



HAL
open science

Role of recombinaison proteins in crossover formation, pairing and synapsis in *Arabidopsis* meiosis: Physiologie et génétique moléculaires

Gunjita Singh

► **To cite this version:**

Gunjita Singh. Role of recombinaison proteins in crossover formation, pairing and synapsis in *Arabidopsis* meiosis: Physiologie et génétique moléculaires. Plants genetics. Université Clermont Auvergne [2017-2020], 2017. English. NNT: 2017CLFAC037 . tel-01781616

HAL Id: tel-01781616

<https://theses.hal.science/tel-01781616>

Submitted on 30 Apr 2018

HAL is a multi-disciplinary open access archive for the deposit and dissemination of scientific research documents, whether they are published or not. The documents may come from teaching and research institutions in France or abroad, or from public or private research centers.

L'archive ouverte pluridisciplinaire **HAL**, est destinée au dépôt et à la diffusion de documents scientifiques de niveau recherche, publiés ou non, émanant des établissements d'enseignement et de recherche français ou étrangers, des laboratoires publics ou privés.

UNIVERSITÉ CLERMONT AUVERGNE

**ÉCOLE DOCTORALE SCIENCES DE LA VIE, SANTÉ,
AGRONOMIE, ENVIRONNEMENT**

ED SVSAE n° d'ordre: 726

Thèse

Présentée à l'Université Clermont Auvergne
pour l'obtention du grade de

DOCTEUR D'UNIVERSITÉ

Spécialité: Physiologie et Génétique Moléculaires

Présentée et soutenue publiquement par

Gunjita Singh

Le 9 Octobre 2017

**ROLE OF RECOMBINATION PROTEINS IN CROSSOVER
FORMATION, PAIRING AND SYNAPSIS
IN ARABIDOPSIS MEIOSIS**

Président : Dr. Pierre Sourdille, UMR 1095, INRA, Clermont Ferrand

Rapporteurs: Dr. Valérie Borde, CNRS, Institute Curie, Paris
Dr. Paul Fransz, University Van Amsterdam, Amsterdam

Examineurs: Dr. Christine Mézard, CNRS, IJPB, INRA, Versailles

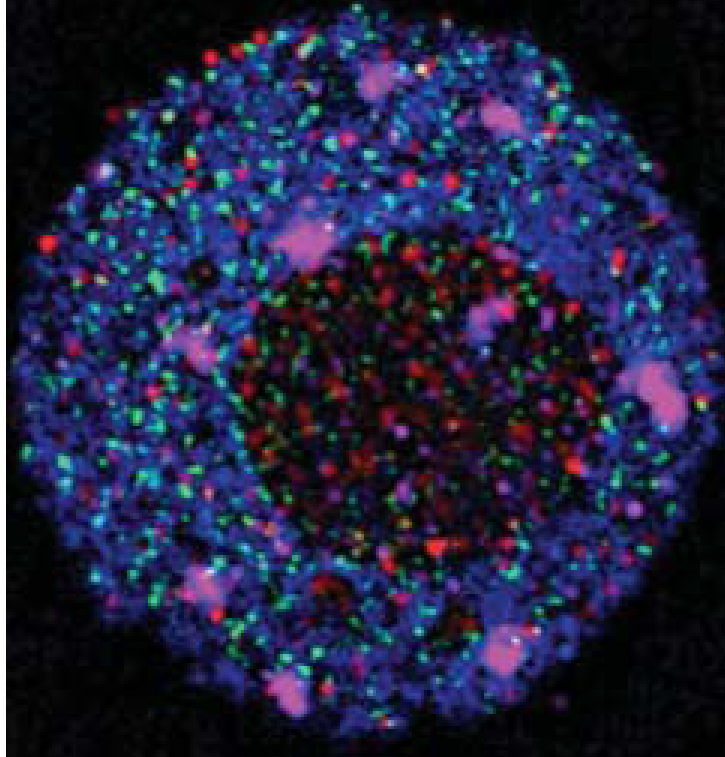
Directeur de thèse: Dr. Charles I. White, CNRS, Clermont-Ferrand

Co-directeur de thèse: Pr. Maria E. Gallego, Université Clermont Auvergne,
Clermont-Ferrand

Laboratoire GRéD - UMR CNRS 6293 - INSERM U1103-
Université Clermont Auvergne

Équipe - RECOMBINAISON ET MAINTENANCE DE L'INTÉGRITÉ DU GÉNOME

“A world of meiotic proteins”
By Gunjita Singh



Leptotene SIM image, showing CENH3 (centromeres in Pink), ASY1 (meiotic protein in Green) and DNA stained with DAPI (Blue), (Imaging has been done with “*Elyra PS.1, Zeiss Microscope*” in IPK, Gatersleben, Germany).

Acknowledgement

This thesis was a great learning experience for me both personally and professionally. I think “Thank You” will be really nothing to define my gratitude towards the people involved throughout my thesis.

I am deeply grateful to my reporters and examiners of my manuscript Dr. Valérie Borde, Dr. Christine Mézard, Dr. Pierre Sourdille and Prof. Paul Fransz, who have agreed to evaluate my thesis work and to be part of my jury.

I would like to thank my supervisor, Dr Charles White and Prof Maria Gallego, for their help and guidance throughout my Ph.D., and for giving me this international opportunity to do this project. I am particularly thankful for their patience during the times when the results were scarce or I was completely lost and unable to perform the experiments.

I would especially like to thank Olivier Da Ines who was always willing to help me whenever I needed, and also for sharing his time and patiently advising (I have a question ☺).

I also wish to thank Chantal and Fabienne for their technical support, helping me to understand the Classical Genetics and also useful advice over the years.

I am grateful for everyone who has spent time in the lab over the years: Heïdi, Matthias, Axel, Angeles, Leticia, Sébastien. It's been a great place to work.

In particular, I want to thank Lauriane (I can't imagine my administrative works being completed on time without her), Pierre, Margaux, Amy, Emeline, Maxime AC, Maxime Voisin for their friendship, crazy parties, celebration and being the shoulder whenever I needed. You guys are my home away from home.

I would like to acknowledge Simon, Cyril, Jérémy, Michel, Nathalie, Olivier Mathieu, Sylvie, Sylviane, Marie-noelle, Aline, Christophe, Samuel, Emmanuel, Thierry, and Maryse Brunel for their collaborative efforts and all the laughs at the lunch table.

I am thankful to the COMREC group for their invaluable contribution to the helpful advice, discussions and sharing of expertise.

I would like to thank the sponsors of this project, the European Commission Marie-Sklodowska Actions (FP7- PEOPLE-2013-ITN. COMREC. 606956) and CNRS.

Finally, I am especially grateful for the support of my friends and family. In particular, I could never thank my Mom enough, for being with me always 24*7 in every circumstance with her unconditional love and support.

And of course a special thanks to my group outside the lab Shifa, Tapish, Bhawana, Siddharth, Harsh, Shyam, Meghana, Indira, Anas, Anne, Gaetano, and Sachin. Thank you guys for being the part of my beautiful journey of PhD.

The visible manifestation of genetic crossing-over, chiasmata link homologous chromosome pairs to permit them to properly orient on the meiotic Anaphase I spindle. They are the result of an intricate and tightly regulated process involving induction of DNA double-strand breaks and their repair through invasion of a homologous template DNA duplex. Recombination is thus essential for the synapsis and accurate segregation of meiotic chromosomes at the first meiotic division, and in doing so, generates genetic variation. Although the processes permitting a chromosome to pair only with its homologue are not fully understood, successful pairing of homologous chromosomes is tightly linked to recombination catalysed by the DNA strand exchange enzymes RAD51 and DMC1. Both proteins share very similar capabilities *in vitro*, but are functionally distinct *in vivo*.

The first part of my thesis shows the impact of eliminating the strand exchange activity of RAD51 in Arabidopsis meiosis, while retaining its function as an accessory factor for the action of DMC1. Recombination can give rise to both crossover (CO) and non-crossover (NCO) outcomes and the meiosis-specific recombinase DMC1 has been thought to be of particular importance is the production of inter-homolog CO. Recent results however suggest strongly that that DMC1 is the only active recombinase in wild-type meiosis and thus must be responsible for both CO and NCO outcomes. Approximately 95% of meiotic homologous recombination in Arabidopsis does not result in inter-homologue crossovers and Arabidopsis is thus a particularly sensitive model for testing the relative importance of the two proteins - even minor effects on the non-crossover event population should produce detectable effects on crossing-over. DMC1 catalyses repair of all meiotic DNA breaks in the presence of the catalytically inactive RAD51 (RAD51-GFP fusion) and the results of my work show that this has no detectable effect on the relative rates of CO and NCO recombination, both locally and chromosome- and genome-wide, nor on the progression of the meiotic division. This work has resulted in a publication in the journal PLoS One (Singh G, Da Ines O, Gallego ME & White CI (2017) Analysis of the impact of the absence of RAD51 strand exchange activity in Arabidopsis meiosis. *PLoS ONE* **12**: e0183006–16).

Previous publications show partial, incomplete homolog synapsis in the absence of *rad51* and *xrcc3* in Arabidopsis meiosis. This is accompanied by the presence of many short ZYP1 fibres in these nuclei, possibly indicating short stretches of Synaptonemal Complex (SC). The partial synapsis is both SPO11- and DMC1-dependent and involves pericentromeres, showing that DMC1 is able to (at least partially) drive synapsis in pericentromeres in the absence of RAD51. In an effort to better characterize this and to test the hypothesis that the short ZYP1 fibres show the presence of initiation of SC at these sites, immunofluorescence and SIM imaging with DAPI staining and ASY1, ZYP1 and CENH3 antisera were carried out for cytogenetic analyses of synapsis in *rad51* and *xrcc3* mutants and the WT in the second part of my thesis work. Although I do observe short ZYP1 fibres including centromeres in the mutants, these are not the rule, so synapsis does not necessarily begin at centromeres or pericentromeres. The superresolution imaging does confirm the presence of stretches of 4-chromatid fibres in *xrcc3* plants and this approach will be extended in future work of the group to probe the nature of the RAD51-independent partial meiotic chromosome synapsis.

Finally, I have designed and built CRISPR/CAS9 constructs with the aim of creating meiotic DSB hotspots at specific genomic loci. Taking advantage of single nucleotide polymorphism data, these constructs were designed to specifically cleave sites in the

Arabidopsis *Col-0* ecotype, and not in *Ler-0* plants. Expression of these constructs in *Col-0* plants and testing recombination rates *in planta*, confirmed their functionality and yielded both hypo- and hyper-recombination effects. Not unexpectedly, these effects varied between different transformant lines and different constructs. Also, a strong effect of chromosome loss was observed in one of the transformants. Crossing this line with *Ler-0* permitted to resolve this problem in the F1 hybrid, suggesting that the presence of a non-cleavable donor chromosome is able to protect against the deleterious effect of too-efficient DSB generation in Arabidopsis meiosis.

Résumé

Manifestation visible des cross-overs génétiques, les chiasmata lient les paires de chromosomes homologues afin de les orienter correctement sur le fuseau méiotique en Métaphase et Anaphase I. Ils résultent d'un processus complexe et étroitement régulé impliquant l'induction de cassures double-brins et de leur réparation par l'invasion d'un duplex d'ADN homologue faisant office de modèle. La recombinaison est ainsi essentielle pour le synapsis et la ségrégation correcte des chromosomes méiotiques à la première division méiotique, et pour la génération de la variabilité génétique. Bien que les processus permettant à un chromosome de s'apparier seulement à son homologue ne soient pas complètement élucidés, l'appariement des chromosomes homologues est étroitement lié à la recombinaison catalysée par les enzymes d'échange de brins d'ADN RAD51 et DMC1. Ces deux protéines ont des capacités très similaires *in vitro*, mais sont fonctionnellement distinctes *in vivo*.

La première partie de ma thèse montre l'impact de l'élimination de l'activité d'échange de brins de RAD51 dans la méiose d'Arabidopsis, tout en conservant sa fonction de facteur accessoire pour l'action de DMC1. La recombinaison peut donner lieu à des cross-over (CO) et non-cross-over (NCO) et la recombinase spécifique de la méiose DMC1 a été jugée particulièrement importante dans la production de CO interhomologue. Des résultats récents suggèrent fortement toutefois que DMC1 est la seule recombinase active dans la méiose et doit donc être responsable des résultats de CO et NCO. Etant donné qu'environ 95% de la recombinaison méiotique homologue dans Arabidopsis n'entraîne pas de cross-overs interhomologues, Arabidopsis est un modèle particulièrement sensible pour tester l'importance relative des deux protéines - même des effets mineurs sur la population d'événements non-cross-over devraient produire des effets détectables sur les cross-overs. DMC1 catalyse la réparation de toutes les cassures d'ADN méiotiques en présence d'une protéine RAD51 catalytiquement inactive (fusion RAD51-GFP), et les résultats de mon travail montrent que cela n'a pas d'effet détectable sur les taux relatifs de recombinaison de CO et de NCO : à la fois localement, à l'échelle du chromosome et du génome. Et non plus sur la progression de la division méiotique. Ce travail a abouti à une publication dans le journal PLoS One (*Singh G, Da Ines O, Gallego ME & White CI (2017) Analyse de l'impact de l'absence d'activité d'échange de brins de RAD51 dans la méiose d'Arabidopsis PLoS ONE 12: e0183006-16*).

Des publications antérieures montrent une synapsis homologue partielle et incomplète en l'absence de *rad51* et *xrcc3* dans la méiose d'Arabidopsis. Cela s'accompagne de la présence de nombreuses fibres courtes ZYP1 dans ces noyaux, ce qui pourrait indiquer de faibles longueurs de complexe synaptonémale (SC). Ce synapsis partielle dépend à la fois de SPO11 et de DMC1 et implique des péricentromères, montrant que DMC1 est capable (au moins partiellement) d'entraîner le synapsis dans les péricentromères en l'absence de RAD51. Afin de mieux caractériser ceci et pour tester l'hypothèse que les fibres ZYP1 courtes montrent la présence d'une initiation de SC à ces sites, j'ai mené des expériences d'immunofluorescence et d'imagerie SIM. Utilisant une coloration DAPI et les antiséras ASY1, ZYP1 et CENH3, j'ai conduit des analyses cytogénétiques de la synapsis dans les mutants *rad51*, *xrcc3* et des plantes sauvages. Ces travaux faisaient l'objet de la deuxième partie de mes travaux de thèse. Dans les plantes mutantes, j'observe

effectivement des fibres courtes ZYP1 comprenant des centromères, mais elles ne sont pas la règle, ce qui signifie que le synapsis ne commence pas nécessairement à des centromères ou des péricentromères. L'imagerie de super-résolution confirme la présence de fibres à 4 chromatides dans les plantes *xrcc3* et cette approche sera étendue dans les futurs travaux de l'équipe pour tester la nature de ce synapsis partiel indépendante de RAD51.

Enfin, j'ai conçu et réalisé des constructions CRISPR / CAS9 dans le but de créer des points chauds méiotiques de cassures double-brins à des loci génomiques spécifiques. Profitant des données de polymorphisme nucléotidique, ces constructions ont été conçues pour couper spécifiquement les sites de l'écotype Arabidopsis *Col-0* et non ceux de l'écotype *Ler-0*. L'expression de ces constructions dans les plantes *Col-0* et les tests des taux de recombinaison *in planta* ont confirmé leur fonctionnalité et ont généré des effets d'hyporecombinaison et d'hyperrecombinaison. De manière attendue, ces effets variaient entre différentes lignées de transformantes et différentes constructions. Un effet important de la perte de chromosome a été observé chez l'un des transformants. Le croisement de cette lignée avec *Ler-0* a résolu ce problème dans l'hybride F1, ce qui suggère que la présence d'un chromosome donneur non clivable est capable de protéger contre l'effet délétère d'une génération de cassures double-brin trop efficace dans la méiose d'Arabidopsis.

RESUME EN FRANCAIS DE LA THESE

INTRODUCTION

Le reproduction sexuée eucaryote nécessite la production de gamètes de ploïdie réduite en deux, la fusion de deux d'entre eux régénère la ploïdie d'origine dans la génération suivante (Barton et Charlesworth, 1998, Buisson et al., 2013). Cette réduction de moitié du nombre de chromosomes est réalisée par méiose : une division cellulaire spécialisée dans laquelle deux divisions successives suivent un seul cycle de réplication de l'ADN. Une seule cellule méiotique produit ainsi quatre noyaux de ploïdie réduite en deux. Cela contraste avec la division cellulaire mitotique, dans laquelle la réplication de l'ADN suivie d'une division unique aboutit à deux noyaux filles de la même ploïdie que la cellule-mère (Fig. 1) (Ma, 2006). La division méiotique résout ainsi le problème du maintien de la ploïdie stable à travers les générations sexuelles, mais cela a un coût. En mitose, la ségrégation équilibrée des chromatides à l'anaphase est assurée par la cohésion des chromatides sœurs établies dans la phase S précédente. Assurant ainsi, que chaque cellule fille reçoit un complément complet de chromosomes. Ceci ne peut être fait qu'une seule fois après chaque phase S, et n'est pas suffisant en méiose, dans laquelle deux divisions nucléaires successives suivent une seule phase S.

Chez la plupart des eucaryotes étudiés, la ségrégation chromosomique méiotique est assurée par des chiasmata, des liens physiques entre chromosomes homologues produits par recombinaison. La recombinaison au cours de la première prophase méiotique garantit ainsi que les chromosomes homologues se séparent avec précision et, ce faisant, casse les liaisons génétiques pour générer la variation génétique responsable de l'évolution (Fig_2) (Osman et al., 2011).

La recombinaison homologue (RH) opère principalement en phases S et G2 dans les cellules mitotiques, favorisant l'utilisation de la chromatide soeur comme modèle pour la réparation, des travaux récents ont conduit à la compréhension, que le choix la RH pour la réparation est essentiellement déterminé par la présence d'une séquence de matrice homologue et une résection extensive des extrémités d'ADN cassées (Ceccaldi et al., 2016). La résection est le processus de dégradation nucléolytique des brins d'ADN à terminaison 5', laissant des extrémités d'ADN monocaténaire à terminaison 3'-OH flanquant le DSB.

La RH pendant la Prophase I méiotique est nécessaire pour la ségrégation appropriée des chromosomes en créant des crossing-over (CO) entre les chromosomes homologues. Ceux-ci mélangent aussi les allèles maternels et paternels pour générer une variation génétique dans les gamètes. Des exceptions existent cependant, notamment chez *Drosophila* et *C. elegans* (Dernburg et al., 1998, Gladyshev et Kleckner, 2017). Chez *C. elegans*, l'appariement homologue SPO11-indépendant se produit entre les régions spécialisées (centres d'appariement) près des extrémités de chaque

chromosome, et aussi entre de nombreux sites interstitiels le long de chaque paire chromosomique (Rog et Dernburg, 2013; Tsai et McKee, 2011). Dans la méiose chez la Drosophile, l'appariement indépendant des chromosomes homologues précède normalement la formation des cassures de l'ADN chez les femelles (Lake et Hawley, 2012) et remplace complètement les mécanismes de recombinaison chez les mâles (McKee et al., 2012).

Notre compréhension des mécanismes de la recombinaison méiotique a été établie partir d'études réalisées dans de nombreux organismes et notamment la levure *S. cerevisiae*. La recombinaison méiotique est initiée par la formation programmée de cassures double brin (DSB), suivie par la résection des brins, la recherche d'homologie et l'invasion, qui conduisent à la formation de structures intermédiaires de molécules liées. Celles-ci sont résolues pour aboutir à des résultats CO ou NCO. Ce sont les CO, qui créent les chiasmata, qui lient physiquement les paires homologues de chromosomes dans la Prophase I tardive et assurent leur ségrégation à l'Anaphase I méiotique (Lambing et al., 2017; Mercier et al., 2014; Smith et Nicolas, 1998).

Le processus de recombinaison méiotique est initié par l'induction programmée de DSB dans tout le génome par le complexe protéique SPO11. Ressemblant à la topoisomérase Topo VI, la structure du complexe eucaryote SPO11 a été récemment clarifiée grâce à l'identification du partenaire essentiel de SPO11 chez *Arabidopsis* (MTOPIVIB), la souris (TOP6BL), *S. cerevisiae* (Rec102), *S. pombe* (Rec6) et *D. melanogaster*

(MEI-P22) (Bouuaert et Keeney, 2016, Liu et al., 2002, Robert et al., 2016a, Vrielynck et al., 2016). Fonctionnant comme hétérodimère ou hétérotétramère, SPO11 agit par attaque nucléophile sur le squelette de l'ADN via ses résidus de tyrosine catalytiquement actifs (Grelon et al., 2001, Hartung et Puchta, 2000, Vrielynck et al., 2016). Au cours de ce processus, SPO11 coupe l'ADN et reste attaché de manière covalente aux extrémités 5' de l'ADN via des liaisons phosphore-tyrosyle, jusqu'à un traitement ultérieur dans l'étape de recombinaison suivante (Bergerat et al., 1997, de Massy, 2013, Keeney et al., 1997).

Trois homologues de SPO11 SPO11-1, SPO11-2 et SPO11-3 ont été identifiés chez des plantes, des algues rouges et des protistes (Grelon et al., 2001, Harting et Puchta, 2001, Lambing et al., 2017, Malik et al., 2007). Les deux SPO11-1 et SPO11-2 sont essentiels pour la formation de DSB méiotique (Grelon et al., 2001, Stacey et al., 2006), tandis que SPO11-3 est impliquée dans l'endoréduplication somatique (Hartung et al., 2007). Seules les plantes mono- et dicotylédones sont connues pour posséder plus d'un paralogue SPO11 dans leur génome (An et al., 2011, Yu et al., 2010). La présence de deux isoformes SPO11 résultant d'un épissage alternatif a été signalée chez la souris et l'homme (Bellani et al., 2010, Keeney et al., 1999, Romanienko et Camerini-Otero, 1999, Shannon et al., 1999), mais SPO11 β seul est capable d'assurer la production de DSB méiotique chez la souris (Kauppi et al., 2011).

Chez *Arabidopsis*, le complexe SPO11 consiste donc en un complexe hétéromérique de deux sous-unités A (SPO11-1 et SPO11-2) et de la sous-

unité B récemment identifiée (MTOFVIB) (Grelon et al., 2001; Hartung et Puchta, 2000; al., 2007, Lambing et al., 2017, Robert et al., 2016, Shingu et al., 2010, Stacey et al., 2006, Vrielynck et al., 2016).

SPO11 de la levure nécessite un certain nombre de protéines accessoires pour initier la recombinaison *in vivo*: RAD50, MRE11, XRS2, MER1, MER2, MEI4, MRE2, REC102, REC104, REC114 et SKI8 (Cole et al., 2010; de Massy, 2013; et Keeney, 2014, Paques et Haber, 1999). Un réseau d'interactions impliquant ces protéines a été établi en utilisant le système de double hybride de levure (Arora et al., 2004; Maleki et al., 2007), montrant que les protéines accessoires SPO11 forment trois sous-complexes pour former un complexe qui se lie à la chromatine (Arora et al., 2004; Maleki et al., 2007; Szekvolgyi et al., 2015). Ces complexes jouent un rôle majeur dans la sélection des régions de DSB potentielles le long des chromosomes, et contribuent finalement au recrutement de SPO11 et au clivage de l'ADN (Szekvolgyi et al., 2015).

Le sous-complexe un: Ski8, Rec102, Rec104 et SPO11 forment le premier sous-complexe. Ski8 a des rôles dans les cellules méiotiques et végétatives. Cependant, le rôle méiotique de Ski8 semble être distinct de sa fonction cytoplasmique dans le métabolisme de l'ARN (Arora et al., 2004). Rec102 et Rec104 se comportent comme une unité fonctionnelle, et sont nécessaires pour la localisation nucléaire de SPO11, l'association avec la chromatine et la liaison aux points chauds (Lam et Keeney, 2014).

Le sous-complexe deux: Le deuxième sous-complexe pré-DSB est composé de Mei4, Mer2 et Rec114. La fonction de ces trois protéines dans

l'induction de DSB n'est pas complètement comprise, mais la localisation différentielle des deux sous-complexes pré-DSB suggère que Mei4 / Mer2/Rec114 peut interagir avec certains composants du complexe SPO11/Ski8/Rec102/Rec104 maintien la boucle de chromatine sur les axes des chromosomes pour activer l'activité SPO11 et former des DSB méiotiques (Lam et Keeney, 2014).

Le sous-complexe trois: Le troisième groupe de protéines est le complexe MRX (Mre11, Rad50 et Xrs2). Ces protéines hautement conservées sont impliquées dans divers aspects du métabolisme de l'ADN dans les cellules végétatives et méiotiques (Arora et al., 2004, Gobbini et al., 2016), avec l'orthologue Xrs2 animale et végétale connue sous le nom de NBS1 (complexe MRN). Mre11 est une endo- et une exonucléase (Myler et Finkelstein, 2017, Paull et Gellert, 1998). Rad50 est un membre de la famille des protéines du maintien structural des chromosomes (SMC) (Anderson et al., 2001, Lee et al., 2013). La liaison des domaines coiled-coil de deux molécules RAD50 à travers un domaine de crochet est critique pour la fonction complexe MRX/MRN, en maintenant les deux extrémités d'ADN d'un DSB (Hohl et al., 2011, Hopfner et al., 2002, Mockel et al., 2012, Myler et Finkelstein, 2017, Wiltzius et al., 2005). Xrs2 est une protéine de liaison à l'ADN structure spécifique qui intervient également dans l'activation des points de contrôle (check points) des dommages à l'ADN (Lee et al., 2013, Trujillo et al., 2003). NBS1 contient trois séquences de localisation nucléaire redondantes (NLS) cruciales pour la

localisation nucléaire du MRN (Desai-Mehta et al., 2001; Tauchi et al., 2002).

Des homologues de MRE11, RAD50 et NBS1 (complexe MRN) ont été caractérisés chez *Arabidopsis thaliana* et se sont avérés jouer les rôles de recombinaison et de réparation d'ADN attendus, mais le complexe n'est pas essentiel à la formation de DSB méiotiques (Bleuyard et al., 2004; Cotterell et al., 2002, Gallego et al., 2001, Puizina et al., 2004, Uanschou et al., 2007).

Il a été démontré que les protéines PRD1, PRD2 et PRD3, DFO, CRC1 et COMET sont impliquées dans la formation de DSB méiotiques chez les plantes (De Muyt et al., 2007, Lambing et al., 2017). AtPRD1 est proposée pour être l'homologue fonctionnel de la protéine MEI1 DSL mammifère, et pour interagir avec AtSPO11-1 pour former des DSB (De Muyt et al., 2007, Lambing et al., 2017, Libby et al., 2003). AtPRD2 semble être un orthologue de MEI4 de la levure et de la souris (De Muyt et al., 2009, Kumar et al., 2010, Lambing et al., 2017). PRD3 est l'orthologue de PAIRI chez le riz, nécessaire pour l'appariement homologue en méiose (De Muyt et al., 2009, Lam et Keeney, 2014, Nonomura et al., 2004). MPO est importante pour la formation des DSB méiotiques. Les mutants *dfo* présentent une asynapsie, des taux de recombinaison fortement réduits et une formation de DSB altérée, comme le montre leur capacité à supprimer la fragmentation des chromosomes méiotiques dans le mutant *mre11* (Zhang et al., 2012). CRC1 d'*O. sativa* est similaire à PCH2 chez *Arabidopsis* et *S. cerevisiae* (Lambing et al., 2017; Miao et al., 2013),

reliant le complexe DSB à l'axe chromosomique et ainsi favorisant la formation de DSB (Osman et al. 2011).

Une fois que les DSB sont formées, les cassures passent à l'étape de résection le terme résection se rapporte à la dégradation 5' -> 3' des extrémités de la DSB pour générer des extrémités 3' sortantes d'ADN simple brin (ADNsb), qui envahiront ensuite la molécule homologue d'ADN pour se réparer. Au cours de la méiose, la liaison covalente de SPO11 aux extrémités du DSB empêche l'accès aux DSB par des exonucléases et elle doit donc être éliminée afin de permettre la réparation de continuer.

L'élimination de SPO11 des extrémités DSB se produit par clivage endonucléolytique dépendant du complexe MRX/MRN, + Com1/Sae2 chez la levure ou CtIP chez les mammifères (Lambing et al., 2017; Mercier et al., 2014; Myler et Finkelstein, 2017, Neale et al., 2005). Chez *S. cerevisiae*, Sae2 favorise l'activité endonucléase de Mre11 dans le complexe MRX (Cannavo et Cejka, 2014). De manière analogue, CtIP (l'orthologue fonctionnel humain de la levure Sae2/Ctp1), ne possède pas d'activité endonucléase, mais peut favoriser l'activité endonucléase de MRE11 (Sartori et al., 2007). Chez les plantes, l'absence de AtMRE11 ou AtCOM1 (l'orthologue fonctionnel de Sae2), conduit à une fragmentation importante des chromosomes et à la persistance de AtSPO11-1 sur la chromatine lors de la Prophase I méiotique (Uanschou et al., 2007). La persistance de AtSPO11-1 liée à la DSB dans les Prophase I des méioses de *Atcom1* et *Atmre11* explique très probablement l'absence de résection

dans ces mutants. Ceci suggère que AtMRE11 et AtCOM1 partagent une fonction similaire avec leurs orthologues de levure (Ji et al., 2012, Puizina et al., 2004, Uanschou et al., 2007).

La résection initiale des extrémités de la DSB forme de courtes extensions d'ADN simple brin. Ces extrémités sont sensibles à l'activité exonucléase pour une résection plus poussée. Au cours de la recombinaison homologue méiotique, l'exonucléase Exo1 est impliquée dans ce traitement de la DSB dans la levure (Zakharyevich et al., 2010). Deux études récentes ont montré que les activités exonucléasiques de Mre11 et Exo1 contribuent à la résection des extrémités de la DSB (Garcia et al., 2011, Zakharyevich et al., 2010). Mre11 traite la DSB avec une activité exonucléase de 3' à 5', Exo1 traite la DSB avec une activité exonucléase de 5' à 3' et son absence entraîne une réduction de la longueur de la résection (Garcia et al., 2011; Zakharyevich et al., 2010). Bien qu'Exo1 ait traité la plupart des extrémités du DSB, certaines étaient normalement traitées en son absence (Zakharyevich et al., 2010). Fait intéressant, la réduction de la longueur du tractus de résection 5'-3' n'a pas affecté significativement la recherche d'homologie par extrémités d'ADNs et la formation de CO (Manfrini et al., 2010; Zakharyevich et al., 2010). Dans les cellules mitotiques de levure, l'hélicase Sgs1 peut dérouler les deux brins d'une extrémité de la DSB pour faciliter l'accès des exonucléases Dna2 et Exo1 et la résection à longue portée (> 3 kb) (Manfrini et al., 2010).

Deux modèles peuvent expliquer la libération de SPO11 pour la résection de DSB. Dans le premier, la résection initiale de la DSB par Mre11/Sae2

pourrait libérer un SPO11-oligonucléotide court, laissant les extrémités de l'ADNs exposées aux activités exonucléasiques de Mre11 et Exo1 (Neale et al., 2005). Alternativement, les oligonucléotides SPO11 formés après la résection initiale par Mre11/Sae2 pourraient rester associés à l'ADNsb complémentaire de l'extrémité 3' jusqu'à la fin de la résection de l'extrémité 5' (Neale et al., 2005). Pour étayer cette deuxième hypothèse, plusieurs études indiquent que le complexe MRX associé à Sae2 peut ancrer des molécules d'ADN (Bhaskara et al., 2007, Clerici et al., 2005, de Jager et al., 2001, Kaye et al., 2004, Lobachev et al. 2004) et pourraient jouer un rôle dans le maintien des oligonucléotides SPO11 associés à l'ADNsb complémentaire. Cependant, une analyse plus approfondie est nécessaire pour élucider ce mécanisme.

Après la résection de la DSB et la génération -d'extrémités 3' sortantes d'ADN à terminaison 3', RAD51 et DMC1 sont chargées sur l'ADNsb pour former un nucléofilament présynaptique. Les nucléofilaments DMC1/RAD51 envahissent l'ADNdb homologue, déplaçant un brin pour former une boucle D. L'extension du brin envahissant, suivi par l'hybridation avec le deuxième côté de la cassure du brin complémentaire résulte dans la formation d'une structure intermédiaire impliquant les deux molécules d'ADN liées par une ou deux jonctions d'Holliday. Une partie minoritaire (ratios DSB: CO de 25-30 chez Arabidopsis, de 15 chez la souris, de 4,4 chez la Drosophile et de 1,8 chez la levure (Serrentino et Borde, 2012) de ces structures intermédiaires seront ensuite résolues pour former des CO, impliquant des chromatides non-sœurs, dans des

chiasmata reliant les chromosomes homologues et le crossing-over génétique.

La formation du nucléofilament présynaptique implique un certain nombre de facteurs accessoires et doit notamment gérer la présence de la protéine RPA1, qui colocalise avec RAD51 pendant la Prophase I chez la levure (Gasior et al., 1998), souris (Moens et al., 2007) et humain (Oliver-Bonet et al., 2007). Chez la levure, RAD51 (Cloud et al., 2012), RAD54, Tid1/Rdh54 (Nimonkar et al., 2012), Mei5-Sae3 (Ferrari et al., 2009, Hayase et al., 2004) et Hop2-Mnd1. (Chan et al., 2014) sont impliquées dans la formation des nucléofilaments présynaptiques DMC1. HOP2/MND1 est nécessaire pour stabiliser le nucléofilament présynaptique (Pezza et al., 2007). Le complexe HOP2/MND1 stabilise l'hétéroduplex d'ADNdb en agissant sur la condensation des molécules d'ADN (Pezza et al., 2010, Pezza et al., 2007, Pezza et al., 2013). Des orthologues de Hop2 et Mnd1 ont été identifiés chez *Arabidopsis* et l'absence d'AtHOP2 ou d'AtMND1 empêche l'appariement méiotique des chromosomes homologues, conduisant à la fragmentation chromosomique à la métaphase I (Uanschou et al., 2013, Vignard et al., 2007). Deux autres protéines, AtRFC1 et AtMCM8, sont également impliquées dans l'étape précoce de la recombinaison homologue (Crismani et al., 2013, Liu et al., 2013, Wang et al., 2012). Les mutants *Atrfc1* (Liu et al., 2013; Wang et al., 2012) et *Atmcm8* (Crismani et al., 2013) présentent une fragmentation chromosomique à partir de l'Anaphase I, et il est proposé que AtRFC1 soit impliquée dans l'extension de l'ADNsb d'invasion par synthèse d'ADN,

alors que la fonction d'AtMCM8 dans la réparation de DSB reste inconnue (Crismani et al., 2013; Wang et al., 2012). Parmi les cinq paralogues RAD51 (XRCC2, XRCC3, RAD51B, RAD51C et RAD51D), seuls XRCC3 et RAD51C sont essentiels pour la recombinaison méiotique RAD51-dépendante chez *Arabidopsis* (Abe et al., 2005, Bleuyard et White, 2004, Li et al., 2005, (Bleuyard et al., 2005) (voir la section RAD51 Paralogs, ci-dessous). *Arabidopsis* a cinq homologues de RPA1 et la mutation de l'un d'entre eux cause des défauts de fertilité résultant d'une formation défectueuse de CO (Osman et al., 2009). De plus, les deux orthologues BRCA2 d'*Arabidopsis*, AtBRCA2a et AtBRCA2b, interagissent avec AtRAD51 et AtDMC1 et sont nécessaires au recrutement des deux recombinaisons sur la chromatine (Seeliger et al., 2012, Siaud et al., 2004).

Concernant les recombinaisons RAD51 et DMC1, le nombre de foyers méiotiques AtDMC1 est réduit en l'absence d'AtRAD51, montrant que la localisation de AtDMC1 sur la chromatine dépend au moins partiellement de AtRAD51 (Kurzbauer et al., 2012, Vignard et al., 2007). Chez la levure et *Arabidopsis*, DMC1 est donc capable de catalyser la réparation de tous les DSB méiotiques en l'absence d'activité d'échange de brins de RAD51 (Cloud et al., 2012, Da Ines et al., 2013b). En l'absence de DMC1, les DSB méiotiques sont efficacement réparés de manière dépendante de RAD51, ce qui entraîne une absence complète de synapses et de formation des bivalents (Couteau et al., 1999). Cependant, lorsque DMC1 est présent, elle inhibe l'activité de réparation RAD51 (Uanschou et al., 2013), rappelant la situation dans la levure, où un mécanisme régulateur négatif

supprimant la fonction RAD51 pendant la méiose est connu (Lao et al., 2013).

Des études antérieures chez *Arabidopsis* ont montré que RAD51 et ses paralogues RAD51C et XRCC3 sont nécessaires pour la réparation méiotique des DSB et la fertilité des plantes. La mutation des gènes individuels provoquent la fragmentation des chromosomes méiotiques dépendant de SPO11. De manière surprenante, on observe une synapse partielle incomplète des homologues dans les méioses mutantes *rad51* et *xrcc3* (et *rad51c*) (Bleuyrd 2004, 2005, Li 2005). Celle-ci est à la fois dépendante de SPO11 et DMC1 et implique des péricentromères, montrant que DMC1 est capable de conduire (au moins partiellement) la synapse dans les péricentromères en l'absence de RAD51 (bleuyard 2004, da ines 2012). Ces observations sont la base du travail que j'ai entrepris pour ma thèse: "Rôle des protéines de recombinaison dans la formation de CO, l'appariement et la synapse méiotique chez *Arabidopsis*". Mon travail expérimental sur ce sujet est divisé en trois parties :

- 1. Analyse de l'impact de l'absence d'activité d'échange de brin de RAD51 dans la méiose d'*Arabidopsis* (Chapitre 3).**
 - 2. Cytogénétique de synapse partielle en l'absence de RAD51 ou XRCC3 (Chapitre 4).**
 - 3. Création de nouveaux points chauds méiotiques ciblés via CRISPR/Cas pour des études des rôles méiotiques de RAD51 et DMC1(Chapitre 5).**
-

CHAPITRE 3 : Analyse de l'impact de l'absence d'activité d'échange de brin RAD51 dans la méiose d'*Arabidopsis*.

Ce travail a été rendu possible par l'utilisation d'une protéine de fusion RAD51-GFP : inactive pour la recombinaison et dominante négative (Da Ines *et al*, 2013). La protéine de fusion RAD51-GFP forme des nucléofilaments sur l'ADN monocaténaire, mais la présence du peptide GFP inactive le second site de liaison à l'ADN de RAD51, ce qui rend le protéine de fusion incapable de catalyser l'étape clé d'invasion de brins de recombinaison (Kobayashi *et al.*, 2014). RAD51-GFP ne peut pas effectuer de recombinaison, mais reste pourtant capable de permettre l'activité de DMC1 dans la méiose (Da Ines *et al*, 2013). Toute recombinaison méiotique est ainsi catalysée par DMC1 dans les plantes RAD51-GFP entièrement fertiles.

- Taux de CO dans les intervalles génétiques marqués par des marqueurs de pollen fluorescent. Les mesures des taux de recombinaison dans un intervalle de bras chromosomiques (I1b) et un intervalle incluant une région centromérique (CEN3) concordante avec nos mesures précédentes sur 2 intervalles génétiques définis par les marqueurs INDEL sur les bras des chromosomes I et III, ne montrent aucun effet significatif de l'absence d'activité d'échange de brin RAD51 fonctionnelle sur les taux de CO

méiotique dans les bras chromosomiques ou à travers le centromère du chromosome 3 d'*Arabidopsis*.

- Le comptage cytologique du nombre de chiasmata par chromosome n'a montré aucune différence significative entre les plantes de type sauvage et les plants exprimant RAD51-GFP. Le nombre de chiasmata à l'échelle du génome a montré une très légère augmentation de la méiose RAD51-GFP ($9,3 \pm 0,11$ (moyenne \pm s.e.m.)) par rapport aux témoins de type sauvage ($9,68 \pm 0,15$), mais de faible importance.

- L'analyse des nombres de CO de type I par immunofluorescence HEI10 n'a montré aucune différence significative entre les méioses RAD51-GFP et de type sauvage. Comme prévu, les nombres de foci HEI10 visibles sur les axes chromosomiques augmentent par le biais du leptotène dans le zygotène tardif à la fois dans le type sauvage et RAD51-GFP et chutent considérablement pour donner 7-11 foci/noyau dans le Pachytène tardif.

- La mesure de la durée de la méiose par l'incorporation d'EDU a montré une cinétique méiotique similaire chez les plantes RAD51-GFP et WT. L'absence d'activité d'échange de brin RAD51 n'a donc provoqué aucune différence détectable dans la synchronisation des stades méiotiques dans cette analyse.

Les recombinaisons RAD51 et DMC1 catalysent l'étape clé de l'invasion des brins de recombinaison et sont toutes les deux essentielles pour la ségrégation ordonnée des chromosomes dans la méiose. Chez la plupart des eucaryotes, la recombinaison méiotique nécessite la coopération des deux protéines d'échange de brin. RAD51 est actif dans la mitose et la

méiose, tandis que DMC1 est spécifique à la méiose. Il y a quelques exceptions où la recombinaison méiotique médiée par DMC1 n'est pas nécessaire parce que plusieurs organismes ne possèdent pas d'orthologue DMC1 (par exemple *Drosophila*, *Caenorhabditis elegans*, *Neurospora crassa* et *Sordaria macrospora*) (Neale et Keeney, 2006).

Pourquoi les eucaryotes ont-ils deux protéines d'échange de brin, et quelles fonctions spécifiques possède DMC1 à la méiose? Une clé de la réponse à cette question vient des travaux récents montrant que l'activité d'invasion de RAD51 n'est pas nécessaire pour la recombinaison méiotique. Des études sur les mutants de séparation de fonction de la levure *rad51-II3A* et *Arabidopsis* RAD51-GFP montrent que l'activité d'échange de brin de DMC1 est suffisante pour la recombinaison méiotique et le besoin de RAD51 est pour la protéine elle-même (comme nucléofilament) et non pour son activité catalytique d'échange de brin (Cloud et al., 2012, Da Ines et al., 2013b). Les phénotypes analogues des mutants de levure et de plante signifient que ces conclusions sont potentiellement applicables de manière générale aux eucaryotes avec un homologue DMC1. DMC1 est donc la recombinase à invasion de brins active dans la recombinaison méiotique. Cette conclusion met donc en doute la croyance généralement admise que DMC1 est spécifiquement impliquée dans le CO et RAD51 dans la recombinaison NCO au cours de la méiose.

En travaillant avec *Arabidopsis thaliana*, nous avons prolongé les études précédentes avec deux autres intervalles génétiques en utilisant

l'intervalle I1b (intervalle de bras) et CEN3 (intervalle centromérique) ainsi qu'à l'échelle chromosomique et du génome entier. Aucun effet significatif sur les rapports CO/NCO ou sur la progression méiotique dans notre expérience EdU au cours du temps en l'absence d'activité d'échange de brins RAD51. Les données de cette première partie de ma thèse étendent le travail précédent et confirment les études antérieures sur la levure et l'Arabidopsis. DMC1 est la protéine d'échange de brin méiotique active dans la méiose WT et semble donc être responsable du CO et du NCO intersoeurs et interhomologues.

<p>CHAPITRE 4 : Cytogénétique de synapsis partiel en l'absence de RAD51 ou XRCC3.</p>
--

La recombinaison homologue pendant la Prophase I est cruciale pour la synapse correcte et la ségrégation des chromosomes homologues dans la première division méiotique (MI) et donc la fertilité. Des progrès très considérables ont été réalisés dans la compréhension des liens entre la recombinaison méiotique et la synapse des homologues, mais nous ne comprenons pas encore complètement ces processus.

RAD51 et les paralogues RAD51, XRCC3 et RAD51C, qui favorisent son activité, sont essentiels pour la réparation de la DSB induite par SPO11 et leur absence entraîne donc la fragmentation chromosomique au cours de la Prophase I chez Arabidopsis (Abe et al., 2005, Bleuyard et al. 2005,

Bleuyard et White, 2004, Li et al., 2005, Vignard et al., 2007). RAD51 (ou DMC1 + RAD51 dans la méiose) catalyse la recherche et l'invasion de la séquence modèle (matrice) homologue et est donc la clé de l'établissement des liens physiques entre les chromosomes homologues. Ainsi, c'est l'induction de la DSB dans le Leptotène et leur réparation qui établit le coalinement des axes chromosomiques homologues visibles dans le Zygotène. Le fait que la fragmentation chromosomique se produit à la fin du Zygotène/début du Pachytène en absence de RAD51 est donc à la fois inattendu et frappant.

Les études d'immunocytologie et de FISH ont confirmé la synapse partielle des homologues dans *rad51* et *xrcc3* et ont mis en évidence une spécificité des régions centromériques et d'ADNr (ADN ribosomique), qui dépendent principalement de la recombinaison DMC1 et non de la RAD51 pour la synapse. (Bleuyard et White, 2004, Da Ines et al., 2012).

La synapse partielle indépendante de RAD51, dépendante de DMC1 et de SPO11 dans les mutants *rad51* et *xrcc3* est donc due à l'appariement des chromosomes homologues dans les régions centromériques et d'DNAr (Da Ines et al., 2012). Ceci, associé à l'absence de synapsis du bras chromosomique chez ces mutants, suggère l'initiation de la synapsie par DMC1 dans ces régions, qui sont ensuite stabilisées et étendues le long des bras chromosomiques par la recombinaison homologue RAD51-dépendante (Da Ines et al., 2012). L'activité de DMC1 dépend de la présence (pas de l'activité d'échange de brin) des nucléofilaments RAD51 (Cloud et al., 2012, Da Ines et al., 2012, Da Ines et al., 2013b, Kobayashi

et al., 2014; Su et al., 2017), et l'appariement et la synapse des régions du bras dépendent à la fois de DMC1 et de RAD51 (qui à son tour dépend de la présence de XRCC3). Ainsi, DMC1 est capable d'établir des synapses (au moins partielles) des régions centromériques et d'ADNr en l'absence de RAD51, mais nécessite la présence de la protéine RAD51 ailleurs. Cette conclusion conduit aux deux questions, qui sont la base de mon travail de thèse:

1) La synapse des chromosomes méiotiques chez *Arabidopsis* commence-t-elle aux centromères/péricentromères et s'étend-elle ensuite aux bras des chromosomes?

2) Quelle est l'interdépendance du centromère et de la synapse des bras?

Pour répondre à ces questions, j'ai réalisé des expériences de co-immunolocalisation, en utilisant des antisérums contre ASY1 (protéine associée à l'axe du complexe synaptonémal), ZYP1 (protéine du filament transversal synaptonémal complexe) et CENH3 (histone centromérique H3). Ces expériences ont été réalisées sur des étalements de chromosomes méiotiques issus de plantes de type sauvage, *rad51* et *xrcc3*, associés à la SIM (Super résolution) et à la microscopie à épifluorescence. Dans ce travail, j'ai analysé les images SIM de WT (15 cellules), *rad51* (19 cellules), *xrcc3* (25 cellules) et aussi des images de microscopie à épifluorescence de WT (30 cellules), *rad51* (30 cellules), *xrcc3* (30 cellules). Cette analyse a donné trois observations importantes:

1. De courtes bandes de fibres ZYP1, et donc vraisemblablement, complexe synaptonémal (CS) ont été observées dans les mutants *xrcc3* et *rad51* aux

stades zygo-pachytène (FIG_16). Bien qu'il ait déjà été conclu que le CS est absent de la méiose *xrcc3* (Vignard et al., 2007), la présence de ces étirements suggère que même si les plantes *xrcc3* et *rad51* sont incapables de compléter la synapse et que leurs chromosomes se fragmentent après le stade zygo-pachytène, ils ont des synapses chromosomiques de courtes étendues .

2. L'appariement des centromères est un événement précoce dans l'appariement des chromosomes méiotiques et a bien été décrit chez *Arabidopsis* (Armstrong et al., 2001). Les centromères d'*Arabidopsis* sont non appariés et dispersés au cours de l'interphase méiotique jusqu'au leptotène, groupés au leptotène/zygotène, les centromères séparés et les homologues s'associent ensuite par paires et synapse dans le zygotène et pachytène. L'observation des centromères méiotiques dans WT, *xrcc3* et *rad51* marqués par l'anticorps CENH3, a montré comme prévu que dans les méiocytes WT il y a 7-9 signaux de centromères au zygotène et 3-5 au pachytène (Fig_2). Même dans *xrcc3* et *rad51*, où les fragments de chromosomes après zygo-pachytène, 7-9 foci centromériques par noyau étaient visibles au zygotène et 3-5 au pachytène (Fig_17). Ces résultats de microscopie sont similaires aux données de couplage centromérique, de regroupement et d'appariement précédemment publiées dans *Arabidopsis* (Da Ines et al., 2012, Da Ines et al., 2014, Fransz et al., 1998, Su et al., 2017).

3. Des travaux antérieurs du laboratoire avec les mutants des paralogues de RAD51, *xrcc3* et *rad51C*, ont montré un appariement centromérique

homologue à la méiose pouvait s'étendre sur au moins 2 Mb à partir du centromère, mais pas dans les régions péri-centromériques euchromatiques (Da Ines et al., 2012). Ceci a conduit à l'hypothèse que les fibres de ZYP1 courtes observées dans ces noyaux correspondent à la synapse et à l'initiation de la formation du CS dans ces régions. J'ai donc réalisé une immunolocalisation en méiose WT, *rad51* et *xrcc3* pour rechercher une colocalisation des fibres ZYP1 et des régions centromériques. Les résultats de cette étude réfutent cette hypothèse. Comme le montre la figure 19, bien que certaines fibres ZYP1 (protéine du CS) commencent à partir des centromères, le plus souvent elles ne le font pas. Cette conclusion a été confirmée par l'analyse d'images de microscopie SIM, qui ont montré à la fois un appariement complet des centromères avant l'apparition de ZYP1 et la présence de fibres courtes de ZYP1 avec des centromères non appariés ou partiellement appariés. Les données de cette expérience montrent clairement que les courtes fibres ZYP1 ne proviennent pas spécifiquement des centromères et donc que les synapses commencent aléatoirement sur les centromères (Fig_19A) ou ailleurs (Fig_19B), ou que les fibres courtes ZYP1 ne marquent pas les régions de synapses homologues.

CHAPITRE 5 : Création de nouveaux points chauds méiotiques ciblés via CRISPR/Cas pour des études des rôles méiotiques de RAD51 et DMC1.

Enfin, la troisième et dernière partie de mon travail de thèse implique le développement d'outils CRISPR/CAS9 pour créer des points chauds de recombinaison méiotique spécifiques à la cible grâce à l'induction ciblée des ruptures d'ADN. Une telle approche sera essentielle pour explorer les rôles des protéines de recombinaison et les mécanismes de la recombinaison méiotique dans les travaux futurs. Quatre constructions CRISPR différentes ciblant des sites dans les intervalles de CEN3 et I1c FTL sur les chromosomes 1 et 3 respectivement, ont été construites et transformées en plantes. Les constructions ont été conçues pour cliver uniquement les chromosomes *Col-0* et non *Ler-0*, en raison de la présence de SNP dans les sites cibles. Dans un hybride F1 *Col-0/Ler-0*, il y aura toujours un donneur intact (2 chromatides) même dans le cas d'un clivage hautement efficace du chromosome *Col-0*. Bien que le temps limité ait fait que je n'ai pas été assez loin pour tirer des conclusions définitives, la mesure des taux de CO méiotique dans les régions ciblées par ces constructions Cas9/gRNA montre des effets évidents sur les taux de CO dans les différents transformants de Cas9-SNP2 : CEN3 (régulation à la hausse et à la baisse) et seulement des effets mineurs avec les autres constructions (peut-être en raison de leur activité plus faible). Ces données confirment l'intérêt de cette approche, et en particulier, que le ciblage

spécifique de la coupure de l'hybride F1 a clairement eu un effet salvateur de la perte chromosomique induite par CRISPR. Ces analyses préliminaires ouvrent des perspectives intéressantes pour la poursuite des travaux sur la compréhension des mécanismes mis en jeu, et son optimisation pour le contrôle ciblé de la recombinaison méiotique.

List of publication and presentations

- 2017 Article:** Gunjita Singh, Olivier Da Ines, Maria E. Gallego, Charles I. White (2017) "Analysis of the impact of the absence of RAD51 strand exchange activity in Arabidopsis meiosis. PLoS ONE Journal. DOI: 10.1371/journal.pone.0183006.
- 2017 Poster:** "Analysis of the impact of the absence of RAD51 strand exchange activity in Arabidopsis meiosis ". EMBO Meiosis Meeting, Hvar, Croatia. August 27 - September 1, 2017.
- 2016 Poster:** "Meiotic crossing-over in the absence of RAD51 activity", "conference on PLANT GENOME STABILITY AND CHANGE". Shonan Village Center Hayama, Kanagawa, Japan. July 7 - 10, 2016.
- 2016 Talk:** " Meiotic crossing-over in the absence of RAD51 activity", at "The Students and Postdocs Meiosis workshop", organized by CNRS & University Montpellier in Montpellier, France 19-20 September.
- 2015 Poster:** " Meiotic crossing-over in the absence of RAD51 activity ". EMBO Meiosis Meeting, Oxford, United Kingdom.

List of Contents

List of Abbreviations	iv
List of Figures	vi
List of Tables	vii
Chapter 1	1
Introduction	1
1.1 Overview of meiosis	2
1.2 Meiotic stages	5
1.2.1 Interphase	5
1.2.2 Meiosis I: Prophase	7
1.2.3 Leptotene.....	7
1.2.4 Zygotene.....	9
1.2.5 Pachytene	10
1.2.6 Diplotene.....	12
1.2.7 Diakinesis	14
1.2.9 Meiosis II.....	16
1.3 Recombination: Double strand breaks and repair pathways.....	17
1.3.1 Initiation (DSB formation)	21
1.3.2 Resection.....	26
1.3.3 Invasion and strand exchange.....	28
1.3.4 RAD51 and DMC1.....	32
1.3.4.1 RAD51	32
1.3.4.2 DMC1	34
1.3.4.3 RAD51 Vs. DMC1: Biochemical and cytological localization	36
1.3.4.4 RAD51 and DMC1 in meiosis	38
1.3.4.5 Rad51 Paralogues	40
1.3.5 Homologous Recombination Repair Pathways:	42
1.3.5.1 Synthesis dependent strand annealing (SDSA).....	44
1.3.5.2 Double-Holiday junction (dHJ) formation.....	48
1.3.6 Crossover resolution	50
1.3.6.1 Interference-dependent-Class I COs	50
1.3.6.2 Interference-independent-Class II COs.....	55
1.3.7 CO Control	58
1.3.8 CO Interference	58
1.3.9 CO Homeostasis	61
Chapter 2	63
Materials and Methods	63
2.1 Materials	64
2.1.1 Bacterial strains.....	64
2.1.2 Vectors	64
2.1.2.1 pEn-Chimera and pDe-CAS9.....	64
2.1.2.2 pGEM®-T Easy Vector (Promega).....	66
2.1.3 Oligonucleotide primer design.....	67
2.1.4 Bacterial growth media	68
2.1.5 Plant Material	68

2.2 Methods:	71
2.2.1 Cytology.....	71
2.2.1.1 Fixation of Buds	71
2.2.1.2 Cytological slide preparation:.....	71
2.2.1.3 DAPI staining	71
2.2.1.4 Fluorescence <i>in situ</i> hybridisation	72
Slide Preparation	72
Pre-Hybridization washes.....	72
Probe mixture preparation and denaturation.....	72
Probes	73
Slide denaturation and hybridization	73
Post-hybridization washes	73
Probe detection.....	74
2.2.1.5 Immunocytology.....	74
2.2.1.6 Microscopy	75
2.2.1.7 EdU meiotic time-course	76
2.2.1.8 Fluorescent Pollen Counting	76
2.2.2 Molecular Biology	77
2.2.2.1 Plant DNA extractions.....	77
2.2.2.2 Polymerase Chain Reactions (PCR).....	78
2.2.2.2 Agarose Gel electrophoresis for DNA.....	79
2.2.3 Cloning.....	80
2.2.3.1 Colony PCR.....	80
2.2.3.2 Gel extraction of DNA.....	80
2.2.3.3 Ligation of DNA fragments entry vectors.....	80
2.2.3.4 Transformation of competent E. coli by heat-shock	81
2.2.3.5 Agrobacterium Transformation by electoporation.....	81
2.2.3.6 Floral dip: Arabidopsis transformation Protocol.....	81
2.2.3.7 Blue/White screening of recombinants	83
2.2.3.8 Purification of plasmid DNA.....	83
2.2.3.9 Sequencing of plasmid DNA	83
2.2.3.10 DNA digestion with restriction enzymes	84
2.2.3.11 Cas9/gRNA Transgenic line formation gRNA preparation	84
2.2.4 Statistics.....	85
Results and Discussion	86
Aims and Objectives	87
of the Thesis	87
Chapter 3.....	90
Publication: “Analysis of the impact of the absence of RAD51 strand exchange activity in Arabidopsis meiosis”	90
3.1 Introduction	91
3.2 Principal Results	92
3.3 Discussion	93
Article	96
Chapter 4.....	113
Cytogenetics of partial synapsis in the absence of RAD51 and XRCC3	113
4.1 Introduction	114
4.2 Result and Discussion	117
Chapter 5.....	124

Creation of specific targeted meiotic recombination hot-spots through the targeted induction of DNA breaks for the study of the roles of RAD51 and DMC1 in peri-centromeric and chromosome arm regions.....	124
5.1 Introduction	125
5.2 Result and Discussion	129
5.3 Conclusion.....	148
Chapter 6.....	149
General Discussion and Perspectives.....	149
Chapter 7.....	156
References	156

List of Abbreviations

AE	Axial elements
Ab	Antibody
ASY1	Asynaptic 1
At	<i>Arabidopsis thaliana</i>
ATP	Adenosine tri-phosphate
BIO	Biotin
BrdU	Bromo-deoxyuridine
BSA	Bovine serum albumin
CAS9	CRISPR associated protein 9
Cdc	Cell-division-cycle protein
cDNA	Copy DNA
CO	Cross-over
Col-0	<i>Arabidopsis Columbia</i> ecotype
CRISPR	Clustered Regularly Interspaced Short Palindromic Repeats
crRNA	CRISPR RNA
Cy3	Cyanine 3
DAPI	4, 6-diaminido-2-phenylindole
dHJ	Double Holliday junction
DIG	Digoxygenin
D-loop	Displacement loop
DMF	N, N-dimethylformamide
DNA	Deoxyribonucleic acid
dsDNA	Double strand Deoxyribonucleic acid
DSB	Double strand break
DsRed	<i>Discosoma</i> sp. red fluorescent protein
eCFP	Enhanced cyan fluorescent protein
EDTA	Ethylene diamine-tetra-acetic acid
EdU	5-ethynyl-2'-deoxyuridine
EM	Electron microscope
eYFP	Enhanced yellow fluorescent protein
FISH	Fluorescent in situ hybridisation
FITC	Fluorescein isothiocyanate
FTLs	Fluorescent-tagged lines
GFP	Green fluorescent protein
gRNA	Guide RNA
HIS	Histidine
HR	Homologous recombination
IPTG	Isopropylthio- β -D-galactosidase
JM	Joint molecule
kb	Kilobase
kDa	KiloDalton
LB	Luria-Bertani Broth
LE	Lateral elements
Ler-0	<i>Landsberg erecta Arabidopsis thaliana</i> ecotype

Mb	Megabase
MI	First meiotic division
mRNA	Messenger RNA
NCO	Non crossover
NHEJ	Non-homologous end joining
NORs	Nucleolar organizing regions
O/N	Overnight
OD	Optical density
PAM	Protospacer adjacent motif
PBS	Phosphate buffered saline
PBST	PBS with triton
PCR	Polymerase chain reaction
PMC	Pollen mother cell
rDNA	Ribosomal DNA
RNA	Ribonucleic acid
RPA	Replication protein A
RT	Room temperature
SEI	Single-end invasion
SC	Synaptonemal complex
SCC	Sister chromatid cohesion protein
SDSA	Synthesis-dependant strand annealing
SEI	Single-end invasion
SIM	Structured illumination microscopy
siRNA	Small interfering RNA
SNP	Single-nucleotide polymorphism
SSC	Saline-sodium citrate
ssDNA	Single-stranded DNA
TALENs	Transcription activator-like effector nuclease
T-DNA	Transfer DNA
TF	Transverse filament
tracrRNA	Trans-activating crRNA
WT	Wild-type
X-Gal	5-bromo-4-chloro-3-indolyl-beta-D-galactopyranoside
ZFNs	Zinc-finger nuclease

List of Figures

Figure_1: Schematic diagram of mitosis	3
Figure_2: Schematic diagram of meiosis	4
Figure_3: Meiosis in Arabidopsis pollen mother cells	6
Figure_4. Schematic representation of synaptonemal complex (SC) in <i>Arabidopsis thaliana</i> .	11
Figure_5: Schematic diagram of cohesin loss from Anaphase I to Anaphase II.	13
Figure_6: Chiasma	15
Figure_7: Schematic representation of DSB and repair pathway	20
Figure_8: Schematic representation of initial common stages of SSA, SDSA and DSBR pathways.	31
Figure_9: Schematic representation SDSA pathway.	46
Figure_10: Schematic representation of dHJs formation.	48
Figure_11: pEn-Chimera vector	64
Figure_12:pDe-CAS9 vector	64
Figure_13: pGEM-T Easy vector	65
Figure_14: Fluorescent tagged pollen markers.	69
Figure_15: Schematic representation of polymerase chain reaction.	78
Figure_16: Immunolocalization of short stretches of ZYP1 fibres.	117
Figure_17: Immunolocalization of CENH3 marking Centromeres.	119
Figure_18: Graphical representation of ZYP1 fragments counts.	121
Figure_19: Immunolocalization of ZYP1 initiation point.	122
Figure_20: CRISPR/Cas9 Genome Editing.	126
Figure_21: Schematic representation of multiple genomic alterations possibility, following cleavage of targets DNA by Cas9.	126
Figure_22: Schematic presentation of Cas9/gRNA designing.	129
Figure_23: Sanger sequencing data of CEN3_SNP1.	131
Figure_24: Sanger sequencing data of CEN3_SNP2.	131
Figure_25: Sanger sequencing data of I1c_SNP1.	132

Figure_26: Sanger sequencing data of I1c SNP2.	132
Figure_27: Genetic map in CEN3_SNP1 interval.	134
Figure_28: Genetic map in CEN3_SNP2 interval.	137
Figure_29: Different possibility of chromosome loss.	140-141
Figure_30: Genetic map in CEN3_SNP2 (down-regulated)*Ler-0 interval.	143

List of Tables

Table_1: Meiotic recombination in the I1C_SNP1 interval.	144
Table_2: Meiotic recombination in the I1C_SNP2 interval.	144

Chapter 1

Introduction

1.1 Overview of meiosis

The process of eukaryotic sexual reproduction is based on the production of gametes of halved ploidy, the fusion of two of which regenerates the original ploidy in the subsequent generation (Barton and Charlesworth, 1998; Buisson et al., 2013). This halving of chromosome number is carried out by meiosis, a specialised cell division in which two successive divisions follow a single round of DNA replication. A single meiotic cell thus produces four nuclei of halved ploidy. This contrasts to the mitotic cell division, in which DNA replication followed by a single division results in two daughter nuclei of the same ploidy as the mother cell (Fig_1) (Ma, 2006). The specialised meiotic cell division thus solves the problem of maintaining ploidy stable across sexual generations, but this comes with a cost. In mitosis, balanced segregation of chromatids at Anaphase is ensured by sister chromatid cohesion established in the preceding S-phase. Thus ensuring that each daughter cell receives a full complement of chromosomes. This can only be done once after each S-Phase however and is not sufficient in meiosis, in which two successive nuclear divisions follow a single S-phase.

In most studied eukaryotes, proper meiotic chromosomal segregation is ensured by chiasmata, physical links between homologous chromosomes produced by recombination. Recombination during the first meiotic prophase ensures that homologous chromosomes accurately segregate

from each other and in doing so, shuffles the genetic information to generate the genetic variation driving evolution (Fig_2) (Osman et al., 2011).

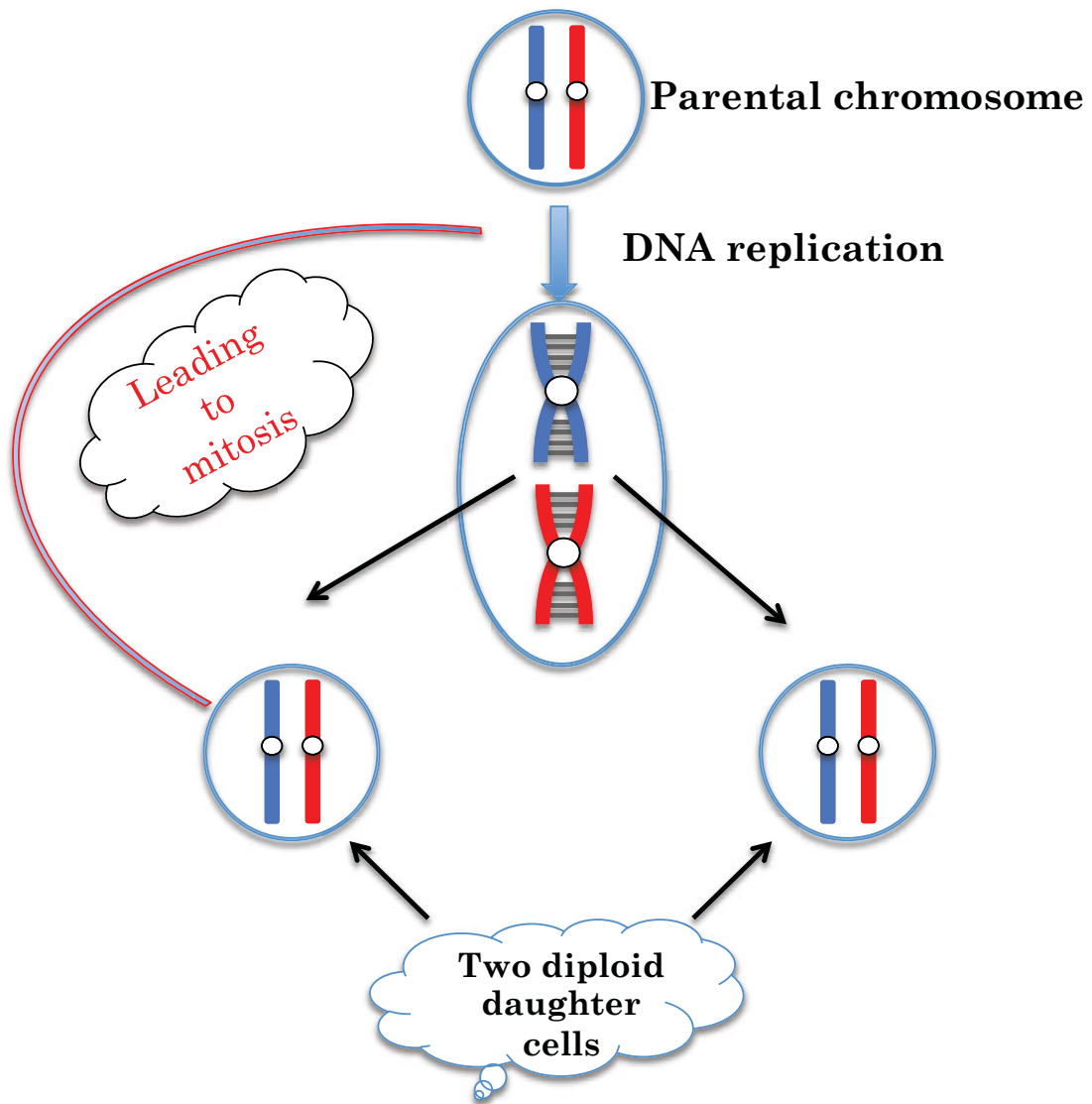


Figure_1: Schematic diagram of mitosis

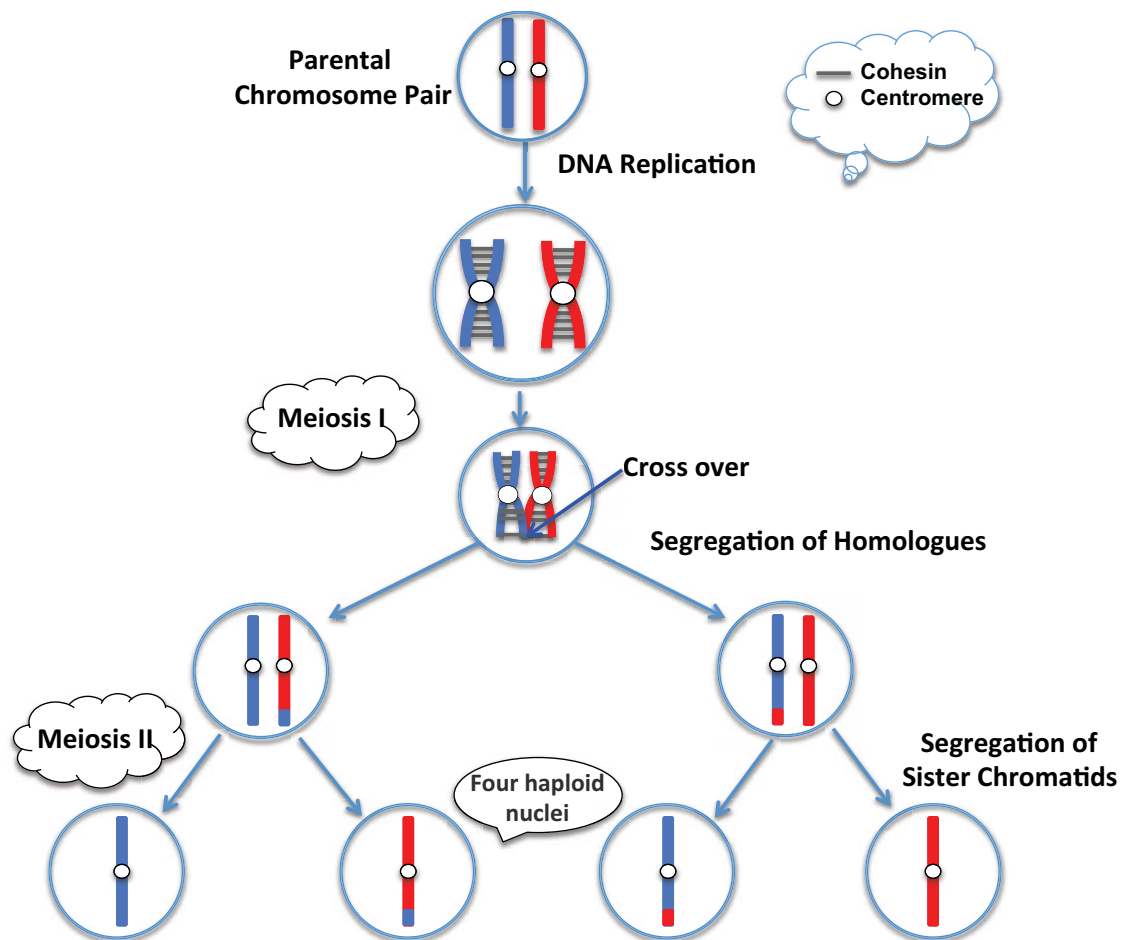


Figure_2: Schematic diagram of meiosis

1.2 Meiotic stages

1.2.1 Interphase

A cell entering into meiosis passes through G1-, S- and G2-phases. In meiotic interphase, G1 cells have a more condensed pericentromeric heterochromatin compared to S and G2 cells. During pre-meiotic S-phase, chromosomes are replicated and each chromosome entering meiosis thus consists of two sister chromatids. Finally, pre-meiotic G2 cells present short stretches of chromosome thread that correspond to the formation of the meiotic chromosome axes as shown by chromosome staining and immunocytochemistry studies using an antibody raised against the axis-associated protein ASY1 (Armstrong and Jones, 2003; Sanchez-Moran et al., 2007).

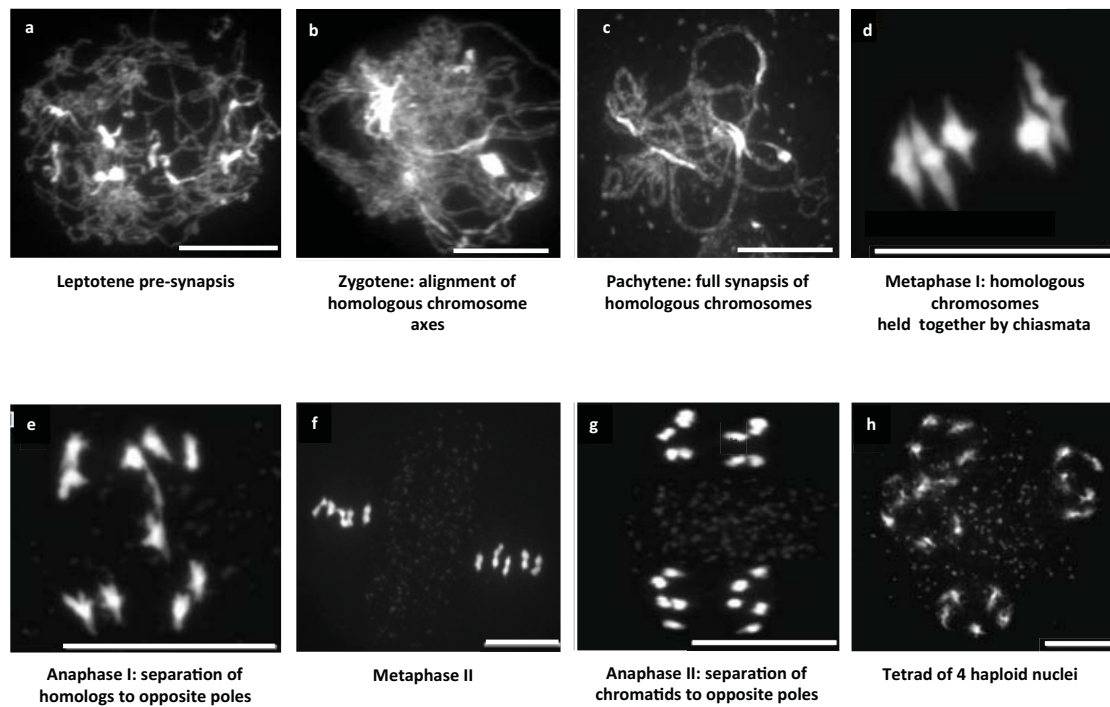


Figure_3: Meiosis in Arabidopsis pollen mother cells

(a) Leptotene, (b) Zygotene, (c) Pachytene, (d) Metaphase I, (e) Anaphase I, (f) Metaphase II, (g) Anaphase II, (h) Tetrad. Nuclei stained with DAPI. Scale bar, 10 μ M.

1.2.2 Meiosis I: Prophase

Meiotic Prophase I consists of five stages: Leptotene, Zygotene, Pachytene, Diplotene, and Diakinesis (Gray and Cohen, 2016; Loidl, 2016; Mercier et al., 2014; Tiang et al., 2012).

1.2.3 Leptotene

Following replication of the chromosomes and the G2 phase, meiotic cells enter Leptotene, the first stage of meiotic Prophase I (Fig_3a). In Leptotene, chromosome condensation results in them becoming visible as fine threads with bead-like chromomeres (Armstrong and Jones, 2003; Zickler and Kleckner, 1999). Chromatin condensation continues, axial element formation begins and, in Arabidopsis, the large nucleolus is found in the centre of the nucleus in early Leptotene. As Leptotene progresses towards zygotene, the nucleolus moves towards the nuclear perimeter where it remains until the end of Prophase I. At this stage, the Arabidopsis centromeres are dispersed in the nucleus, while the telomeres are clustered and associated with the nucleolus, rather than adopting the classical bouquet arrangement found in many eukaryotes (Armstrong et al., 2001).

This clustering in a "bouquet" on the nuclear envelope occurs near the microtubule organizing center (MTOC) in *C. elegans*, the spindle pole body (SPB) in fungi, or the centrosome in animals. The bouquet arrangement and subsequent chromosomal movements during Prophase I are thought

to facilitate alignment of chromosome arms and to play an important role in the initiation of homolog pairing in a number of species (Da Ines and White, 2015; Loidl, 2016). The link between chromosome movement and telomere clustering during meiosis is particularly well characterized in the fission yeast *Schizosaccharomyces pombe*, in which deletion of genes critical for bouquet formation disrupts homolog pairing and recombination (Chikashige et al., 2006; Klutstein et al., 2015).

The bouquet is also found in plants. In Maize bouquet formation is required for homolog pairing. This is not a general rule however, as in *Arabidopsis* the onset of pairing is often observed prior to bouquet formation and is recombination independent (Armstrong et al., 2001; Li et al., 2005; Roberts et al., 2009). In *Arabidopsis thaliana*, rather than a classical bouquet, loose telomere clustering associated with the nucleolus is observed during interphase and early meiosis (Armstrong et al., 2001; Roberts et al., 2009). At the onset of leptotene, telomeres pair, dissociate from the nucleolus, and disperse but remain confined to one hemisphere of the nucleus. As is the case for bouquet formation, this atypical telomere clustering has been suggested to facilitate homolog pairing and appears to be recombination independent (Golubovskaya et al., 2002; Lee et al., 2012; Loidl, 2016; Roberts et al., 2009; Varas et al., 2015; Zickler, 2006).

Centromeres may also contribute to the reorganization of meiotic prophase chromosomes in various ways (Da Ines and White, 2015; Kurdzo and Dawson, 2015). In many organisms, centromere clustering occurs at

the onset of meiosis, for example in *Arabidopsis* centromeres cluster just after telomere clustering (Da Ines et al., 2012; Da Ines et al., 2014). Interactions between centromeric regions during early Prophase I are a common feature of meiotic chromosome behavior, and these can be placed into different classes: Centromere clustering (centromeres associated in groups), centromere coupling (Non-homologous centromere association), and centromere pairing (homologous centromere association) (Da Ines and White, 2015). Such associations have been observed in all studied organisms, including yeast, mammals, *Drosophila*, and plants, and often precede chromosome arm pairing, suggesting a role in the establishment of proper meiotic chromosome synapsis (Da Ines and White, 2015; Loidl, 2016; Subramanian and Hochwagen, 2011; Zhang and Han, 2017).

In *Arabidopsis*, centromeres are unpaired and dispersed during pre-meiotic interphase, clustered at the Lepto-Zygotene stage prior to the chromosome arm pairing, then separated and subsequently associated in pairs at zygotene and Pachytene stage (Zhang and Han, 2017) (more details are in the discussion of Chapter 2).

1.2.4 Zygotene

During Zygotene, chromosome alignments begin and chromosomes are clumped towards one side of the nucleus (Fig_3b). Homologous chromosomes start to synapse and the formation of the synaptonemal complex (SC) initiates, seen as thicker chromosome threads and by immunocytochemistry using an antibody against the SC transverse

filament protein - AtZYP1 in Arabidopsis; (Higgins et al., 2005).

It is believed that SC preferably initiate from DSB sites, as these are the sites of homology recognition and recombination (Mercier et al., 2014; Zickler, 2006), but there are exceptions to this rule. For example in *Drosophila*, SC assembles first in the vicinity of centromere and then at numerous sites along the chromosome arms (Takeo et al., 2011; Tanneti et al., 2011).

1.2.5 Pachytene

Chromosome compaction and formation of SC continues from Zygotene to Pachytene. At the end of the Pachytene stage, the highly compacted homologous chromosomes are fully associated in the SC and the telomeres dispersed (Armstrong and Jones, 2003; Dawe, 1998; Roeder, 1997; Shaw and Moore, 1998) (Fig_3c).

First described almost 60 years ago in salamander meiosis (Moses, 1958), the Synaptonemal Complex (SC) is a multi-protein structure which links synapsed pairs of homologous chromosomes into a single fiber in Pachytene (Cahoon and Hawley, 2016; Zickler and Kleckner, 2015). In the SC the pairs of homologous chromosomes are closely associated in a tripartite structure with two conjoined axes named lateral elements (LE) linked via transverse filaments (TF) (Borner et al., 2004; Page and Hawley, 2004). Transverse filaments overlap in the middle of the central space to form central element (CE) of SC (Heyting, 1996) (Fig_4)

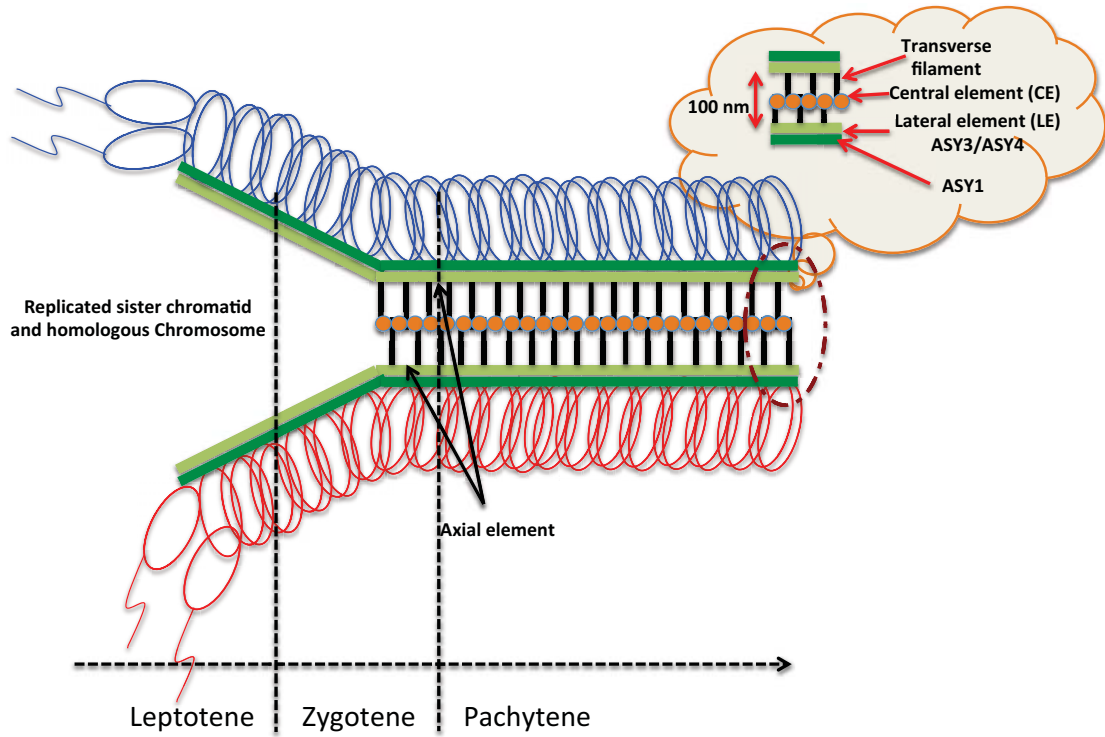


Figure_4. Schematic representation of synaptonemal complex (SC) in *Arabidopsis thaliana*.

1.2.6 Diplotene

The Diplotene stage is marked by the breakdown of the SC and the progressive separation of the homologues along their length from the sites of cross-overs (CO), where the two homologous chromosomes have reciprocally exchanged genetic information. This separation leaves the homologous pairs linked at the sites of the CO and can be cytologically visualised as discrete structural connections, called chiasmata, between the homologous chromosomes (Fig_6).

Together with sister chromatid cohesion, CO physically connect homologous chromosomes until the onset of anaphase I (Fig_5) (Buonomo et al., 2000; Kudo et al., 2006; Lacefield and Murray, 2007; Sanchez Moran et al., 2001). At late diplotene, homologous chromosomes condense to form discrete bivalent structures. The centromeres are unpaired (Armstrong et al., 2001; Da Ines et al., 2012) and each chromosome presents a prominent pericentromeric heterochromatin block.

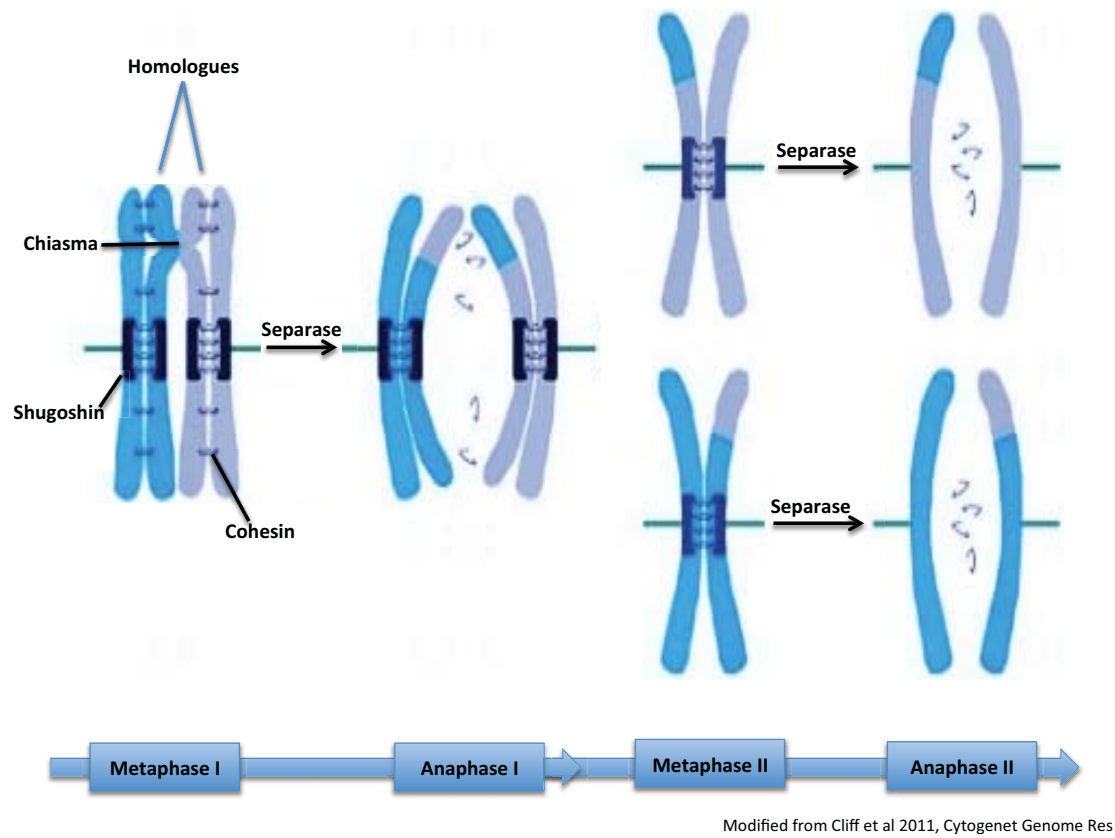


Figure_5: Schematic diagram of cohesin loss from Anaphase I to Anaphase II.

1.2.7 Diakinesis

Diakinesis is the last stage of Prophase I, where the chromosomes become shorter and further condense by a spiralling process (Dawe, 1998).

1.2.8 Metaphase I to telophase I

Cells enter into pro-metaphase with highly condensed chromosomes, the nuclear envelope disrupts, microtubules organize into a spindle and attach to the linked centromeres of sister chromatids at the kinetochore (Dawe, 1998; Kleckner, 1996; Shaw and Moore, 1998). The chromosomes align at the equatorial plate at Metaphase I with the kinetochores co-oriented for the separation of homologues in Anaphase I (Dawe, 1998) (Fig_3d and Fig_5). Separase cleaves the cohesin on chromosome arms at Anaphase I, with the cohesion at centromeres being protected due to the presence of Shugoshin until Anaphase II (Katis et al., 2004; Kitajima et al., 2004; Marston, 2015; Marston et al., 2004). The dissolution of sister chromatid cohesion of chromosome arms in Anaphase I (Fig_3e and Fig_5) (Clift and Marston, 2011; Dawe, 1998; Kleckner, 1996; Shaw and Moore, 1998), permits one chromosome from each pair of homologues to move to each pole of the spindle (Armstrong and Jones, 2003; Dawe, 1998; Kleckner, 1996; Shaw and Moore, 1998). At Telophase I the chromosomes at each pole are partially decondensed (Armstrong and Jones, 2003). There is no DNA replication or interphase and cells enter immediately into the second division of meiosis.

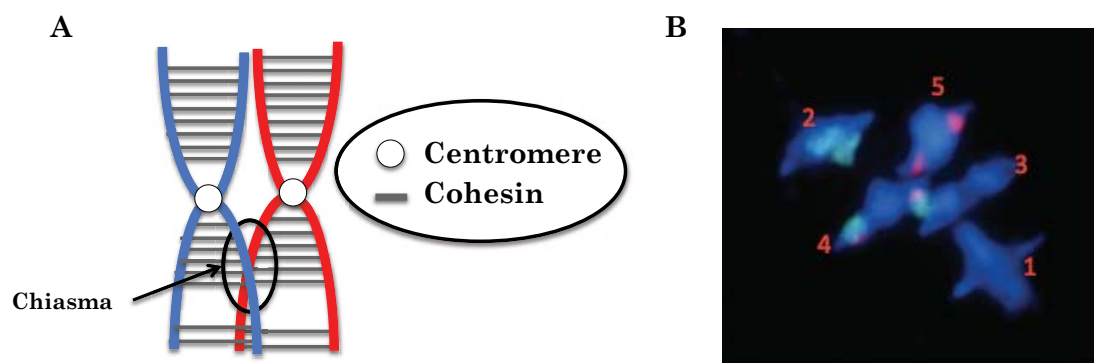


Figure_6: Chiasma. (A) Schematic representation of chiasmata between homologous chromosomes. (B) Cytological image of Arabidopsis chiasmata, The five Arabidopsis chromosomes (numbered) are identified by FISH with a 45S rDNA probe marking chromosomes 2 and 4 in green and a 5S rDNA probe marking chromosomes 3, 4 and 5 in red.

1.2.9 Meiosis II

Meiosis II is the second meiotic division, and in general involves equational segregation, or separation of sister chromatids. Mechanically, the process is similar to mitosis, although its genetic results are fundamentally different.

Meiotic Prophase II leads to disappearance of the two nuclei and thickening of the chromosomes. The microtubule organizing centers (MTOC) begin arranging two spindles perpendicular to that of Meiosis I. The kinetochores of sister chromatids have opposite orientation thus enabling each sister chromatid in a particular pair to attach itself to opposing poles. The chromosomes align at the middle of the spindle at the end of Metaphase II, (fig_3f). In order for sister chromatids to separate in Anaphase II, the protection of centromere cohesion by Shugoshin must be removed. It has been proposed that tension between sister chromatids is required to inactivate Shugoshin in Meiosis II, however the process of cohesin deprotection during Meiosis II is not yet fully understood (Clift and Marston, 2011) review Marston 2015). The loss of centromeric cohesion permits separation of sister chromatids to opposing poles in Anaphase II (fig_3g). Meiosis ends with the four separate groups of sister chromatids and the reformation of the nuclear membranes around each group in Telophase II, resulting in four haploid nuclei (fig_3h). Finally cytoplasmic division results in four haploid gametic cells.

1.3 Recombination: Double strand breaks and repair pathways

The importance of correct DSB-repair to living cells is underlined by the evolution of multiple DSB-repair pathways and their presence in all studied organisms. These pathways are grouped into two general classes on the basis of the implication (homologous recombination or HR), or not (non-homologous end-joining or NHEJ), of sequence homology between the recombining DNA molecules (Mehta and Haber, 2014; Paques and Haber, 1999). Briefly, NHEJ joins broken DNA molecules without the necessity of significant sequence homology between the recombining DNA ends. At its simplest, NHEJ can religate a broken DNA molecule without loss or addition of sequence. It is however frequently associated with the insertion or deletion of nucleotides at the repaired break due to processing of the ends before ligation and/or the involvement of flanking microhomologies. HR also acts to repair DNA breaks, but does so with the use of a homologous template DNA and is thus in general error-free. The mechanisms of HR are described in more detail in the following sections.

HR operates principally in S and G2 phases in mitotic cells, favouring the use of the sister chromatid as template for repair, while NHEJ is particularly important in G1 cells in the absence of sister chromatids (Kakarougkas and Jeggo, 2014; Kim et al., 2005; Lieber, 2010). Elucidation of the factors determining the use of HR or NHEJ to repair a

given DNA break has been the focus of much work in recent years and has led to the understanding that the choice of HR for repair is essentially determined by the presence of a homologous template sequence and by extensive resection of the broken DNA ends (Ceccaldi et al., 2016). Resection is the process of nucleolytic degradation of 5'-ended DNA strands, leaving 3'-OH ended single-stranded DNA overhangs flanking the DSB.

HR during meiotic Prophase I is required for proper chromosome segregation by creating COs between homologous chromosomes. These also shuffle maternal and paternal alleles to generate genetic variation in the gametes. Exceptions to the need for recombination to ensure pairing and synapsis of homologues do exist however, notably in *Drosophila* and *C. elegans* (Dernburg et al., 1998; Gladyshev and Kleckner, 2017). In *C. elegans*, Spo11-independent homologous pairing occurs between specialized regions (pairing centers) near one end of each chromosome, and also between numerous interstitial sites along each chromosome pair (Rog and Dernburg, 2013; Tsai and McKee, 2011). In *Drosophila* meiosis, recombination-independent pairing of homologous chromosomes normally precedes the formation DNA breaks in females (Lake and Hawley, 2012), and fully substitutes recombinational mechanisms in males (McKee et al., 2012).

The mechanisms of meiotic recombination have been established from studies in many organisms and notably in budding yeast. Meiotic

recombination is initiated by the programmed formation of double-strand breaks (DSBs), followed by strand resection, homology search and invasion, which lead to the formation of joint molecule intermediate structures. These are resolved to result in CO or NCO outcomes. It is the CO, which create the chiasmata, which physically link homologous pairs of chromosomes in late meiotic Prophase I and ensure their proper segregation at meiotic Anaphase I (Lambing et al., 2017; Mercier et al., 2014; Smith and Nicolas, 1998) (Fig_7).

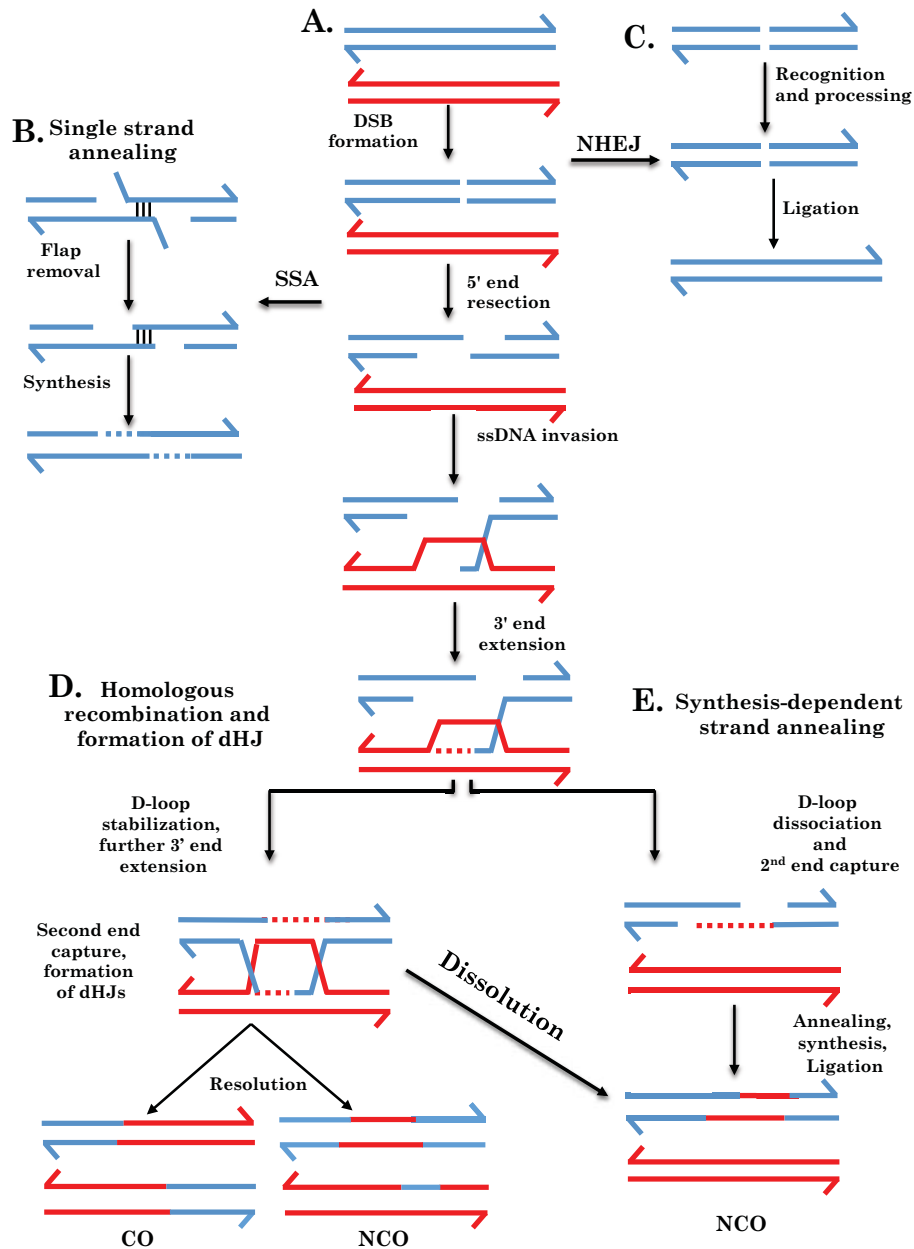


Figure_7: Schematic representation of DSB repair pathways. (A) resection of 5'-ended DNA strands at double-strand breaks produces 3'-ended ss DNA overhangs which can invade a homologous duplex DNA template to produce the single-end invasion (SEI) intermediate structure. DNA synthesis from the invading 3'-end copies the template sequence across the break site. (B) If the break is flanked by direct repeat sequences, the Single-Strand Annealing or SSA pathway can act to repair the break by annealing of the flanking repeat sequences. (C) Alternatively, prior to resection, the DSB can be religated by nonhomologous end joining (NHEJ) (D) Completion of repair of the SEI structure can proceed through formation of the dHJ intermediate and either resolution to produce either CO or NCO outcomes, or dissolution to separate the recombining molecules as a NCO. If the CO occurs between two non-sister chromatids of homologous chromosomes, it will result in the formation of a chiasma physically linking the two chromosomes. (E) repair of the SEI structure through the

synthesis-dependent strand annealing (SDSA) pathway or dissolution of the dHJ structure completes repair with NCO outcomes.

1.3.1 Initiation (DSB formation)

The process of meiotic recombination is initiated by the programmed induction of DSB throughout the genome by the Spo11 protein complex. Resembling the archeal Topo VI topoisomerase, the structure of the eukaryotic SPO11 complex has recently been clarified through the identification of the essential Topo VIB-like partner of SPO11 in *Arabidopsis* (MTOFVIB), mouse (TOP6BL), *S. cerevisiae* (Rec102), *S. pombe* (Rec6) and *D. melanogaster* (MEI-P22) (Bouuaert and Keeney, 2016; Liu et al., 2002; Robert et al., 2016a; Vrielynck et al., 2016). Functioning as a heterodimer or heterotetramer, SPO11 acts through nucleophilic attack on the DNA backbone via its catalytically active tyrosine residues (Grelon et al., 2001; Hartung and Puchta, 2000; Vrielynck et al., 2016). During this process, SPO11 cuts the DNA and remains covalently attached to the 5' ends of DNA via phosphor-tyrosyl linkages, until further processing in the subsequent step of recombination (Bergerat et al., 1997; de Massy, 2013; Keeney et al., 1997).

Three several SPO11 homologues, have been identified in plants, red algae and protists (Grelon et al., 2001; Hartung and Puchta, 2001; Lambing et al., 2017; Malik et al., 2007). Both SPO11-1 and SPO11-2 are essential for meiotic DSB formation (Grelon et al., 2001; Stacey et al., 2006), while SPO11-3 is implicated in somatic endo-reduplication

(Hartung et al., 2007). Mono- and dicotyledonous plants are known to possess more than one SPO11 paralogue in their genome (An et al., 2011; Yu et al., 2010). The presence of two SPO11 isoforms resulting from alternative splicing has been reported in mouse and human (Bellani et al., 2010; Keeney et al., 1999; Romanienko and Camerini-Otero, 1999; Shannon et al., 1999), but SPO11 β alone is able to ensure meiotic DSB production in mouse (Kauppi et al., 2011).

In Arabidopsis, the SPO11 complex thus consists of a heteromeric complex of two A subunits (SPO11-1 and SPO11-2) and the recently identified B subunit (MTOPIVIB) (Grelon et al., 2001; Hartung and Puchta, 2000; Hartung et al., 2007; Lambing et al., 2017; Robert et al., 2016; Shingu et al., 2010; Stacey et al., 2006; Vrielynck et al., 2016).

Budding yeast SPO11 requires a number of accessory proteins to initiate recombination *in vivo*: RAD50, MRE11, XRS2, MER1, MER2, MEI4, MRE2, REC102, REC104, REC114 and SKI8 (Cole et al., 2010; de Massy, 2013; Lam and Keeney, 2014; Paques and Haber, 1999). A network of interactions involving these proteins has been established using the yeast two-hybrid system (Arora et al., 2004; Maleki et al., 2007), showing that Spo11 accessory proteins form three sub-complexes to form a larger pre-DSB complex that binds to the chromatin (Arora et al., 2004; Maleki et al., 2007; Szekvolgyi et al., 2015). These complexes play a major role to selecting the potential DSB regions along the chromosomes, and ultimately contribute to the recruitment of Spo11 and triggering cleavage

(Szekvolgyi et al., 2015).

Sub-complex one: Ski8, Rec102, Rec104 and Spo11 form the first sub-complex. Ski8 has roles in both meiotic and vegetative cells. However, the meiotic role of Ski8 seems to be distinct from its cytoplasmic function in RNA metabolism (Arora et al., 2004). Rec102 and Rec104 behave as a functional unit, and are required for Spo11 nuclear localization, chromatin association, and binding to hot spots (Lam and Keeney, 2014).

Sub-complex two: The second pre-DSB sub-complex is composed of Mei4, Mer2 and Rec114. The function of these three proteins in DSB induction not fully understood but the differential localization of the two pre-DSB sub-complexes suggests that Mei4/Mer2/Rec114 may interact with some components of Spo11/Ski8/Rec102/Rec104 complex and tether the chromatin loop to the chromosome axes to activate Spo11 activity and form meiotic DSBs (Lam and Keeney, 2014).

Sub-complex three: The third group of proteins is the MRX complex (Mre11, Rad50 and Xrs2). These highly conserved proteins are involved in various aspects of DNA metabolism in both vegetative and meiotic cells (Arora et al., 2004; Gobbini et al., 2016), with the animal and plant Xrs2 ortholog known as NBS1 (MRN complex). Mre11 is an endo- and exonuclease (Myler and Finkelstein, 2017; Paull and Gellert, 1998). Rad50 is a member of the structural maintenance of chromosome (SMC) protein family (Anderson et al., 2001; Lee et al., 2013). Linking of the coiled-coil domains of two RAD50 molecules through a hook domain is critical for

MRX/MRN complex function, bridging the two DNA ends of a DSB (Hohl et al., 2011; Hopfner et al., 2002; Mockel et al., 2012; Myler and Finkelstein, 2017; Wiltzius et al., 2005). Xrs2 is a structure-specific DNA-binding protein that also mediates DNA damage checkpoint activation (Lee et al., 2013; Trujillo et al., 2003). NBS1 contains three redundant nuclear localization sequences (NLS) crucial for the nuclear localization of MRN (Desai-Mehta et al., 2001; Tauchi et al., 2002).

Homologues of MRE11, RAD50 and NBS1 (MRN complex) have been characterized in *Arabidopsis thaliana* and shown to play the expected recombination and DNA repair roles, however the complex is not essential for the formation of meiotic DSBs (Bleuyard et al., 2004; Daoudal-Cotterell et al., 2002; Gallego et al., 2001; Puizina et al., 2004; Uanschou et al., 2007).

The proteins PRD1, PRD2 and PRD3, DFO, CRC1 and COMET have been shown to be involved in meiotic DSB formation in plants (De Muyt et al., 2007; Lambing et al., 2017). AtPRD1 is proposed to be the functional homologue of the mammalian DSB protein MEI1, and to interact with AtSPO11-1 to form DSBs (De Muyt et al., 2007; Lambing et al., 2017; Libby et al., 2003). AtPRD2 appears to be an ortholog of budding yeast and mouse MEI4 (De Muyt et al., 2009; Kumar et al., 2010; Lambing et al., 2017). PRD3 is the ortholog of PAIR1 in rice, required for homologous pairing in meiosis (De Muyt et al., 2009; Lam and Keeney, 2014; Nonomura et al., 2004). DFO is important for meiotic DSB formation. *dfo*

mutants exhibit asynapsis, severely reduced recombination rates, and impaired DSB formation as shown by the ability to suppress *mre11* chromosome fragmentation defects (Zhang et al., 2012). CRC1 from *O. sativa* is similar to PCH2 in Arabidopsis and *S. cerevisiae* (Lambing et al., 2017; Miao et al., 2013), possibly promoting DSB formation by linking the DSB complex to the chromosome axis (Osman et al., 2011).

1.3.2 Resection

The term resection refers to the processing of the DSB ends to generate 3'-ended, single-stranded DNA (ssDNA) overhangs, that will subsequently invade the homologous DNA template molecule for repair. During meiosis, the covalent binding of SPO11 to the DSB ends prevents the processing of the DSB ends by exonucleases. Removal of SPO11 from the DSB ends occurs by endonucleolytic cleavage dependent on the MRX/MRN complex, together with Com1/Sae2 in yeast and with CtIP in mammals (Lambing et al., 2017; Mercier et al., 2014; Myler and Finkelstein, 2017; Neale et al., 2005) (Fig_8).

In *S. cerevisiae*, Sae2 promotes endonuclease activity of Mre11 in the MRX complex (Cannavo and Cejka, 2014). Analogously, CtIP (the human functional orthologue of the yeast Sae2/Ctp1), lacks a endonuclease activity and may promote the endonuclease activity of MRE11 (Sartori et al., 2007). In plants, the absence of AtMRE11 or AtCOM1, the functional orthologue of Sae2), leads to extensive fragmentation of chromosomes and the persistence of AtSPO11-1 on the chromatin during meiotic Prophase I (Uanschou et al., 2007). The persistence of AtSPO11-1 bound to DSB in *Atcom1* and *Atmre11* Prophase I likely accounts for the absence of DSB end resection. This suggests that AtMRE11 and AtCOM1 share similar function with their budding yeast orthologues (Ji et al., 2012; Puizina et al., 2004; Uanschou et al., 2007).

The initial resection of the DSB ends forms short single-stranded DNA overhangs. These ends are sensitive to exonuclease activity for further resection. During meiotic homologous recombination, the exonuclease Exo1 is involved in this processing of DSB ends in budding yeast (Zakharyevich et al., 2010). Two recent studies showed that the exonuclease activities of Mre11 and Exo1 contribute to the resection of the DSB ends (Garcia et al., 2011; Zakharyevich et al., 2010). Mre11 processes the DSB ends with a 3' to 5' exonuclease activity, while Exo1 processes the DSB ends with a 5' to 3' exonuclease activity and its absence results in a reduction of the resection tract length (Garcia et al., 2011; Zakharyevich et al., 2010). Although Exo1 processed most DSB ends, some were normally processed in its absence (Zakharyevich et al., 2010). Interestingly, the reduction of the 5'-3' resection tract length did not significantly affect the homology search of the ssDNA tail and the formation of CO (Manfrini et al., 2010; Zakharyevich et al., 2010). In budding yeast mitotic cells, Sgs1 has a helicase activity and can unwind the two strands of a DSB end to facilitate access of the exonucleases Dna2 and Exo1 and formation of long range resection tracts (> 3 kb) (Manfrini et al., 2010).

Two models can explain the release of covalently bound Spo11 at DSB ends and resection. The initial resection of the DSB ends by Mre11/Sae2 could release a short Spo11-oligonucleotide, leaving the free ssDNA ends exposed to the exonuclease activities of Mre11 and Exo1 (Neale et al., 2005). Alternatively, Spo11-oligonucleotides formed after the initial resection by Mre11/Sae2 could remain associated with the complementary

unresected 3' end ssDNA until completion of the processing of the 5' end (Neale et al., 2005). Several studies indicate that the MRX complex in association with Sae2 can tether DNA molecules (Bhaskara et al., 2007; Clerici et al., 2005; de Jager et al., 2001; Kaye et al., 2004; Lobachev et al., 2004) and could have a role in maintaining Spo11-oligonucleotides associated with the complementary ssDNA. However, further analysis is required to elucidate this mechanism.

1.3.3 Invasion and strand exchange

Two RecA-related recombinases, RAD51 and DMC1, are involved in the repair of SPO11-dependent DSBs in most sexually reproducing organisms (Aboussekhra et al., 1992; Bishop et al., 1992; Lambing et al., 2017; Mercier et al., 2014; Shinohara et al., 1992) Following the resection of DSBs and the generation of 3' ended ssDNA overhangs, RAD51 and DMC1 protomers are loaded onto the ssDNA to form a pre-synaptic nucleofilament. Dmc1/Rad51 pre-synaptic nucleofilaments invade the homologous dsDNA template, displacing one strand to form a D-loop and annealing with the complementary strand to form a strand-invasion complex duplex. A subset of these repair events results in physical exchanges or cross-overs (CO) between the interacting DNA molecules and if these are non-sister chromatids, in chiasmata linking the homologous chromosomes and genetic CO. Strikingly, numbers of meiotic DSB commonly exceed numbers of chiasmata, with DSB:CO ratios of 25-30 in *Arabidopsis*, 15 in mouse, 4.4 in *Drosophila* and 1.8 in budding yeast

(Serrentino and Borde, 2012).

Formation of the pre-synaptic nucleofilament involves a number of accessory factors and must deal with the presence of the single-strand binding protein RPA1, which co-localizes with RAD51 during Prophase I in yeast (Gasior et al., 1998), mice (Moens et al., 2007) and humans (Oliver-Bonet et al., 2007). In budding yeast, Rad51 (Cloud et al., 2012), Rad54, Tid1/Rdh54 (Nimonkar et al., 2012), Mei5-Sae3 (Ferrari et al., 2009; Hayase et al., 2004) and Hop2-Mnd1 (Chan et al., 2014) complexes are involved in the formation of Dmc1 pre-synaptic nucleofilaments. HOP2/MND1 is necessary to stabilise the pre-synaptic nucleofilament (Pezza et al., 2007). HOP2/MND1 complex stabilises the dsDNA heteroduplex by acting on the condensation of DNA molecules (Pezza et al., 2010; Pezza et al., 2007; Pezza et al., 2013). Orthologs of Hop2 and Mnd1 have been identified in Arabidopsis. The absence of AtHOP2 or AtMND1 prevented meiotic chromosome pairing between homologs and led to chromosome fragmentation at Metaphase I (Uanschou et al., 2013; Vignard et al., 2007). Two other proteins, AtRFC1 and AtMCM8, are also involved in the early step of homologous recombination (Crismani et al., 2013; Liu et al., 2013; Wang et al., 2012). *Atrfc1* (Liu et al., 2013; Wang et al., 2012) and *Atmcm8* (Crismani et al., 2013) mutant lines presented chromosome fragmentation from Anaphase I onwards. It is proposed that AtRFC1 may be involved in the extension of the invading ssDNA by DNA-synthesis, while the function of AtMCM8 in DSB repair is more elusive (Crismani et al., 2013; Wang et al., 2012). Of the five RAD51 paralogs

(XRCC2, XRCC3, RAD51B, RAD51C, and RAD51D), only XRCC3 and RAD51C are essential for RAD51-dependent meiotic recombination in *Arabidopsis* (Abe et al., 2005; Bleuyard and White, 2004; Li et al., 2005; Mercier et al., 2014), (see RAD51 Paralogs section, below). *Arabidopsis* has five homologs of RPA1 and mutation of one of these causes fertility defects resulting from defective CO formation (Osman et al., 2009). Also, the two BRCA2 orthologs of *Arabidopsis*, AtBRCA2a and AtBRCA2b, interact with AtRAD51 and AtDMC1 and are required for the recruitment of both recombinases on the chromatin (Seeliger et al., 2012; Siaud et al., 2004).

The stoichiometry of both RAD51 and DMC1 recombinases in the nucleofilament is still under debate. The number of meiotic AtDMC1 foci is reduced in the absence of ATRAD51, showing the localisation of AtDMC1 on the chromatin is at least partially dependent on AtRAD51 (Kurzbaueer et al., 2012; Vignard et al., 2007). In yeast and *Arabidopsis*, DMC1 is thus capable of catalysing the repair of all meiotic DSB in the absence of RAD51 strand-exchange activity (Cloud et al., 2012; Da Ines et al., 2013b). In the absence of DMC1, meiotic DSBs are efficiently repaired in a RAD51-dependent manner, resulting however in a complete absence of synapsis and bivalent formation (Couteau et al., 1999; Mercier et al., 2014). However, when DMC1 is present, it represses RAD51 repair activity (Uanschou et al., 2013), reminiscent of the situation in yeast, where a negative regulatory mechanism suppressing RAD51 function during meiosis is known to operate (Lao et al., 2013) (More details below and discussion of Chapter one).

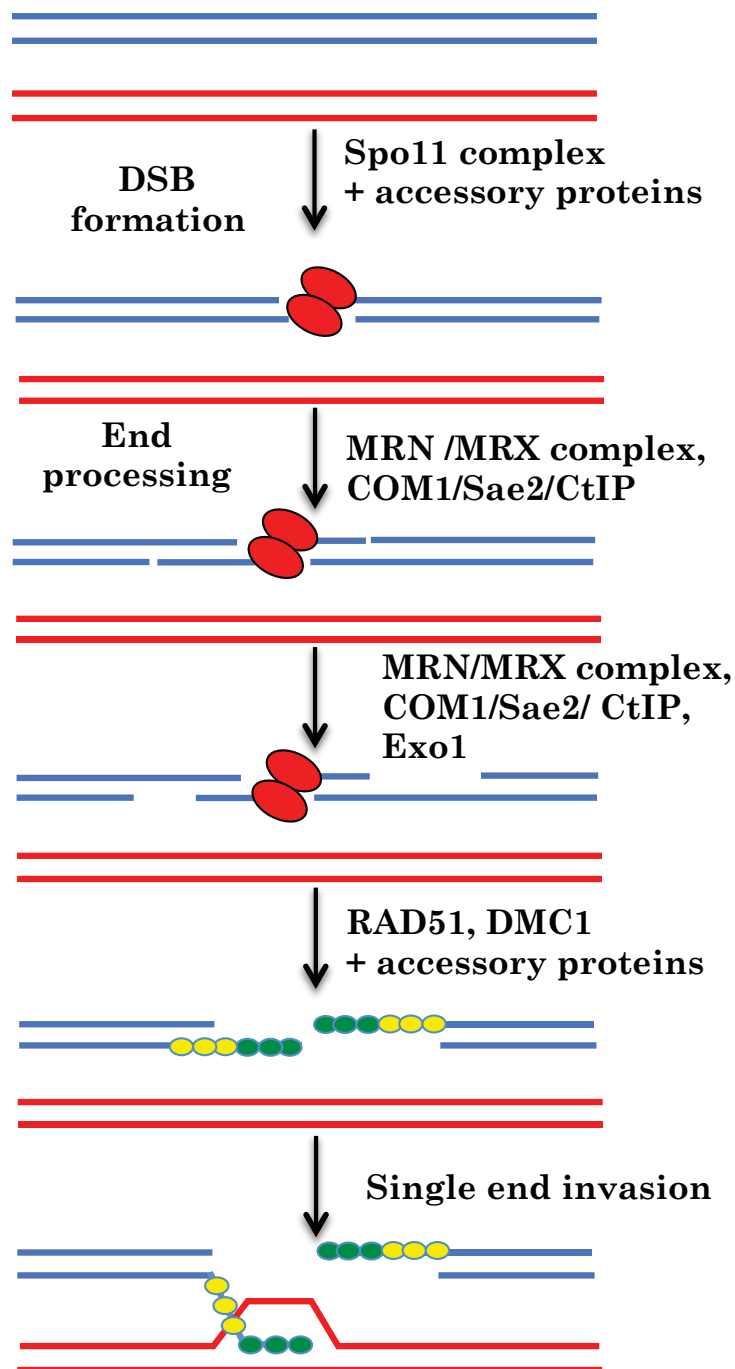


Figure_8: Schematic representation of initial common stages of SDSA and DSBR pathways. The different stages (Initiation, recognition, and invasion) and the protein complexes involved in these pathways are presented here. The broken DNA is shown in blue and the intact DNA molecule in red serving as a template for repair. This can be either a sister chromatid or the homologous chromosome.

1.3.4 RAD51 and DMC1

1.3.4.1 RAD51

In 1974, Game and Mortimer identified RAD51 as well as the other members of the RAD50-57 epistasis group, as being needed for ionizing radiation resistance (Game and Mortimer, 1974). RAD51 is the eukaryotic homolog of the RecA protein from *E. coli*, which catalyses the key strand-invasion step of mitotic and meiotic recombination (Brown and Bishop, 2014; Morriscal, 2015). In each species of eubacteria only one RecA gene is present (Eisen, 1995), in contrast to archeal species such as *Pyrococcus abyssi*, which have two RecA-like genes known as RadA and RadB (DiRuggiero et al., 1999; Komori et al., 2000). A variable number of RecA-like genes are found in eukaryotes. Budding and fission yeast have four RAD51-like genes: RAD51, DMC1, RAD55/rhp55, RAD57/rhp57 (Bishop et al., 1992; Game, 1993; Lovett, 1994; Shinohara et al., 1992), while vertebrates and plants have seven different RAD51-like genes, RAD51, DMC1, RAD51B, RAD51C, RAD51D, XRCC2, and XRCC3 (Hamant et al., 2006; Li and Ma, 2006).

In yeast, *rad51* null mutants exhibit a drastic increase in radiation sensitivity and severe defects in mitotic and meiotic recombination. In meiotic cells, an accumulation of DSBs at recombination hotspots, a reduced formation of recombination intermediates and reduced spore viability were observed (Donovan, Milne et al., 1994, Fasullo, Giallanza et

al., 2001, Rattray & Symington, 1995, Shinohara, Ogawa et al., 1992). The lethality of RAD51 knockouts in mice and humans has complicated study of its role in meiosis (Lim and Hasty, 1996; Tsuzuki et al., 1996), but a recent study has succeeded in testing the effects of RAD51 knockdown in mouse meiosis through injection of siRNA into seminiferous tubules. This produced Leptotene arrest and loss of Zygotene nuclei through p53-dependent apoptosis (Dai et al., 2017). In chicken, DT40 cells depleted of RAD51 show massive chromosome abnormalities and accumulate in the G2/M phase of the cell cycle before dying (Sonoda et al., 1998).

In plants, Maize has two redundant RAD51 genes, RAD51A1 and RAD51A2 (Franklin et al., 1999). *rad51a rad51b* mutant plants are viable with no visible developmental defects, but are male sterile with reduced numbers of chiasmata and evidence of non-homologue synapsis in male meiosis. Residual female fertility however showed apparently normal crossing-over rates in surviving meiocytes (Li et al., 2007). In rice, the *japonica* cultivar has two RAD51 proteins (RAD51A1 and RAD51A2) with *in vitro* data suggesting RAD51A2 has the major role in homologous pairing, while *indica* rice has only one (Morozumi et al., 2013; Rajanikant et al., 2008). Arabidopsis has one RAD51 gene and *rad51* mutants are viable but have severe defects in homologous recombination in both mitosis and meiosis, leading to meiotic Prophase I chromosome fragmentation and fully sterile plants (Li et al., 2004).

RAD51 functions in all three phases of HR: presynapsis, synapsis and post-synapsis (Sung et al., 2003). The presynaptic phase begins with loading of RAD51 onto single-strand DNA to form a RAD51–ssDNA filament, called the presynaptic filament. Forming a heptameric ring in the absence of ATP, RAD51 forms a presynaptic filament on single-stranded DNA in the presence of ATP. This right-handed filament comprises six RAD51 molecules and 18 nucleotides per helical turn with the DNA within the filament is stretched 50% more than the length of B-DNA (Lee et al., 2005; Ogawa et al., 1993). Single-molecule microscopy of RAD51-DNA filaments shows that the filament is elongated in the presence of ATP and that as the ATP is hydrolyzed the filament is compressed (Robertson et al., 2009). This process of stretching is believed to be essential for efficient homology search (Chen et al., 2007; Klapstein et al., 2004).

1.3.4.2 DMC1

DMC1 (Disrupted meiotic cDNA 1) was identified in yeast on the basis of its meiosis-specific expression (Bishop et al., 1992). Known as Lim15 in *Lilium longiflorum* and *Coprinus cinereus* (Hotta et al., 1995; Kobayashi et al., 1994), yeast DMC1 is 45% identical with yeast RAD51 and approximately 26% similar to *E. coli* RecA (Bishop et al., 1992; Shinohara et al., 1992).

DMC1 mutated yeast gets cells arrest in late Prophase of meiosis I, with defects in synaptonemal complex formation, inter-chromosomal

recombination and spindle body formation, resulting in reduction of spore viability. *dmc1* mutant cells arrest in meiotic Prophase due to meiosis specific checkpoints at the end of Prophase I. This is the last checkpoint where cells can return to the mitotic division without further following the meiotic division. They stay arrested at meiotic Prophase for approximately 30h and then return to mitotic pathway (Bishop et al., 1992; Schwacha and Kleckner, 1997). In mice, mutation of DMC1 also causes arrest of gametogenesis in Prophase I and infertility (Pittman et al., 1998). As for RAD51, rice has two redundant DMC1 proteins (DMC1A and DMC1B) and rice DMC1 is required for normal meiotic recombination, proper CO formation and synapsis (Deng and Wang, 2007; Ding et al., 2001; Kathiresan et al., 2002; Wang et al., 2016). Arabidopsis *dmc1* mutants complete meiosis and produce gametes, but have only 3-5% fertility due to the absence of meiotic chiasmata giving apparently random segregation of chromosomes at Anaphase I (Couteau et al., 1999; Mercier et al., 2014).

As for RAD51, DMC1 mediates the DNA strand exchange reaction, which consists of presynaptic filament formation, homology search and strand invasion, and strand displacement. Upon formation of a double strand break, the DNA ends are nucleolytically processed to generate 3' ssDNA tails, which serve as the nucleation site for the DMC1. DMC1 can form stacked rings with ssDNA passed through the centre of the rings (Passy et al., 1999; Sehorn et al., 2004), but the stacked ring form of DMC1 is inactive and the helical nucleoprotein filament is the catalytic form (Bugreev et al., 2005; Passy et al., 1999; Sehorn et al., 2004). The DMC1

nucleofilament catalyses the search for homology and invasion of the homologous template, forming the synaptic complex.

DMC1 is capable of catalysing ATP-dependent DNA strand exchange, with Ca^{2+} ions activating DMC1 and promote DMC1-mediated HR (Sehron (2004)(Bugreev et al., 2005). Similarly, Ca^{2+} has also been shown to promote *S. cerevisiae* DMC1-mediated HR (Lee et al., 2005). Bugreev et al. (2005) showed that Ca^{2+} stimulates DMC1 by promoting formation of long, stable presynaptic filaments and a conformational change in DMC1, and that free Ca^{2+} ion binds to a specific site in DMC1, different from the ATP-Mg $^{2+}$ binding site, which may induce a conformational change in the protein resulting in efficient DNA strand exchange.

1.3.4.3 RAD51 Vs. DMC1: Biochemical and cytological localization

Originally identified in yeast (Aboussekhra et al., 1992; Bishop et al., 1992; Game and Mortimer, 1974; Game et al., 1980; Shinohara et al., 1992), the RAD51 and DMC1 proteins are weak DNA-dependent ATPases with similar biochemical properties. Binding to ssDNA and dsDNA to form nucleoprotein filaments, the former catalyse the search for, and invasion of a homologous DNA template molecule (Baumann et al., 1996; Brown and Bishop, 2014; Hong et al., 2001; Kagawa and Kurumizaka, 2010; Li et al., 1997; Masson and West, 2001; Sheridan et al., 2008; Sung, 1994). The activities of the two proteins are not however identical, as illustrated by the observation of greater resistance to dissociation of D-loops formed by

human DMC1 compared to RAD51 (Bugreev et al., 2011) and the differing substrate requirements for the formation of four-strand joint molecules suggesting opposite polarities of polymerization of RAD51 (3'-5') and DMC1 (5'-3') on ssDNA (Murayama et al. 2011) discussed by (Brown and Bishop, 2014).

RAD51 plays key roles in both meiosis and mitosis, while DMC1 is meiosis-specific (Bishop et al., 1992; Shinohara et al., 1992). In meiosis, RAD51 has been generally believed to act chiefly in inter-sister and non-CO recombination, with DMC1 being important for recombination between non-sister chromatids of homologs. DMC1 can however catalyse inter-sister/non-CO recombination and RAD51 is now believed to serve as a support for DMC1 activity in meiosis, rather than catalysing recombination itself (Cloud et al., 2012; Da Ines et al., 2013b; Hong et al., 2013; Schwacha and Kleckner, 1997).

The precise arrangement of RAD51 and DMC1 filaments in meiotic recombination remains uncertain. *S. cerevisiae* immunolocalization data showed that RAD51 and DMC1 foci colocalise on DSB sites in meiotic recombination (Bishop, 1994). A later publication confirmed that they mark recombination sites and the foci of RAD51 and DMC1 are next to each other, side-by-side (Shinohara et al., 2000). These studies led the research to the hypothesis, arguing that the two DNA ends of a DSB behave differently and that this could be due to loading of RAD51 on one end and DMC1 on the other (Brown and Bishop, 2014; Hong et al., 2013; Hunter and Kleckner, 2001; Kim et al., 2010; Lao et al., 2008; Neale et al.,

2005). In this sense, a publication in *Arabidopsis* showed data supporting RAD51 and DMC1 localisation to different sides of meiotic DSB, and thus an asymmetric loading model. (Kurzbaue et al., 2012). Recent data from yeast and *Arabidopsis* have however provided a major advance in sorting out this puzzle. These studies show that only the presence of RAD51 protein is essential in meiosis, not its strand-exchange activity, and thus DMC1 is the only active strand-invasion enzyme in meiosis (Cloud et al., 2012; Da Ines et al., 2013b). Furthermore, a recent analysis of meiotic Rad51 and Dmc1 foci shows that Rad51-only and Dmc1-only actually are associated with previously undetected Dmc1 or Rad51, respectively (Brown et al., 2015). Taken together, these data lead to the conclusion that both Rad51 and Dmc1 are present on both sides of meiotic DSB, although in varying relative amounts (discussed by (Brown and Bishop, 2014)).

1.3.4.4 RAD51 and DMC1 in meiosis

Present in most eukaryotic organisms, both RAD51 and DMC1 are structural and functional homologs of the bacterial strand-exchange protein RecA, which cooperate during meiotic recombination. RAD51 contributes to both mitotic and meiotic recombination, while DMC1 is meiosis specific to meiosis. The RAD51 and DMC1 genes diverged following a gene duplication that occurred around the time of divergence of the pro- and eukaryotic kingdoms (Ramesh et al., 2005; Stassen et al., 1997). Most organisms that undergo meiosis fall into one of two categories with respect to RAD51 and DMC1. The first category has orthologs of both

RAD51 and DMC1; in these organisms both proteins are involved in meiotic recombination and required for the pairing and synapsis of homologs. The second category of organisms has RAD51, but lacks DMC1. Organisms that possess both RAD51 and DMC1 include budding and fission yeast, plants, and mammals. The group, which only has RAD51, is *Drosophila melanogaster*, *Caenorhabditis elegans*, and the fungus *Sordaria macrospora*. *D. melanogaster* and *C. elegans* are both able to pair and synapse homologs in the absence of recombination (Brown and Bishop, 2014; Dernburg et al., 1998; McKim et al., 1998; Villeneuve and Hillers, 2001). In contrast *S. macrospora* lacks DMC1, but depends on RAD51 for meiotic homolog alignment and synapsis (Brown and Bishop, 2014; Storlazzi et al., 2003).

In HR, resection of 5'-ended DNA strands flanking the DSB generates 3' ssDNA overhangs that are rapidly bound by the single-strand binding protein, Replication Protein A (RPA). Assisted by mediator proteins, RAD51 and DMC1 are loaded onto exposed ssDNA, displacing RPA and forming the helical NPF (Sugiyama and Kowalczykowski, 2002; Yu et al., 2001). Presynaptic filament assembly requires ATP binding but not hydrolysis (Chi et al., 2006). Formation and maintenance of the RAD51-ssDNA NPF is required for the DNA homology search and strand exchange (Baumann et al., 1996). Homology search is by random collision and transient nonspecific interactions with dsDNA (Bianco et al., 1998). Human RAD51 facilitates homology search by a rapid A:T base-flipping mechanism (Gupta et al., 1999). Once a homologous sequence is found,

RAD51 promotes the formation of a physical connection between the invading ssDNA and a homologous duplex DNA template (Baumann et al., 1996). This results in the generation of heteroduplex DNA with D-loop (displacement-loop) structure. Subsequent dissociation of RAD51 from DNA, linked to ATP hydrolysis, permits to expose the invading 3'-OH end (Kowalczykowski, 1991). This extremity is used as a primer for DNA synthesis with the homologous sequence as a template.

1.3.4.5 Rad51 Paralogues

In addition to Dmc1, the yeast *S. cerevisiae* has two RAD51 paralogues, RAD55 and RAD57 (Kans and Mortimer, 1991; Lovett, 1994). These paralogues form a heterodimeric complex, which is able to integrate into the RAD51-DNA nucleofilament (Liu et al., 2011; Sung, 1997). Two structural and functional orthologues of Rad55 and Rad57 have been identified in the fission yeast *Schizosaccharomyces pombe*, Rhp55 and Rhp57, respectively (Khasanov et al., 1999; Tsutsui et al., 2000), RFS-1/RIP-1 heterodimer of RAD51 paralog in *C. elegans* and RAD51C-XRCC3 complex in humans. (Liu et al., 2002b; Masson et al., 2001b; Taylor et al., 2015; Wiese et al., 2002).

Apart from DMC1, in plants and vertebrates there are five RAD51 paralogues, RAD51B (RAD51L1/REC2), RAD51C (RAD51L2), RAD51D (RAD51L3), XRCC2, and XRCC3 (Bleuyard et al., 2005; Kawabata et al., 2005; Osakabe et al., 2002; Shinohara and Ogawa, 1999). In mice, mutation in any of the paralogs, except DMC1, leads to embryonic

lethality (Kuznetsov et al., 2009; Lim and Hasty, 1996; Pittman and Schimenti, 2000; Shu et al., 1999). In contrast, none of the seven RAD51 family proteins is required for vegetative growth in Arabidopsis (Abe et al., 2005; Bleuyard et al., 2005; Bleuyard and White, 2004; Couteau et al., 1999; Li et al., 2004; Li et al., 2005; Su et al., 2017; Wang et al., 2014).

Yeast two-hybrid and co-immunoprecipitation studies have shown two complexes of the five RAD51 paralogues: RAD51C + XRCC3 (CX3), RAD51B + RAD51C + RAD51D +XRCC2 (BCDX2). Two sub-complexes have also been described: RAD51B + RAD51C (BC) and RAD51D+ XRCC2 (DX2) (Liu et al., 2002b; Masson et al., 2001a; Miller et al., 2004; Miller et al., 2002; Osakabe et al., 2005; Osakabe et al., 2002; Schild et al., 2000; Wiese et al., 2002). Both major complexes, CX3 and BCDX2, are involved in mitotic DNA repair and HR, but only CX3 is essential for meiotic HR (Bleuyard et al., 2005; Bleuyard and White, 2004; Li et al., 2005; Osakabe et al., 2005). *rad51c* and *xrcc3* mutants in Arabidopsis are sterile due to chromosome fragmentation during Prophase I of meiosis. (Abe et al., 2005; Bleuyard et al., 2005; Bleuyard and White, 2004; Da Ines et al., 2012; Kuznetsov et al., 2007; Li et al., 2005; Liu et al., 2007; Su et al., 2017) and show a reduction in meiotic RAD51 foci (Su et al., 2017). Meiosis proceeds normally in *rad51b*, *rad51d* and *xrcc2* plants (Bleuyard et al., 2005; Osakabe et al., 2005) and the triple mutant is fertile (Serra et al., 2013; Wang et al., 2014). No reduction in somatic RAD51 foci was reported for irradiated Arabidopsis *xrcc2*, *rad51b* and *rad51d* mutants (Da Ines et al., 2013a) and Arabidopsis *rad51b* and *xrcc2* mutants show mild meiotic

hyper-recombination phenotypes (Da Ines et al., 2013a). Similar results have been published concerning the rice RAD51 paralogs, where *xrcc3* and *rad51c* mutants present sterility and chromosome fragmentation (Tang et al., 2014; Zhang et al., 2015).

1.3.5 Homologous Recombination Repair Pathways:

Strand invasion by Rad51/Dmc1 nucleoprotein filaments forms a stable single-end invasion (SEI) intermediate structure linking the broken and template DNA molecules. Copying the template through DNA synthesis primed by the invading 3'-ended strand can be followed by two events: unwinding of the joint structure (SDSA pathway - see below) or capture of the 3' ended strand of the other side of the break to give a symmetric double Holliday junction (dHJ) intermediate, which is subsequently stabilized and resolved to form CO or NCO (Bishop and Zickler, 2004; Schwacha and Kleckner, 1995).

In general, the number of meiotic DSB exceeds the number of COs (Serrentino and Borde, 2012), meaning the majority of DSB are repaired as NCOs: for example the DSB/CO ratio in Arabidopsis is 25-30 and 15 in mice. Surprisingly, the decision as to which repair pathway a DSB will take, CO or NCO, is made early on in the recombination process, even before stable strand exchange has occurred (Borner et al., 2004; Hunter and Kleckner, 2001; Sanchez-Moran et al., 2007). Although dHJs can theoretically be resolved as either CO or NCO products, most NCOs are

thought to result from the synthesis dependent strand annealing pathway (SDSA), where the process does not proceed as far as the formation of a dHJ (Allers and Lichten, 2001; McMahill et al., 2007).

As CO between sister chromatids are not identifiable genetically, such events would commonly be classed as NCO. During meiosis in budding yeast, HR takes place preferentially using the (non-sister) homologous chromosome, with around 20-30% being repaired using the sister chromatid (Goldfarb and Lichten, 2010; Kim et al., 2010). Relatively little information is however available concerning this in other organisms, as the products of inter-sister recombination are inherently more difficult to detect than inter-homolog recombination due to the genetically identical nature of sister chromatids.

1.3.5.1 Synthesis dependent strand annealing (SDSA)

Following formation of SPO11-dependent DSBs and their subsequent resection, DMC1/RAD51 pre-synaptic nucleofilaments are formed on the 3'-OH ended overhangs flanking the break and invade the homologous template DNA molecule. Annealing between the invading pre-synaptic nucleofilament (receiver) and the complementary strand of the donor forms a dsDNA heteroduplex and a displacement loop (D-loop) structure. The 3' end of the invading chromatid is then extended by DNA-synthesis, which further enlarges the D-loop. The heterologous duplexes are thought to be very unstable and most heterologous duplexes dissociate after a short elongation of the receiver chromatid by DNA-synthesis (McMahill et al., 2007). The authors proposed that invading chromatids could repeat the step of strand invasion/DNA synthesis/dissociation several times before being repaired by the SDSA pathway (Danilowicz et al., 2013; McMahill et al., 2007) (Fig_9).

The SDSA pathway leads only to the formation of NCOs. The presence of nucleotide polymorphisms between the donor chromatid and around the break site on the receiver chromatid results in the transfer of genetic information from the donor chromatid towards the receiver chromatid by DNA synthesis. Dissociation of the invading strand from the donor, annealing of the newly synthesized region of the invading ssDNA with the non-invading complementary ssDNA repairs the broken chromatid. Any transfer of genetic information will thus go from the donor to the receiver

chromatid (gene conversion). Annealing between the newly synthesized region of the invading ssDNA and the undamaged region of the non-invading ssDNA will result in the formation of a dsDNA heteroduplex if a nucleotide polymorphism exists at this locus between the donor and recipient chromosomes. The dsDNA heteroduplex can be recognised by the mismatch repair system which, depending upon which strand is "repaired", can either generate a gene conversion or restore the parental genotype (Berchowitz and Copenhaver, 2010; McMahon et al., 2007). Tetrad analysis in fungi showed that gene conversion of a marker is frequently associated with reciprocal exchange of flanking markers (Fogel and Hurst, 1967; McMahon et al., 2007; Mitchell, 1955). In one publication in *Saccharomyces cerevisiae*, they created a random spore system in which it was possible to identify a subset of NCO recombinants that can readily be accounted for by SDSA, but not by dHJ-mediated recombination. Tetrad analysis using the system provided evidence that SDSA is a major pathway for NCO gene conversion in meiosis (McMahon et al., 2007). Recent advances in DNA sequencing have made the analysis of meiotic NCO more easier (Lu et al., 2012; Wijnker et al., 2013; Yang et al., 2012). Gene conversion associated with NCO result in allelic changes at polymorphic sites without exchange of flanking sequences, they are more difficult to detect. In a recent study in *Arabidopsis*, Yang et al. (2012) crossed two inbred ecotypes, Columbia and *Landsberg erecta*, and analysed 40 F2 plants by sequencing. The authors reported that over 90 % of the recombination events were GC events and that the average GC

track length was 402 base pairs (Yang et al., 2012). However this sequencing data have been re-analyzed by Qi et al. 2014 and have been shown to have a high background due to miscall of genome variants (SNPs and INDEL) (Qi et al., 2014). In a separate study, Sun et al. used a tetrad pollen assay showed a variable locus-to-locus frequency of GC and estimated the average frequency of GC events per locus per meiosis at 3.5×10^{-4} but the author was unable to distinguish between the association of GC with CO or NCO (Sun et al., 2012).

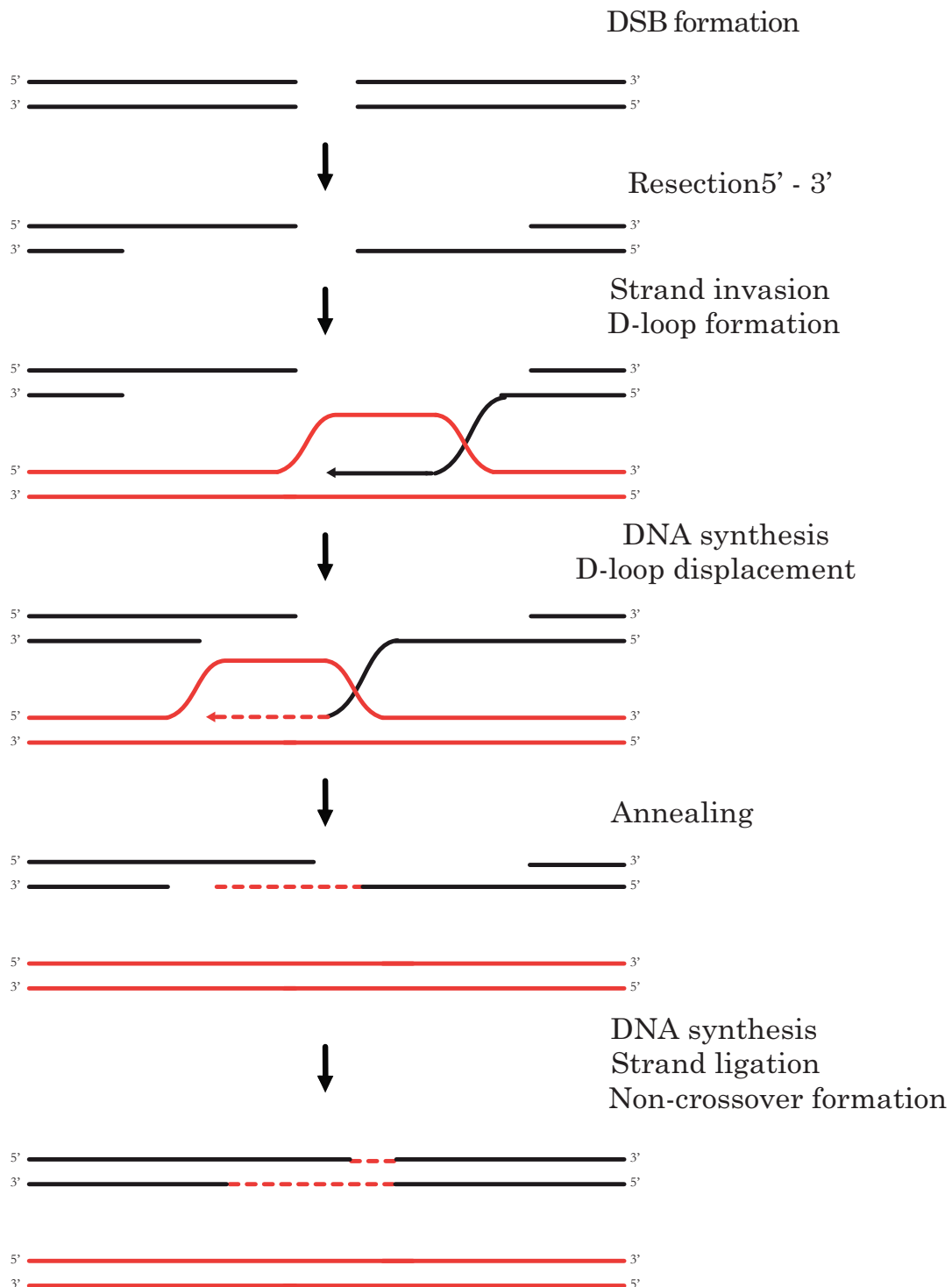


Figure_9: Schematic representation of the SDSA pathway. The broken DNA is shown in black and the intact DNA serving as a template for repair in red. This can be either sister chromatin or the homologous chromosome. The separation of the two molecules occurs via dissolution of the D-loop structure through the action of helicases.

1.3.5.2 Double-Holiday junction (dHJ) formation

Strand-invasion recombination intermediates can also proceed to the CO-producing pathway of DSB repair. Once the invading strand has formed a D-loop in the homologous chromosome, the 3' end of the invading strand is then extended, using the receiving strand as a template. If the structure is not destabilised and resolved via SDSA, the pathway will instead be set on a course which results in the formation of a double Holliday junction (dHJ) (Holliday, 1964). A dHJ is formed following a process called second end capture, where the displaced strand of the D-Loop associates with the resected 3' ssDNA end on the other side of the DSB. A stable dHJ can be resolved either as a crossover or a non-crossover, depending on which strands are cut in the junction (Holliday, 1964). In meiotic recombination however it appears that most dHJs are resolved as COs, and most or all NCOs are thought to be generated by SDSA (Allers and Lichten, 2001; Jessop and Lichten, 2008; Martini et al., 2006) (Fig_10).

Two classes of meiotic COs have been characterised. COs of Class I are sensitive to interference, where the formation of one CO limits the formation of an additional CO in the adjacent chromosomal region. The strength of interference is maximum at the region surrounding the CO site and is proportionally reduced further away. In contrast, COs of Class II are interference-independent and the COs are randomly distributed along the chromosomes (Berchowitz et al., 2007; Higgins et al., 2008a; Hollingsworth and Brill, 2004; Holloway et al., 2008).

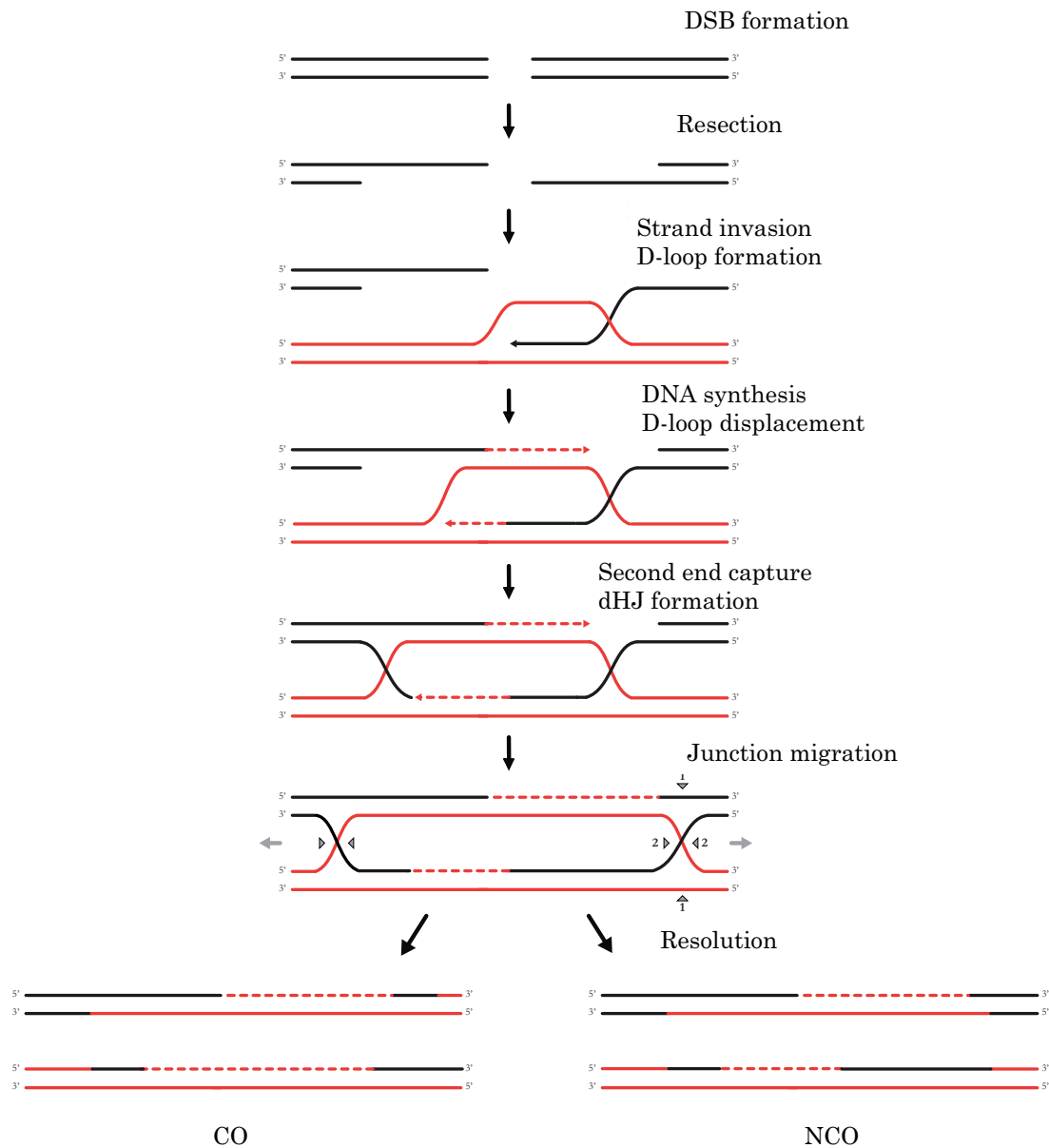


Figure_10: Schematic representation of dHJ formation and resolution. The broken DNA is shown in black and the intact DNA serving as a template for repair in red. The template molecule can be either the sister chromatid or the homologous chromosome. The dHJ joint molecule structure is separated through resolution of the Holliday junctions by endonucleases. Depending on the strands cleaved (gray triangles), this resolution may result in Crossover or Non-Crossover products.

1.3.6 Crossover resolution

1.3.6.1 Interference-dependent-Class I COs

Formation of Class I COs relies on the ZMM group of proteins initially identified in budding yeast: ZIP1, ZIP2, ZIP3, ZIP4, MER3, MSH4, MSH5, SPO16 and PPH3 (Borner et al., 2004; Mercier et al., 2014). These proteins localise on the chromatin. The designation and implementation of a DSB to be repaired towards the formation of a CO are not fully understood. However, it is thought that the ZMM complex implements the decision to repair a CO-designated DSB site towards inter-homologue recombination and CO formation by counter-acting the anti-recombinase activities of helicases (Crismani et al., 2012; Hunter, 2015; Knoll et al., 2012; Mercier et al., 2014). Intermediate joint molecules are sensitive to the anti-recombinase activity of helicases such as Sgs1 (Lorenz et al., 2012) and AtFANCM (Crismani et al., 2012; Knoll et al., 2012), in budding yeast and Arabidopsis, respectively. Anti-recombinases can dissolve dHJ intermediates and prevent inter-homologue recombination and CO formation (Bugreev et al., 2007; Chelysheva et al., 2008; De Muyt et al., 2012; Wu and Burgess, 2006).

MSH4 and MSH5 are homologues of the bacterial MutS protein (MutS Homologue), required for DNA mismatch repair (MMR) in prokaryotes (Fishel, 2015). They play a key role in promoting CO formation and CO interference during meiotic recombination in eukaryotes (Ross-Macdonald

and Roeder, 1994; Zalevsky et al., 1999). In budding yeast, *msh4* and *msh5* mutants show approximately an 85% reduction in CO and the remaining CO are interference insensitive. Similar results have been reported in Arabidopsis where *Atmsh4* and *Atmsh5* mutant revealed severe reduction in fertility due to a decrease in chiasma frequency at Metaphase I (Higgins et al., 2004; Higgins et al., 2008b). *in vitro* biochemical studies using recombinant human hMSH4/5 suggest that MSH4 and MSH5 work as a heterodimer that can bind to Holliday junctions (HJ) and pro-HJs such as D-loops. These observations led to the hypothesis that during meiotic recombination, the MSH4-MSH5 heterodimer encompass two DNA duplexes side by side via a sliding clamp mechanism to convert and stabilize them into dHJs, which are subsequently resolved to COs or NCOs (Snowden et al., 2004). Heterodimers of the MSH proteins thus are thought to stabilize the single end invasion step, while MER3 functions as a DNA helicase, unwinding double stranded DNA and allowing dHJ formation (Mazina et al., 2004; Nakagawa and Kolodner, 2002; Snowden et al., 2004) (Ross-Macdonald and Roeder, 1994).

MSH4/MSH5 homologues are also identified in Arabidopsis (Higgins et al., 2004; Higgins et al., 2008b). Immunolocalization in Arabidopsis shows that MSH4 is present as numerous foci in Leptotene, similar to the number of RAD51 foci, and that the number of foci decreases during zygotene until only a few are left by Pachytene (Higgins et al., 2004). Proper MSH4 localisation is dependent on various upstream meiotic

proteins, including retinoblastoma related protein (RBR) (Chen et al., 2011).

As in yeast, the *Arabidopsis* homologue of MER3 (also known as rock-n-rollers (RCK) is required for Class I crossover formation, with a loss-of-function mutation producing a phenotype similar to that of MSH4, where crossovers are reduced by ~85%, leaving only interference- insensitive COs (Chen et al., 2005; Mercier et al., 2005; Snowden et al., 2004).

In addition to the MutS homologues and Mer3, the Zip proteins (Zip1,2,3 and 4) are also required for crossover formation (Borner et al., 2004). Mutation of these ZMM genes lead to severe reductions in crossover numbers, while the crossovers that do form occur with a Poisson distribution, suggesting that they are not subject to crossover interference (Hollingsworth and Brill, 2004).

Another important protein of ZMM pathway found in plants, mammals and *Sordaria*, is HEI10. HEI10 is member of a family of proteins possessing E3 SUMO/ubiquitin ligase activity: similar to Zip3 in budding yeast, ZHP-3 in *C. elegans* and RNF212 in mammals (in addition to HEI10) (Agarwal and Roeder, 2000; Bhalla et al., 2008; Chelysheva et al., 2012; Reynolds et al., 2013). Zip3 acts as a negative regulator of Zip1 polymerisation in the formation of SC in budding yeast. Synapsis is dependent on earlier inter-homolog interactions in the Wild-Type, but in a *spo11/zip3* background, the SC is still able to assemble without recombination or pairing (Macqueen and Roeder, 2009). This synapsis was

however initiated at centromeric regions, where recombination is unlikely to occur. In mammals, this activity is due to the antagonistic effect which HEI10 has on RNF212, a SUMO-ligase, which also has similarities with Zip3 and is required for stabilisation of the MSH4-MSH5 complex and subsequent CO formation (Qiao et al., 2014; Reynolds et al., 2013). In *Arabidopsis* and rice, the functional orthologue of HEI10 has been characterised. Similarly to mammals, the plant HEI10 is dispensable for SC formation but essential for the formation of MLH1-dependent COs (Chelysheva et al., 2012; Wang et al., 2012a).

The XPF-family endonuclease SHOC1 is another ZMM protein found in *Arabidopsis*. This protein has a human homologue, and shares a distant similarity to the budding yeast ZMM protein Zip2 (Macaisne et al., 2008). Mutation of SHOC1 causes a phenotype typical of ZMM mutations: CO frequency was reduced by 86%, from 9.2 (wild type) to 1.27 CO per meiosis (Macaisne et al., 2008). The *Arabidopsis* PTD protein also has been found to function similarly to ZMM proteins (Wijeratne et al., 2006). *ptd* mutants display a 74% reduction in chiasma frequency from 2.5 from 9.7 per meiosis in wild-type. Further analysis revealed that MSH4-dependent COs were absent in *ptd* meiosis and the residual COs did not display interference and were distributed at random (Wijeratne et al., 2006). The PTD protein displays sequence similarities with ERCC1, which forms a complex with XPF to cleave branched DNA structures (Sancar et al., 2004; Wijeratne et al., 2006). In support of the suggestion that these two proteins work together as a structure-specific endonuclease, PTD has been

shown to interact with SHOC1 in a two-hybrid assay. These observations suggest that SHOC1 and PTD may work as a complex in the formation of MSH4-dependent COs (Macaisne et al., 2008; Macaisne et al., 2011).

The resolvase involved in the resolution of dHJs towards the formation of COs of Class I is unknown. Recently one publication showed that Exo1, Mlh1 and Mlh3 are required for the formation of interference-dependent COs (Zakharyevich et al., 2012). Exo1 and Mlh3 have a nuclease activity (Nishant et al., 2008; Ranjha et al., 2014; Rogacheva et al., 2014). However, Zakharyevich et al. (2012) showed that the nuclease activity of Exo1 was dispensable for the resolution of dHJs (Zakharyevich et al., 2012). Further study is required to understand the role of Exo1, Mlh1 and Mlh3 in the resolution of dHJs.

In Arabidopsis, the spatiotemporal localisation of AtMLH1 and AtMLH3 differs from the spatiotemporal localisation of ZMM proteins. AtMLH1 and AtMLH3 form few foci (around 10 foci) in late pachytene of Arabidopsis PMCs (Ferdous et al., 2012; Jackson et al., 2006). The number of MLH1 foci observed on chromosome spread preparations (Ferdous et al., 2012; Jackson et al., 2006) is consistent with the number of chiasmata observed at Metaphase I of Arabidopsis PMCs (Sanchez-Moran et al., 2002) and the rate of COs per genome identified by genome wide genotyping plants from crosses between Arabidopsis *Columbia* and *Landsberg erecta* ecotypes (Giraut et al., 2011). Jackson et al. (2006) showed that loss of AtMLH3 resulted in the presence of residual COs of

Class I (Jackson et al., 2006). Conversely, in *Atmsh4* (Higgins et al., 2004) or *Atmsh5* (Higgins et al., 2008b) mutant lines, the formation of COs of Class I was abolished. This indicates that additional components of the late recombination nodules account for the resolution of dHJs and formation of CO sensitive to interference, independently of AtMLH3. The significance of the residual level of COs of Class I formed in *Atmlh3* remains to be investigated.

1.3.6.2 Interference-independent-Class II COs

COs of Class II are distributed randomly along the chromosomes and are not sensitive to interference. Recent studies suggest that three proteins with an endonuclease activity, Mus81, Yen1 and Slx1, are involved in the resolution of dHJs and the formation of COs of Class II. It is thought that these nucleases cleave dHJs both symmetrically and asymmetrically (Nishino et al., 2005). Hence, dHJs resolved by these nucleases lead to the formation of COs and NCOs in equal proportions. Zakharyevich et al. (2012) and De Muyt et al. (2012) showed that the joint molecule resolution activities of Mus81-Mms4 and Yen1 are partially redundant in budding yeast (De Muyt et al., 2012; Zakharyevich et al., 2012). In the absence of Mus81 or Mms4, Yen1 and Slx1-Slx4 promote joint molecule resolution, although not as efficiently as Mus81. Matos et al. (2011) reported that the endonuclease activity of Yen1 and Mus81 are differentially regulated by phosphorylation (Matos et al., 2011). Mus81 activity is promoted by Cdc5-mediated phosphorylation of its regulator Mms4 (Gallo-Fernandez et al.,

2012; Matos et al., 2011). In contrast, phosphorylation of Yen1 by an as yet unknown kinase, inhibits its endonuclease activity during Meiosis I (Matos et al., 2011). The authors suggested that Yen1 acts as a safeguard system. In this model, the dephosphorylation of Yen1 at Meiosis II activates its endonuclease activity and joint molecules unresolved by Mus81 during Meiosis I can be processed by Yen1 during Meiosis II (Matos et al., 2011). Oh et al. (2008) showed that Mus81 has an additional role by resolving aberrant joint molecules, such as multi-chromatid joint molecules, in the *sgs1* mutant (Oh et al., 2008).

Plant homologues of Yen1/Gen1 and Mus81 have been identified, exemplified by AtGEN1, AtSEND1 and AtMUS81 (Bauknecht and Kobbe, 2014; Furukawa et al., 2003; Olivier et al., 2016) in Arabidopsis, with AtSEND1 being the functional homolog of Yen1/Gen1 (Bauknecht and Kobbe, 2014; Furukawa et al., 2003; Olivier et al., 2016). Yang et al. (2012) reported that OsGEN-L, a member of the class 4 RAD2/XPG family nucleases in rice, has a 5'-flap endonuclease activity and a HJ resolvase activity. In meiosis, OsGEN1 has indispensable roles in chiasmata formation and DNA lesion repair in rice male gametophytes (Wang et al., 2017). In Arabidopsis, COs of Class II represents 15 % of the total number of COs (Higgins et al., 2004; Higgins et al., 2008a), as seen in the 1.6 chiasmata per meiosis in the *Atmsh4* mutant (Higgins et al., 2004). In the *Atmsh4 Atmus81* double mutant, the mean chiasma frequency is reduced to 0.85 per nucleus compared to 1.25 per nucleus in *atmsh4* single mutant, suggesting that some dHJs are resolved to form COs of Class II

independently of the endonuclease activity of AtMUS81 (Higgins et al., 2008a). A similar observation was reported in budding yeast (De Muyt et al., 2012; Zakharyevich et al., 2012). Investigation of *Atmus81 Atsend1* and *Atmsh4 Atmus81 Atsend1* mutants may reveal additional functions of these nucleases in the resolution of dHJs and the formation of COs during meiosis.

The difference of sensitivity of COs of Classes I and II towards interference is poorly understood, presumably in large part because of the poor understanding of the implementation and spreading of interference along chromosomes. That the resolution of joint molecules towards COs of Class I and II involves different resolvases suggests that different forms of joint molecules may exist with one type being resolved by a complex composed of Exo1-Mlh1-Mlh3-unknown resolvase and hence forming COs of Class I. The other type of joint molecules will be resolved by the Mus81-Mms4-Yen1-Slx1-Slx4 pathway to form COs of Class II. Alternatively, although sensitive to the two types of resolvases, similar joint molecules could be under the control of different factors and resolved to form one of the two classes of COs. In this model, the MUS81 pathway is inactive under wild-type condition (Berchowitz et al., 2007; Higgins et al., 2008a). In contrast, in the absence of factors involved in the inter-homologue recombination pathway and the formation of COs of Class I, the MUS81 pathway becomes active and processes dHJs to form COs of Class II (Ferdous et al., 2012; Franklin et al., 2006; Higgins et al., 2004).

1.3.7 CO Control

COs do not form at random points in the genome and the control over their formation occurs at multiple levels. Various studies have revealed that meiotic COs are tightly regulated in all organisms (Jones, 1984), with the number and distribution of COs ensuring that in a typical wild-type meiosis, every chromosome will produce at least one CO, no matter how small that chromosome might be relative to the others. This is known as the 'obligate CO' and is essential for proper segregation of chromosomes during meiosis (Jones, 1984; Jones and Franklin, 2006; Shinohara et al., 2008).

1.3.8 CO Interference

First identified in *Drosophila* (Sturtevant, 1915), interference between COs is a phenomenon by which formation of a CO reduces the probability of formation of another CO in adjacent region (Jones and Franklin, 2006). This is due to the property of interfering CO-designated sites inhibiting the formation of other interfering COs in a distance-dependent manner, thereby increasing the chance of a second CO occurring further from the initial CO. Tetrad analysis in budding yeast showed approx. 85% of the COs exhibited interference based on their fit to the Chi-squared distribution (Copenhaver et al., 2002) and similar results are seen in *Arabidopsis* (Higgins et al., 2004).

There is some conflicting evidence as to whether or not interference

requires formation of the SC. In *C. elegans*, the SC has been shown to influence interference based on its structure, but also have its structure modified by CO formation (Libuda et al., 2013). In yeast, cytological examination of meiosis has demonstrated that synapsis initiation complexes, based on measuring foci of Zip2 and Zip3, showed interference operating on their distribution even the absence of Zip1, which is required for SC formation (Fung et al., 2004). It has also been demonstrated that interference is established early in the recombination pathway, prior to SC formation (Borner et al., 2004). Together with the finding that the CO/NCO repair pathway decision is made prior to strand exchange, including in *zip1* mutants, we can infer that the SC is not required for interference in yeast. Similarly, Arabidopsis *zyp1* mutants, which cannot form an SC, still produce COs which are subject to interference (Higgins et al., 2005).

There are several models to explain the mechanisms governing interference.

- The first model is the "counting model" (Stahl et al., 2004), which proposes that crossovers are separated by a specific number of non-crossover events, which may define the length of space between any two adjacent COs. This model satisfactorily accounts for CO data from budding yeast (Stahl et al., 2004).
- The second model of interference postulates that interference is imposed by an unknown factor which polymerises out from CO-

designated recombination sites preventing other DSB sites from being processed as COs (King and Mortimer, 1990). The "Polymerization" model fits to CO data of *Drosophila* and budding yeast (King and Mortimer, 1990). This model proposes that the early recombination structures are distributed independently to each other and have an equal opportunity to perform and spread a bi-directional polymerization event. This polymer can inhibit additional early pre-CO structures with the condition that the interference is strongest nearest to the initiated events, which would be subsequently referred to as COs (King and Mortimer, 1990).

- The "mechanical stress" or "beam-film" CO interference model postulates that mechanical stress in the chromosome fiber is required for the production of CO, and that the formation of a crossover somehow relieves this physical tension in its local vicinity on that chromosome, (Kleckner et al., 2004). The term 'beam-film' refers to the analogy of a metal beam coated with a ceramic film. Upon heating, the metal would expand, producing cracks in the ceramic film. Crossover distribution patterns in yeast, flies, grasshopper and tomato agree with this model (Zhang et al., 2014a).
- The fourth model is the "chromosome oscillatory movement" (COM) model which fits CO data from human and mouse (Hulten, 2011). During Prophase I, oscillatory movements would occur along

homologous chromosomes and that chiasma are formed via the proximity of homologous chromosomes at the nodal regions of the waves along the length of chromosome pairs that are created by the oscillatory movements from the telomeres and the kinetochores (Hulten, 2011).

The mechanism, which governs CO interference has been shown to be distinct from CO assurance, as one can be disrupted without affecting the other. CO interference is set up earlier than assurance, and seems to require assembly of Msh4/Msh5 containing interference-sensitive recombination complexes, while CO assurance requires ZMM proteins involved later in the CO pathway and full extension of the synaptonemal complex (Bishop and Zickler, 2004; Shinohara et al., 2008). A whole-genome recombination mapping study in yeast showed that interference does not only act on COs, but also NCOs, providing strong support to the theory that interference is established very early in the recombination pathway, preceding CO/NCO designation (Mancera et al., 2008).

1.3.9 CO Homeostasis

The ratio of numbers of Spo11-induced meiotic DSBs to COs varies considerably among organisms, For example, Arabidopsis has 25-30 DSB/CO, budding yeast has 1.8 DSB/CO and mouse 15 DSB/CO (Serrentino and Borde, 2012). Reducing the number of DSBs does not cause a parallel reduction in the number of COs, instead there is a

tendency for COs to be maintained at the expense of NCOs. This is known as COs homeostasis and is necessary for assuring the formation of at least one CO between each chromosome pair, thus ensuring proper segregation of homologous chromosomes during Meiosis I. This has been demonstrated in yeast using alleles of *spo11* with varying levels of reduced and increased activity (Cole et al., 2012; Henderson and Keeney, 2004; Martini et al., 2006). CO Homeostasis is thought to be linked to interference, as it disappears when interference is absent and displays a stronger or weaker effect as interference increases or decreases (Zhang et al., 2014a).

Chapter 2

Materials and Methods

2.1 Materials

2.1.1 Bacterial strains

- One Shot™ TOP10 Chemically Competent *E. coli*
F- mcrA Δ(mrr-hsdRMS-mcrBC) Φ80lacZΔM15 Δ lacX74 recA1 araD139
Δ(araleu)7697 galU galK rpsL (Str^R) endA1 nupG
- DH5 α.
F- Φ80lacZΔM15 Δ(lacZYA-argF) U169 recA1 endA1 hsdR17(r_k
m_k⁺) phoA supE44 thi-1 gyrA96 relA1 λ⁻
- One Shot™ ccdB Survival™ 2T1R Competent Cells
 (Invitrogen™)
F- mcrA Δ(mrr-hsdRMS-mcrBC) Φ80lacZΔM15 ΔlacX74 recA1 araΔ139
Δ(ara-leu)7697 galU galK rpsL (Str^R) endA1 nupG fhuA::IS2

2.1.2 Vectors

2.1.2.1 pEn-Chimera and pDe-CAS9

These vectors for the expression of Cas9 protein and sgRNA in *Arabidopsis* were obtained from Holger Puchta, KIT, Germany (Fauser et al., 2014). The sgRNA construct for any target site of interest is built in pChimera transferred to pDe-CAS9 via Gateway® cloning (LR reaction) (Fig_11 and Fig_12). The plant codon-optimised Cas9 open reading frame is driven by the Ubiquitin4-2 promoter from *Petroselinum crispum* (parsley) and terminated by the pea3A terminator from *Pisum sativum*

(pea). The principle architecture of the codon-optimised Cas9 was adapted from that published by the group of George M. Church (Mali et al., 2013).

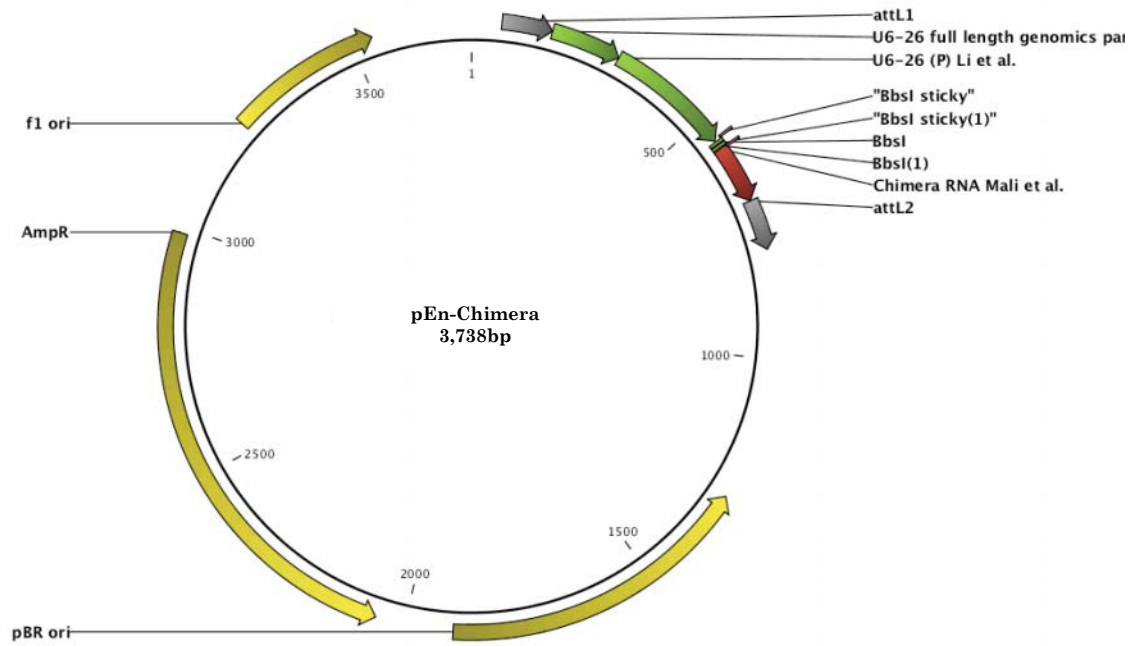


Figure_11: pEn-Chimera vector

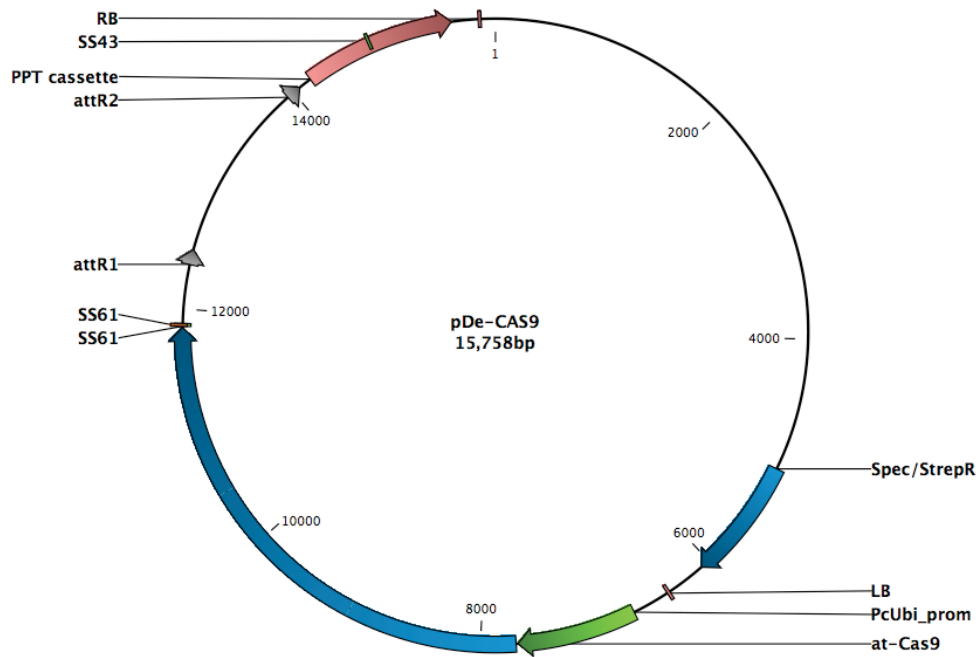


Figure_12:pDe-CAS9 vector

2.1.2.2 pGEM®-T Easy Vector (Promega)

These vectors are linearized vectors from Promega with a single 3'-terminal thymidine at both ends. The T-overhangs at the insertion site greatly improve the efficiency of ligation of PCR products by preventing re-circularization of the vector and providing a compatible overhang for PCR products (Fig_13).

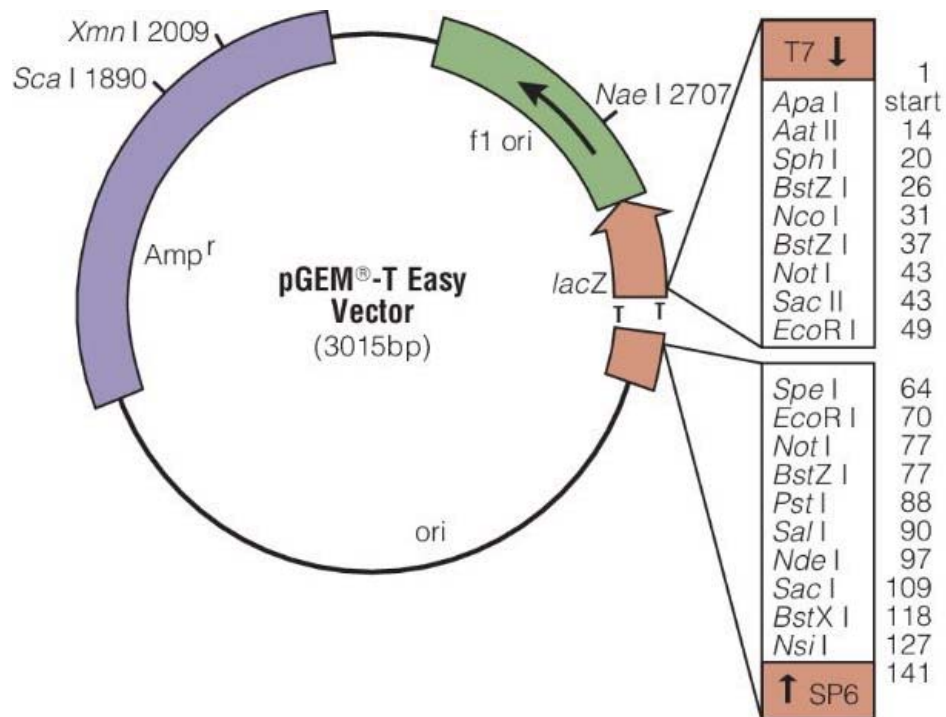


Figure_13: pGEM-T Easy vector

2.1.3 Oligonucleotide primer design

All Oligos were ordered from GATC:

Lab ref	Name	Sequence	T _m (°C)
1521	SS-42 (Genotyping of pde-CAS9 construct) Fauser et al. Plant J 2014	TCCCAGGATTAGAATGATTAGG	46°C
1522	SS-43 (Genotyping of pde-CAS9 construct) Fauser et al. Plant J 2014	CGACTAAGGGTTTCTTATATGC	46°C
1523	SS-61 (Genotyping of pde-CAS9 construct) Fauser et al. Plant J 2014	GAGCTCCAGGCCTCCCAGCTTT CG	59.1 °C
1524	SS-129 (Genotyping of pde-CAS9 construct) Fauser et al. Plant J 2014	CACAGGAAACAGCTATGAC	56°C
1598	gRNA targeting Chr 2 end seq including 1st telom repeat (same as that in pCW747) 'F'	ATTGtaaaatTTTgtatgagtt ta	38.6 °C
1599	gRNA targeting Chr 2 end seq including 1st telom repeat (same as that in pCW747) 'R'	AAACtaaactcatacaaaatTT ta	38.6 °C
1600	gRNA targeting DGU_US ISCE1 site (same as that in pCW745) 'F'	ATTGactattaccctgTTatcc ct	47.2 °C
1601	gRNA targeting DGU_US ISCE1 site (same as that in pCW745)	AAACagggataacagggtaata gt	47.2 °C
1612	For the amplification of pde-CAS9 and add attB sites for gateway cloning. 'F'	ggggACAAGTTTGTACAAAAA GCAGGCTtCATGGATAAGAAGT ACTC	62.9 °C
1613	For the amplification of pde-CAS9 and add attB sites for gateway cloning. 'R'	gggGacCACTTTGTACAAGAAA GCTGGGTcTCAAACCTTCTCT TC	65.7 °C
1643	gRNA to target in-between CEN3 markers. SNP T/A grna for	ATTGGTTCGAGCCTACGATCGAT TA	50.6 °C
1644	gRNA to target in-between CEN3 markers. SNP T/A grna rev	AAACTAATCGATCGTAGGCTCG AC	50.6 °C
1645	gRNA to target in-between CEN3 markers. SNP A/C grna for	ATTGTTTCAAGCTTATGGAATT CG	45.4 °C
1646	gRNA to target in-between CEN3 markers. SNP A/C grna rev	AAACCGAATTCATAAGCTTGA AA	45.4 °C
1726	gRNA to target in-between I1bc markers SNP T/C I1bc gRNA 'F'	ATTGAAAACGCTAGTAAACAAT CA	43.7 °C
1727	gRNA to target in-between I1bc markers SNP T/C I1bc gRNA 'R'	AAACTGATTGTTTACTAGCGTT TT	43.7 °C
1728	gRNA to target in-between I1bc markers SNP C/G I1bc gRNA 'F'	ATTGGAATGTACCCGCGTTTCA AG	50.6 °C
1729	gRNA to target in-between I1bc markers SNP C/G I1bc gRNA 'R'	AAACCTTGAAACGCGGGTACAT TC	50.6 °C
1730	gRNA to target in-between I1bc markers SNP C/A I1bc gRNA 'F'	ATTGCAGGTGCATGGGAAGTAA GA	50.6 °C
1731	gRNA to target in-between I1bc markers SNP C/A I1bc gRNA 'R'	AAACACCCATCTTACTTCCCAT GC	50.6 °C
1732	gRNA to target in-between I1bc markers SNP C/T I1bc gRNA 'F'	ATTGCAGAGATCTTGAGCACAA CT	48.9 °C
1733	gRNA to target in-between I1bc markers SNP C/T I1bc gRNA 'R'	AAACAGTTGTGCTCAAGATCTC AG	48.9 °C

1734	gRNA to target in-between I1bc markers SNP T/G I1bc gRNA 'F'	ATTGGAAAACAATTGGGCTTTG TT	45.4 °C
1735	gRNA to target in-between I1bc markers SNP T/G I1bc gRNA 'R'	AAACAACAAAGCCCAATTGT TC	45.4 °C
1761	Oligos for seq and pcr SNP1 CEN3 interval: 'F'	TATATGGCCACATACAAAAC	54°C
1762	Oligos for seq and pcr SNP1 CEN3 interval:'R'	CAAATTTATGCTTCATTTAG	50°C
763	Oligos for seq and pcr SNP2 CEN3 interval:'F'	CCAGTACGATTACTGCTAAC	58°C
1764	Oligos for seq and PCR of SNP2 CEN3 interval 'R'	AGAGGCGTGCTCTTCTTC	56°C
1790	To amplify SNP1 I1bc (C/G):'F'	TGCTCGTCCTCCTGTAAGTC	62°C
1791	To amplify SNP1 I1bc (C/G):'R'	CAATATGTAGCCGCCGTCC	60°C
1792	To amplify SNP2 I1bc (T/C):'F'	TGCGTTTAGATTTGATTTTC	52°C
1793	To amplify SNP2 I1bc (T/C): 'R'	TCAGGTTTAAGTGGGACG	54°C

2.1.4 Bacterial growth media

All media were sterilized by autoclaving (15 psi, 121°C for 20 minutes). Luria-Bertani Broth (LB) media: 10g/L bacto-tryptone, 5g/L bacto-yeast extract, 10g/L NaCl; plus 15g/L bacto-agar for LB-agar. Incubations for Bacterial cultures were :*E. coli* 37°C overnight or 16h; *A. tumefaciens* 29°C for 48h). Antibiotics for selection were 100µg/ml ampicillin; 50µg/ml kanamycin; 25µg/ml rifampicin.

2.1.5 Plant Material

All plants used in this study are of the Columbia and Landsberg ecotypes (Col-0 and Ler-0) of *Arabidopsis thaliana*. The *rad51* RAD51-GFP plant was built in our lab (Da Ines et al., 2013b) in the Col-0 background. In this line, the meiotic defects and sterility due to the absence of RAD51 protein is complemented by expression of the RAD51-GFP fusion protein (Da Ines

et al., 2013b; Kobayashi et al., 2014). The fluorescent pollen tagged lines (FTL) CEN3 and I1b were kindly provided by Ian Henderson (University of Cambridge, U.K.) (Yelina et al., 2013). The line is tagged with red and yellow and I1bc line is tagged with red, yellow and cyan fluorescent protein fusions expressed in these permit visual scoring of meiotic crossing-over in defined genetic intervals of 10.43 cM between FTL2536 (DsRED):FTL3332 (eYFP) spanning the centromere of Chromosome 3 (CEN3) or 8.16 cM between FTL567 (eYFP) - FTL1262 (DsRed) and 19.2 cM between FTL1262 (DsRed) - FTL992 (CFP) (I1bc) on the left arm of Chromosome 1 (Berchowitz and Copenhaver, 2008; Francis et al., 2007; Yelina et al., 2013) (Fig_14). Homozygous I1b and CEN3 lines were crossed with wild type Col-0 and with homozygous *rad51/rad51* RAD51-GFP/RAD51-GFP plants to obtain heterozygous F1 lines, which were selfed to generate the WT and *rad51* RAD51-GFP F2 homozygotes, heterozygous for the pollen markers in coupling (problems with scoring the CFP fluorescence meant that I was not able to use the I1c interval in the work described in Chapter 3).

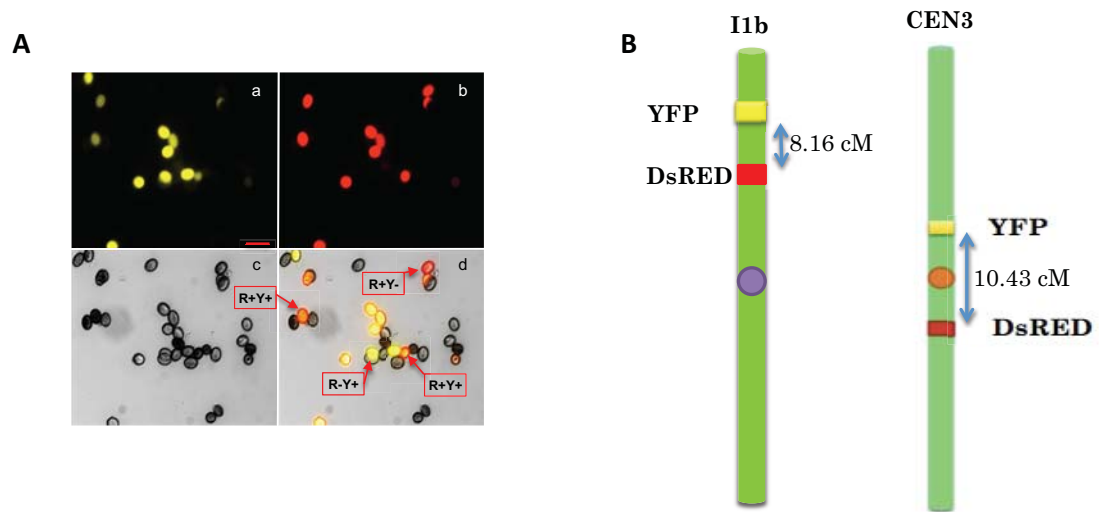


Figure_14: Fluorescent tagged pollen markers. YFP (A.a), RFP (A.b), bright-field (A.c), and merged (A.d) images of pollen from CEN3xCol0 F1 plants carrying the fluorescent markers. Examples of pollen with the different combinations of fluorescence are arrowed (Scale bar is 5 μ m). (B) Schematic representation of the marked genetic intervals: I1bc, 8.16 cM (I1b) and 19.2 cM (I1c) interval on Chromosome 1 marked with Yellow, Red and Cyan FTL; CEN3, 10.43 cM spanning the centromere of Chromosome 3, marked with Red and Yellow FTL. Scale bar 5 μ m.

2.2 Methods:

2.2.1 Cytology

2.2.1.1 Fixation of Buds

Whole inflorescences were fixed in ice-cold ethanol/glacial acetic acid (3:1) and stored at -20°C until further use.

2.2.1.2 Cytological slide preparation:

Immature flower buds of appropriate size were selected under a binocular microscope, rinsed twice at room temperature in distilled water for 5 min followed by two washes in 1× citrate buffer for 5 min. Then incubated for 2h on a slide in 100µl of enzyme mixture (0.3% w/v cellulase, 0.3% w/v pectolyase, 0.3% cytohelicase (Sigma) in a moist chamber at 37°C. Buds were softened for 1 minute in 15 µl 60% acetic acid on a microscope slide at 45°C, fixed with ice-cold ethanol/glacial acetic acid (3:1) and air dried.

2.2.1.3 DAPI staining

Slides were mounted in Vectashield mounting medium with DAPI (Vector Labs, Burlingame, CA, USA) for microscopy. We use approx. 8µl DAPI/slide and then covered the slide with 22×22 mm coverslip, removed the excess of DAPI with tissue paper.

2.2.1.4 Fluorescence *in situ* hybridisation

Slide Preparation

Fluorescence in situ hybridisation (FISH) of Pollen Mother Cell (PMC) meiotic chromosome spreads was carried out following the method of (Sanchez Moran et al., 2001). Chromosome spreads were prepared as described above (Cytological slide preparation section).

Pre-Hybridization washes

The slides were washed in 2xSSC (diluted from 20xSSC; 3M NaCl, 3M tri-sodium citrate, pH 7) in coplin jars for 10 minutes at room temperature followed by digestion with pepsin (0.01mg pepsin in 0.01M HCl, total volume 100 ml) for 90 seconds at 37°C. The pepsin-digested slides were washed in 2xSSC for 10 minutes and fixed with 4% paraformaldehyde for 10 minutes after which briefly rinsed with sterile distilled water twice, 5 minutes each. The slides were then dehydrated with a series of alcohol concentrations of 70%, 90%, 100% respectively for 2 minutes each and then air-dried (30min-1h, RT).

Probe mixture preparation and denaturation

Prepared 20 µl of probe mixture per slide: 14 µl hybridization mix (1g dextran sulphate, 5 ml deionized formamide and 1 ml 20X SSC, dissolve at -20°C) + 0.5-3.0 µl of labeled probe + sterile water up to 20 µl. Denature

the probe by heating at 80°C, 10 min then immediately cool on ice for 5 min.

Probes

5S ribosomal DNA (rDNA) probes: Plasmid pCT4.2 containing the 5S rDNA gene from *A. thaliana* as a 500 bp insert cloned in pGEM-T Easy vector (Campbell et al., 1992).

45S rDNA probe: 8.9kb EcoR1 fragment of wheat 45S rDNA originally cloned in pAC184 then sub cloned into pUC19. Use Nick translation (11745808910:ROCHE) for probe preparation for FISH (Gerlach and Bedbrook, 1979; Molnar et al., 1989).

Slide denaturation and hybridization

Add 20 µl of the probe mixture to meiotic chromosome spreads on a previously prepared slide, cover with a coverslip, heat at 75°C on a hot plate for 4 minutes to denature the probes and incubate for hybridization in a sealed plastic container with damp tissue paper at 37°C O/N.

Post-hybridization washes

After overnight incubation, coverslips were removed and the slides washed at 45°C three times 5 minutes in 50% formamide-2X SSC, then once in 2X SSC at 45°C for 5 minutes, and once in 4T (4X SSC, 0.05% tween20) buffer at 45°C for 5 minutes. A final wash was done in 4T buffer at room temperature for 5 minutes.

Probe detection

The secondary labeling reaction with fluorescent-labeled secondary antibodies (anti-digoxigenin conjugated with FITC or streptavidin (anti-biotin) conjugated with Cy3) (Cy3-Streptavidin PA43001 Amersham GE Healthcare and Anti-digoxigenin-fluorescein Fab fragments Cat No. 11.207741910 Roche) was then carried out to visualize the probes. The secondary antibodies were diluted in Immunolocalization blocking buffer (5ng/ μ l) and used 50 μ l/slide, covered with parafilm and incubated the slide for 1h in dark, humid chamber at 37°C. After 1h removed the parafilm and washed the slides in 4T buffer 3 times, 5 minutes each wash and left them to dry. At the end performed counter-staining with 8 μ l Vectashield mounting medium with DAPI.

2.2.1.5 Immunocytology

Collect the inflorescences on wet tissue paper and separate the buds containing meiotic stages avoiding the bigger ones with pollen. Took 6-8 buds in a 10 μ l of digestion enzyme mix (containing; Cytohelicase 0.1 g, Sucrose 0.375 g, SDW 25 ml, Polyvinyl pyrrollidone (Mw 40,000) 0.25 g) on a slide and dissected them to get the anthers containing meiocytes. Incubate the slide in a humid chamber at 37°C for 5 minutes and then squash the anthers using a brass rod to release the meiocytes. Add another 10 μ l digestion enzyme mix and mix well with needle and incubate at 37°C for 7 minutes. After 7 minutes, add 10 μ l of 1% lipsol and

tap the outer circle of the droplet for 1-2 minutes with the brass rod to generate the bubbles, leave for 5 min at room temperature. Fix using 30 μ l of 4% paraformaldehyde pH 8 and leave the slide to dry under the fume hood at RT for 4h. Dry slides were then washed in PBST (1% PBS buffer, 0.1% Triton) 3 times, 5 minutes each wash. After washing, blocked the slides using EM blocking buffer (1% Bovine Serum Albumin, 1X PBS, 0.1% Triton). Prepared the primary antibody mix in EM blocking buffer using the following dilutions: Anti-ASY1 from Guinea-Pig (1:250 dilution) (Higgins et al., 2004) and Hei10 from Rabbit (1:150 dilution) (Chelysheva et al., 2012). Used 50 μ l of primary antibody/slide, covered the slide with parafilm and incubated in humid chamber at 4°C O/N. Next morning the slides were washed in PBST 3 times, 5 minute each wash. Then after used secondary antibody with desired fluorescence and incubate in humid chamber in dark at RT for 1h. Washed it again 3 times, 5 minutes each with PBST buffer.

Counter-stain the slide with 8 μ l Vectashield mounting medium with DAPI for microscopy.

2.2.1.6 Microscopy

All observations were made with a motorised Zeiss AxioImager Z1 epifluorescence microscope (Carl Zeiss AG, Germany) using a PL Apochromat 100X/1.40 oil objective, an Axio Cam Mrm camera (Carl Zeiss AG, Germany) and appropriate Zeiss filter sets: 25HE (DAPI), filter set 38HE (Alexa 488), 43HE (Alexa 596). Image stacks were deconvoluted

with the deconvolution module (theoretical PSF, iterative algorithm) of Zen imaging software. Collapsed Z-stack projections obtained using the AxioVision Extended-focus module (projection method) for presentation.

2.2.1.7 EdU meiotic time-course

Floral stems (~8 cm) of well grown, 6 week-old (Armstrong, 2012; Stronghill et al., 2014) were cut under running tap water and transferred in 10mM EdU for 2h (Click-IT assay kit Invitrogen, California, USA). The floral tips were then rinsed under running water for 2-3 times and transferred to glass tubes containing tap water and incubated at 23°C, 100-130 $\mu\text{m}^2/\text{s}$ light intensity). Samples were collected at 0h, 12h, 16h, 24h & 36h time points, fixed in ethanol: glacial acetic acid (3:1 ratio) and stored at 4°C. Meiotic chromosome spreads were prepared following the basic cytology slide preparation method of (Fransz et al., 1998; Ross et al., 1996). EdU was detected using an anti EdU Kit (Click-IT assay kit, Invitrogen, California, USA) following the company's manual. At the end, final staining with 8 μl Vectashield mounting medium with DAPI.

2.2.1.8 Fluorescent Pollen Counting

Analysis of meiotic recombination rate in the CEN3 and I1b intervals was carried out with plants carrying the fluorescent pollen markers developed by the Copenhaver and Henderson labs (Berchowitz and Copenhaver, 2008; Francis et al., 2007; Yelina et al., 2013). As described above in the Plant Material section, *rad51* RAD51-GFP and WT F2 plants

heterozygous for the I1b and CEN3 markers in coupling were used for this work.

Seeds were sown in soil, stratified for two days at 4°C and grown in plant growth cabinets (SANYO MLR-351H) under standard long day conditions (16h/day, 23°C, humidity 50-60%) for 4-5 weeks before collecting pollen for analysis. Only flowers from primary stems were used in this study. Opened flowers were collected and tapped on slides into 20 µl droplets of water to release the pollen. The droplets were then covered with 22×22mm coverslips and examined under the fluorescence microscope through DsRed2 and eYFP channels (Zeiss filtersets: DsRed: ; TURBOYFP:). The I1b interval is flanked by a third eCFP marker (FTL992), but this did not provide consistent data in my hands and was not used further in my work (Yelina et al., 2013). Numbers of Red Yellow, Red not-Yellow, Yellow not-Red and non-fluorescent pollen were counted and used to determine genetic map distances between the markers in the WT and *rad51* RAD51-GFP plants. In each case, the 1:1 segregation of the individual markers in the pollen (RED:not-Red and Yellow:not-Yellow) was tested by χ^2 to safeguard against counting artefacts. Pollen lots, which did not pass the χ^2 test, were discarded.

2.2.2 Molecular Biology

2.2.2.1 Plant DNA extractions

1-2 small green leaves of 3 week-old plants were placed in 2ml Eppendorf

tubes containing 300 μ l extraction buffer and one 7 mM diam. stainless steel bead. The Eppendorf tubes were placed in the adapter sets of the tissue lyser machine (TissueLyser II, Qiagen) and the tissue ground for 2 times 30 seconds. The tubes were shaken by hand to ensure thorough mixing, incubated in a water-bath at 65°C for 10 minutes, centrifuged at 10000 rpm for 15-20 minutes and the supernatant transferred to - another tube containing 300 μ l of isopropanol. After mixing well, tubes were incubated at RT for 5 min and centrifuged at 10000 rpm for 20 minutes. Supernatants were decanted and tubes air-dried. Finally, the pellets were dissolved in 100 μ l of ddH₂O.

2.2.2.2 Polymerase Chain Reactions (PCR)

Gene specific primers were used for PCR depending on the type of genotype.

Master Mix	1X reaction (μ l)
DNA	1.5
5X buffer	4
MgCl ₂	1.6
dNTPs 10mM	0.4
Oligo 'F' 10 μ M	1
Oligo 'R' 10 μ M	1
GoTaq	0.1
ddH ₂ O	10.4
Total	20

PCR reactions were done in Biometra thermocycler/T3000 PCR machines. The gene specific primers and specific cycling conditions used depending upon the genes. In general, the standard PCR cycle is 94°C for 5 minutes at the first cycle for preparing denaturation followed by 35 cycles of 94°C for 2 minute, 60°C for 30 second for annealing (generally being around 4°C below the lowest of the primer T_m) and 72°C for 1 minute (depends on the size of the PCR product) DNA extension. Finally, reactions were incubated at 72°C for 5 minutes (PCR cycles can vary as per standardization of protocol).

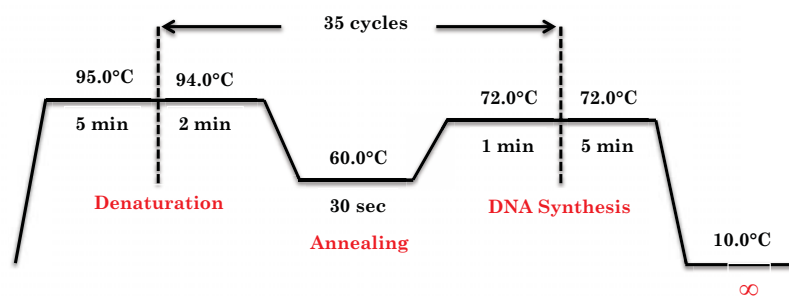


Figure_15: Schematic representation of polymerase chain reaction (PCR).

2.2.2.2 Agarose Gel electrophoresis for DNA

1% agarose gels in 0.5x TBE (5x TBE: 0.45M Tris, 0.45M Orthoboric acid, 12.5 mM EDTA) with 0.5µg/ml ethidiumbromide were poured in Bio-Rad electrophoresis apparatus. The size of PCR products were compared with aliquot of 1kb DNA Ladder (Invitrogen), 50µl DNA Loading Buffer (40% (v/v) glycerol, 0.25% (w/v) bromophenol blue, 0.25% (w/v) xylene cyanol, 135 µl SDW). PCR products were visualized using a Syngene gel imaging

and analysis system.

2.2.3 Cloning

2.2.3.1 Colony PCR

Colonies were tested by colony PCR using the one primer specific to vector and one to insert. Colonies were picked with sterile toothpicks under the Laminar-flow hood and mixed in PCR mix (described in Polymerase chain reaction section).

2.2.3.2 Gel extraction of DNA

DNA bands were visualised and excised from gels under UV light. DNA was extracted using the PCR clean-up & Gel Extraction Kit (Machery-Nagel. Ref. 740609.250)

DNA concentrations were estimated by UV absorbance with a Nanodrop apparatus (Thermo-Fisher Scientific).

2.2.3.3 Ligation of DNA fragments entry vectors

Using insert:vector ratios of 2:1 or 3:1, samples were ligated at 16°C overnight in 10µl ligation mix: 1µl 10x ligation buffer (300mM Tris-HCl pH 7.8 at 25°C, 100mM MgCl₂, 100mM DTT, 10mM ATP) + 0.5µl T4 DNA ligase (Promega) + DNA + ddH₂O to 10µl.

2.2.3.4 Transformation of competent *E. coli* by heat-shock

50 µl competent cells of *E. coli* DH5α stored at -80°C was gently thawed and mixed with 2-4 µl of ligation reaction. The transformation reaction was then incubated on ice for 20-30 minutes, heat shocked at 42°C for 45 seconds, followed by 3-5 minutes on ice. 600µl of LB medium was added and tubes shaken at 37°C, 200 rpm for 1 hour. Transformed cells were spread on 5 mm thick LB-agar plates containing the appropriate selective agent. Plates were then inverted for incubation at 37°C for 16 hours.

2.2.3.5 Agrobacterium Transformation by electroporation

40 µl competent cells of *Agrobacterium tumefaciens* (C58C1) stored at -80°C was gently thawed and mixed with 100 ng of DNA. Following incubation on ice for 30 minutes, they were transferred to electroporation cuvettes and given one 1.8 KV pulse in the *E. coli* Pulser (Bio-RAD). The mix was transferred from the cuvette to a 15 ml falcon tube, 1 ml of LB medium added, mixed gently and shaken at 29°C, 200 rpm for 3h. Cells were spread onto LB-agar plates with the appropriate selective antibiotics. Plates were then inverted for incubation at 29°C for 48h.

2.2.3.6 Floral dip: Arabidopsis transformation Protocol

This Arabidopsis floral dip protocol was used to transform plants (modified from Bechtold et al., 1993; Clough and Bent, 1998).

Grow healthy *Arabidopsis* plants until they are flowering under 16 hour light/8 hour short days. First bolts were clipped to encourage proliferation of secondary bolts. Plants will be ready roughly 4-6 days after clipping. Optimal plants have many immature flower clusters and not many fertilized siliques.

Prepare *Agrobacterium tumefaciens* strain carrying the gene of interest on a binary vector. Grow a liquid culture @ 28°C first O/N primary culture in LB with antibiotics to select for the binary plasmid, and then next day secondary culture for 4-6 hour. Check the OD600 = >1, spin down *Agrobacterium* cells, resuspend to OD600 = 0.8 in 5% Sucrose solution (if made fresh, no need to autoclave), 100-200 ml of suspension will be required for each two or three small pots to be dipped, or 400-500 ml for each two or three 3.5" (9cm) pots. Before dipping, add Silwet L-77 to a concentration of 0.05% (500 µl/L) and mix well. Dip above-ground parts of plant in *Agrobacterium* solution for 2 to 3 seconds.

Place dipped plants under a dome or cover for 16 to 24 hours to maintain high humidity (plants can be laid on their side if necessary). Do not expose to excessive sunlight (air under dome can get hot). Water and grow plants normally, tying up loose bolts with tape. Stop watering as seeds become mature.

Harvest dry seed. Transformants are usually all independent, but are guaranteed to be independent if they come off of separate plants.

Select for transformants using antibiotic or herbicide selectable marker.

2.2.3.7 Blue/White screening of recombinants

pGEM-Teasy vector is a high-copy-number plasmid containing T7 and SP6 RNA polymerase promoters flanking a multiple cloning region within the coding region of the α -peptide of the enzyme β galactosidase. Insertional inactivation of the α -peptide allows identification of recombinants by blue/white screening on indicator plates. LB agar for blue/white screening of colonies with plasmids containing inserts included 10 μ l X-Gal solution (20mg/ml in DMF) + 10 μ l IPTG (100mM) per ml. + the desired antibiotic.

2.2.3.8 Purification of plasmid DNA

Plasmid DNA purification (Macherey-Nagel. Ref.) was used for plasmid DNA purification from bacterial cultures following the manufacturer's guidelines.

2.2.3.9 Sequencing of plasmid DNA

Plasmid DNA sequencing was performed by the GATC Biotech, (Germany). CLC main workbench software was used to analyze the DNA sequencing data and BLAST (www.ncbi.nlm.nih.gov . NCBI, Bethesda, USA) used for homology searches.

2.2.3.10 DNA digestion with restriction enzymes

Restriction enzymes were obtained from New England Biolabs (NEB) or Promega. Digestions were performed in appropriate buffers supplied with the enzymes. The length of digestion for plasmid DNA was between 1h-16h at 37°C; for plant genomic DNA was 16 hours at 37°C.

2.2.3.11 Cas9/gRNA Transgenic line formation gRNA preparation

I designed my 20 nt protospacer sequence from each specific target site (Oligo forward: 5'ATTG+ protospacer; Oligo 'R': 5'AAAC+ rev-com protospacer) following the protocol from (Fauser et al., 2014).

Oligo-Annealing

2 µl of each oligo 'F' and 'R' (100 mM) + 46 µl of ddH₂O to make the total volume of 50µl. Denature at 95°C (In thermocycler), and incubate at RT for 20 min.

Vector digestion using BbsI restriction enzyme and ligation format.

Digestion of pEN-Chimera (see vector section) using *BbsI* restriction enzyme and purified digested DNA with it using purification kit (Machery-Nagel).

Once the digestion was done and purified, I set up the ligation reaction using T4 DNA ligase (Digestion and ligation protocol are described above).

After O/N ligation reaction, transformed 5 μ l of this ligation mix in DH5 α *E. coli* and checked the positive colony by colony PCR (Methods in detail described in colony PCR and *E. coli* transformation section).

Gateway Cloning

Gateway reaction using pDe-Cas9 (containing gateway site - see vector section) and pEN-Chimera.

2 μ l	Entry vector (pEn-Chimera)
3 μ l	pDe-Cas9
4 μ l	TE buffer; pH 8
1 μ l	LR clonase II
10 μ l	Total

Incubate at 25°C O/N or 2h at RT

1 μ l of Proteinase K, and incubate at 37°C for 10 min to stop the reaction.



E. coli transformation, plating and colony PCR (to confirm the +ve clone). Agrobacterium and plant transformation were performed as described in previous sections.

2.2.4 Statistics

GraphPad Prism software was used for all statistical calculations.

Results and Discussion

*Aims and Objectives
of the Thesis*

Meiotic recombination is a highly regulated process that faithfully repairs programmed DSBs, ensuring accurate synapsis and reductional chromosome segregation at Meiosis I. Following pre-meiotic DNA replication, the SPO11 complex introduces DSBs across the genome. These DSBs are nucleolytically resected, revealing 3'-ended single strand DNA (ssDNA) tracts upon which loading of RAD51 and DMC1 forms a helical nucleofilament. The nucleofilament is the active species in the search to locate an intact, homologous double strand DNA (dsDNA) repair template. The ssDNA nucleofilament then invades the intact dsDNA duplex creating a displacement-loop structure. The invading 3' end serves as a primer for restorative DNA synthesis using the donor as template, facilitating the completion of the DNA repair process.

During meiosis, the eukaryotic RecA homologs Rad51 and Dmc1 cooperate to promote homology search and strand exchange, the central step in homologous recombination. Like RecA, RAD51 and DMC1 form nucleoprotein filaments on ssDNA and catalyze strand exchange *in vitro*. RAD51 is responsible for catalyzing strand exchange *in vivo* in both mitotic and meiotic cells, while DMC1 is meiosis-specific. Recent work has shown that the meiosis-specific protein DMC1 is the meiotic strand-exchange recombinase with RAD51 playing an essential, but non-catalytic role promoting DMC1 nucleofilament assembly and function.

Previous studies in *Arabidopsis* have shown that *RAD51* and its paralogs *RAD51C* and *XRCC3* are required for meiotic DSB repair and plant

fertility and mutation of individual genes cause SPO11-dependent meiotic chromosome fragmentation. Surprisingly, partial, incomplete homolog synapsis is seen in *rad51* and *xrcc3* (and presumably *rad51c*) mutant meiosis. This is both SPO11- and DMC1-dependent and involves pericentromeres, showing that DMC1 is able to (at least partially) drive synapsis in pericentromeres in the absence of RAD51. These observations are the basis for the work I have undertaken for my thesis: “Role of recombination protein in CO formation, pairing and synapsis in *Arabidopsis* meiosis”. My experimental work on this subject is divided into three parts as follows:

- Analysis of the impact of the absence of RAD51 strand exchange activity in *Arabidopsis* meiosis.
- Cytogenetics of partial synapsis in the absence of RAD51 or XRCC3.
- Creation of novel targeted meiotic hot-spots via CRISPR/Cas for studies of the roles of RAD51 and DMC1 in meiotic crossing-over in the context of centromeric chromatin structure.

Chapter 3

Publication: “Analysis of the impact of the absence of RAD51 strand exchange activity in Arabidopsis meiosis”

**Gunjita Singh, Olivier Da Ines,
Maria Eugenia Gallego, Charles I. White***

PLoS ONE (2017)- 8(12): e0183006

3.1 Introduction

Recombination establishes the chiasmata that physically link pairs of homologous chromosomes in meiosis. These chiasmata ensure balanced segregation of homologous chromosomes at the first meiotic division and generate genetic variation in the production of gametes. The visible manifestation of genetic crossing-overs, chiasmata are the result of an intricate and tightly regulated process involving induction of DNA double-strand breaks and their repair through invasion of a homologous template DNA duplex, catalysed by RAD51 and DMC1 in most eukaryotes. Recombination can give rise to both crossover (CO) and non-crossover (NCO) outcomes and the meiosis-specific recombinase DMC1 has been thought to be of particular importance in the production of inter-homolog CO. Recent results however suggest strongly that that DMC1 is the only active recombinase in wild-type meiosis and thus must be responsible for both CO and NCO outcomes. Through testing the roles of RAD51 and DMC1, in this publication we confirm and extend this conclusion. Given that repair of more than 95% of meiotic DSBs in Arabidopsis does not result in inter-homologue CO, Arabidopsis is a particularly sensitive model for testing the relative importance of the two proteins—even minor effects on the non-crossover event population should produce detectable effects on crossing-over. Although the presence of RAD51 protein provides essential support for the action of DMC1, our results show no significant effect of the absence of RAD51 strand-exchange activity on meiotic

crossing-over rates or patterns in different chromosomal regions or across the whole genome of *Arabidopsis*, strongly supporting the argument that DMC1 catalyses repair of all meiotic DNA breaks, not only non-sister cross-overs.

3.2 Principal Results

- This work took advantage of a dominant-negative, inactive rad51 protein fusion previously characterized in the group. The fusion protein can form nucleofilaments on single-stranded DNA but the presence of the GFP peptide inactivates the second DNA binding site of RAD51, rendering the fusion protein incapable of catalysing the key strand-invasion step of recombination. RAD51-GFP cannot carry out recombination, but remains able to support the activity of DMC1 in meiosis. All meiotic recombination is thus catalysed by DMC1 in the fully fertile RAD51-GFP plants.
- CO rates in genetic intervals marked by fluorescent pollen markers. Measurements of recombination rates in a chromosome arm interval (I1b) and a interval including a centromeric region (CEN3) concord with our previous measurements on 2 genetic intervals defined by INDEL markers on the arms of chromosomes I and III, showing no significant effect of the absence of functional RAD51 strand-exchange activity on meiotic CO rates in chromosome arms or across the centromere of *Arabidopsis* chromosome 3.

- Cytological counting of numbers of chiasmata per chromosome showed no significant differences between wild-type and RAD51-GFP plants. Genome-wide numbers of chiasmata showed a very slight increase in RAD51-GFP meiosis (9.3 ± 0.11 (mean \pm s.e.m.)) compared to the Wild-Type controls (9.68 ± 0.15), but this was of weak significance.
- Analysis of numbers of type I CO by HEI10 immunofluorescence showed no significant difference between RAD51-GFP and wild-type meiosis. As expected, the numbers of HEI10 foci visible on chromosome axes increase through leptotene into late zygotene in both wild type and RAD51-GFP and drop dramatically to give 7–11 foci/nucleus in late Pachytene.
- Meiotic experiment through EdU pulse-chase meiotic time course showed similar meiotic kinetics in RAD51-GFP and WT plants. The absence of RAD51 strand-exchange activity thus caused no detectable differences in the timing of meiotic stages in this analysis.

3.3 Discussion

The RAD51 and DMC1 recombinases catalyse the key strand-invasion step of recombination and are both essential for ordered segregation of chromosomes in meiosis. In most eukaryotes, meiotic recombination requires the co-operation of both strand-exchange proteins. RAD51 is

active in both mitosis and meiosis while DMC1 is specific to meiosis. There are some exceptions where DMC1 mediated meiotic recombination is not necessary because several organisms do not possess a DMC1 orthologue (e.g. *Drosophila*, *Caenorhabditis elegans*, *Neurospora crassa* and *Sordaria macrospora*) (Neale and Keeney, 2006).

Why do eukaryotes have two strand-exchange proteins, and what unique functions are accomplished by the meiosis-specific DMC1 protein? A key to the answer to this question comes from the recent work showing that the joint molecule forming activity of RAD51 is not needed for meiotic recombination. Studies of the yeast *rad51-II3A* and Arabidopsis RAD51-GFP separation-of-function mutants that the strand-exchange activity of DMC1 alone is sufficient for meiotic recombination and the requirement for RAD51 is for the protein itself (as a nucleofilament) and not for its catalytic strand-exchange activity (Cloud et al., 2012; Da Ines et al., 2013b). The analogous phenotypes to the yeast and plant mutants carry the implication that these conclusions are potentially applicable in general to eukaryotes with a DMC1 homologue. DMC1 is thus the active strand-invasion recombinase in meiotic recombination. This conclusion thus brings into doubt the generally held belief that DMC1 is specifically implicated in CO and RAD51 in NCO recombination in meiosis.

Working with *Arabidopsis thaliana* we extended the previous studies into two more genetic intervals using I1b (arm interval) and CEN3 (centromeric interval) interval and to whole-chromosome and whole-

genome levels. No evidence was found for any significant effect on CO/NCO ratios or on meiotic progression in our EdU time-course experiment in the absence of RAD51 strand-exchange activity. The data in this first part of my thesis extend the previous work and confirm the earlier yeast and Arabidopsis studies. DMC1 is the active meiotic strand-exchange protein in WT meiosis and thus appears to be responsible for inter-sister and inter-homologue CO and NCO.

Article

RESEARCH ARTICLE

Analysis of the impact of the absence of RAD51 strand exchange activity in Arabidopsis meiosis

Gunjita Singh, Olivier Da Ines, Maria Eugenia Gallego, Charles I. White*

Génétique, Reproduction et Développement, UMR CNRS 6293 - INSERM U1103 - Université Clermont Auvergne Campus Universitaire des Cézeaux, Aubiere, France

* charles.white@uca.fr



OPEN ACCESS

Citation: Singh G, Da Ines O, Gallego ME, White CI (2017) Analysis of the impact of the absence of RAD51 strand exchange activity in Arabidopsis meiosis. PLoS ONE 12(8): e0183006. <https://doi.org/10.1371/journal.pone.0183006>

Editor: Arthur J. Lustig, Tulane University Health Sciences Center, UNITED STATES

Received: May 29, 2017

Accepted: July 27, 2017

Published: August 10, 2017

Copyright: © 2017 Singh et al. This is an open access article distributed under the terms of the [Creative Commons Attribution License](https://creativecommons.org/licenses/by/4.0/), which permits unrestricted use, distribution, and reproduction in any medium, provided the original author and source are credited.

Data Availability Statement: All relevant data are within the paper and its Supporting Information files.

Funding: This work was funded by the European Commission Marie-Sklodowska Actions (FP7-PEOPLE-2013-ITN. COMREC. 606956), the Centre National de la Recherche Scientifique, Institut National de la Santé et de la Recherche Médicale, and the Université Clermont Auvergne. The funders had no role in study design, data collection and analysis, decision to publish, or preparation of the manuscript.

Abstract

The ploidy of eukaryote gametes must be halved to avoid doubling of numbers of chromosomes with each generation and this is carried out by meiosis, a specialized cell division in which a single chromosomal replication phase is followed by two successive nuclear divisions. With some exceptions, programmed recombination ensures the proper pairing and distribution of homologous pairs of chromosomes in meiosis and recombination defects thus lead to sterility. Two highly related recombinases are required to catalyse the key strand-invasion step of meiotic recombination and it is the meiosis-specific DMC1 which is generally believed to catalyse the essential non-sister chromatid crossing-over, with RAD51 catalysing sister-chromatid and non-cross-over events. Recent work in yeast and plants has however shown that in the absence of RAD51 strand-exchange activity, DMC1 is able to repair all meiotic DNA breaks and surprisingly, that this does not appear to affect numbers of meiotic cross-overs. In this work we confirm and extend this conclusion. Given that more than 95% of meiotic homologous recombination in Arabidopsis does not result in inter-homologue crossovers, Arabidopsis is a particularly sensitive model for testing the relative importance of the two proteins—even minor effects on the non-crossover event population should produce detectable effects on crossing-over. Although the presence of RAD51 protein provides essential support for the action of DMC1, our results show no significant effect of the absence of RAD51 strand-exchange activity on meiotic crossing-over rates or patterns in different chromosomal regions or across the whole genome of Arabidopsis, strongly supporting the argument that DMC1 catalyses repair of all meiotic DNA breaks, not only non-sister cross-overs.

Introduction

The process of eukaryotic sexual reproduction is based on the production of gametes of halved ploidy, the fusion of two of which regenerates the original ploidy in the subsequent generation [1, 2]. This halving of chromosome number is carried out by meiosis, a specialised cell division in which two successive divisions follow a single round of DNA replication. A single meiotic

Competing interests: The authors have declared that no competing interests exist.

cell thus produces four nuclei of halved ploidy, in contrast to mitosis, in which DNA replication is followed by a single division, resulting in two daughter nuclei of the same ploidy as the mother cell.

The specialised meiotic cell division thus solves the problem of maintaining ploidy stable across sexual generations, but this comes with a cost. In mitosis, balanced segregation of chromatids, is ensured by sister chromatid cohesion established in the preceding S-phase, but this can only work once and is thus not sufficient in meiosis, in which two successive nuclear divisions follow a single S-phase. In most studied eukaryotes, the problem of proper meiotic chromosomal segregation is ensured by chiasmata, physical links between homologous chromosomes produced by non-sister-chromatid cross-over recombination (CO) in the first meiotic division. Recombination during the first meiotic prophase thus ensures that homologous chromosomes accurately segregate from each other and in doing so, shuffles the genetic information to generate the genetic variation driving evolution.

The work of many authors has contributed to understanding the molecular processes underlying the repair of programmed meiotic DNA double-strand breaks (DSB) and the relationships between CO and non-CO meiotic recombination outcomes. Readers are directed to [3–5] for recent reviews of this subject. Briefly, the process of meiotic recombination is initiated by the programmed induction of DSB throughout the genome by the SPO11 protein complex, followed by resection of the broken DNA ends to generate 3' single-stranded DNA (ssDNA) overhangs on both sides of the DSB. Binding of the RAD51 and DMC1 proteins to these overhangs generates nucleoprotein filaments, which search for and invade an homologous template DNA duplex. Copying of the template DNA molecule and resolution of the joint recombination intermediates repairs the break. A subset of these repair events result in physical exchanges or CO between the interacting DNA molecules and if these are non-sister chromatids, in chiasmata linking the homologous chromosomes and genetic CO. Strikingly, numbers of meiotic DSB commonly exceed numbers of chiasmata, with DSB:CO ratios of 25–30 in *Arabidopsis*, 15 in mouse, 4.4 in *Drosophila* and 1.8 in budding yeast (reviewed by [6]).

The highly conserved RAD51 protein family consists of 7 members in plants and animals: RAD51, DMC1 and the five RAD51 paralogs: RAD51B, RAD51C, RAD51D, XRCC2 and XRCC3. RAD51 and DMC1 catalyse the key recognition and invasion of a homologous DNA template molecule, with the 5 RAD51 paralogs playing essential roles in supporting this activity [7–11]. Originally identified in yeast [12–16], RAD51 and DMC1 are believed to derive from Archaeal *RadA* through a duplication early in eukaryotic evolution [17–19]. The two proteins are weak DNA-dependent ATPases with similar biochemical properties. Binding to ssDNA and dsDNA to form nucleoprotein filaments, which catalyse the search for, and invasion of a homologous DNA template molecule [3, 20–26]. The activities of the two proteins are not however identical, as illustrated by the observation of greater resistance to dissociation of D-loops formed by human DMC1 compared to RAD51 [27] and the differing substrate requirements for the formation of four-strand joint molecules—suggesting opposite polarities of polymerization of RAD51 (3'-5') and DMC1 (5'-3') on ssDNA (Murayama et al. 2011) discussed by [3].

RAD51 plays key roles in both meiosis and mitosis, while DMC1 is meiosis-specific [12, 16]. In meiosis, RAD51 is generally believed to play roles chiefly in inter-sister and non-CO recombination, with DMC1 being important for recombination between non-sister chromatids of homologs, although it can catalyse inter-sister/non-CO recombination in the absence of RAD51 activity [28–31]. Budding yeast *dmc1* mutants arrest in meiotic prophase, accumulate meiotic DSB and have strong defects in accumulation of joint molecule (JM) recombination intermediates [12, 28, 32]. Return to growth experiments do permit recovery of JM intermediates in the yeast *dmc1* mutant, but these are only between sister chromatids [28]. Meiotic

prophase arrest is not observed in the yeast *rad51* mutant, which does however show delayed appearance of JM intermediates with a strong bias towards inter-sister versus inter-homologue JM [28] and produces viable spores. The severity of the *dmc1* and *rad51* meiotic phenotypes in yeast is however strain-dependent [33–35].

In mouse, *dmc1* meiosis shows zygotene arrest without synapsis [36, 37], while absence of RAD51 is embryonic lethal [38, 39]. A recent study has succeeded in testing the effects of RAD51 knockdown in mouse meiosis through injection of siRNA into seminiferous tubules and shows leptotene arrest and loss of zygotene nuclei through p53-dependent apoptosis [40]. A few cells escape this apoptosis and these show increased sex-chromosome asynapsis and reduced CO, further supporting the conclusion that RAD51 is needed for DMC1 to function in mouse [40].

Maize has two redundant *RAD51* genes, *RAD51A1* and *RAD51A2* [41]. *rad51a rad51b* mutant plants are viable with no visible developmental defects, but are male sterile with reduced numbers of chiasmata and evidence of non-homologue synapsis in male meiosis. Residual female fertility however permitted apparently normal CO rates in surviving meiocytes [42]. The *japonica* cultivar of rice has two RAD51 proteins (*RAD51A1* and *RAD51A2*) with *in vitro* data suggesting *RAD51A2* has the major role in homologous pairing, while *indica* rice plants have only one RAD51 [43, 44]. Rice also has two redundant DMC1 proteins (*DMC1A* and *DMC1B*) and rice DMC1 is required for normal meiotic recombination, proper CO formation and synapsis [45–49]. It is however the model plant *Arabidopsis thaliana*, which provides the most clear illustration of the different meiotic phenotypes of *dmc1* and *rad51* mutants. *Arabidopsis* plants lacking either protein are viable and complete meiosis, but achiasmate meiosis leads to random segregation of intact (fully repaired) chromosomes and residual fertility in the *dmc1* mutant. In striking contrast, the lack of DSB repair leads to meiotic Prophase I chromosome fragmentation in the fully sterile *rad51* mutant [50, 51].

A considerable body of data thus points to a specific role for DMC1 in meiotic inter-homologue CO recombination, but the complexity of the mutant phenotypes has complicated clarification of the specific roles of RAD51 and DMC1 in this process. Recent data from yeast and *Arabidopsis* have however provided a major advance in sorting out this puzzle. Inactivation of the secondary DNA binding site of RAD51 in *rad51-II3A* mutant yeast blocks its ability to catalyse recombination but does not affect fertility [30]. This is also seen upon expression of the dominant-negative RAD51-GFP fusion protein in *Arabidopsis* [31], which also lacks secondary DNA binding and strand-invasion activity [52]. In contrast to the effect of absence of RAD51, these mutant RAD51 proteins are unable to catalyse invasion of the template DNA duplex and are defective in mitotic DSB repair, but remain able to support the activity of DMC1 in meiosis [30, 31, 52]. These studies unequivocally show that DMC1 is capable of catalysing the repair of all meiotic DSB in the absence of RAD51 strand-exchange activity. Given the excess of meiotic DSB over CO and the general belief that DMC1 is specifically responsible for meiotic inter-homologue CO recombination, both yeast and plant studies tested for effects on meiotic CO rates. No effect on CO was found in the defined genetic intervals used for these tests, suggesting that DMC1 is the only active strand-invasion enzyme in meiosis and that only the presence of RAD51 is essential, not its strand-exchange activity.

All meiotic recombination is catalysed by DMC1 in the (fully fertile) *rad51 + RAD51-GFP* *Arabidopsis* plants, and they thus provide an opportunity for better understanding of the specificities of the roles of DMC1 and RAD51 in inter-homologue meiotic CO and pairing. We present here an analysis of the effects of the absence of RAD51 strand-exchange activity on meiotic CO patterns in different chromosomal regions and across the whole *Arabidopsis* genome. We find no significant effect of the absence of RAD51 strand-exchange activity on

meiosis in Arabidopsis—arguing that DMC1 is the unique active meiotic strand-exchange protein in WT plants.

Results

Recombination rates

FTL marker lines [53, 54] were used to test for effects of the absence of RAD51 strand exchange activity on meiotic CO rates in pericentromeric regions. The pollen-expressed, red and yellow fluorescent protein markers in these lines provide a rapid and precise means of measuring genetic map-distance in defined genetic intervals in Arabidopsis. We used the FTL lines I1b carrying linked insertions on the arm of chromosome 1 (I1b: FTL567 and FTL1262, and; FTL567: FTL1262 = 8.16 cM), and CEN3, with two insertions spanning the centromere of chromosome 3 (CEN3: FTL3332: FTL2536 = 11.04 cM) [54] (S1 Fig). The I1b and CEN3 lines were crossed with Col-0 WT and *rad51/rad51 RAD51-GFP/RAD51-GFP* homozygotes to generate F1 lines in which both DMC1 and RAD51 (WT), or only DMC1 (*rad51/RAD51 RAD51-GFP*) strand exchange activities are present during meiosis. F2 plants were derived by selfing the F1 and genotyped to identify the *RAD51/RAD51* and *rad51/rad51 RAD51-GFP/RAD51-GFP* F2 mapping lines.

Pollen from the WT and *rad51 RAD51-GFP* mapping lines were scored for the fluorescent markers and to guard against biases in scoring, the 1:1 ratio of presence/absence of the markers individual markers was verified with a Chi-squared test in each data set (Tables 1 and 2).

As expected and in agreement with our previous data on different chromosome-arm genetic intervals [31], absence of RAD51 strand exchange activity had no detectable effect on meiotic CO rate in the chromosome I1b interval (Fig 1, Table 2; WT: mean±sem = 8.45±0.20 cM; 6 plants, total pollen scored = 6261; RAD51-GFP: mean±sem = 8.68±0.35 cM; 6 plants, total pollen scored = 6923. unpaired 2-tailed t-test. P = 0.5751 t = 0.5795 df = 10). Neither was any significant effect of the absence of RAD51 strand-exchange activity observed in the centromere-spanning chromosome 3 interval, CEN3 (Fig 1, Table 1; WT: mean±sem = 11.68±0.06 cM; 5 plants, total pollen scored = 6304; RAD51-GFP: 11.62±0.10 cM; 5 plants, total pollen scored = 5142. unpaired 2-tailed t-test. P = 0.6103 t = 0.5303 df = 8).

These results concord with our previous measurements on 2 genetic intervals defined by INDEL markers on the arms of chromosomes I and III [31], showing no significant effect of the absence of functional RAD51 strand-exchange activity on meiotic CO rates in chromosome arms or across the centromere of Arabidopsis chromosome 3.

Table 1. Meiotic recombination in the CEN3 interval.

Plant#	R	Y	R+Y	neither	total	r	Chi2 R:not R	Chi2 Y:not Y
WT#1	74	68	514	550	1206	0.118	0.750	1.460
WT#2	52	40	360	335	787	0.117	1.740	0.210
WT#3	72	68	544	520	1204	0.116	0.651	0.332
WT#4	103	107	798	772	1780	0.118	0.272	0.506
WT#5	75	78	594	580	1327	0.115	0.091	0.218
RAD51-GFP#1	45	40	312	320	717	0.119	0.010	0.240
RAD51-GFP#2	46	30	285	290	651	0.117	0.190	0.680
RAD51-GFP#3	66	70	542	512	1190	0.114	0.568	0.971
RAD51-GFP#4	75	80	614	590	1359	0.114	0.266	0.619
RAD51-GFP#5	78	65	534	548	1225	0.117	0.001	0.595

<https://doi.org/10.1371/journal.pone.0183006.t001>

Table 2. Meiotic recombination in the I1b interval.

Plant#	R	Y	R+Y	neither	total	r	Chi2 R:not R	Chi2 Y:not Y
WT#1	31	20	276	275	602	0.085	0.239	0.166
WT#2	45	36	436	438	955	0.085	0.051	0.013
WT#3	54	50	628	630	1362	0.076	0.003	0.026
WT#4	53	62	645	627	1387	0.083	0.058	0.526
WT#5	35	42	386	402	865	0.089	0.612	0.094
WT#6	54	43	486	507	1090	0.089	0.092	0.939
RAD51-GFP#1	32	23	273	264	592	0.093	0.547	0.000
RAD51-GFP#2	49	51	447	451	998	0.100	0.036	0.004
RAD51-GFP#3	45	24	437	414	920	0.075	2.104	0.004
RAD51-GFP#4	62	41	556	552	1211	0.085	0.516	0.239
RAD51-GFP#5	90	63	842	830	1825	0.084	0.833	0.123
RAD51-GFP#6	60	55	637	625	1377	0.084	0.210	0.036

Numbers of Red (R), Yellow (Y) and Red+Yellow (R+Y) fluorescent and non-fluorescent (neither) pollen from flowers of wild-type and *rad51 RAD51-GFP* plants used to calculate genetic map distances (r cM) in the CEN3 (a) and I1b (b) marked intervals in WT and *RAD51-GFP* plants.

<https://doi.org/10.1371/journal.pone.0183006.t002>

Chiasmata counting

Fluorescence *in situ* hybridisation (FISH) using probes for the 5S and 45S rDNA loci [55], permits identification of all 5 Arabidopsis chromosomes in meiotic metaphase I and the form of the bivalents can be used to infer mean CO numbers per chromosome and per meiosis (Fig 2a) [55].

Counting chiasmata showed means of 9.3 ± 0.11 (mean \pm s.e.m.) and 9.68 ± 0.15 chiasmata per meiosis in Col-0 (wild type) and RAD51-GFP plants respectively (Fig 2c and Table 3). The absence of RAD51 strand exchange activity thus results in a mild increase in CO of borderline significance (unpaired 2-tailed t-test. $P = 0.045$, $t = 2.08$ $df = 37$). Taking the five chromosomes individually, numbers of chiasmata numbers per chromosome showed no significant differences between wild-type and RAD51-GFP plants (adjusted P values of 0.957, 0.957, 0.383, 0.725, 0.957 for chromosomes 1 to 5 respectively. Fig 2b, Table 3).

Meiotic HEI10 foci

Arabidopsis HEI10/ZYP3 is structurally and functionally related to yeast Zip3 and mammalian HEI10 and is required for the formation of Type I COs [56]. HEI10 immunolocalization (IF) foci can be used to quantify numbers of Type I COs. Fig 3 shows representative IF images of WT (a-d) and RAD51-GFP (e-h) Arabidopsis pollen mother cells (PMC) spreads with DAPI (blue), anti-ASY1 (green) and anti-HEI10 (red). As expected [56], the numbers of HEI10 foci visible on chromosome axes increase through leptotene into late zygotene in both wild type and RAD51-GFP and drop dramatically to give 7–11 foci/nucleus in late Pachytene. Mean (\pm s.e.m, number of meioses counted) numbers of HEI10 foci in Leptotene, Zygotene and Pachytene were $72.43 (\pm 1.50, n = 7)$, $140.5 (\pm 1.83, 10)$ and $9.5 (\pm 0.183, n = 40)$ respectively for WT meioses. Leptotene, Zygotene and Pachytene values for RAD51-GFP meioses were $70.29 (\pm 2.00, n = 7)$, $139.7 (\pm 1.67, 10)$ and $9.73 (\pm 0.168, n = 48)$ respectively. No significant differences were thus observed in numbers of HEI10 foci between WT and RAD51-GFP (2-tailed t-tests. Leptotene: $P = 0.41$, $t = 0.859$, $df = 12$; Zygotene: $P = 0.750$, $t = 0.3234$, $df = 18$; Pachytene: $P = 0.382$, $t = 0.924$, $df = 86$).

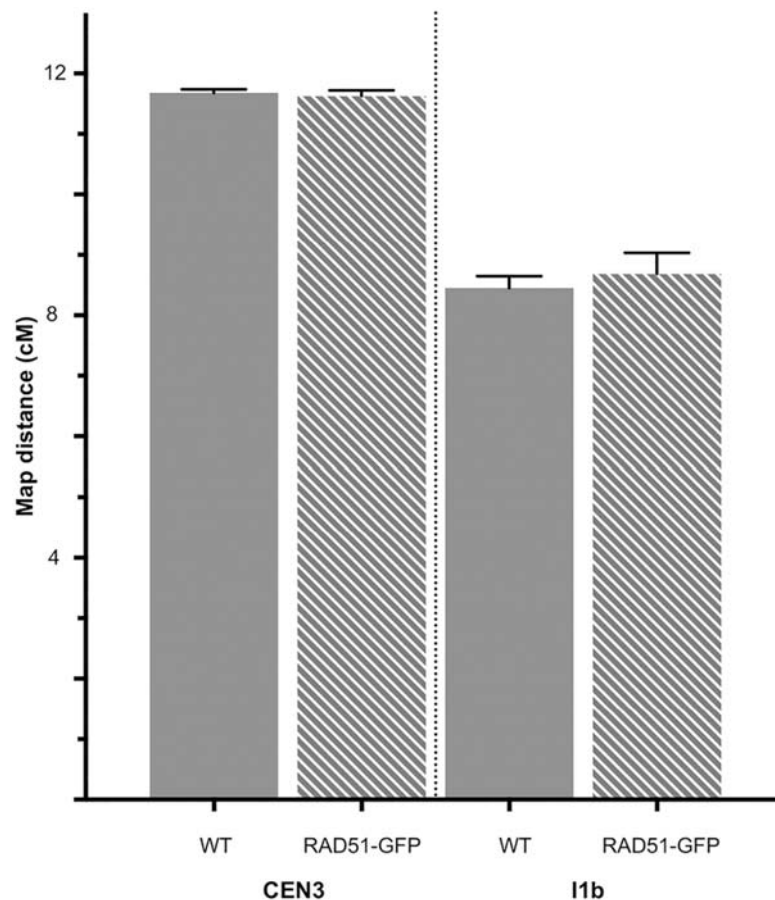


Fig 1. Genetic map distances of the I1b and CEN3 intervals in WT and *RAD51-GFP* meioses. Mean map lengths (cM) of the I1b and CEN3 genetic intervals in Wild type (filled bars) and *RAD51-GFP* plants (striped bars). Error bars are standard errors of the mean.

<https://doi.org/10.1371/journal.pone.0183006.g001>

Meiotic time-course

Previous reports have shown that perturbation of homologous recombination and synapsis causes delays in meiotic prophase I with, for example, the *zyp1* mutant causing an extension of prophase I by approximately 6 hours [57]. We thus tested for effects of the absence of RAD51 strand-exchange activity on the progression of the meiotic division using an EdU pulse-chase (see [Methods](#)). Briefly, a pulse of the thymidine analogue EdU is taken up through the transpiration stream and incorporated into DNA in replicating cells, including those in pre-meiotic S-phase. Anthers are collected and fixed across a time-course, and meiotic Pollen Mother Cell nuclei observed for the first occurrence of EdU labeled chromosomes at specific meiotic stages.

Meiocytes that incorporated EdU into their replicating DNA at the end of S-phase took approximately 6–8 hours to progress through G2 into early leptotene [58]. As seen in [Fig 4](#), EdU signal was observed in leptotene nuclei 12 hours following the EdU pulse ([Fig 4](#), panels d-f and iv-vi). EdU signal was detected in chromosomes of early zygotene meiocytes 16 hours after the pulse ([Fig 4](#), panels g-i and vii-ix). At the 20h point, labelled chromosomes were observed in Zygotene/Pachytene ([Fig 4](#), panel j-l and x-xii). At 24h Pachytene chromosomes were completely labelled with EdU ([Fig 4](#), panel m-o and xiii-xiv), At 36h, EdU staining is

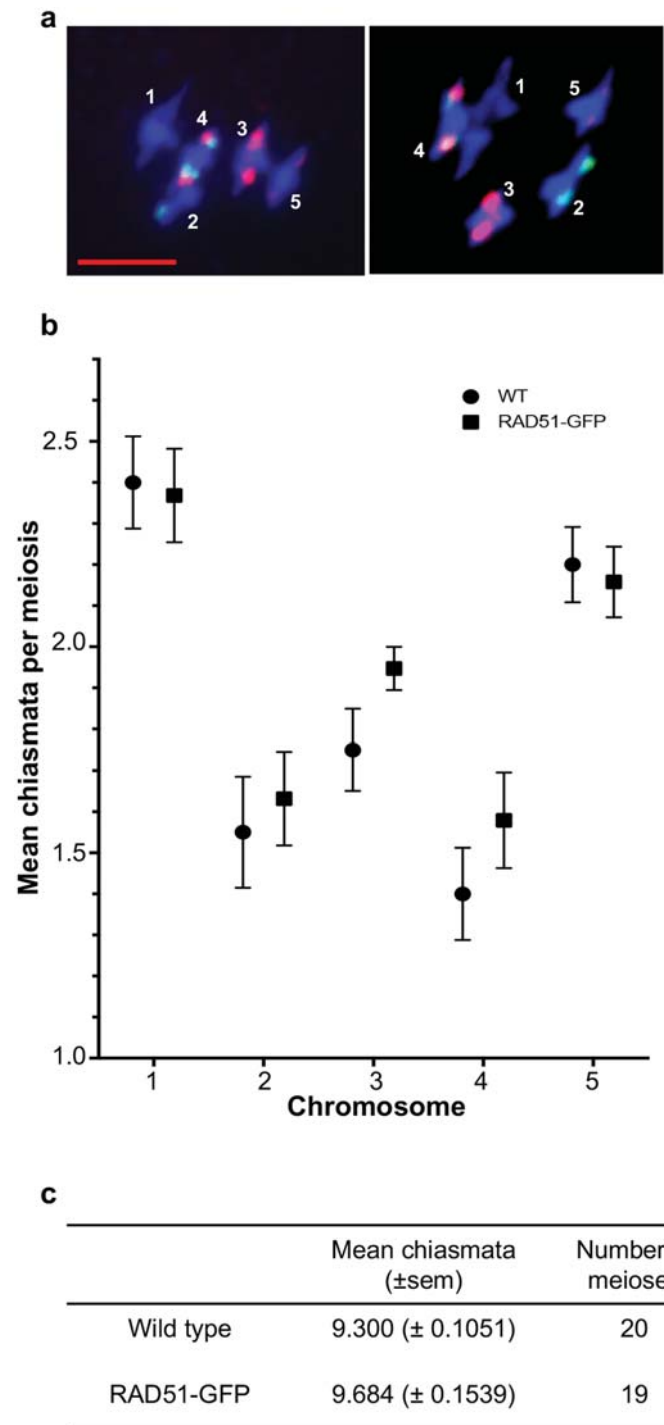


Fig 2. Chiasmata counts in wild type and RAD51-GFP meioses. DAPI-stained (blue) meiotic Metaphase I of wild type (a, left panel) and RAD51-GFP (a, right panel). Green (45S rDNA) and red (5S rDNA) FISH signals are used to identify each of the 5 chromosomes (numbered) and the shape of the bivalents permits counting chiasmata. Scale bar is 5µm. Mean numbers of chiasmata per chromosome (b) in wild type (blue) and RAD51-GFP (red) and per meiosis (c) (errors are s.e.m.).

<https://doi.org/10.1371/journal.pone.0183006.g002>

Table 3. Chiasmata counts.

	WT	RAD51-GFP	P	significant?
Chr 1	2.4±0.11	2.37±0.11	0.957	no
Chr 2	1.55±0.14	1.63±0.11	0.957	no
Chr 3	1.75±0.10	1.95±0.05	0.383	no
Chr 4	1.4±0.11	1.58±0.12	0.725	no
Chr 5	2.2±0.09	2.16±0.09	0.957	no
all	9.3 ± 0.11	9.7 ± 0.15	0.0445	yes*

Mean (±s.e.m.) numbers of chiasmata per chromosome and per meiosis in WT (N = 20) and RAD51-GFP (N = 19) plants. Adjusted P values (unpaired 2-tailed t-tests, Holm-Sidak method) show no significant differences for the chromosomes taken individually. A small difference of borderline significance is seen in the per-meiosis counts (*unpaired 2-tailed t-test. P = 0.045, t = 2,08 df = 37).

<https://doi.org/10.1371/journal.pone.0183006.t003>

visible only in meiosis II in both wild type and RAD51-GFP plants (Fig 4 panels p-r and xvi-xviii). EdU labelling thus followed the same kinetics in RAD51-GFP and WT plants, showing that the absence of RAD51 strand-exchange activity thus caused no detectable differences in the timing of meiotic stages in this analysis.

Discussion

Notwithstanding the similar activities of the two proteins, *rad51* and *dmc1* mutants have very different meiotic phenotypes and the Arabidopsis *rad51* and *dmc1* mutants provide a very clear illustration of these differences. Accumulation of unrepaired meiotic DSB leads to Mek1-dependent meiotic arrest in the yeast *dmc1* mutant [3, 12, 59, 60]. The Arabidopsis *dmc1* mutant is however able to fully repair meiotic DSB created by the SPO11 complex, but has achiasmate meiosis and fertility is reduced to only a few percent of that of wild type plants. In striking contrast, the Arabidopsis *rad51* mutant is sterile due to chromosomal fragmentation in meiotic prophase I. In the absence of RAD51 protein, DMC1 alone is thus unable to repair meiotic DSB, while RAD51 (in the absence of DMC1) does repair meiotic DSB but without generating interhomologue CO and chiasmata [50, 51, 61, 62]. The dependence of DMC1 on the presence of RAD51 can also be seen in increased numbers of univalents and non-homologous chromosome associations caused by the Arabidopsis *rad51-2* knock-down allele [63] and the partial suppression of the *rad51* phenotype in the absence of ATR kinase [61]. The key to answering these puzzling differences came from the demonstration that inactivation of the secondary DNA binding site of RAD51 did not affect the fertility of *rad51-II3A* mutant yeast [30], nor RAD51-GFP in Arabidopsis [31]. The mutant *rad51-II3A* and RAD51-GFP proteins are unable to catalyse invasion of the template DNA duplex and are defective in mitotic DSB repair, but remain able to support the activity of DMC1 in meiosis [30, 31, 52].

DMC1 is thus capable of catalysing the repair of all meiotic DSB in the absence of RAD51 strand-exchange activity, but the question remains as to whether it does so in wild type meiosis or whether this result is specific to the *rad51*-mutant context. Given the excess of meiotic DSB over CO and the long-standing belief that the involvement of DMC1 in the repair of a given meiotic DSB was the key to it potentially resulting in a CO, both yeast and plant studies tested for effects on meiotic CO rates. The absence of detectable effects on CO patterns in yeast *rad51-II3A* [30] and Arabidopsis RAD51-GFP [31], suggested that this is the case. In this work we have taken advantage of the 25- to 30-fold excess of meiotic DSB over CO in Arabidopsis to extend our previous results on the possible effects of absence of RAD51 strand-exchange activity on meiotic CO patterns [31]. Compared to only 44% in budding yeast, more than 95% of

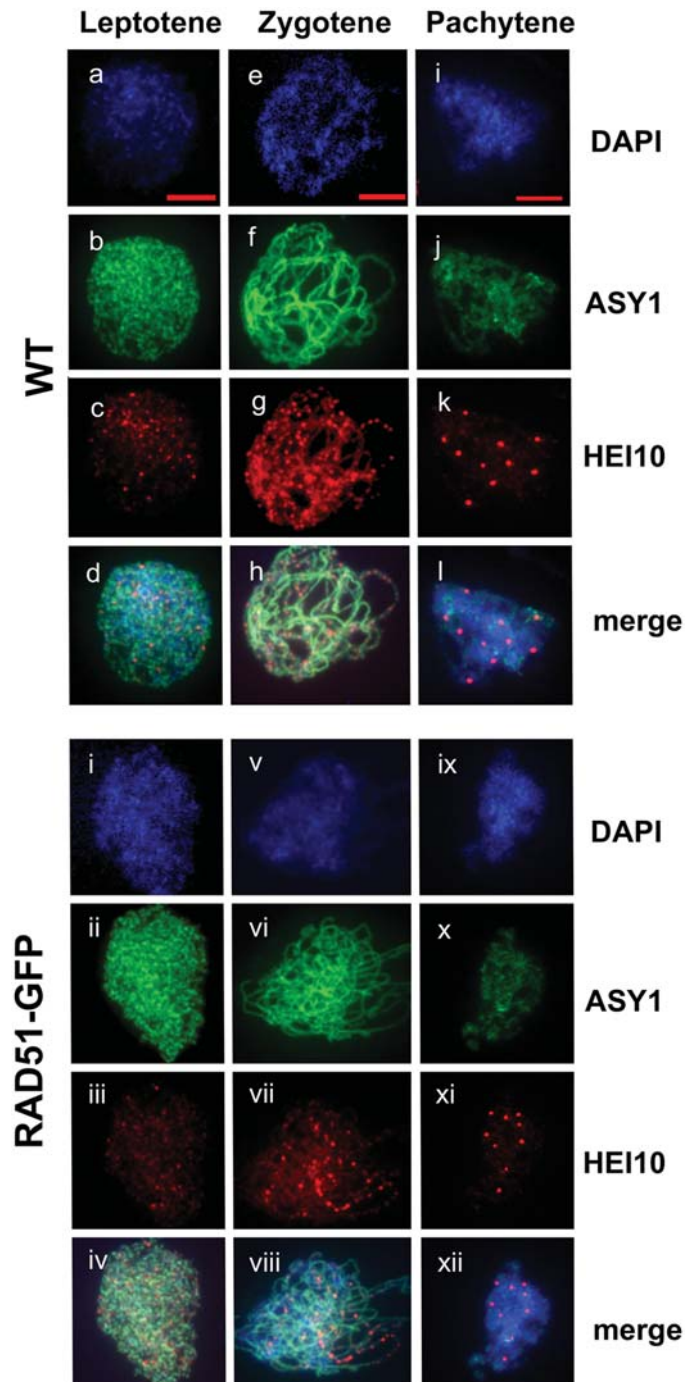


Fig 3. HEI10 foci in wild type and RAD51-GFP Pachytene. Immunolocalization of the ZMM protein HEI10 (red) and the meiotic protein ASY1 (green) in wild type Leptotene (a-d), Zygotene (e-h) and Pachytene (i-l) and RAD51-GFP Leptotene (i-iv), Zygotene (v-viii) and Pachytene (ix-xii) Pollen Mother Cell nuclei. Scale bar is 5µm.

<https://doi.org/10.1371/journal.pone.0183006.g003>

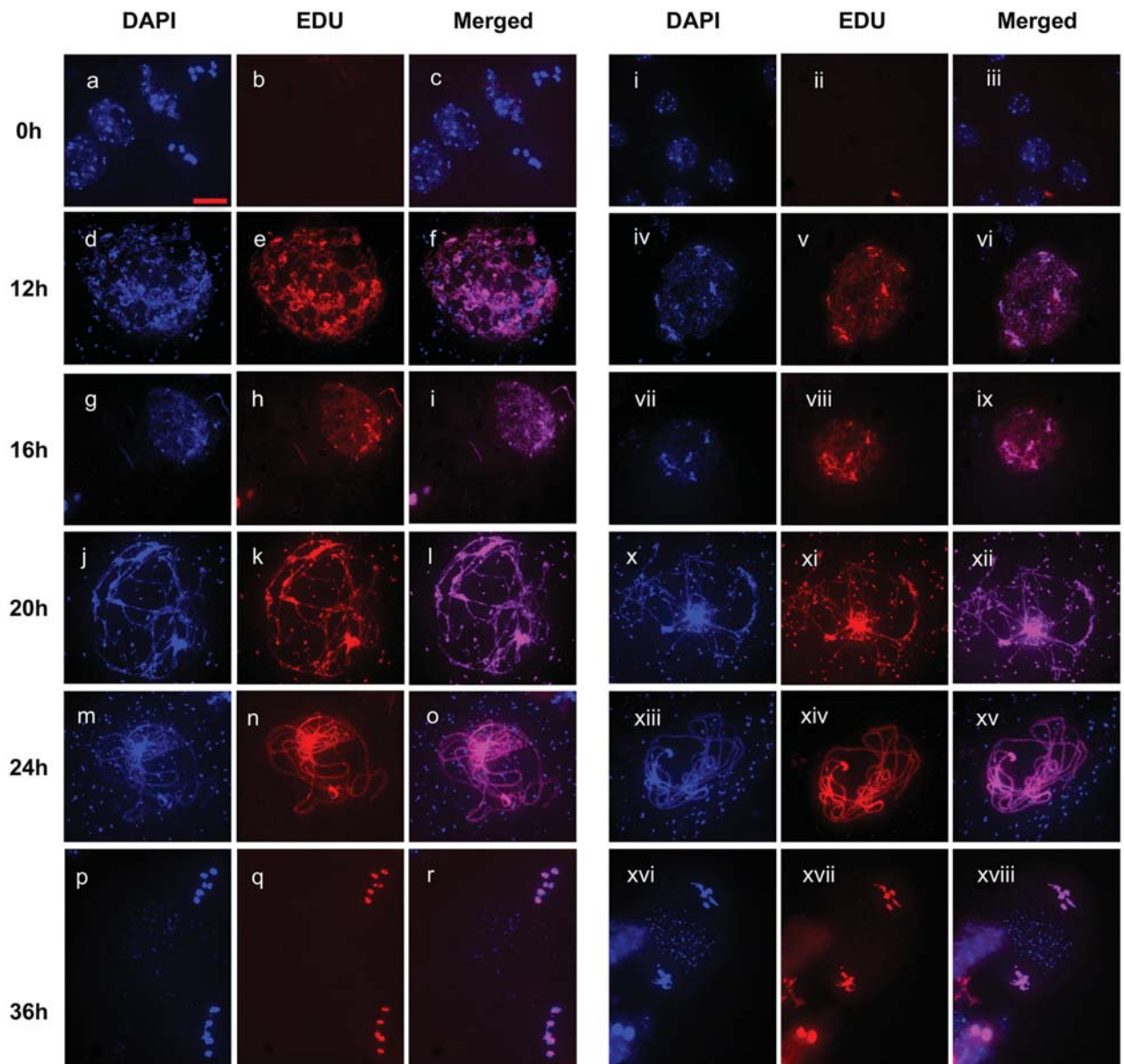


Fig 4. EdU pulse-chase meiotic time-course in wild type and RAD51-GFP plants. Wild type (a-r) and RAD51-GFP (i-xviii) pollen mother cells are in the pre-meiotic S/G2-phase 2 hours after the EdU pulse (+2 h), in leptotene at +12h, early zygotene at +16h, zygo-pachytene at +20h, pachytene at +24h and meiosis II at +36h. Scale bar is 10µm.

<https://doi.org/10.1371/journal.pone.0183006.g004>

meiotic DSB give rise to non-CO outcomes in WT Arabidopsis, making the plant a sensitive model to test for changes in their metabolism. Extending our previous results to more genetic intervals and to whole-chromosome and whole-genome measurements of chiasmata, we find no evidence for any significant effect in the absence of RAD51 strand-exchange activity on CO numbers or meiotic progression. This work thus extends and confirms the earlier yeast and Arabidopsis studies—arguing that DMC1 is the unique active meiotic strand-exchange protein in WT meiosis and thus appears to be responsible for intersister and inter-homologue CO, and very probably conversion.

Materials and methods

Plant material

All plants used in this study are of the Columbia ecotype of *Arabidopsis thaliana*. The *rad51-1* RAD51-GFP plant has been previously described [31]. The fluorescent pollen marked lines CEN3 and I1b [54] were kindly provided by Ian Henderson.

Seeds were sown in soil, stratified for two days at 4°C and grown in plant growth cabinets (SANYO MLR-351H) under standard conditions (16h day, 23°C, humidity 50–60%).

Analysis of meiotic recombination rates

FTL marker lines [53, 54] were used to test for effects of the absence of RAD51 strand exchange activity on meiotic CO rates in peri-centromeric regions. The I1bc line carries three linked insertions on the right arm of chromosome 1 (FTL567, FTL1262, and FTL992). The CFP marker (FTL992) did not however yield repeatable results in our hands and so the I1b interval (FTL567:FTL1262 = 8.16 cM) was used in this work. The CEN3 line has two markers spanning the centromere of chromosome 3 (CEN3: FTL3332:FTL2536 = 10.43 cM—11.06 cM) [54, 64]). The I1b and CEN3 lines were crossed with Col-0 WT and *rad51/rad51* RAD51-GFP/RAD51-GFP homozygotes to generate F1 mapping lines heterozygous for the pollen markers in coupling, in which both DMC1 and RAD51 (WT), or only DMC1 (*rad51* RAD51-GFP) strand exchange activities are present during meiosis. Seeds of these plants were sown and the F2 plants genotyped to identify the homozygote F2 mapping lines for collection of pollen. The *rad51* KO allele and RAD51-GFP insertion were followed by PCR genotyping [31] and presence of the fluorescent markers was scored by visual examination of the pollen from flowers of the principal stems with a fluorescence microscope [53, 54].

FISH

Meiotic chromosome spreads were prepared according to [55]. Briefly, whole inflorescences were fixed in ice-cold ethanol/glacial acetic acid (3:1) and stored at -20°C until further use. Immature flower buds of appropriate size were selected under a binocular microscope, rinsed twice at room temperature in distilled water for 5 min followed by two washes in 1X citrate buffer for 5 min. Flower buds were then incubated for 2 h on a slide in 100µl of enzyme mixture (0.3% w/v cellulase, 0.3% w/v pectolyase, 0.3% cytohelicase (Sigma)) in a moist chamber at 37°C. Buds were softened for 1 minute in 15µl 60% acetic acid on a microscope slide at 45°C, fixed with ice-cold ethanol/glacial acetic acid (3:1) and air dried. Finally, slides were mounted in Vectashield mounting medium with DAPI (Vector Labs, Burlingame, CA, USA) for microscopy.

Immunocytology

Slide preparation for immunolocalization of proteins were carried out as described by [65]. Anti-ASY1 from Guinea-Pig (1:250 dilution) [66] and HEI10 from Rabbit (1:150 dilution) [56] were kindly provided by Chris. Franklin (Univ. Birmingham, U.K.) and Mathilde Grelon (INRA, Versailles, France).

Microscopy

All observations were made with a motorised Zeiss AxioImager Z1 epifluorescence microscope (Carl Zeiss AG, Germany) using a PL Apochromat 100X/1.40 oil objective, AxioCam Mrm camera (Carl Zeiss AG, Germany) and appropriate Zeiss filter sets: 25HE (DAPI), 38HE (Alexa 488), 43HE (Alexa 596).

Pulse chase experiment

Floral stems (approx. 8cm) of well-grown, 6 week-old *rad51/rad51 RAD51-GFP/RAD51-GFP* and WT plants [58, 67] were cut under running tap water and transferred in 10 mM EdU for 2h (Click-IT assay kit Invitrogen, California, USA). The floral tips were then rinsed under running water for 2–3 times and transferred to glass tubes containing tap water and incubated at 23°C, ~100–120 $\mu\text{m}^2/\text{s}^{-1}$ light intensity). Samples were collected at 0h, 12h, 16h, 24h & 36h time points and fixed in ethanol: glacial acetic acid (3:1 ratio) and stored at 4°C. Meiotic chromosome spreads were prepared and stained and analysed as described [68, 69].

Supporting information

S1 Fig. Scoring fluorescent pollen. YFP (a), RFP (b), bright-field and merged (d) images of pollen from CEN3xCol-0 F1 plants carrying the fluorescent markers. Examples of the different combinations of fluorescence are arrowed. Scale bar is 5 μm .
(PDF)

Acknowledgments

Our thanks to the members of the recombination group and the COMREC network for helpful discussions, to Ian Henderson and Greg. Copenhagen for the pollen-marker lines, to Chris. Franklin and Mathilde Grelon for antisera and to Juan-Luis Santos and Monica Pradillo for help with the chiasmata counting.

Author Contributions

Conceptualization: Gunjita Singh, Maria Eugenia Gallego, Charles I. White.

Data curation: Gunjita Singh, Charles I. White.

Formal analysis: Gunjita Singh, Charles I. White.

Funding acquisition: Maria Eugenia Gallego, Charles I. White.

Methodology: Gunjita Singh, Olivier Da Ines, Charles I. White.

Project administration: Charles I. White.

Resources: Maria Eugenia Gallego, Charles I. White.

Supervision: Olivier Da Ines, Maria Eugenia Gallego.

Validation: Maria Eugenia Gallego, Charles I. White.

Visualization: Charles I. White.

Writing – original draft: Gunjita Singh, Maria Eugenia Gallego, Charles I. White.

Writing – review & editing: Gunjita Singh, Maria Eugenia Gallego, Charles I. White.

References

1. Hunter N (2007) Meiotic Recombination. In: Aguilera A. and Rothstein R., editors. Molecular Genetics of Recombination. Springer. pp. 381–442.
2. Barton NH, Charlesworth B. Why sex and recombination? Science. 1998. 281: 1986–1990. PMID: [9748151](https://pubmed.ncbi.nlm.nih.gov/9748151/)
3. Brown MS, Bishop DK. DNA strand exchange and RecA homologs in meiosis. Cold Spring Harb Perspect Biol. 2014. 7: a016659. <https://doi.org/10.1101/cshperspect.a016659> PMID: [25475089](https://pubmed.ncbi.nlm.nih.gov/25475089/)

4. Hunter N. Meiotic Recombination: The Essence of Heredity. *Cold Spring Harb Perspect Biol.* 2015. 7: a016618. <https://doi.org/10.1101/cshperspect.a016618> PMID: [26511629](https://pubmed.ncbi.nlm.nih.gov/26511629/)
5. Zickler D, Kleckner N. Recombination, Pairing, and Synapsis of Homologs during Meiosis. *Cold Spring Harb Perspect Biol.* 2015. 7: a016626. <https://doi.org/10.1101/cshperspect.a016626> PMID: [25986558](https://pubmed.ncbi.nlm.nih.gov/25986558/)
6. Serrentino M-E, Borde V. The spatial regulation of meiotic recombination hotspots: are all DSB hotspots crossover hotspots? *Exp Cell Res.* 2012. 318: 1347–1352. <https://doi.org/10.1016/j.yexcr.2012.03.025> PMID: [22487095](https://pubmed.ncbi.nlm.nih.gov/22487095/)
7. Godin SK, Sullivan MR, Bernstein KA. Novel insights into RAD51 activity and regulation during homologous recombination and DNA replication. *Biochem Cell Biol.* 2016. 94: 407–418. <https://doi.org/10.1139/bcb-2016-0012> PMID: [27224545](https://pubmed.ncbi.nlm.nih.gov/27224545/)
8. Taylor MR, Spirek M, Jian Ma C, Carzaniga R, Takaki T, Collinson LM, et al. A Polar and Nucleotide-Dependent Mechanism of Action for RAD51 Paralogs in RAD51 Filament Remodeling. *Mol Cell.* 2016. 64: 926–939. <https://doi.org/10.1016/j.molcel.2016.10.020> PMID: [27867009](https://pubmed.ncbi.nlm.nih.gov/27867009/)
9. Su H, Cheng Z, Huang J, Lin J, Copenhaver GP, Ma H, et al. Arabidopsis RAD51, RAD51C and XRCC3 proteins form a complex and facilitate RAD51 localization on chromosomes for meiotic recombination. *PLoS Genet.* 2017. 13: e1006827. <https://doi.org/10.1371/journal.pgen.1006827> PMID: [28562599](https://pubmed.ncbi.nlm.nih.gov/28562599/)
10. Suwaki N, Klare K, Tarsounas M. RAD51 paralogs: roles in DNA damage signalling, recombinational repair and tumorigenesis. *Semin Cell Dev Biol.* 2011. 22: 898–905. <https://doi.org/10.1016/j.semcdb.2011.07.019> PMID: [21821141](https://pubmed.ncbi.nlm.nih.gov/21821141/)
11. Zelensky A, Kanaar R, Wyman C. Mediators of homologous DNA pairing. *Cold Spring Harb Perspect Biol.* 2014. 6: a016451. <https://doi.org/10.1101/cshperspect.a016451> PMID: [25301930](https://pubmed.ncbi.nlm.nih.gov/25301930/)
12. Bishop DK, Park D, Xu L, Kleckner N. DMC1: a meiosis-specific yeast homolog of *E. coli* recA required for recombination, synaptonemal complex formation, and cell cycle progression. *Cell.* 1992. 69: 439–456. PMID: [1581960](https://pubmed.ncbi.nlm.nih.gov/1581960/)
13. Game JC, Mortimer RK. A genetic study of x-ray sensitive mutants in yeast. *Mutat Res.* 1974. 24: 281–292. PMID: [4606119](https://pubmed.ncbi.nlm.nih.gov/4606119/)
14. Game JC, Zamb TJ, Braun RJ, Resnick M, Roth RM. The Role of Radiation (rad) Genes in Meiotic Recombination in Yeast. *Genetics.* 1980. 94: 51–68. PMID: [17248996](https://pubmed.ncbi.nlm.nih.gov/17248996/)
15. Aboussekhra A, Chanet R, Adjiri A, Fabre F. Semidominant suppressors of Srs2 helicase mutations of *Saccharomyces cerevisiae* map in the *RAD51* gene, whose sequence predicts a protein with similarities to procaryotic RecA proteins. *Mol Cell Biol.* 1992. 12: 3224–3234. PMID: [1620127](https://pubmed.ncbi.nlm.nih.gov/1620127/)
16. Shinohara A, Ogawa H, Ogawa T. Rad51 protein involved in repair and recombination in *S. cerevisiae* is a RecA-like protein. *Cell.* 1992. 69: 457–470. PMID: [1581961](https://pubmed.ncbi.nlm.nih.gov/1581961/)
17. Lin Z, Kong H, Nei M, Ma H. Origins and evolution of the *recA/RAD51* gene family: evidence for ancient gene duplication and endosymbiotic gene transfer. *Proc Natl Acad Sci U S A.* 2006. 103: 10328–10333. <https://doi.org/10.1073/pnas.0604232103> PMID: [16798872](https://pubmed.ncbi.nlm.nih.gov/16798872/)
18. Ramesh MA, Malik S-B, Logsdon JM. A phylogenomic inventory of meiotic genes; evidence for sex in *Giardia* and an early eukaryotic origin of meiosis. *Curr Biol.* 2005. 15: 185–191. <https://doi.org/10.1016/j.cub.2005.01.003> PMID: [15668177](https://pubmed.ncbi.nlm.nih.gov/15668177/)
19. Stassen NY, Logsdon JM Jr., Vora GJ, Offenberg HH, Palmer JD, Zolan ME. Isolation and characterization of *rad51* orthologs from *Coprinus cinereus* and *Lycopersicon esculentum*, and phylogenetic analysis of eukaryotic *recA* homologs. *Curr Genet.* 1997. 31: 144–157. PMID: [9021132](https://pubmed.ncbi.nlm.nih.gov/9021132/)
20. Baumann P, Benson FE, West SC. Human Rad51 protein promotes ATP-dependent homologous pairing and strand transfer reactions in vitro. *Cell.* 1996. 87: 757–766. PMID: [8929543](https://pubmed.ncbi.nlm.nih.gov/8929543/)
21. Hong EL, Shinohara A, Bishop DK. *Saccharomyces cerevisiae* Dmc1 protein promotes renaturation of single-strand DNA (ssDNA) and assimilation of ssDNA into homologous super-coiled duplex DNA. *J Biol Chem.* 2001. 276: 41906–41912. <https://doi.org/10.1074/jbc.M105563200> PMID: [11551925](https://pubmed.ncbi.nlm.nih.gov/11551925/)
22. Li Z, Golub EI, Gupta R, Radding CM. Recombination activities of HsDmc1 protein, the meiotic human homolog of RecA protein. *Proc Natl Acad Sci U S A.* 1997. 94: 11221–11226. PMID: [9326590](https://pubmed.ncbi.nlm.nih.gov/9326590/)
23. Masson JY, West SC. The Rad51 and Dmc1 recombinases: a non-identical twin relationship. *Trends Biochem Sci.* 2001. 26: 131–136. PMID: [11166572](https://pubmed.ncbi.nlm.nih.gov/11166572/)
24. Sheridan SD, Yu X, Roth R, Heuser JE, Sehorn MG, Sung P, et al. A comparative analysis of Dmc1 and Rad51 nucleoprotein filaments. *Nucleic Acids Res.* 2008. 36: 4057–4066. <https://doi.org/10.1093/nar/gkn352> PMID: [18535008](https://pubmed.ncbi.nlm.nih.gov/18535008/)
25. Sung P. Catalysis of ATP-dependent homologous DNA pairing and strand exchange by yeast RAD51 protein. *Science.* 1994. 265: 1241–1243. PMID: [8066464](https://pubmed.ncbi.nlm.nih.gov/8066464/)

26. Kagawa W, Kurumizaka H. From meiosis to postmeiotic events: uncovering the molecular roles of the meiosis-specific recombinase Dmc1. *FEBS J.* 2010. 277: 590–598. <https://doi.org/10.1111/j.1742-4658.2009.07503.x> PMID: 20015079
27. Bugreev DV, Pezza RJ, Mazina OM, Voloshin ON, Camerini-Otero RD, Mazin AV. The resistance of DMC1 D-loops to dissociation may account for the DMC1 requirement in meiosis. *Nat Struct Mol Biol.* 2011. 18: 56–60. <https://doi.org/10.1038/nsmb.1946> PMID: 21151113
28. Schwacha A, Kleckner N. Interhomolog bias during meiotic recombination: meiotic functions promote a highly differentiated interhomolog-only pathway. *Cell.* 1997. 90: 1123–1135. PMID: 9323140
29. Hong S, Sung Y, Yu M, Lee M, Kleckner N, Kim KP. The logic and mechanism of homologous recombination partner choice. *Mol Cell.* 2013. 51: 440–453. <https://doi.org/10.1016/j.molcel.2013.08.008> PMID: 23973374
30. Cloud V, Chan YL, Grubb J, Budke B, Bishop DK. Rad51 Is an Accessory Factor for Dmc1-Mediated Joint Molecule Formation During Meiosis. *Science.* 2012. 337: 1222–1225. <https://doi.org/10.1126/science.1219379> PMID: 22955832
31. Da Ines O, Degroote F, Goubely C, Amiard S, Gallego ME, White CI. Meiotic recombination in Arabidopsis is catalysed by DMC1, with RAD51 playing a supporting role. *PLoS Genet.* 2013. 9: e1003787. <https://doi.org/10.1371/journal.pgen.1003787> PMID: 24086145
32. Hunter N, Kleckner N. The single-end invasion: an asymmetric intermediate at the double-strand break to double-holliday junction transition of meiotic recombination. *Cell.* 2001. 106: 59–70. PMID: 11461702
33. Rockmill B, Roeder GS. The yeast med1 mutant undergoes both meiotic homolog nondisjunction and precocious separation of sister chromatids. *Genetics.* 1994. 136: 65–74. PMID: 8138177
34. Rockmill B, Sym M, Scherthan H, Roeder GS. Roles for two RecA homologs in promoting meiotic chromosome synapsis. *Genes Dev.* 1995. 9: 2684–2695. PMID: 7590245
35. Tsubouchi H, Roeder GS. The importance of genetic recombination for fidelity of chromosome pairing in meiosis. *Dev Cell.* 2003. 5: 915–925. PMID: 14667413
36. Pittman DL, Cobb J, Schimenti KJ, Wilson LA, Cooper DM, Brignull E, et al. Meiotic prophase arrest with failure of chromosome synapsis in mice deficient for Dmc1, a germline-specific RecA homolog. *Mol Cell.* 1998. 1: 697–705. PMID: 9660953
37. Yoshida K, Kondoh G, Matsuda Y, Habu T, Nishimune Y, Morita T. The mouse RecA-like gene Dmc1 is required for homologous chromosome synapsis during meiosis. *Mol Cell.* 1998. 1: 707–718. PMID: 9660954
38. Lim DS, Hasty P. A mutation in mouse *rad51* results in an early embryonic lethal that is suppressed by a mutation in *p53*. *Mol Cell Biol.* 1996. 16: 7133–7143. PMID: 8943369
39. Tsuzuki T, Fujii Y, Sakumi K, Tominaga Y, Nakao K, Sekiguchi M, et al. Targeted disruption of the *Rad51* gene leads to lethality in embryonic mice. *Proc Natl Acad Sci U S A.* 1996. 93: 6236–6240. PMID: 8692798
40. Dai J, Voloshin O, Potapova S, Camerini-Otero RD. Meiotic Knockdown and Complementation Reveals Essential Role of RAD51 in Mouse Spermatogenesis. *Cell Rep.* 2017. 18: 1383–1394. <https://doi.org/10.1016/j.celrep.2017.01.024> PMID: 28178517
41. Franklin AE, McElver J, Sunjevaric I, Rothstein R, Bowen B, Cande WZ. Three-dimensional microscopy of the Rad51 recombination protein during meiotic prophase. *Plant Cell.* 1999. 11: 809–824. PMID: 10330467
42. Li J, Harper LC, Golubovskaya I, Wang CR, Weber D, Meeley RB, et al. Functional analysis of maize RAD51 in meiosis and double-strand break repair. *Genetics.* 2007. 176: 1469–1482. <https://doi.org/10.1534/genetics.106.062604> PMID: 17507687
43. Rajanikant C, Melzer M, Rao BJ, Sainis JK. Homologous recombination properties of OsRad51, a recombinase from rice. *Plant Mol Biol.* 2008. 68: 479–491. <https://doi.org/10.1007/s11103-008-9385-6> PMID: 18695945
44. Morozumi Y, Ino R, Ikawa S, Mimida N, Shimizu T, Toki S, et al. Homologous pairing activities of two rice RAD51 proteins, RAD51A1 and RAD51A2. *PLoS One.* 2013. 8: e75451. <https://doi.org/10.1371/journal.pone.0075451> PMID: 24124491
45. Deng ZY, Wang T. OsDMC1 is required for homologous pairing in *Oryza sativa*. *Plant Mol Biol.* 2007. 65: 31–42. <https://doi.org/10.1007/s11103-007-9195-2> PMID: 17562186
46. Wang H, Hu Q, Tang D, Liu X, Du G, Shen Y, et al. OsDMC1 Is Not Required for Homologous Pairing in Rice Meiosis. *Plant Physiol.* 2016. 171: 230–241. <https://doi.org/10.1104/pp.16.00167> PMID: 26960731
47. Kathiresan A, Khush GS, Bennet J. Two rice *DMC1* genes are differentially expressed during meiosis and during haploid and diploid mitosis. *J Sex Plant Reprod.* 2002. 14: 257–267.

48. Ding Z-J, Wang T, Chong K, Bai S. Isolation and characterization of *OsDMC1*, the rice homologue of the yeast *DMC1* gene essential for meiosis. *J Sex Plant Reprod.* 2001. 13: 285–288.
49. Shimazu J, Matsukura C, Senda M, Ishikawa R, Akada S, Harada T, et al. Characterization of a *DMC1* homologue, *RiLIM15*, in meiotic panicles, mitotic cultured cells and mature leaves of rice (*Oryza sativa* L.). *Theor Appl Genet.* 2001. 102: 1159–1163.
50. Couteau F, Belzile F, Horlow C, Grandjean O, Vezon D, Doutriaux MP. Random chromosome segregation without meiotic arrest in both male and female meiocytes of a *dmc1* mutant of *Arabidopsis*. *Plant Cell.* 1999. 11: 1623–1634. PMID: [10488231](#)
51. Li W, Chen C, Markmann-Mulisch U, Timofejeva L, Schmelzer E, Ma H, et al. The *Arabidopsis AtRAD51* gene is dispensable for vegetative development but required for meiosis. *Proc Natl Acad Sci U S A.* 2004. 101: 10596–10601. <https://doi.org/10.1073/pnas.0404110101> PMID: [15249667](#)
52. Kobayashi W, Sekine S, Machida S, Kurumizaka H. Green fluorescent protein fused to the C terminus of RAD51 specifically interferes with secondary DNA binding by the RAD51-ssDNA complex. *Genes Genet Syst.* 2014. 89: 169–179. <https://doi.org/10.1266/ggs.89.169> PMID: [25747041](#)
53. Berchowitz LE, Copenhaver GP. Fluorescent *Arabidopsis* tetrads: a visual assay for quickly developing large crossover and crossover interference data sets. *Nat Protoc.* 2008. 3: 41–50. <https://doi.org/10.1038/nprot.2007.491> PMID: [18193020](#)
54. Yelina NE, Ziolkowski PA, Miller N, Zhao X, Kelly KA, Muñoz DF, et al. High-throughput analysis of meiotic crossover frequency and interference via flow cytometry of fluorescent pollen in *Arabidopsis thaliana*. *Nat Protoc.* 2013. 8: 2119–2134. <https://doi.org/10.1038/nprot.2013.131> PMID: [24113785](#)
55. Sanchez Moran E, Armstrong SJ, Santos JL, Franklin FC, Jones GH. Chiasma formation in *Arabidopsis thaliana* accession Wassilewskija and in two meiotic mutants. *Chromosome Res.* 2001. 9: 121–128. PMID: [11321367](#)
56. Chelysheva L, Vezon D, Chambon A, Gendrot G, Pereira L, Lemhemdi A, et al. The *Arabidopsis* HEI10 is a New ZMM Protein Related to Zip3. *PLoS Genet.* 2012. 8: e1002799. <https://doi.org/10.1371/journal.pgen.1002799> PMID: [22844245](#)
57. Higgins JD, Sanchez-Moran E, Armstrong SJ, Jones GH, Franklin FC. The *Arabidopsis* synaptonemal complex protein ZYP1 is required for chromosome synapsis and normal fidelity of crossing over. *Genes Dev.* 2005. 19: 2488–2500. <https://doi.org/10.1101/gad.354705> PMID: [16230536](#)
58. Armstrong S (2013) A time course for the analysis of meiotic progression in *Arabidopsis thaliana*. In: Pawlowski W., Grelon M. and Armstrong S., editors. *Plant Meiosis Methods in Molecular Biology (Methods and Protocols)*. Totowa, NJ: Humana Press. pp. 119–123.
59. Lydall D, Nikolsky Y, Bishop DK, Weinert T. A meiotic recombination checkpoint controlled by mitotic checkpoint genes. *Nature.* 1996. 383: 840–843. <https://doi.org/10.1038/383840a0> PMID: [8893012](#)
60. Callender TL, Laureau R, Wan L, Chen X, Sandhu R, Laljee S, et al. Mek1 Down Regulates Rad51 Activity during Yeast Meiosis by Phosphorylation of Hed1. *PLoS Genet.* 2016. 12: e1006226. <https://doi.org/10.1371/journal.pgen.1006226> PMID: [27483004](#)
61. Kurzbauer M-T, Uanschou C, Chen D, Schlögelhofer P. The recombinases DMC1 and RAD51 are functionally and spatially separated during meiosis in *Arabidopsis*. *Plant Cell.* 2012. 24: 2058–2070. <https://doi.org/10.1105/tpc.112.098459> PMID: [22589466](#)
62. Uanschou C, Ronceret A, Von Harder M, De Muyt A, Vezon D, Pereira L, et al. Sufficient amounts of functional HOP2/MND1 complex promote interhomolog DNA repair but are dispensable for intersister DNA repair during meiosis in *Arabidopsis*. *Plant Cell.* 2013. 25: 4924–4940. <https://doi.org/10.1105/tpc.113.118521> PMID: [24363313](#)
63. Pradillo M, López E, Linacero R, Romero C, Cuñado N, Sanchez-Moran E, et al. Together yes, but not coupled: new insights into the roles of RAD51 and DMC1 in plant meiotic recombination. *Plant J.* 2012. 69: 921–933. <https://doi.org/10.1111/j.1365-313X.2011.04845.x> PMID: [22066484](#)
64. Yelina NE, Choi K, Chelysheva L, Macaulay M, de Snoo B, Wijnker E, et al. Epigenetic remodeling of meiotic crossover frequency in *Arabidopsis thaliana* DNA methyltransferase mutants. *PLoS Genet.* 2012. 8: e1002844. <https://doi.org/10.1371/journal.pgen.1002844> PMID: [22876192](#)
65. Armstrong S, Caryl A, Jones G, Franklin F. Asy1, a protein required for meiotic chromosome synapsis, localizes to axis-associated chromatin in *Arabidopsis* and *Brassica*. *J Cell Sci.* 2002. 115: 3645–3655. PMID: [12186950](#)
66. Higgins JD, Armstrong SJ, Franklin FCH, Jones GH. The *Arabidopsis* MutS homolog ATM5H4 functions at an early step in recombination: evidence for two classes of recombination in *Arabidopsis*. *Genes Dev.* 2004. 18: 2557–2570. <https://doi.org/10.1101/gad.317504> PMID: [15489296](#)
67. Stronghill PE, Azimi W, Hasenkampf CA. A novel method to follow meiotic progression in *Arabidopsis* using confocal microscopy and 5-ethynyl-2'-deoxyuridine labeling. *Plant Methods.* 2014. 10: 33. <https://doi.org/10.1186/1746-4811-10-33> PMID: [25337148](#)

68. Ross KJ, Franz P, Jones GH. A light microscopic atlas of meiosis in *Arabidopsis thaliana*. Chromosome Res. 1996. 4: 507–516. PMID: [8939362](#)
69. Franz P, Armstrong S, Alonso-Blanco C, Fischer TC, Torres-Ruiz RA, Jones G. Cytogenetics for the model system *Arabidopsis thaliana*. Plant J. 1998. 13: 867–876. PMID: [9681023](#)

Chapter 4

Cytogenetics of partial synapsis in the absence of RAD51 and XRCC3

4.1 Introduction

Homologous recombination during Prophase 1 is crucial for correct synapsis and segregation homologous chromosomes in the first meiotic division (MI) and thus fertility. Very considerable advances have been made in understanding of the links between meiotic recombination and synapsis of homologues, but we do not still fully understand these processes.

RAD51 and the RAD51 paralogues XRCC3 and RAD51C, which support its activity, are essential for the repair of meiotic SPO11-induced DSB and their absence thus results in meiotic prophase I chromosome fragmentation in *Arabidopsis* (Abe et al., 2005; Bleuyard et al., 2005; Bleuyard and White, 2004; Li et al., 2005; Vignard et al., 2007). RAD51 (or DMC1 + RAD51 in meiosis) catalyses the search for, and invasion of the homologous template sequence and is thus key to the establishment of the physical links between homologous chromosomes. Thus, it is the induction of DSB in Leptotene and their repair that establishes the co-alignment of homologous chromosome axes visible in Zygotene, making the observation that the chromosomal fragmentation occurs in late Zygotene/early Pachytene both unexpected and striking.

Immunocytology and FISH studies confirmed the partial synapsis of homologues in *rad51* and *xrcc3* and pointed to a specificity of centromeric and rDNA regions, which depend principally on DMC1 and not on RAD51

recombination for synapsis. (Bleuyard and White, 2004; Da Ines et al., 2012).

RAD51-independent, DMC1- and SPO11-dependent partial synapsis in *rad51* and *xrcc3* mutants is thus due to homologous chromosome pairing at centromeric and rDNA regions (Da Ines et al., 2012). This, together with the absence of chromosome arm synapsis in these mutants suggests DMC1-driven initiation of synapsis in these regions, which is further stabilised and extended along chromosome arms through RAD51-dependent homologous recombination (Da Ines et al., 2012). The activity of DMC1 depends upon the presence (not the strand-exchange activity) of RAD51 nucleofilaments (Cloud et al., 2012; Da Ines et al., 2012; Da Ines et al., 2013b; Kobayashi et al., 2014; Su et al., 2017), and the pairing and synapsis of arm regions is dependent on both DMC1 and RAD51 (which in turn is dependent upon the presence of XRCC3). Thus, DMC1 is capable of (at least partial) synapsis of centromeric and rDNA regions in the absence of RAD51, but requires the presence of RAD51 protein elsewhere, pointing to a specificity of peri-centromeric and rDNA regions in the requirement for the presence of RAD51 to support the action of DMC1. This conclusion leads to the two questions, which are the basis of the work resented in this part of my thesis work:

- 1) Does meiotic chromosome synapsis in Arabidopsis begin at centromeres/peri-centromeres and then extend though the chromosome arms?

2) What is the interdependence of centromere and arm synapsis?

4.2 Result and Discussion

To answer these questions I performed Co-Immunolocalisation experiments, using antisera against ASY1 (Synaptonemal Complex axis-associated protein), ZYP1 (Synaptonemal Complex transverse filament protein) and CENH3 (centromeric histone H3). These experiments were carried out on meiotic chromosome spreads from wild type, *rad51* and *xrcc3* plants, combined with SIM (Super resolution) and epi-fluorescence microscopy. In this work I analysed the SIM images of WT (15 cells), *rad51* (19 cells), *xrcc3* (25 cells) and also epi-fluorescence microscopy images of WT (30 cells), *rad51* (30 cells), *xrcc3* (30 cells). This analysis yielded three important observations:

1. Short stretches of ZYP1 fibre, and thus presumably SC, were observed in *xrcc3* and *rad51* mutants at zygo-pachytene stages (FIG_16). Although it has previously been concluded that SC is absent in *xrcc3* meiosis (Vignard et al., 2007), presence of these stretches suggests that even if *xrcc3* and *rad51* plants are unable to complete synapsis and their chromosomes fragment after the zygo-pachytene stage, they have some short stretches of synapsed chromosomes.

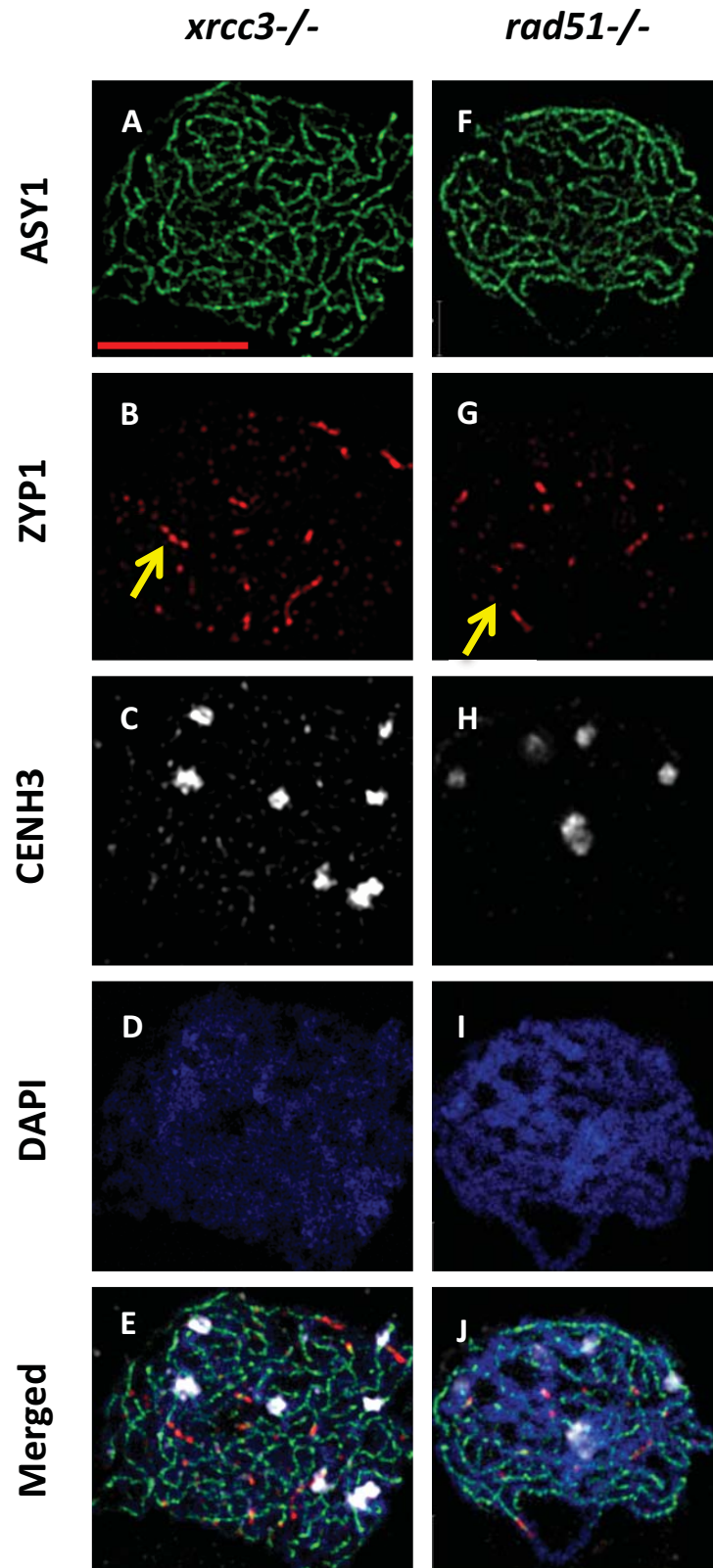


Figure_16: Immunolocalization of short stretches of ZYP1 fibres. ASY1 (green), ZYP1 (red) and CENH3 (white) during Prophase I. (A-E) *xrcc3/xrcc3* (F-J) *rad51/rad51*. Short stretches of ZYP1 fibres are visible in *xrcc3* and *rad51* mutants. Scale bar 5 μ m.

2. Centromere pairing is an early event in meiotic chromosome pairing and has been well described in *Arabidopsis* (Armstrong et al., 2001). *Arabidopsis* centromeres are unpaired and dispersed during meiotic interphase up to leptotene, cluster at leptotene/zygotene, separate and homologous centromeres then associate in pairs and synapse in zygotene and pachytene. Observation of meiotic centromeres in WT, *xrcc3* and *rad51* marked by CENH3 antibody, showed as expected that in WT meiocytes there are 7-9 signals of centromere at zygotene and 3-5 at pachytene (Fig_2). Even in *xrcc3* and *rad51*, in which chromosomes fragment after zygo-pachytene, 7-9 centromeric foci per nucleus were visible at zygotene and 3-5 at pachytene (Fig_17). These microscopy results are similar to previously published centromere coupling, clustering and pairing data in *Arabidopsis* (Da Ines et al., 2012; Da Ines et al., 2014; Fransz et al., 1998; Su et al., 2017).

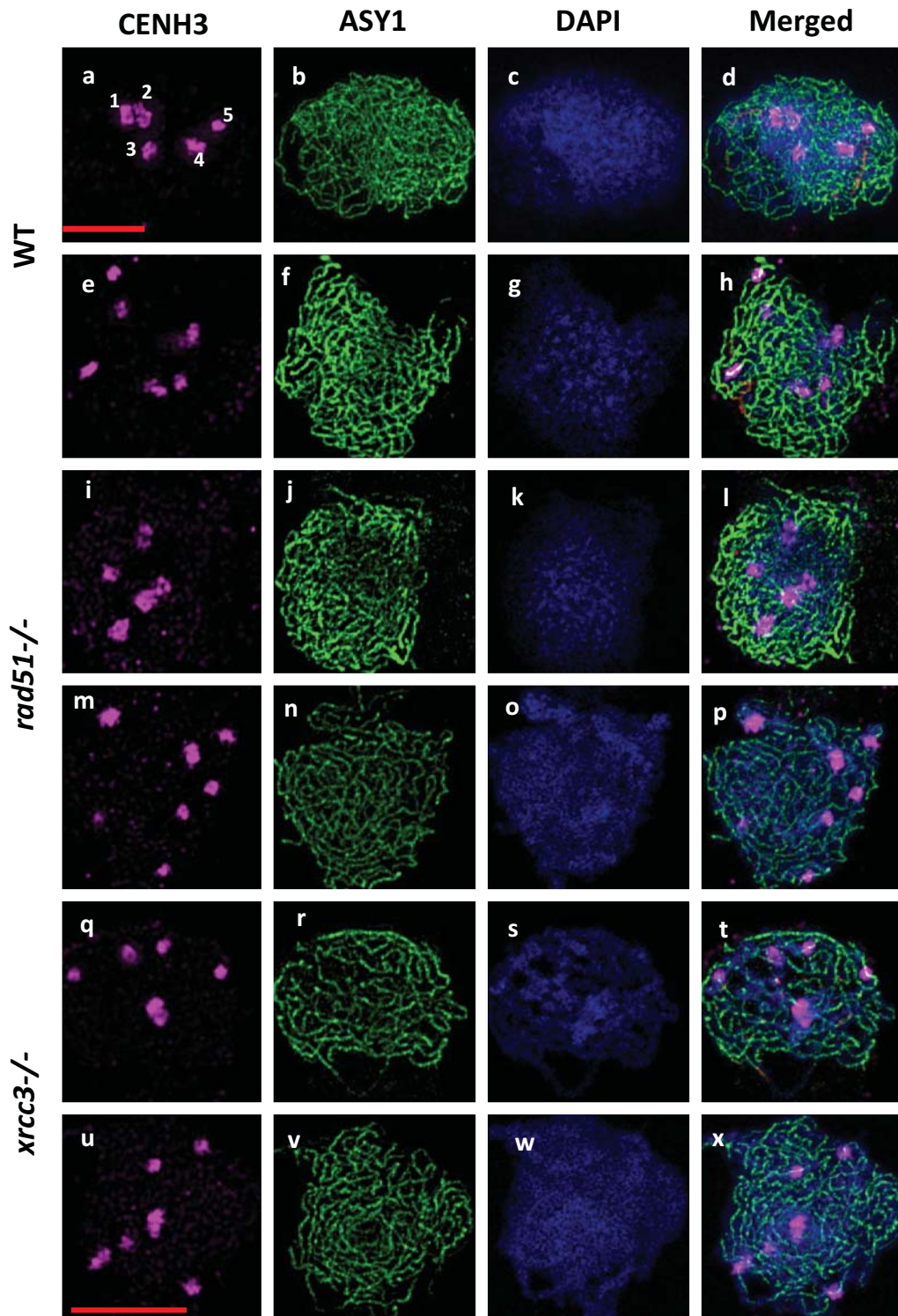


Figure_17: Immunolocalization of CENH3 marking Centromeres. ASY1 (green), DAPI (blue) and CENH3 (magenta) during Prophase I. CENH3 marking the centromere (a-d, e-h) in WT, (i-l, m-p) in *rad51* (q-t, u-x) in *xrc3* plants. Centromeres are completely paired in images (a), (i) and (q), and partial in (e), (m) and (u). Scale bar 5 μ m.

3. Previous work from the lab with the RAD51 paralogue mutants, *xrcc3* and *rad51C*, showed homologous centromere pairing at meiosis which can extend for at least 2 Mb from centromere, well into the euchromatic pericentromeric regions (Da Ines et al., 2012). This led to the hypothesis that the short ZYP1 fibres observed in these nuclei correspond to synapsis and initiation of SC formation in these regions. I thus carried out immunolocalisation in WT, *rad51* and *xrcc3* meiosis to look for colocalisation of ZYP1 fibres and centromeric regions. The results of this study disprove this hypothesis. As shown in Fig_19, although some ZYP1 fibers (SC protein) initiate from centromeres, more often they do not. This conclusion was confirmed by the analysis of SIM microscopy images, which showed both full pairing of centromeres before the appearance of ZYP1 and the presence of short ZYP1 fibres with centromeres being unpaired or partly paired. The data from this experiment clearly shows that the short ZYP1 fibres do not specifically originate at centromeres and thus that either synapsis begins randomly on centromeres (Fig_19A) or elsewhere (Fig_19B), or that the short ZYP1 fibres do not mark regions of homologous synapsis.

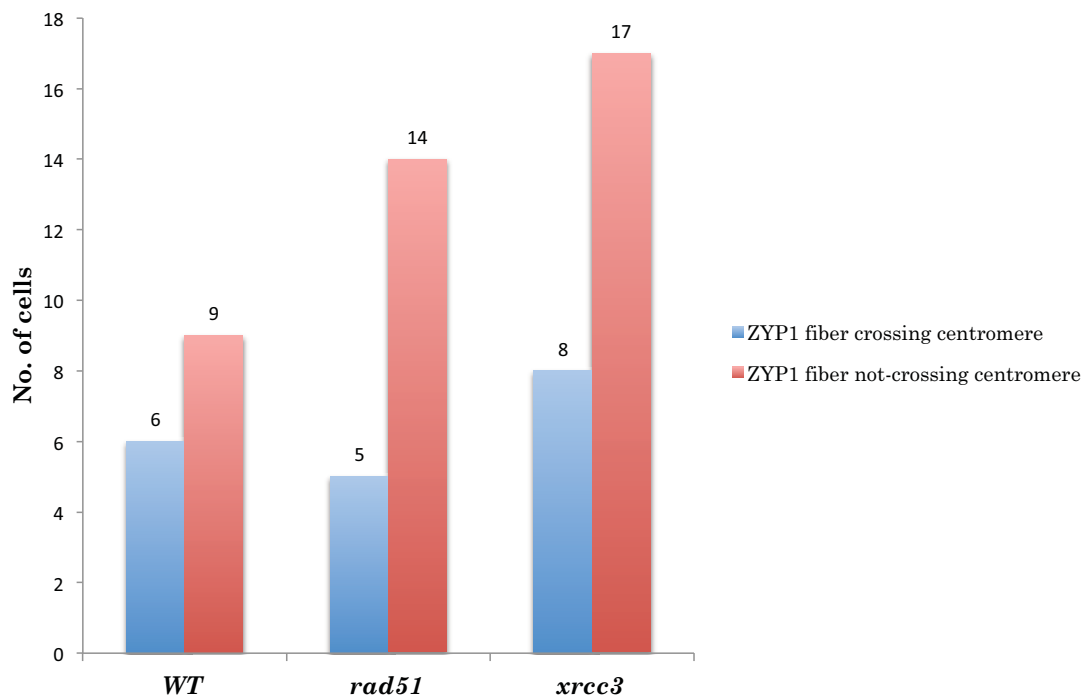


Figure_18: Graphical representation of ZYP1 fragments counts, crossing or not crossing the centromere in *WT*, *xrcc3* and *rad51* mutants.

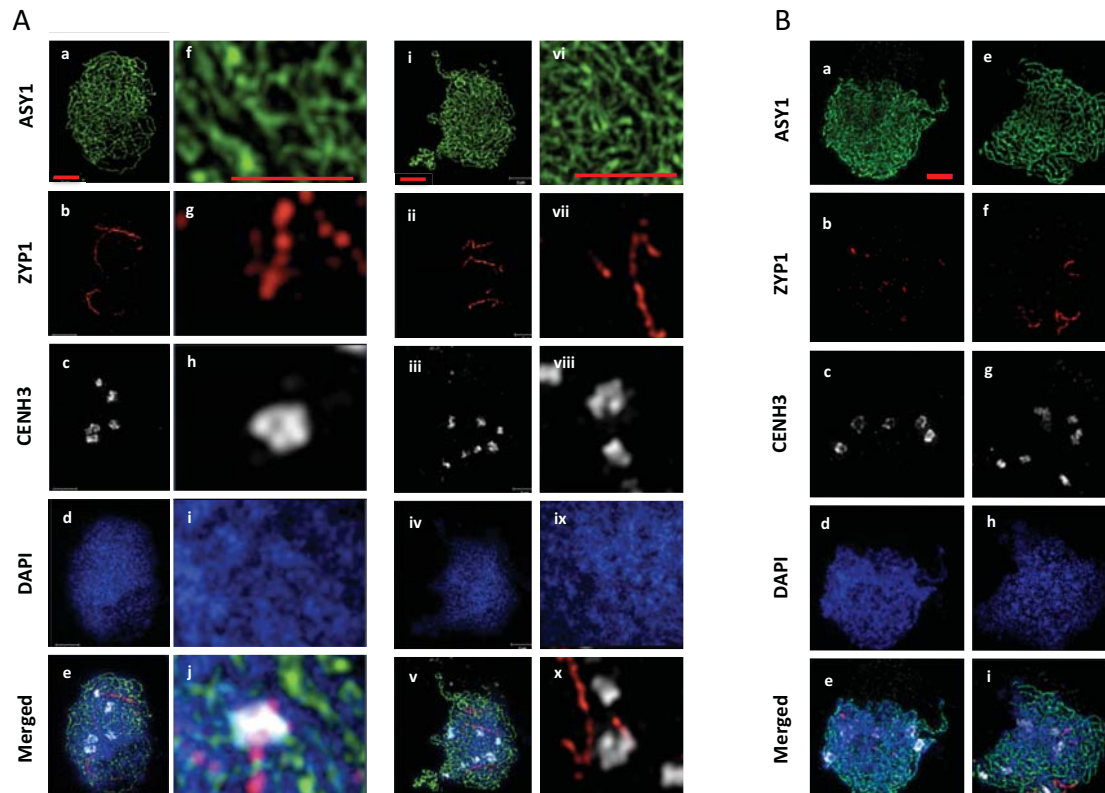


Figure_19: Immunolocalization of ZYP1 initiation point. ASY1 (green), ZYP1 (red) and CENH3 (white) during Zygotene. In image (A) (a-e) and (i-v)) showing the ZYP1 initiating from centromere. (A (f-j) and (vi-x)) is the zoom in of (A (a-e) and (i-v)). In image (B (A-E) and (F-J)) showing the ZYP1 initiating from centromere. (A (f-j) and (vi-x)) is the zoom in of (A (a-e) and (i-v)). Scale bar 5µm.

Chapter 5

Creation of specific targeted meiotic recombination hot-spots through the targeted induction of DNA breaks for the study of the roles of RAD51 and DMC1 in peri-centromeric and chromosome arm regions.

5.1 Introduction

Engineering of human, animal and plant genomes is key to basic biology research, medical advances and crop improvement. The ability to insert, remove or even edit DNA sequences easily and precisely has attracted the interest of the scientific community in a wide range of biotechnology areas, such as medicine, energy and even environmental studies. Targetable nucleases are paving the way for this and a new era is emerging fast with new tools and techniques able to engineer the genome with even greater facility and impact. Targetable nucleases enable scientists to target and modify theoretically any gene in any organism (Ding et al., 2016; Komor et al., 2017; Takasu et al., 2010). Three classes of sequence-specific nucleases have been employed for the majority of this work: meganucleases, zinc-finger nucleases (ZFNs) and transcription activator-like effector nucleases (TALENs). They all permit targeting double-strand breaks (DSBs) in DNA to allow gene editing via endogenous DNA lesion repair pathways (Gaj et al., 2013; Li et al., 2012; Mussolino and Cathomen, 2013; Streubel et al., 2012; Zhang et al., 2010; Zhang et al., 2013). However, the issue with these technologies is that they require elaborate designing and assembly of individual DNA-binding proteins for each DNA target site. Recently a new addition to this list has solved this problem and is being actively employed in all imaginable biological contexts. This is a bacterial CRISPR/Cas system (Segal and Meckler, 2013). CRISPR/Cas is a simple, versatile and efficient RNA-guided gene-editing tool (Jinek et al., 2012),

programmed to target specific genomic sites with a single chimeric RNA (single guide RNA, sgRNA), with a higher degree of flexibility for target selection than protein-guided targeting tools. This system has been demonstrated to facilitate genome editing in diverse species, including animals (including humans), microbes, and plants (Fan et al., 2015; Feng et al., 2013; Li et al., 2013; Miao et al., 2013; Schiml et al., 2014; Shan et al., 2013; Sun et al., 2015; Wang et al., 2013; Xie and Yang, 2013; Xu et al., 2015; Zhang et al., 2014). Expression of the *S. pyogenes* Cas9 (SpCas9) and an artificial chimera of crRNA and tracrRNA called guide RNA (gRNA) in eukaryotic cells (Fig_20), targeted genome editing has been readily achieved via either error-prone non-homologous end joining (NHEJ) or homology-directed repair (HDR) of the cleavage site (Fig_21) (Cho et al., 2013; Cong et al., 2013; DiCarlo et al., 2013; Hwang et al., 2013; Jinek et al., 2012; Jinek et al., 2013; Mali et al., 2013; Wang et al., 2013).

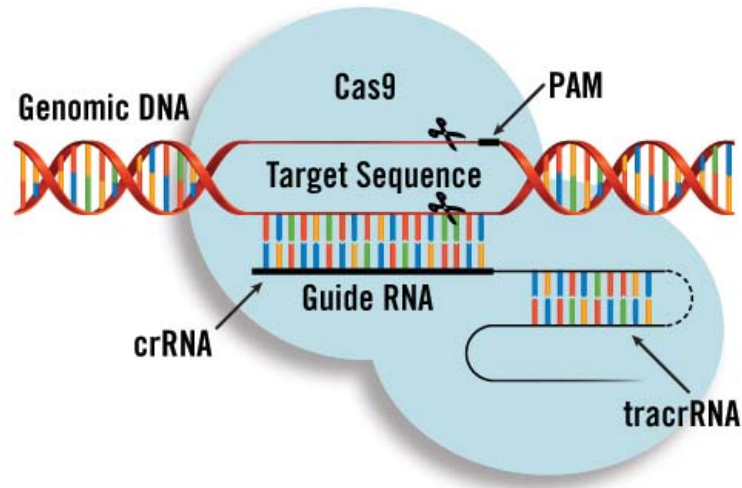


Figure_20: CRISPR/Cas9 Genome Editing. The Cas9 endonuclease (blue) is targeted to DNA by a guide RNA, which can be supplied as a two-part system consisting of crRNA and tracrRNA or as a single guide RNA, where the crRNA and tracrRNA are connected by a linker (dotted line). Target recognition is facilitated by the protospacer-adjacent motif (PAM). Cleavage occurs on both strands (scissors) 3-4 bp upstream of the PAM.

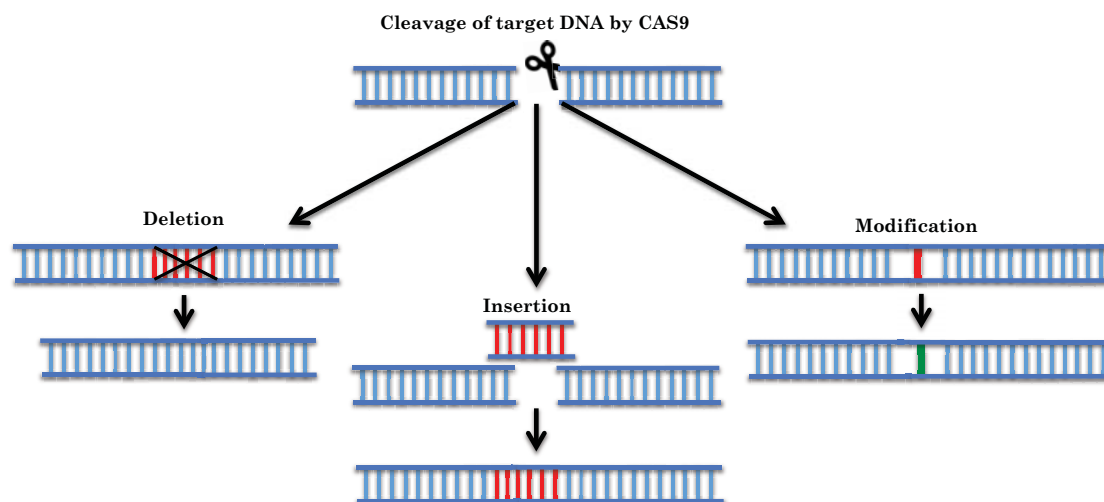


Figure_21: Schematic representation of multiple genomic alterations possibility, following cleavage of target DNA by Cas9. Variable length insertions and/or deletions (indels) can result near the DNA break due to mistakes in DNA repair by the endogenous non-homologous end-joining (NHEJ) pathway. These indels frequently result in disruption of gene function. Alternatively, by supplying a DNA repair template, researchers can leverage the homology-directed repair (HDR) pathway to create defined deletions, insertions or modifications.

With the aim of creating targeted initiation of meiotic recombination at specific pre-determined sites in order to extend our studies of the meiotic roles of RAD51 and DMC1, I built tools to induce DSB in the centromere-spanning CEN3 and chromosome-arm I1bc genetic intervals described in Chapter 1 and the PLoS One article (Singh et al., 2017). This work was carried out using the plant codon-optimized pDE-Cas9 system kindly provided by the Puchta lab (Fauser et al., 2014).

Through comparison of the *Arabidopsis Col-0* and *Ler-0* ecotype genome sequences, I identified target sequences containing single nucleotide polymorphisms (SNP) to make them specific for the *Col-0* ecotype. This was done with the aim of studying the effects on meiotic recombination (and ultimately the molecular mechanisms) of the targeted induction of chromosomal DSB. The use of *Col-0*-specific Cas9/gRNA cleavage in *Col-0/Ler-0* F1 hybrid plants was planned for three reasons: firstly, it will determine which of the two homologues is the initiator of recombination (the *Col-0* one); secondly, the presence of SNPs in sequences flanking the DSB site will permit the analyses of both CO and NCO events and gene conversion tracks and finally, will avoid the possibility of both the target sequence of the *Col-0* chromosome and its *Ler-0* homologue being cut simultaneously. The targets were also chosen such that the SNPs created restriction site polymorphisms to facilitate further work. gRNA targeting the *Arabidopsis thaliana Col-0* genome within the centromeric and arm interval site were built. (Fig_22).

5.2 Result and Discussion

FTL marker lines (Berchowitz and Copenhaver, 2008; Yelina et al., 2013) were used to test for effects of Cas9/gRNA on recombination and meiotic CO rates targeting in pericentromeric regions and mid arm intervals. The pollen-expressed, red, cyan and yellow fluorescent protein markers in these lines provide a rapid and precise means of measuring genetic map-distance in defined genetic intervals in Arabidopsis. We used the FTL lines I1c carrying linked insertions on the arm of chromosome 1 (I1c: FTL992 and FTL1262, and; FTL992: FTL1262 = 19.2 cM), and CEN3, with two insertions spanning the centromere of chromosome 3 (CEN3: FTL3332: FTL2536 = 11.04 cM) (Yelina et al., 2013). The I1c and CEN3 lines were crossed with Col-0 WT homozygotes to generate F1 lines. These F1 lines were transformed by the CRISPR/Cas9 (driven by ubiquitin promoter) + gRNA (driven by U6-26 also ubiquitin promoter) constructs targeting in Col-0 background (detail vector map in Material and Methods).

I designed two different gRNA targeting in each interval and named them SNP1 and SNP2. Thus four different CRISPR constructs were built, two targeting sites within the CEN3 (Cas9:SNP1_CEN3 and Cas9:SNP2_CEN3) and two in I1c (Cas9:SNP1_I1c and Cas9:SNP2_I1c) FTL intervals in *Col-0* background, but not *Ler-0* plants (because of the presence of SNPs in targets in *Ler-0* these Cas9 constructs should not cut the *Ler-0* (Fig_22B)) were built and transformed into plants (Fig_22).

The four target sites are shown in Fig_22 with the Ler-0 SNPs and restriction site polymorphism shown in each case. These transformations were carried out in Col-0 mapping lines to permit testing of the efficiency of target cleavage and to check for effects on meiotic crossing-over for each Cas9/gRNA pair. Thus, the CEN3-target constructs (Cas9:SNP1_CEN3 and Cas9/SNP2_CEN3) were transformed into double heterozygote (coupling) CEN3 Col-0 plants and the I1c target constructs (Cas9:SNP1_I1c and Cas9:SNP2_I1c) were transformed into I1c Col-0 plants.

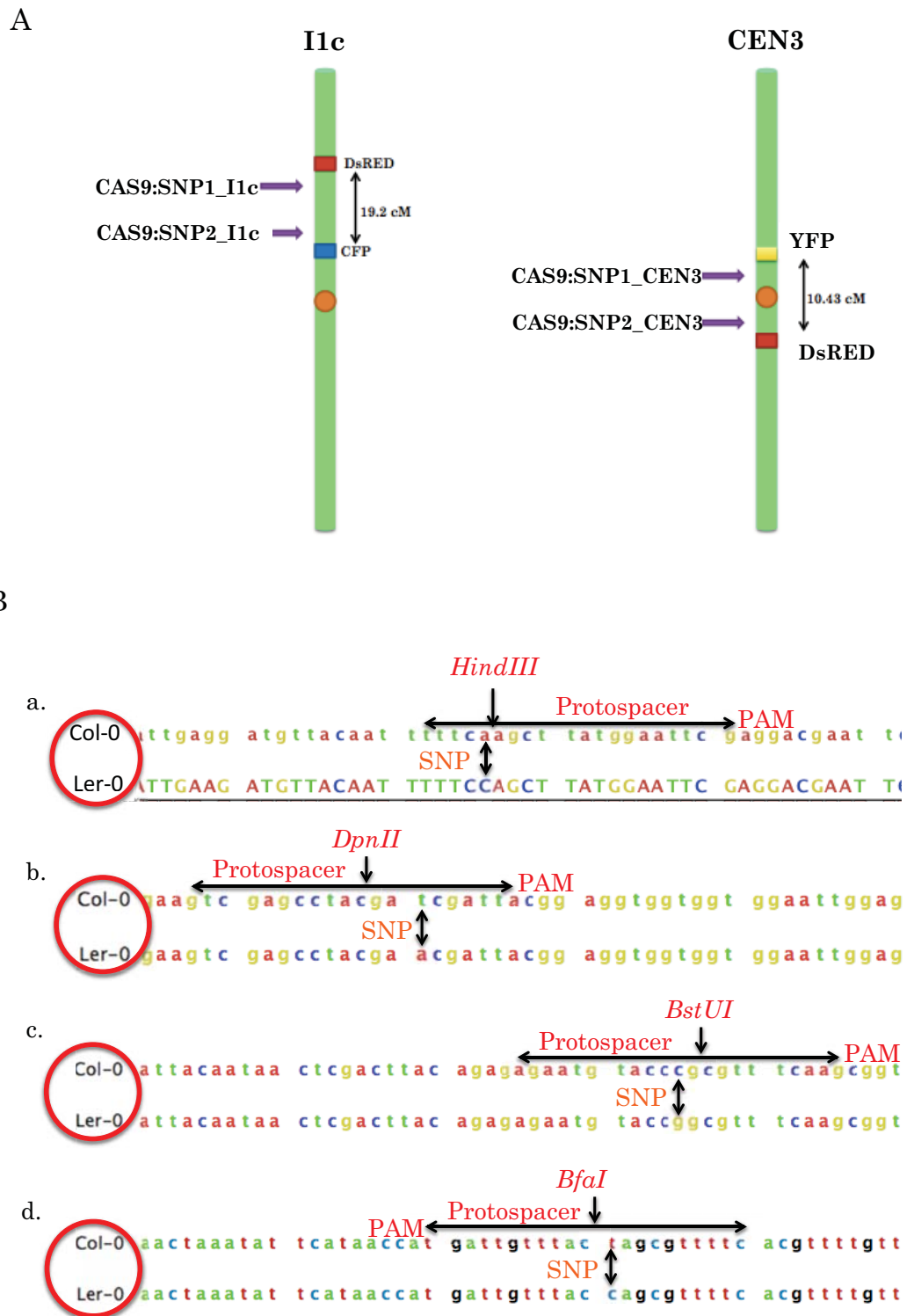


Figure_22: Schematic presentation of Cas9/gRNA designing. (A) Cas9_gRNA targeting in I1C and CEN3 intervals. (B) The targets were chosen to include SNP that confer specificity to the *Col-0* ecotype. (Ba) Cas9:SNP1_CEN3, (Bb) Cas9:SNP2_CEN3, (Bc) Cas9:SNP1_I1c, & (Bd) Cas9:SNP2_I1C. The expected Cas9 cleavage sites lie 4-5bp upstream of the PAM sequence in each case.

The expression of these constructs in *Col-0* FTL lines background will induce DSB and their repair by NHEJ will result in elevated site-specific mutagenesis at the target sites. To test this I amplified the target sites of transformed plants by PCR, cloned them into pGEM-Teasy vector and sent 96 clones of each for sequencing.

Analysis of the sequences of 96 well plate Sanger sequencing data of genomic target sites of the transformed *Col-0* FTL lines (CEN3 and I1c) confirmed strong activity of the Cas9:SNP2_CEN3 construct (10 mutations/60 sequences) (Fig_24), and less so in the other three; Cas9:SNP1_CEN3, Cas9:SNP1_I1c, Cas9:SNP2_I1c (3/92, 0/90, 1/83) (Fig_23, Fig_25, and Fig_26). Such variability in mutagenesis efficiencies at different target sites is to be expected and these results confirm that one, and probably 2 or 3 of the constructs Cas9:CEN3_SNP1 and Cas9:CEN3_SNP2 are working efficiently.

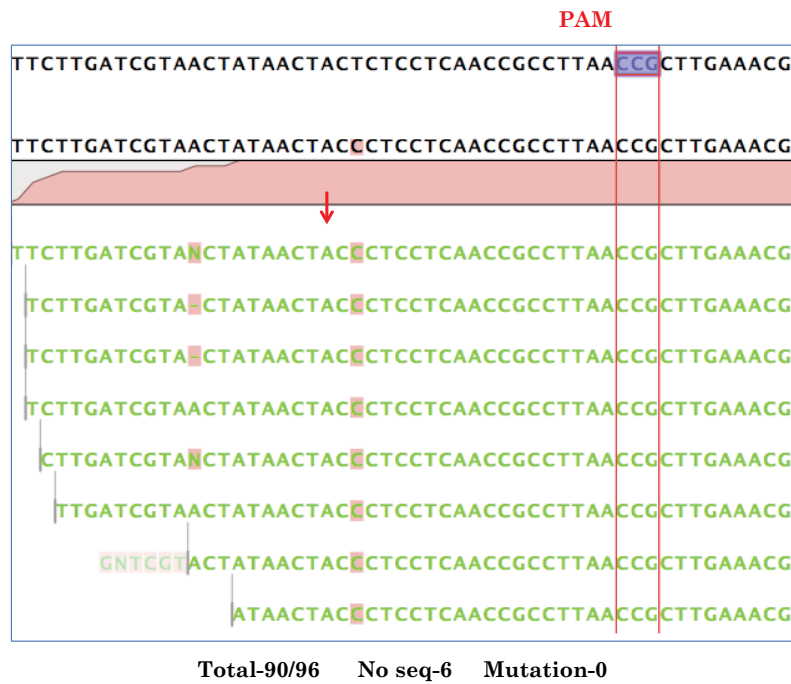


Figure_25: Sanger sequencing data of Cas9:SNP1_I1c

The 20nt Cas9 is expected to cut the target site between the fourth and fifth nt. upstream of the PAM sequence. Mutations detected in the sequencing results are marked with red.



Figure_26: Sanger sequencing data of Cas9:SNP2_I1c.

The 20nt Cas9 is expected to cut the target site between the fourth and fifth nt. upstream of the PAM sequence. Mutations detected in the sequencing results are marked with red.

Effects on recombination of targeting the CEN3 interval in meiosis.

After validation by the sequencing data from these CRISPR/gRNA transformants, The transformed double heterozygote mapping lines (CEN3, I1c) carrying the *Cas9/gRNA* constructs were tested for effect of meiotic crossing-over rate. To guard against biases in scoring, the 1:1 ratio of presence/absence of the individual markers was verified with a Chi-squared test in each data set (Fig_27B, 28B, 30B and Table_1 & 2).

Recombination data in CEN3 interval

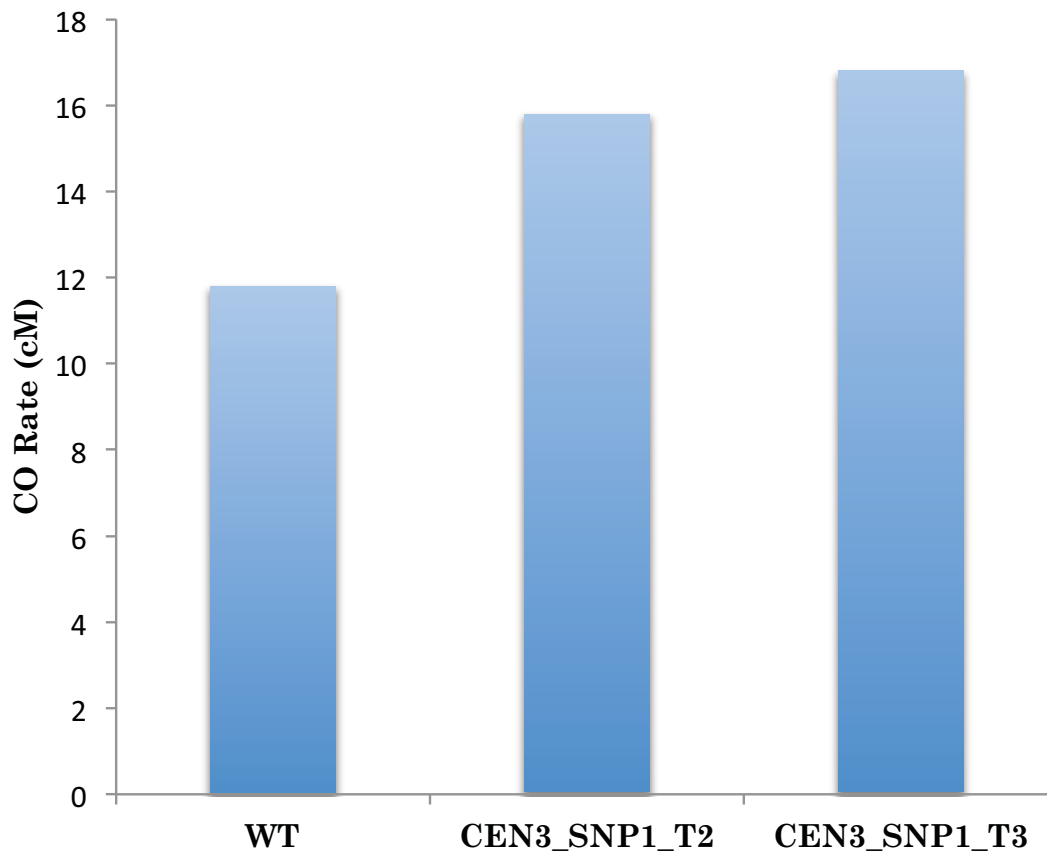
For the first target in the CEN3 interval Cas9:SNP1_CEN3. the pollen count data and statistical analysis showed the recombination rate was increased in both T2 and T3 generations as compared to WT controls (Cas9^{-/-}).

WT: mean±sem = 11.8±0.001 cM; 2 plants, total pollen scored = 1448 (Fig_27B)

Cas9:SNP1_CEN3_T2 (up-regulated): mean±sem = 15.8±0.003 cM; 2 plants, total pollen scored = 1530.

Cas9:SNP1_CEN3_T3 (up-regulated): mean±sem = 16.8±0.006 cM; 2 plants, total pollen scored = 1497 (Fig_27).

A.



B.

Pollen Counts								
Plant#	R	Y	R+Y	neither	total	r	Chi2 R:not R	Chi2 Y:not Y
WT#1	40	45	300	329	714	0.119	1.619	0.807
WT#2	46	40	317	331	734	0.117	0.087	0.545
T2 generation								
Cas9:SNP1_CEN3#1	65	80	386	369	900	0.161	0.044	1.138
Cas9:SNP1_CEN3#2	51	62	301	316	730	0.155	0.926	0.882
T3 generation								
Cas9:SNP1_CEN3#1.1	64	54	288	322	728	0.162	0.791	2.659
Cas9:SNP1_CEN3#1.2	60	74	300	335	769	0.174	3.122	0.573

Figure_27: Genetic map distance in Cas9:SNP1_CEN3 interval (A) Graphical representation of genetic map distance of the Cas9:SNP1_CEN3 and WT interval. (B) Pollen counts and recombination rate (r) in the Cas9:SNP1_CEN3 interval.

A simple mapping of the second target in the CEN3 interval, Cas9:SNP2_CEN3, showed that in one transformant the CO rate was up regulated in both generation T2 and T3.

WT: mean \pm sem = 11.8 \pm 0.001 cM; 2 plants, total pollen scored = 1448

Transformant1:

Cas9:SNP2_CEN3_T2 (up-regulated): mean \pm sem = 15.65 \pm 0.0075cM; 2 plants, total pollen scored = 1276.

Cas9:SNP2_CEN3_T3: mean \pm sem = 11.45 \pm 0.0185 cM; 2 plants, total pollen scored = 1493 (Fig_28).

On the other hand, in the second tested transformant line the recombination rate was decreased.

Transformant 2:

Cas9:SNP2_CEN3_T2 (down-regulated): mean \pm sem = 4.2 \pm 0.016cM; 2 plants, total pollen scored = 1603

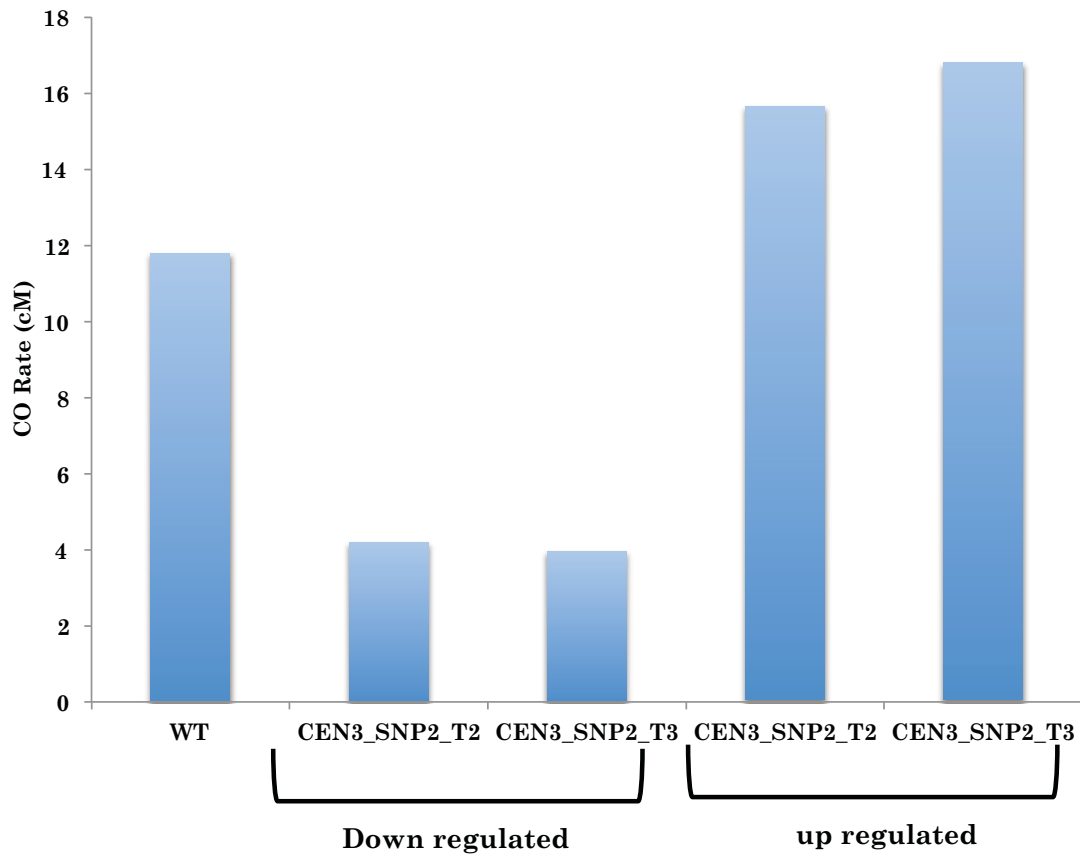
Cas9:SNP2_CEN3_T3 (down-regulated): mean \pm sem = 3.95 \pm 0.006 cM; 2 plants, total pollen scored = 3782 (Fig_28).

Thus in this line (Cas9:SNP2_CEN3) recombination rates differed markedly between different T2 plants from different transformants (both hyper-rec and hypo-rec. Fig_28B). One hyper-rec (Cas9:SNP2_CEN3#1) and one hypo-rec (Cas9:SNP2_CEN3#2). I took these plants to the T3 generation and performed the pollen count from two plants of each (Cas9:SNP2_CEN3#1 and Cas9:SNP2_CEN3#2).

T3 plants from the hyper-rec line (Cas9:SNP2_CEN3#3.1, Cas9:SNP2_CEN3#3.2) showed again differing recombination rates, remaining weakly hyper-rec (Fig. 28B, C).

T3 plants from the hypo-rec line (Cas9:SNP2_CEN3#1.1, Cas9:SNP2_CEN3#1.2) were strong hypo-rec, however this was accompanied by strong bias in pollen numbers against one of the parental chromosomes (not Red, not Yellow; Fig_28).

A.



B.

Pollen Counts								
Plant#	R	Y	R+Y	neither	total	r	Chi2 R:not R	Chi2 Y:not Y
T2 generation: Transformant 1								
Cas9:SNP2_CEN3#1	27	5	266	255	553	0.058	1.969	0.219
Cas9:SNP2_CEN3#2	6	13	349	355	723	0.026	0.234	0.001
T2 generation: Transformant 2								
Cas9:SNP2_CEN3#3	40	38	220	224	522	0.149	0.008	0.069
Cas9:SNP2_CEN3#4	96	81	430	474	1081	0.164	0.778	3.220
T3 generation								
Cas9:SNP2_CEN3#1.1	26	67	1882	61	2036	0.046	1556.18	1702.87
Cas9:SNP2_CEN3#1.2	25	32	1618	71	1746	0.033	1358.30	1383.11
Cas9:SNP2_CEN3#3.1	39	35	322	371	767	0.096	2.640	3.662
Cas9:SNP2_CEN3#3.2	54	43	303	326	726	0.133	0.198	1.592

Figure_28: Genetic map in Cas9:SNP2_CEN3 interval (A) Genetic map distance of the Cas9:SNP2_CEN3 and WT interval. (B) Pollen count and recombination rate (r) in the Cas9:SNP2_CEN3 interval.

Pollen Counts								
Plant#	P	R	Total	r(WT)	expP	expR	Chi2 (=WT)	p
Wild type	629	85	714	0.119	629.034	84.966	1.544	0.997
T2 generation: Transformant 1								
Cas9:SNP2_CEN3#1	521	32	553	0.119	487.193	65.807	19.713	8.996E-06
Cas9:SNP2_CEN3#2	704	19	723	0.119	636.963	86.037	59.288	1.362E-14
T2 generation: Transformant 2								
Cas9:SNP2_CEN3#3	444	78	522	0.119	459.882	62.118	4.609	0.032
Cas9:SNP2_CEN3#4	904	177	1081	0.119	952.361	128.639	20.637	5.552E-06

Fig_28C: Chi-squared (1df) test on the null hypothesis that the recombination rates measured in the Cas9 transformant lines do not differ from the non-transformant WT rate (0.119). Plants Cas9:SNP2_CEN3#1, Cas9:SNP2_CEN3#2, Cas9:SNP2_CEN3#3 and Cas9:SNP2_CEN3#4 differ significantly from the expectation, while the non-transformant Wild type control (no cas9) doesn't. (P = number of parental pollen; R = number of recombinant pollen; r(WT) = recombination rate of WT; expR = expected number of recombinant pollen if recombination rate is r(WT); expP = expected number of parental pollen if recombination rate is r(WT)).

Hypothesis for one of the parental Chromosome loss in Cas9:SNP2_CEN3 line

To find out the reason behind the loss of one parental chromosome first I checked the meiotic stages in PMCs and all the stages were normal (Fig_29II), with no defects suggesting the presence of unrepaired broken chromosomes. It is of course possible that the effect is not visible at this level. To go further with the search for the explanation of this bias against the RFP- YFP- chromosome 3, I hypothesized that if the target site on one of the two chromosomes is mutated, Cas9 would not be able to cut it and it would thus be protected (Fig_29I). If so, only one of the chromosomes would be cut by Cas9 and if not repaired, this chromosome could be lost with high frequency. If this is the case, half of the target chromosomes in this line should show a mutation of the target sequence and this would be visible by sequencing. I thus amplified the target site from this line by PCR, cloned it into pGEM-Teasy and sent multiple clones for sequencing. Analysis of the sequencing data showed no mutations were observed at the target site.

It is possible that there is a larger deletion, which covers the target in this chromosome and so it wouldn't have been amplified and thus not visible in the sequencing. To check that, this wasn't the case, I crossed the line Cas9:SNP2_CEN3#1, which was losing one of the parental chromosome (table: 28B) to *Ler-0* (*Ler-0* have no Fluorescent markers) and selected RFP+ YFP+/RFP- YFP- F1 plants. The RFP+ YFP+ chromosome 3 in these

F1 plants is the chromosome that was over-represented in the *Col-0* plants. If the target site mutation hypothesis is correct, this chromosome should not be cleavable and the *Col/Ler* hybrid (described in the beginning of the text (5.2 result and discussion section)) would thus not have Cas9 targets on neither of the chromosomes 3. In this case, the presence of the Cas9 expression would not be expected to have any effect on crossing-over rates in the CEN3 interval in these plants.

Fluorescent pollen counting on the *Col/Ler* F1 lines tested showed a hyporec effect (less pronounced than that of the parental line), supporting the argument that the RFP+ YFP+ chromosome 3 from the parent is a target for Cas9 cutting and thus invalidating the target-site mutation hypothesis for explaining the specific loss of the RFP- YFP- chromosome 3 in the original transformed line (*Col-0* background). Strikingly however, no biases in inheritance of the two parental chromosomes were observed in pollen from the *Col/Ler* hybrid plants, suggesting that the presence of the non-cleavable (*Ler*) chromosome 3 protects against this effect (discussed below).

I.

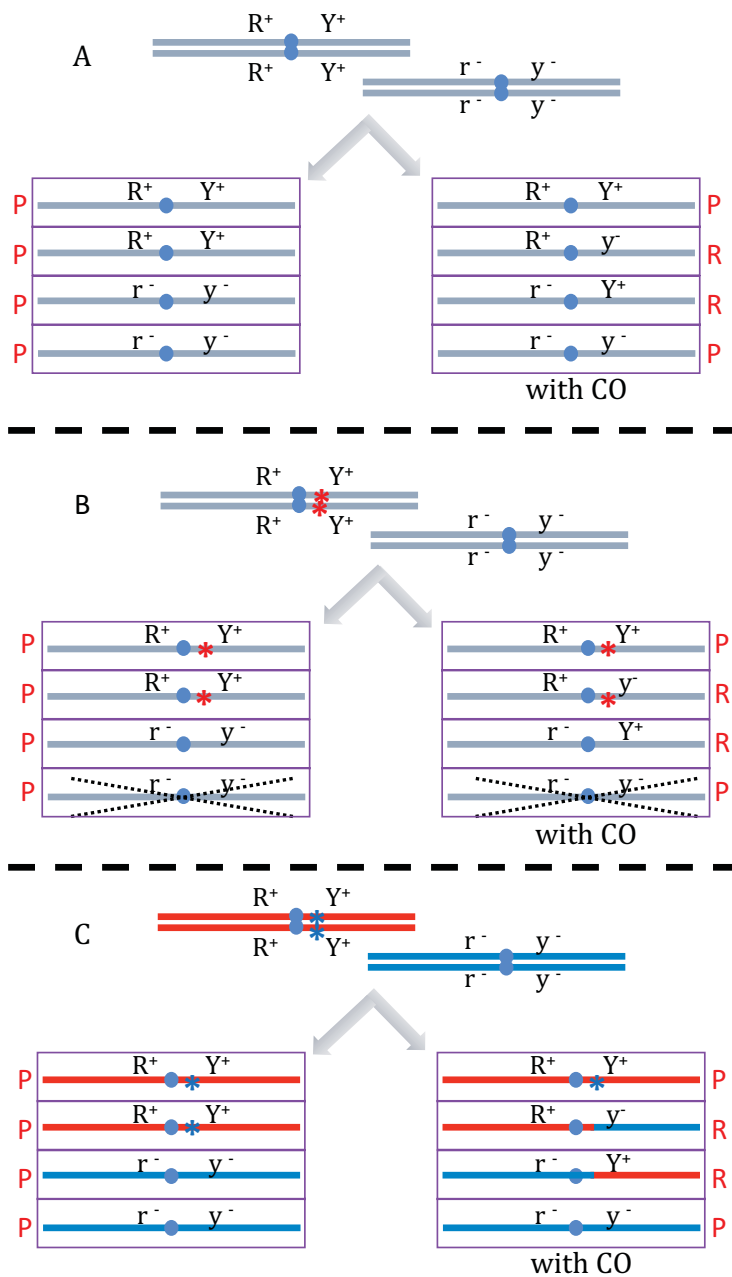


Figure_29_(I) Schema of our hypotheses to explain the loss of one parental chromosome in the Cas9/gRNA lines. (A) In normal meiosis, a CO outside the marked interval will give rise to 4 parental meiotic products (left) or a CO between the markers will give 2 parental and 2 recombinant products (right). (B) Too-efficient by Cas9 could lead to loss of the both target parental chromosomes with equal frequency. However I observed a strong bias to loss of one of the two parental chromosomes (without markers). A possible explanation for this could be that the Cas9 target of the other parental chromosome (with markers) is mutated (showed with asterisks). In this case, only the non-mutated chromosome will be lost due to too-efficient Cas9 cutting. (C) A *Col-0/Ler-0* F1 hybrid carrying the mutated

Col-0 chromosome would have a Cas9 target site neither on the *Col-0* chromosome (red), nor on the *Ler-0* chromosome (blue), and the presence of Cas9/gRNA should thus have no effect on recombination. * represents mutation of the Cas9 target site.

II.

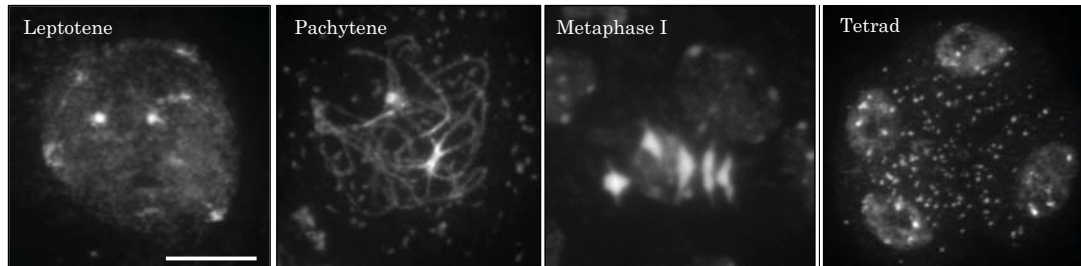


Figure_29(II). Normal meiotic stages in PMCs losing one of the parental chromosome, carrying Cas9/gRNA.

The variability of effects of the CRISPR/Cas9 constructs between individual transformant lines is not unexpected, nor is the detection of loss of chromosomes. From discussions with other groups in the European meiosis network (EU Marie Skłodowska-Curie ITN: COMREC), other groups encounter similar problems with chromosome loss in analogous systems. This effect is presumably due to the too-efficient cutting of the chromosome and possibly to the cutting of two or more chromatids at the same time, thus affecting the availability of an intact donor sequence for DSB repair.

In the case of my work, the constructs were designed such that there was a target site only in *Col-0* and not in *Ler-0*. In a *Col-0* / *Ler-0* F1 hybrid there will thus be an intact donor (2 chromatids) even in the case of highly efficient cleavage of the *Col-0* chromosome. Although much more work needs to be done in characterizing this system, to my satisfaction such a backcross of Cas9:CEN3_SNP2 lines (in *Col-0* background) with *Ler-0* resolved the chromosome loss problem, while retaining a hypo-rec effect of the Cas9 (Table_5).

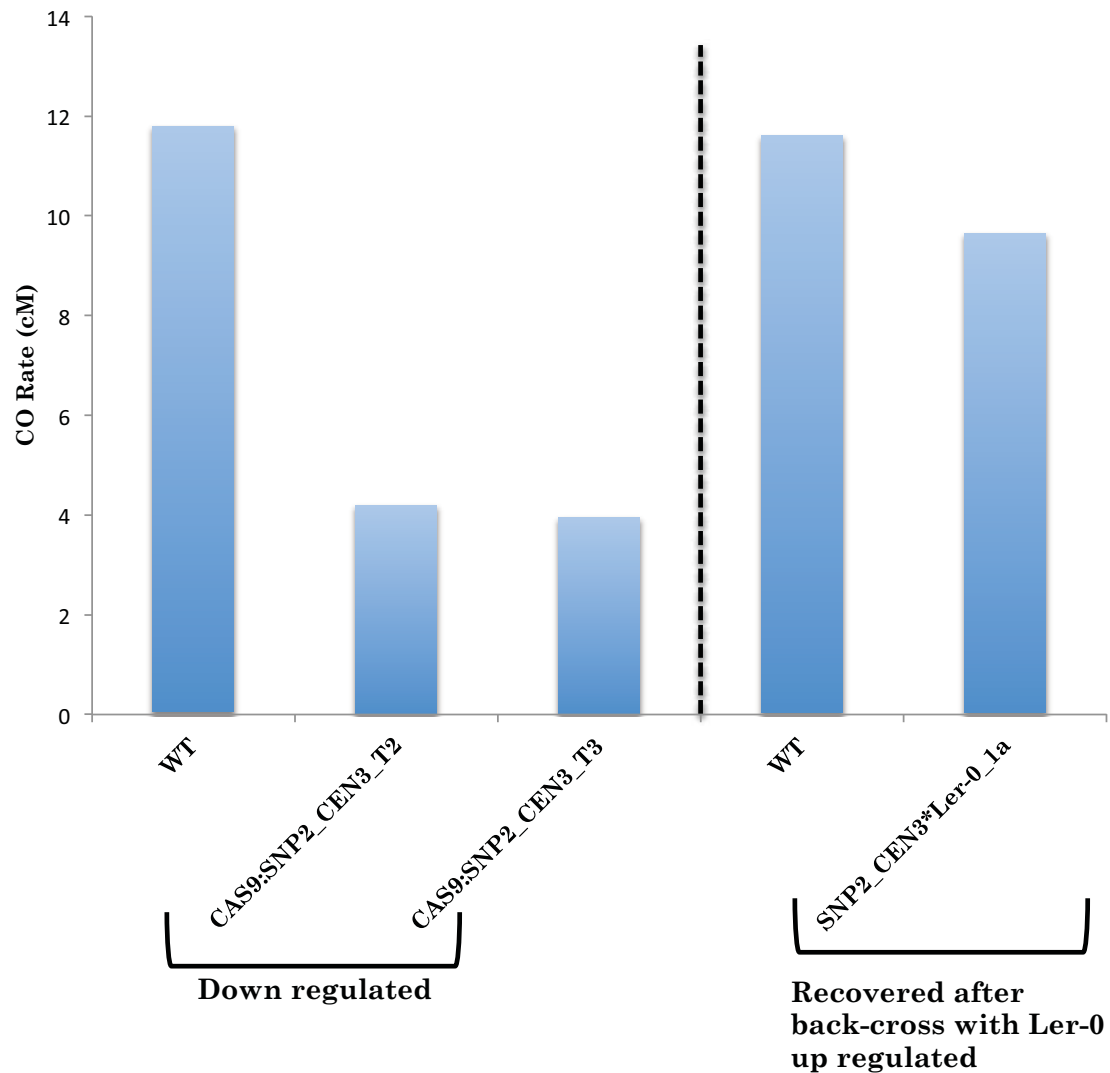
Cas9:SNP2_CEN3hyperec*Ler-0: mean±sem = 9.65±0.0245 cM; 2 plants, total pollen scored = 2069.

The non-recombinant (parental) pollen counts were:

Cas9:SNP2_CEN3*Ler-0_1a - R+Y= 450; No color=430

Cas9:SNP2_CEN3*Ler-0_1b- R+Y=494 & No color=490 (Fig_30).

A.



B.

Plant#	Pollen Counts					r	Chi2 R:not R	Chi2 Y:not Y
	R	Y	R+Y	neither	total			
WT	54	57	407	440	958	0.116	1.353	0.939
Cas9:SNP2_CEN3*Ler0_1a	62	60	457	430	1009	0.121	0.833	0.619
Cas9:SNP2_CEN3*Ler0_1b	37	39	494	490	1060	0.072	0.004	0.034

Figure_30: Genetic map in Cas9:SNP2_CEN3 (down-regulated)*Ler-0 interval. (A) Genetic map distance of the Cas9:SNP2_CEN3 (down-regulated), Cas9:SNP2_CEN3 (down-regulated)*Ler-0 and WT interval. (B) Pollen counts and recombination rates (r) in the Cas9:SNP2CEN3*Ler0_T1 interval.

Effects on recombination of targeting the I1c interval in meiosis.

As with the CEN3 interval I tested the effects of expressing Cas9+gRNA targeting at two different sites in I1c interval in Col-0 background (Fig_22) and performed pollen counts experiment in the I1c interval of chromosome arm region. Unfortunately, difficulties were encountered with pollen counting due to the poor fluorescence of pollen in I1c line and although mild hypo-rec effects were observed, the results are not conclusive.

I1c_WT: mean±sem = 19.5±0 cM; 1 plants, total pollen scored = 620.

Cas9:SNP1_I1c_T2 (hyporec): mean±sem = 17.33±0.007 cM; 3 plants, total pollen scored = 1936.

Cas9:SNP2_I1c_T2 (hyporec): mean±sem = 16.7±0.018 cM; 2 plants, total pollen scored = 1276 (Table_1 & 2).

Table_1: Meiotic recombination in the I1C_SNP1 interval

Pollen Counts								
Plant#	R	Y	R+C	neither	total	r	Chi2 R:not R	Chi2 C:not C
WT	68	53	239	260	620	0.195	0.058	2.090
Cas9:SNP1_I1c#1	55	50	265	271	641	0.164	0.001	0.189
Cas9:SNP1_I1c#2	68	54	253	275	650	0.188	0.098	1.994
Cas9:SNP1_I1c#3	56	57	260	299	672	0.168	2.381	2.149

Table_2: Meiotic recombination in the I1C_SNP2 interval

Pollen Counts								
Plant#	R	C	R+C	neither	total	r	Chi2 R:not R	Chi2 C:not C
WT	68	53	239	260	620	0.195	0.058	2.090
Cas9:SNP2_I1c#1	47	45	258	267	553	0.149	0.778	0.196
Cas9:SNP2_I1c#2	58	55	255	243	723	0.185	0.544	0.133

5.3 Conclusion

Although I have not been able to take these analyses far enough to draw definite conclusions, measurement of meiotic CO rates in the regions targeted by these Cas9/gRNA constructs show clear effects on CO rates in different transformants of Cas9:SNP2_CEN3 (both up- and down-regulation) and only minor effects with the other constructs (perhaps due to their lower activity?). These data confirm the interest of this approach and particularly, the F1 hybrid + ecotype-specific targeting of cleavage has clearly had an effect rescuing the CRISPR induced chromosome loss. These preliminary analyses open interesting perspectives for further work on understanding the mechanisms brought into play and optimizing this approach for the targeted control of meiotic recombination.

Chapter 6

General Discussion
and
Perspectives

Since the mid-90s *Arabidopsis thaliana* has been developed as a model system for the study of meiotic homologous recombination in plants. Over the past decade studies in cereals have also provided numerous insights into this field. The identification and study of meiotic mutants has been key to advances in the study of plant meiosis and the availability of the *Arabidopsis* tagged mutant collections and genome sequence, together with developments in sequencing, proteomics and bioinformatics provide a rich toolkit for the identification of proteins involved in meiotic recombination and analysis of their functional interrelationships.

The results presented in Chapter I of my thesis work are focused on the study of the recombinases RAD51 and DMC1 in *Arabidopsis thaliana*, both of which are key actors in homologous recombination in meiosis. This work took advantage of the dominant-negative *Arabidopsis* RAD51-GFP fusion protein, which lacks strand-transfer (and thus DSB repair) activity, but retains the capacity to assemble at DNA breaks (Da Ines et al., 2013b; Kobayashi et al., 2014). This approach thus permits unambiguous study of meiosis in which DMC1 is the only active strand-transfer recombinase and I used this to determine whether this fact has an impact on rates of meiotic crossing-over. The results of this work have recently been published: Singh G, Da Ines O, Gallego ME & White CI (2017) Analysis of the impact of the absence of RAD51 strand exchange activity in *Arabidopsis* meiosis. *PLoS ONE* **12**: e0183006–16

In a first approach, CO rates were determined in two marked genetic

intervals, one spanning the centromere of chromosome 3 and the second on the arm region of chromosome 1. These data were extended to chiasmata counts per chromosome and per meiosis (whole genome), and to counting HEI10 foci to specifically quantify Class I CO. These data showed no significant differences in CO numbers and patterns between WT and RAD51-GFP plants. The genome-wide numbers of chiasmata did show a very slight increase in RAD51-GFP meiosis (9.3 ± 0.11 (mean \pm s.e.m.)) compared to the WT controls (9.68 ± 0.15), but this was of weak significance. I also checked the kinetics of meiotic progression by an EdU pulse-chase time course experiment and this confirmed the similar meiotic kinetics in RAD51-GFP and WT plants. These results thus lead to the conclusion that absence of RAD51 strand-exchange activity caused no detectable differences in meiosis in Arabidopsis. The data from this part of my thesis confirm and extend the earlier yeast and Arabidopsis studies (Cloud et al., 2012; Da Ines et al., 2013b). Although depending upon the presence of RAD51 nucleofilaments for its activity, DMC1 appears to be the only active meiotic strand-exchange protein in WT meiosis and thus is be responsible for inter-sister and inter-homologue CO and NCO.

The second results chapter describes my work focused on understanding the cytogenetics of partial synapsis observed in the absence of RAD51 and XRCC3 (Abe et al., 2005; Bleuyard et al., 2005; Bleuyard and White, 2004; Li et al., 2005; Vignard et al., 2007). Recombination induced in Leptotene establishes the co-alignment of homologous chromosome axes visible in Zygotene, making the observation partial meiotic synapsis in

Zygotene/early Pachytene of centromeric and 5S rDNA regions of homologs in *xrcc3*, *rad51c* and *rad51* mutants, both unexpected and striking. I thus undertook work to better characterise this partial synapsis in these mutant meiosis, aiming to respond to two specific questions:

- Does meiotic chromosome synapsis in Arabidopsis begin at centromeres/peri-centromeres and then extend though the chromosome arms?
- What is the interdependence of centromere and arm synapsis?

I performed Co-Immunolocalisation experiments, using antisera against ASY1 (Synaptonemal Complex axis-associated protein), ZYP1 (Synaptonemal Complex transverse filament protein) and CENH3 (centromeric histone H3). These experiments were carried out on meiotic chromosome spreads from wild type, *rad51* and *xrcc3* plants, combined with SIM (Super resolution) and epi-fluorescence microscopy.

Previous work from the lab with the RAD51 paralogue mutants *xrcc3* and *rad51C*, showed homologous centromere pairing at meiosis which can extend for at least 2 Mb from centromere, well into the euchromatic pericentromeric regions (Da Ines et al., 2012). This led to the hypothesis that the short ZYP1 fibres observed in these nuclei correspond to synapsis and initiation of SC formation in these regions. The results of my work disprove this hypothesis. Although some ZYP1 fibers (SC protein) initiate from centromeres, more often they do not. This conclusion was confirmed by the analysis of SIM microscopy images, which showed both full pairing

of centromeres before the appearance of ZYP1 and the presence of short ZYP1 fibres with centromeres being unpaired or partly paired.

My observations of in *xrcc3* and *rad51* meiosis showed 7-9 centromeric foci per nucleus were at zygotene and 3-5 at early pachytene, prior to chromosome fragmentation, confirming that centromeres do pair in these mutants. The microscopy images concord with previously published centromere coupling, clustering and pairing data in *Arabidopsis* (Da Ines et al., 2012; Da Ines et al., 2014; Fransz et al., 1998; Su et al., 2017).

Finally, the third and final part of my thesis work involves the development of CRISPR/CAS9 tools to create target specific meiotic recombination hot-spots through the targeted induction of DNA breaks. Such an approach will be key to probing the roles of recombination proteins and the mechanisms of meiotic recombination in future work. Four different CRISPR constructs targeting sites within the CEN3 and I1c FTL intervals on chromosomes 1 and 3 respectively, were built and transformed into plants. The constructs were designed to cleave only *Col-0* and not *Ler-0* chromosomes, due to the presence of SNPs in the target sites. In a *Col-0 / Ler-0* F1 hybrid there will thus always be an intact donor (2 chromatids) even in the case of highly efficient cleavage of the *Col-0* chromosome. Although limited time has meant that I have not been able to take these analyses far enough to draw definite conclusions, measurement of meiotic CO rates in the regions targeted by these Cas9/gRNA constructs show clear effects on CO rates in different

transformants of Cas9-SNP2:CEN3 (both up- and down-regulation) and only minor effects with the other constructs (perhaps due to their lower activity). These data confirm the interest of this approach and particularly, that the F1 hybrid + ecotype-specific targeting of cleavage has clearly had an effect rescuing CRISPR induced chromosome loss. These preliminary analyses open interesting perspectives for further work on understanding the mechanisms brought into play and optimizing this approach for the targeted control of meiotic recombination.

PERSPECTIVES

- RAD51 is an essential accessory factor for the activity of DMC1. How does it play this role - does the loading of RAD51 influence the specificity of the DMC1 nucleofilament? What are the roles of in this?
- Extending this to other essential recombination factors such as XRCC3 and RAD51C will permit clarifying the dynamics of recombination complex assembly/disassembly and hopefully lead to better understanding of the specificities of meiotic recombination. Why does a give DSB result in a NCO or an inter-sister or inter-homolog CO?
- The biological significance of formation of early homologous centromere associations in meiosis remains to be determined. The discovery and analysis of new mutants that are defective only in this

early centromeric pairing and/or clustering will be key to answering this puzzle.

- How centromere associations are formed in time and space remains to be characterized. Most of our knowledge comes from analyses of fixed nuclei, which necessarily provide only frozen snapshots of this dynamic process. Live-imaging microscopy should help to decipher the mechanisms and regulation of centromere associations.
- Telomere and centromere associations are frequently contemporaneous and sometimes interdependent. Better understanding of how meiotic chromosome pairing is achieved would benefit from new imaging strategies to follow meiotic chromosome movements and in particular the dynamics of these two prominent chromosomal landmarks.
- What are the small stretches of ZYP1 in *xrcc3* and *rad51* meiosis? Do they correspond to true synapsis or to transient intermediate structures?

Chapter 7

References

- Abe, K., Osakabe, K., Nakayama, S., Endo, M., Tagiri, A., Todoriki, S., Ichikawa, H., and Toki, S. (2005). Arabidopsis RAD51C gene is important for homologous recombination in meiosis and mitosis. *Plant Physiol* *139*, 896-908.
- Aboussekhra, A., Chanet, R., Adjiri, A., and Fabre, F. (1992). Semidominant suppressors of Srs2 helicase mutations of *Saccharomyces cerevisiae* map in the RAD51 gene, whose sequence predicts a protein with similarities to procaryotic RecA proteins. *Mol Cell Biol* *12*, 3224-3234.
- Agarwal, S., and Roeder, G.S. (2000). Zip3 provides a link between recombination enzymes and synaptonemal complex proteins. *Cell* *102*, 245-255.
- Allers, T., and Lichten, M. (2001). Differential timing and control of noncrossover and crossover recombination during meiosis. *Cell* *106*, 47-57.
- An, X.J., Deng, Z.Y., and Wang, T. (2011). OsSpo11-4, a rice homologue of the archaeal TopVIA protein, mediates double-strand DNA cleavage and interacts with OsTopVIB. *PLoS One* *6*, e20327.
- Anderson, D.E., Trujillo, K.M., Sung, P., and Erickson, H.P. (2001). Structure of the Rad50 x Mre11 DNA repair complex from *Saccharomyces cerevisiae* by electron microscopy. *J Biol Chem* *276*, 37027-37033.
- Armstrong, S.J. (2012). A time course for the analysis of meiotic progression in *Arabidopsis thaliana*. *Methods Mol Biol* *990*, 119-123.
- Armstrong, S.J., Franklin, F.C., and Jones, G.H. (2001). Nucleolus-associated telomere clustering and pairing precede meiotic chromosome synapsis in *Arabidopsis thaliana*. *J Cell Sci* *114*, 4207-4217.
- Armstrong, S.J., and Jones, G.H. (2003). Meiotic cytology and chromosome behaviour in wild-type *Arabidopsis thaliana*. *J Exp Bot* *54*, 1-10.
- Arora, C., Kee, K., Maleki, S., and Keeney, S. (2004). Antiviral protein Ski8 is a direct partner of Spo11 in meiotic DNA break formation, independent of its cytoplasmic role in RNA metabolism. *Mol Cell* *13*, 549-559.

- Barton, N.H., and Charlesworth, B. (1998). Why sex and recombination? *Science* *281*, 1986-1990.
- Bauknecht, M., and Kobbe, D. (2014). AtGEN1 and AtSEND1, two paralogs in Arabidopsis, possess holliday junction resolvase activity. *Plant Physiol* *166*, 202-216.
- Baumann, P., Benson, F.E., and West, S.C. (1996). Human Rad51 protein promotes ATP-dependent homologous pairing and strand transfer reactions in vitro. *Cell* *87*, 757-766.
- Bellani, M.A., Boateng, K.A., McLeod, D., and Camerini-Otero, R.D. (2010). The expression profile of the major mouse SPO11 isoforms indicates that SPO11beta introduces double strand breaks and suggests that SPO11alpha has an additional role in prophase in both spermatocytes and oocytes. *Mol Cell Biol* *30*, 4391-4403.
- Berchowitz, L.E., and Copenhaver, G.P. (2008). Fluorescent Arabidopsis tetrads: a visual assay for quickly developing large crossover and crossover interference data sets. *Nat Protoc* *3*, 41-50.
- Berchowitz, L.E., and Copenhaver, G.P. (2010). Genetic interference: don't stand so close to me. *Curr Genomics* *11*, 91-102.
- Berchowitz, L.E., Francis, K.E., Bey, A.L., and Copenhaver, G.P. (2007). The role of AtMUS81 in interference-insensitive crossovers in *A. thaliana*. *PLoS Genet* *3*, e132.
- Bergerat, A., de Massy, B., Gadelle, D., Varoutas, P.C., Nicolas, A., and Forterre, P. (1997). An atypical topoisomerase II from Archaea with implications for meiotic recombination. *Nature* *386*, 414-417.
- Bhalla, N., Wynne, D.J., Jantsch, V., and Dernburg, A.F. (2008). ZHP-3 acts at crossovers to couple meiotic recombination with synaptonemal complex disassembly and bivalent formation in *C. elegans*. *PLoS Genet* *4*, e1000235.

- Bhaskara, V., Dupre, A., Lengsfeld, B., Hopkins, B.B., Chan, A., Lee, J.H., Zhang, X., Gautier, J., Zakian, V., and Paull, T.T. (2007). Rad50 adenylate kinase activity regulates DNA tethering by Mre11/Rad50 complexes. *Mol Cell* 25, 647-661.
- Bianco, P.R., Tracy, R.B., and Kowalczykowski, S.C. (1998). DNA strand exchange proteins: a biochemical and physical comparison. *Front Biosci* 3, D570-603.
- Bishop, D.K. (1994). RecA homologs Dmc1 and Rad51 interact to form multiple nuclear complexes prior to meiotic chromosome synapsis. *Cell* 79, 1081-1092.
- Bishop, D.K., Park, D., Xu, L., and Kleckner, N. (1992). DMC1: a meiosis-specific yeast homolog of E. coli recA required for recombination, synaptonemal complex formation, and cell cycle progression. *Cell* 69, 439-456.
- Bishop, D.K., and Zickler, D. (2004). Early decision; meiotic crossover interference prior to stable strand exchange and synapsis. *Cell* 117, 9-15.
- Bleuyard, J.Y., Gallego, M.E., Savigny, F., and White, C.I. (2005). Differing requirements for the Arabidopsis Rad51 paralogs in meiosis and DNA repair. *Plant J* 41, 533-545.
- Bleuyard, J.Y., Gallego, M.E., and White, C.I. (2004). Meiotic defects in the Arabidopsis rad50 mutant point to conservation of the MRX complex function in early stages of meiotic recombination. *Chromosoma* 113, 197-203.
- Bleuyard, J.Y., and White, C.I. (2004). The Arabidopsis homologue of Xrcc3 plays an essential role in meiosis. *EMBO J* 23, 439-449.
- Borner, G.V., Kleckner, N., and Hunter, N. (2004). Crossover/noncrossover differentiation, synaptonemal complex formation, and regulatory surveillance at the leptotene/zygotene transition of meiosis. *Cell* 117, 29-45.
- Bouuaert, C.C., and Keeney, S. (2016). DNA. Breaking DNA. *Science* 351, 916-917.
- Brown, M.S., and Bishop, D.K. (2014). DNA strand exchange and RecA homologs in meiosis. *Cold Spring Harb Perspect Biol* 7, a016659.

- Brown, M.S., Grubb, J., Zhang, A., Rust, M.J., and Bishop, D.K. (2015). Small Rad51 and Dmc1 Complexes Often Co-occupy Both Ends of a Meiotic DNA Double Strand Break. *PLoS Genet* *11*, e1005653.
- Bugreev, D.V., Golub, E.I., Stasiak, A.Z., Stasiak, A., and Mazin, A.V. (2005). Activation of human meiosis-specific recombinase Dmc1 by Ca²⁺. *J Biol Chem* *280*, 26886-26895.
- Bugreev, D.V., Pezza, R.J., Mazina, O.M., Voloshin, O.N., Camerini-Otero, R.D., and Mazin, A.V. (2011). The resistance of DMC1 D-loops to dissociation may account for the DMC1 requirement in meiosis. *Nat Struct Mol Biol* *18*, 56-60.
- Bugreev, D.V., Yu, X., Egelman, E.H., and Mazin, A.V. (2007). Novel pro- and anti-recombination activities of the Bloom's syndrome helicase. *Genes Dev* *21*, 3085-3094.
- Buisson, A., Joubert, A., Montoriol, P.F., Da Ines, D., Hordonneau, C., Pereira, B., Garcier, J.M., Bommelaer, G., and Petitcolin, V. (2013). Diffusion-weighted magnetic resonance imaging for detecting and assessing ileal inflammation in Crohn's disease. *Aliment Pharmacol Ther* *37*, 537-545.
- Buonomo, S.B., Clyne, R.K., Fuchs, J., Loidl, J., Uhlmann, F., and Nasmyth, K. (2000). Disjunction of homologous chromosomes in meiosis I depends on proteolytic cleavage of the meiotic cohesin Rec8 by separin. *Cell* *103*, 387-398.
- Cahoon, C.K., and Hawley, R.S. (2016). Regulating the construction and demolition of the synaptonemal complex. *Nat Struct Mol Biol* *23*, 369-377.
- Campbell, B.R., Song, Y., Posch, T.E., Cullis, C.A., and Town, C.D. (1992). Sequence and organization of 5S ribosomal RNA-encoding genes of *Arabidopsis thaliana*. *Gene* *112*, 225-228.
- Cannavo, E., and Cejka, P. (2014). Sae2 promotes dsDNA endonuclease activity within Mre11-Rad50-Xrs2 to resect DNA breaks. *Nature* *514*, 122-125.

- Ceccaldi, R., Rondinelli, B., and D'Andrea, A.D. (2016). Repair Pathway Choices and Consequences at the Double-Strand Break. *Trends Cell Biol* 26, 52-64.
- Chan, Y.L., Brown, M.S., Qin, D., Handa, N., and Bishop, D.K. (2014). The third exon of the budding yeast meiotic recombination gene HOP2 is required for calcium-dependent and recombinase Dmc1-specific stimulation of homologous strand assimilation. *J Biol Chem* 289, 18076-18086.
- Chelysheva, L., Vezon, D., Belcram, K., Gendrot, G., and Grelon, M. (2008). The Arabidopsis BLAP75/Rmi1 homologue plays crucial roles in meiotic double-strand break repair. *PLoS Genet* 4, e1000309.
- Chelysheva, L., Vezon, D., Chambon, A., Gendrot, G., Pereira, L., Lemhemdi, A., Vrielynck, N., Le Guin, S., Novatchkova, M., and Grelon, M. (2012). The Arabidopsis HEI10 Is a New ZMM Protein Related to Zip3. *PLoS Genet* 8, e1002799.
- Chen, C., Zhang, W., Timofejeva, L., Gerardin, Y., and Ma, H. (2005). The Arabidopsis ROCK-N-ROLLERS gene encodes a homolog of the yeast ATP-dependent DNA helicase MER3 and is required for normal meiotic crossover formation. *Plant J* 43, 321-334.
- Chen, L.T., Ko, T.P., Chang, Y.C., Lin, K.A., Chang, C.S., Wang, A.H., and Wang, T.F. (2007). Crystal structure of the left-handed archaeal RadA helical filament: identification of a functional motif for controlling quaternary structures and enzymatic functions of RecA family proteins. *Nucleic Acids Res* 35, 1787-1801.
- Chen, Z., Higgins, J.D., Hui, J.T., Li, J., Franklin, F.C., and Berger, F. (2011). Retinoblastoma protein is essential for early meiotic events in Arabidopsis. *EMBO J* 30, 744-755.
- Chi, P., Van Komen, S., Sehorn, M.G., Sigurdsson, S., and Sung, P. (2006). Roles of ATP binding and ATP hydrolysis in human Rad51 recombinase function. *DNA Repair (Amst)* 5, 381-391.

- Chikashige, Y., Tsutsumi, C., Yamane, M., Okamasa, K., Haraguchi, T., and Hiraoka, Y. (2006). Meiotic proteins bqt1 and bqt2 tether telomeres to form the bouquet arrangement of chromosomes. *Cell* *125*, 59-69.
- Cho, S.W., Kim, S., Kim, J.M., and Kim, J.S. (2013). Targeted genome engineering in human cells with the Cas9 RNA-guided endonuclease. *Nat Biotechnol* *31*, 230-232.
- Clerici, M., Mantiero, D., Lucchini, G., and Longhese, M.P. (2005). The *Saccharomyces cerevisiae* Sae2 protein promotes resection and bridging of double strand break ends. *J Biol Chem* *280*, 38631-38638.
- Clift, D., and Marston, A.L. (2011). The role of shugoshin in meiotic chromosome segregation. *Cytogenet Genome Res* *133*, 234-242.
- Cloud, V., Chan, Y.L., Grubb, J., Budke, B., and Bishop, D.K. (2012). Rad51 Is an Accessory Factor for Dmc1-Mediated Joint Molecule Formation During Meiosis. *Science* *337*, 1222-1225.
- Cole, F., Kauppi, L., Lange, J., Roig, I., Wang, R., Keeney, S., and Jasin, M. (2012). Homeostatic control of recombination is implemented progressively in mouse meiosis. *Nat Cell Biol* *14*, 424-430.
- Cole, F., Keeney, S., and Jasin, M. (2010). Evolutionary conservation of meiotic DSB proteins: more than just Spo11. *Genes Dev* *24*, 1201-1207.
- Cong, L., Ran, F.A., Cox, D., Lin, S., Barretto, R., Habib, N., Hsu, P.D., Wu, X., Jiang, W., Marraffini, L.A., *et al.* (2013). Multiplex genome engineering using CRISPR/Cas systems. *Science* *339*, 819-823.
- Copenhaver, G.P., Housworth, E.A., and Stahl, F.W. (2002). Crossover interference in *Arabidopsis*. *Genetics* *160*, 1631-1639.
- Couteau, F., Belzile, F., Horlow, C., Grandjean, O., Vezon, D., and Doutriaux, M.P. (1999). Random chromosome segregation without meiotic arrest in both male and female meiocytes of a *dmc1* mutant of *Arabidopsis*. *Plant Cell* *11*, 1623-1634.

Crismani, W., Girard, C., Froger, N., Pradillo, M., Santos, J.L., Chelysheva, L., Copenhaver, G.P., Horlow, C., and Mercier, R. (2012). FANCM limits meiotic crossovers. *Science* 336, 1588-1590.

Crismani, W., Portemer, V., Froger, N., Chelysheva, L., Horlow, C., Vrielynck, N., and Mercier, R. (2013). MCM8 is required for a pathway of meiotic double-strand break repair independent of DMC1 in *Arabidopsis thaliana*. *PLoS Genet* 9, e1003165.

Da Ines, O., Abe, K., Goubely, C., Gallego, M.E., and White, C.I. (2012). Differing requirements for RAD51 and DMC1 in meiotic pairing of centromeres and chromosome arms in *Arabidopsis thaliana*. *PLoS Genet* 8, e1002636.

Da Ines, O., Degroote, F., Amiard, S., Goubely, C., Gallego, M.E., and White, C.I. (2013a). Effects of XRCC2 and RAD51B mutations on somatic and meiotic recombination in *Arabidopsis thaliana*. *Plant J* 74, 959-970.

Da Ines, O., Degroote, F., Goubely, C., Amiard, S., Gallego, M.E., and White, C.I. (2013b). Meiotic recombination in *Arabidopsis* is catalysed by DMC1, with RAD51 playing a supporting role. *PLoS Genet* 9, e1003787.

Da Ines, O., Gallego, M.E., and White, C.I. (2014). Recombination-independent mechanisms and pairing of homologous chromosomes during meiosis in plants. *Mol Plant* 7, 492-501.

Da Ines, O., and White, C.I. (2015). Centromere Associations in Meiotic Chromosome Pairing. *Annu Rev Genet* 49, 95-114.

Dai, J., Voloshin, O., Potapova, S., and Camerini-Otero, R.D. (2017). Meiotic Knockdown and Complementation Reveals Essential Role of RAD51 in Mouse Spermatogenesis. *Cell Rep* 18, 1383-1394.

Danilowicz, C., Peacock-Villada, A., Vlassakis, J., Facon, A., Feinstein, E., Kleckner, N., and Prentiss, M. (2013). The differential extension in dsDNA bound to Rad51 filaments may play important roles in homology recognition and strand exchange. *Nucleic Acids Res* 42, 526-533.

- Daoudal-Cotterell, S., Gallego, M.E., and White, C.I. (2002). The plant Rad50-Mre11 protein complex. *FEBS Lett* 516, 164-166.
- Dawe, R.K. (1998). Meiotic Chromosome Organization and Segregation in Plants. *Annu Rev Plant Physiol Plant Mol Biol* 49, 371-395.
- de Jager, M., van Noort, J., van Gent, D.C., Dekker, C., Kanaar, R., and Wyman, C. (2001). Human Rad50/Mre11 is a flexible complex that can tether DNA ends. *Mol Cell* 8, 1129-1135.
- de Massy, B. (2013). Initiation of meiotic recombination: how and where? Conservation and specificities among eukaryotes. *Annu Rev Genet* 47, 563-599.
- De Muyt, A., Jessop, L., Kolar, E., Sourirajan, A., Chen, J., Dayani, Y., and Lichten, M. (2012). BLM helicase ortholog Sgs1 is a central regulator of meiotic recombination intermediate metabolism. *Mol Cell* 46, 43-53.
- De Muyt, A., Pereira, L., Vezon, D., Chelysheva, L., Gendrot, G., Chambon, A., Laine-Choinard, S., Pelletier, G., Mercier, R., Nogue, F., *et al.* (2009). A high throughput genetic screen identifies new early meiotic recombination functions in *Arabidopsis thaliana*. *PLoS Genet* 5, e1000654.
- De Muyt, A., Vezon, D., Gendrot, G., Gallois, J.L., Stevens, R., and Grelon, M. (2007). AtPRD1 is required for meiotic double strand break formation in *Arabidopsis thaliana*. *EMBO J* 26, 4126-4137.
- Deng, Z.Y., and Wang, T. (2007). OsDMC1 is required for homologous pairing in *Oryza sativa*. *Plant Mol Biol* 65, 31-42.
- Dernburg, A.F., McDonald, K., Moulder, G., Barstead, R., Dresser, M., and Villeneuve, A.M. (1998). Meiotic recombination in *C. elegans* initiates by a conserved mechanism and is dispensable for homologous chromosome synapsis. *Cell* 94, 387-398.

- Desai-Mehta, A., Cerosaletti, K.M., and Concannon, P. (2001). Distinct functional domains of nibrin mediate Mre11 binding, focus formation, and nuclear localization. *Mol Cell Biol* 21, 2184-2191.
- DiCarlo, J.E., Norville, J.E., Mali, P., Rios, X., Aach, J., and Church, G.M. (2013). Genome engineering in *Saccharomyces cerevisiae* using CRISPR-Cas systems. *Nucleic Acids Res* 41, 4336-4343.
- Ding, Y., Li, H., Chen, L.L., and Xie, K. (2016). Recent Advances in Genome Editing Using CRISPR/Cas9. *Front Plant Sci* 7, 703.
- Ding, Z.-j., Wang, T., Chong, K., and Bai, S. (2001). Isolation and characterization of OsDMC1, the rice homologue of the yeast DMC1 gene essential for meiosis. *Sexual Plant Reprod* 13, 285-288.
- DiRuggiero, J., Brown, J.R., Bogert, A.P., and Robb, F.T. (1999). DNA repair systems in archaea: mementos from the last universal common ancestor? *J Mol Evol* 49, 474-484.
- Eisen, J.A. (1995). The RecA protein as a model molecule for molecular systematic studies of bacteria: comparison of trees of RecAs and 16S rRNAs from the same species. *J Mol Evol* 41, 1105-1123.
- Fan, D., Liu, T., Li, C., Jiao, B., Li, S., Hou, Y., and Luo, K. (2015). Efficient CRISPR/Cas9-mediated Targeted Mutagenesis in *Populus* in the First Generation. *Sci Rep* 5, 12217.
- Fausser, F., Schiml, S., and Puchta, H. (2014). Both CRISPR/Cas-based nucleases and nickases can be used efficiently for genome engineering in *Arabidopsis thaliana*. *Plant J* 79, 348-359.
- Feng, Z., Zhang, B., Ding, W., Liu, X., Yang, D.L., Wei, P., Cao, F., Zhu, S., Zhang, F., Mao, Y., *et al.* (2013). Efficient genome editing in plants using a CRISPR/Cas system. *Cell Res* 23, 1229-1232.

Ferdous, M., Higgins, J.D., Osman, K., Lambing, C., Roitinger, E., Mechtler, K., Armstrong, S.J., Perry, R., Pradillo, M., Cunado, N., *et al.* (2012). Inter-homolog crossing-over and synapsis in *Arabidopsis* meiosis are dependent on the chromosome axis protein AtASY3. *PLoS Genet* 8, e1002507.

Ferrari, S.R., Grubb, J., and Bishop, D.K. (2009). The Mei5-Sae3 protein complex mediates Dmc1 activity in *Saccharomyces cerevisiae*. *J Biol Chem* 284, 11766-11770.

Fishel, R. (2015). Mismatch repair. *J Biol Chem* 290, 26395-26403.

Fogel, S., and Hurst, D.D. (1967). Meiotic gene conversion in yeast tetrads and the theory of recombination. *Genetics* 57, 455-481.

Francis, K.E., Lam, S.Y., Harrison, B.D., Bey, A.L., Berchowitz, L.E., and Copenhaver, G.P. (2007). Pollen tetrad-based visual assay for meiotic recombination in *Arabidopsis*. *Proc Natl Acad Sci U S A* 104, 3913-3918.

Franklin, A.E., McElver, J., Sunjevaric, I., Rothstein, R., Bowen, B., and Cande, W.Z. (1999). Three-dimensional microscopy of the Rad51 recombination protein during meiotic prophase. *Plant Cell* 11, 809-824.

Franklin, F.C., Higgins, J.D., Sanchez-Moran, E., Armstrong, S.J., Osman, K.E., Jackson, N., and Jones, G.H. (2006). Control of meiotic recombination in *Arabidopsis*: role of the MutL and MutS homologues. *Biochem Soc Trans* 34, 542-544.

Fransz, P., Armstrong, S., Alonso-Blanco, C., Fischer, T.C., Torres-Ruiz, R.A., and Jones, G. (1998). Cytogenetics for the model system *Arabidopsis thaliana*. *Plant J* 13, 867-876.

Fung, J.C., Rockmill, B., Odell, M., and Roeder, G.S. (2004). Imposition of crossover interference through the nonrandom distribution of synapsis initiation complexes. *Cell* 116, 795-802.

- Furukawa, T., Kimura, S., Ishibashi, T., Mori, Y., Hashimoto, J., and Sakaguchi, K. (2003). OsSEND-1: a new RAD2 nuclease family member in higher plants. *Plant Mol Biol* *51*, 59-70.
- Gaj, T., Gersbach, C.A., and Barbas, C.F., 3rd (2013). ZFN, TALEN, and CRISPR/Cas-based methods for genome engineering. *Trends Biotechnol* *31*, 397-405.
- Gallego, M.E., Jeanneau, M., Granier, F., Bouchez, D., Bechtold, N., and White, C.I. (2001). Disruption of the Arabidopsis RAD50 gene leads to plant sterility and MMS sensitivity. *Plant J* *25*, 31-41.
- Gallo-Fernandez, M., Saugar, I., Ortiz-Bazan, M.A., Vazquez, M.V., and Tercero, J.A. (2012). Cell cycle-dependent regulation of the nuclease activity of Mus81-Eme1/Mms4. *Nucleic Acids Res* *40*, 8325-8335.
- Game, J.C. (1993). DNA double-strand breaks and the RAD50-RAD57 genes in *Saccharomyces*. *Semin Cancer Biol* *4*, 73-83.
- Game, J.C., and Mortimer, R.K. (1974). A genetic study of x-ray sensitive mutants in yeast. *Mutat Res* *24*, 281-292.
- Game, J.C., Zamb, T.J., Braun, R.J., Resnick, M., and Roth, R.M. (1980). The Role of Radiation (rad) Genes in Meiotic Recombination in Yeast. *Genetics* *94*, 51-68.
- Garcia, V., Phelps, S.E., Gray, S., and Neale, M.J. (2011). Bidirectional resection of DNA double-strand breaks by Mre11 and Exo1. *Nature* *479*, 241-244.
- Gasior, S.L., Wong, A.K., Kora, Y., Shinohara, A., and Bishop, D.K. (1998). Rad52 associates with RPA and functions with rad55 and rad57 to assemble meiotic recombination complexes. *Genes Dev* *12*, 2208-2221.
- Gerlach, W.L., and Bedbrook, J.R. (1979). Cloning and characterization of ribosomal RNA genes from wheat and barley. *Nucleic Acids Res* *7*, 1869-1885.

- Giraut, L., Falque, M., Drouaud, J., Pereira, L., Martin, O.C., and Mezard, C. (2011). Genome-wide crossover distribution in *Arabidopsis thaliana* meiosis reveals sex-specific patterns along chromosomes. *PLoS Genet* 7, e1002354.
- Gladyshev, E., and Kleckner, N. (2017). Recombination-independent recognition of DNA homology for repeat-induced point mutation. *Curr Genet* 63, 389-400.
- Gobbini, E., Cassani, C., Villa, M., Bonetti, D., and Longhese, M.P. (2016). Functions and regulation of the MRX complex at DNA double-strand breaks. *Microb Cell* 3, 329-337.
- Goldfarb, T., and Lichten, M. (2010). Frequent and efficient use of the sister chromatid for DNA double-strand break repair during budding yeast meiosis. *PLoS Biol* 8, e1000520.
- Golubovskaya, I.N., Harper, L.C., Pawlowski, W.P., Schichnes, D., and Cande, W.Z. (2002). The *pam1* gene is required for meiotic bouquet formation and efficient homologous synapsis in maize (*Zea mays* L.). *Genetics* 162, 1979-1993.
- Gray, S., and Cohen, P.E. (2016). Control of Meiotic Crossovers: From Double-Strand Break Formation to Designation. *Annu Rev Genet* 50, 175-210.
- Grelon, M., Vezon, D., Gendrot, G., and Pelletier, G. (2001). *AtSPO11-1* is necessary for efficient meiotic recombination in plants. *EMBO J* 20, 589-600.
- Gupta, R.C., Folta-Stogniew, E., O'Malley, S., Takahashi, M., and Radding, C.M. (1999). Rapid exchange of A:T base pairs is essential for recognition of DNA homology by human Rad51 recombination protein. *Mol Cell* 4, 705-714.
- Hamant, O., Ma, H., and Cande, W.Z. (2006). Genetics of meiotic prophase I in plants. *Annu Rev Plant Biol* 57, 267-302.
- Hartung, F., and Puchta, H. (2000). Molecular characterisation of two paralogous SPO11 homologues in *Arabidopsis thaliana*. *Nucleic Acids Res* 28, 1548-1554.

Hartung, F., and Puchta, H. (2001). Molecular characterization of homologues of both subunits A (SPO11) and B of the archaebacterial topoisomerase 6 in plants. *Gene* 271, 81-86.

Hartung, F., Wurz-Wildersinn, R., Fuchs, J., Schubert, I., Suer, S., and Puchta, H. (2007). The catalytically active tyrosine residues of both SPO11-1 and SPO11-2 are required for meiotic double-strand break induction in Arabidopsis. *Plant Cell* 19, 3090-3099.

Hayase, A., Takagi, M., Miyazaki, T., Oshiumi, H., Shinohara, M., and Shinohara, A. (2004). A protein complex containing Mei5 and Sae3 promotes the assembly of the meiosis-specific RecA homolog Dmc1. *Cell* 119, 927-940.

Henderson, K.A., and Keeney, S. (2004). Tying synaptonemal complex initiation to the formation and programmed repair of DNA double-strand breaks. *Proc Natl Acad Sci U S A* 101, 4519-4524.

Heyting, C. (1996). Synaptonemal complexes: structure and function. *Curr Opin Cell Biol* 8, 389-396.

Higgins, J.D., Armstrong, S.J., Franklin, F.C.H., and Jones, G.H. (2004). The Arabidopsis MutS homolog AtMSH4 functions at an early step in recombination: evidence for two classes of recombination in Arabidopsis. *Genes Dev* 18, 2557-2570.

Higgins, J.D., Buckling, E.F., Franklin, F.C., and Jones, G.H. (2008a). Expression and functional analysis of AtMUS81 in Arabidopsis meiosis reveals a role in the second pathway of crossing-over. *Plant J* 54, 152-162.

Higgins, J.D., Sanchez-Moran, E., Armstrong, S.J., Jones, G.H., and Franklin, F.C. (2005). The Arabidopsis synaptonemal complex protein ZYP1 is required for chromosome synapsis and normal fidelity of crossing over. *Genes Dev* 19, 2488-2500.

- Higgins, J.D., Vignard, J., Mercier, R., Pugh, A.G., Franklin, F.C., and Jones, G.H. (2008b). AtMSH5 partners AtMSH4 in the class I meiotic crossover pathway in *Arabidopsis thaliana*, but is not required for synapsis. *Plant J* 55, 28-39.
- Hohl, M., Kwon, Y., Galvan, S.M., Xue, X., Tous, C., Aguilera, A., Sung, P., and Petrini, J.H. (2011). The Rad50 coiled-coil domain is indispensable for Mre11 complex functions. *Nat Struct Mol Biol* 18, 1124-1131.
- Holliday, R. (1964). A mechanism for gene conversion in fungi. *Genet Res* 5, 282-304.
- Hollingsworth, N.M., and Brill, S.J. (2004). The Mus81 solution to resolution: generating meiotic crossovers without Holliday junctions. *Genes Dev* 18, 117-125.
- Holloway, J.K., Booth, J., Edelmann, W., McGowan, C.H., and Cohen, P.E. (2008). MUS81 generates a subset of MLH1-MLH3-independent crossovers in mammalian meiosis. *PLoS Genet* 4, e1000186.
- Hong, E.L., Shinohara, A., and Bishop, D.K. (2001). *Saccharomyces cerevisiae* Dmc1 protein promotes renaturation of single-strand DNA (ssDNA) and assimilation of ssDNA into homologous super-coiled duplex DNA. *J Biol Chem* 276, 41906-41912.
- Hong, S., Sung, Y., Yu, M., Lee, M., Kleckner, N., and Kim, K.P. (2013). The logic and mechanism of homologous recombination partner choice. *Mol Cell* 51, 440-453.
- Hopfner, K.P., Craig, L., Moncalian, G., Zinkel, R.A., Usui, T., Owen, B.A., Karcher, A., Henderson, B., Bodmer, J.L., McMurray, C.T., *et al.* (2002). The Rad50 zinc-hook is a structure joining Mre11 complexes in DNA recombination and repair. *Nature* 418, 562-566.
- Hotta, Y., Furukawa, K., and Tabata, S. (1995). Meiosis specific transcription and functional proteins. *Adv Biophys* 31, 101-115.

- Hulten, M.A. (2011). On the origin of crossover interference: A chromosome oscillatory movement (COM) model. *Mol Cytogenet* 4, 10.
- Hunter, N. (2015). *Meiotic Recombination: The Essence of Heredity*. Cold Spring Harb Perspect Biol 7.
- Hunter, N., and Kleckner, N. (2001). The single-end invasion: an asymmetric intermediate at the double-strand break to double-holliday junction transition of meiotic recombination. *Cell* 106, 59-70.
- Hwang, W.Y., Fu, Y., Reyon, D., Maeder, M.L., Tsai, S.Q., Sander, J.D., Peterson, R.T., Yeh, J.R., and Joung, J.K. (2013). Efficient genome editing in zebrafish using a CRISPR-Cas system. *Nat Biotechnol* 31, 227-229.
- Jackson, N., Sanchez-Moran, E., Buckling, E., Armstrong, S.J., Jones, G.H., and Franklin, F.C. (2006). Reduced meiotic crossovers and delayed prophase I progression in AtMLH3-deficient Arabidopsis. *EMBO J* 25, 1315-1323.
- Jessop, L., and Lichten, M. (2008). Mus81/Mms4 endonuclease and Sgs1 helicase collaborate to ensure proper recombination intermediate metabolism during meiosis. *Mol Cell* 31, 313-323.
- Ji, J., Tang, D., Wang, K., Wang, M., Che, L., Li, M., and Cheng, Z. (2012). The role of OsCOM1 in homologous chromosome synapsis and recombination in rice meiosis. *Plant J* 72, 18-30.
- Jinek, M., Chylinski, K., Fonfara, I., Hauer, M., Doudna, J.A., and Charpentier, E. (2012). A programmable dual-RNA-guided DNA endonuclease in adaptive bacterial immunity. *Science* 337, 816-821.
- Jinek, M., East, A., Cheng, A., Lin, S., Ma, E., and Doudna, J. (2013). RNA-programmed genome editing in human cells. *Elife* 2, e00471.
- Jones, G.H. (1984). The control of chiasma distribution. *Symp Soc Exp Biol* 38, 293-320.

- Jones, G.H., and Franklin, F.C. (2006). Meiotic crossing-over: obligation and interference. *Cell* *126*, 246-248.
- Kagawa, W., and Kurumizaka, H. (2010). From meiosis to postmeiotic events: uncovering the molecular roles of the meiosis-specific recombinase Dmc1. *FEBS J* *277*, 590-598.
- Kakarougkas, A., and Jeggo, P.A. (2014). DNA DSB repair pathway choice: an orchestrated handover mechanism. *Br J Radiol* *87*, 20130685.
- Kans, J.A., and Mortimer, R.K. (1991). Nucleotide sequence of the RAD57 gene of *Saccharomyces cerevisiae*. *Gene* *105*, 139-140.
- Kathiresan, A., Khush, G.S., and Bennett, J. (2002). Two rice DMC1 genes are differentially expressed during meiosis and during haploid and diploid mitosis. *Sexual Plant Reprod* *14*, 257-267.
- Katis, V.L., Galova, M., Rabitsch, K.P., Gregan, J., and Nasmyth, K. (2004). Maintenance of cohesin at centromeres after meiosis I in budding yeast requires a kinetochore-associated protein related to MEI-S332. *Curr Biol* *14*, 560-572.
- Kauppi, L., Barchi, M., Baudat, F., Romanienko, P.J., Keeney, S., and Jasin, M. (2011). Distinct properties of the XY pseudoautosomal region crucial for male meiosis. *Science* *331*, 916-920.
- Kawabata, M., Kawabata, T., and Nishibori, M. (2005). Role of recA/RAD51 family proteins in mammals. *Acta Med Okayama* *59*, 1-9.
- Kaye, J.A., Melo, J.A., Cheung, S.K., Vaze, M.B., Haber, J.E., and Toczyski, D.P. (2004). DNA breaks promote genomic instability by impeding proper chromosome segregation. *Curr Biol* *14*, 2096-2106.
- Keeney, S., Baudat, F., Angeles, M., Zhou, Z.H., Copeland, N.G., Jenkins, N.A., Manova, K., and Jasin, M. (1999). A mouse homolog of the *Saccharomyces cerevisiae* meiotic recombination DNA transesterase Spo11p. *Genomics* *61*, 170-182.

- Keeney, S., Giroux, C.N., and Kleckner, N. (1997). Meiosis-specific DNA double-strand breaks are catalyzed by Spo11, a member of a widely conserved protein family. *Cell* *88*, 375-384.
- Khasanov, F.K., Savchenko, G.V., Bashkirova, E.V., Korolev, V.G., Heyer, W.D., and Bashkirov, V.I. (1999). A new recombinational DNA repair gene from *Schizosaccharomyces pombe* with homology to *Escherichia coli* RecA. *Genetics* *152*, 1557-1572.
- Kim, J.S., Krasieva, T.B., Kurumizaka, H., Chen, D.J., Taylor, A.M., and Yokomori, K. (2005). Independent and sequential recruitment of NHEJ and HR factors to DNA damage sites in mammalian cells. *J Cell Biol* *170*, 341-347.
- Kim, K.P., Weiner, B.M., Zhang, L., Jordan, A., Dekker, J., and Kleckner, N. (2010). Sister cohesion and structural axis components mediate homolog bias of meiotic recombination. *Cell* *143*, 924-937.
- King, J.S., and Mortimer, R.K. (1990). A polymerization model of chiasma interference and corresponding computer simulation. *Genetics* *126*, 1127-1138.
- Kitajima, T.S., Kawashima, S.A., and Watanabe, Y. (2004). The conserved kinetochore protein shugoshin protects centromeric cohesion during meiosis. *Nature* *427*, 510-517.
- Klapstein, K., Chou, T., and Bruinsma, R. (2004). Physics of RecA-mediated homologous recognition. *Biophys J* *87*, 1466-1477.
- Kleckner, N. (1996). Meiosis: how could it work? *Proc Natl Acad Sci U S A* *93*, 8167-8174.
- Kleckner, N., Zickler, D., Jones, G.H., Dekker, J., Padmore, R., Henle, J., and Hutchinson, J. (2004). A mechanical basis for chromosome function. *Proc Natl Acad Sci U S A* *101*, 12592-12597.

- Klutstein, M., Fennell, A., Fernandez-Alvarez, A., and Cooper, J.P. (2015). The telomere bouquet regulates meiotic centromere assembly. *Nat Cell Biol* 17, 458-469.
- Knoll, A., Higgins, J.D., Seeliger, K., Reha, S.J., Dangel, N.J., Bauknecht, M., Schropfer, S., Franklin, F.C., and Puchta, H. (2012). The Fanconi anemia ortholog FANCM ensures ordered homologous recombination in both somatic and meiotic cells in *Arabidopsis*. *Plant Cell* 24, 1448-1464.
- Kobayashi, T., Kobayashi, E., Sato, S., Hotta, Y., Miyajima, N., Tanaka, A., and Tabata, S. (1994). Characterization of cDNAs induced in meiotic prophase in lily microsporocytes. *DNA Res* 1, 15-26.
- Kobayashi, W., Sekine, S., Machida, S., and Kurumizaka, H. (2014). Green fluorescent protein fused to the C terminus of RAD51 specifically interferes with secondary DNA binding by the RAD51-ssDNA complex. *Genes Genet Syst* 89, 169-179.
- Komor, A.C., Badran, A.H., and Liu, D.R. (2017). CRISPR-Based Technologies for the Manipulation of Eukaryotic Genomes. *Cell* 168, 20-36.
- Komori, K., Miyata, T., DiRuggiero, J., Holley-Shanks, R., Hayashi, I., Cann, I.K., Mayanagi, K., Shinagawa, H., and Ishino, Y. (2000). Both RadA and RadB are involved in homologous recombination in *Pyrococcus furiosus*. *J Biol Chem* 275, 33782-33790.
- Kowalczykowski, S.C. (1991). Biochemistry of genetic recombination: energetics and mechanism of DNA strand exchange. *Annu Rev Biophys Biophys Chem* 20, 539-575.
- Kudo, N.R., Wassmann, K., Anger, M., Schuh, M., Wirth, K.G., Xu, H., Helmhart, W., Kudo, H., McKay, M., Maro, B., *et al.* (2006). Resolution of chiasmata in oocytes requires separase-mediated proteolysis. *Cell* 126, 135-146.

- Kumar, R., Bourbon, H.M., and de Massy, B. (2010). Functional conservation of Mei4 for meiotic DNA double-strand break formation from yeasts to mice. *Genes Dev* 24, 1266-1280.
- Kurdzo, E.L., and Dawson, D.S. (2015). Centromere pairing--tethering partner chromosomes in meiosis I. *FEBS J* 282, 2458-2470.
- Kurzbauer, M.-T., Uanschou, C., Chen, D., and Schlögelhofer, P. (2012). The recombinases DMC1 and RAD51 are functionally and spatially separated during meiosis in *Arabidopsis*. *Plant Cell* 24, 2058-2070.
- Kuznetsov, S., Pellegrini, M., Shuda, K., Fernandez-Capetillo, O., Liu, Y., Martin, B.K., Burkett, S., Southon, E., Pati, D., Tessarollo, L., *et al.* (2007). RAD51C deficiency in mice results in early prophase I arrest in males and sister chromatid separation at metaphase II in females. *J Cell Biol* 176, 581-592.
- Kuznetsov, S.G., Haines, D.C., Martin, B.K., and Sharan, S.K. (2009). Loss of Rad51c leads to embryonic lethality and modulation of Trp53-dependent tumorigenesis in mice. *Cancer Res* 69, 863-872.
- Lacefield, S., and Murray, A.W. (2007). The spindle checkpoint rescues the meiotic segregation of chromosomes whose crossovers are far from the centromere. *Nat Genet* 39, 1273-1277.
- Lake, C.M., and Hawley, R.S. (2012). The molecular control of meiotic chromosomal behavior: events in early meiotic prophase in *Drosophila* oocytes. *Annu Rev Physiol* 74, 425-451.
- Lam, I., and Keeney, S. (2014). Mechanism and regulation of meiotic recombination initiation. *Cold Spring Harb Perspect Biol* 7, a016634.
- Lambing, C., Franklin, F.C., and Wang, C.R. (2017). Understanding and Manipulating Meiotic Recombination in Plants. *Plant Physiol* 173, 1530-1542.
- Lao, J.P., Cloud, V., Huang, C.C., Grubb, J., Thacker, D., Lee, C.Y., Dresser, M.E., Hunter, N., and Bishop, D.K. (2013). Meiotic crossover control by concerted

action of Rad51-Dmc1 in homolog template bias and robust homeostatic regulation. *PLoS Genet* 9, e1003978.

Lao, J.P., Oh, S.D., Shinohara, M., Shinohara, A., and Hunter, N. (2008). Rad52 Promotes Postinvasion Steps of Meiotic Double-Strand-Break Repair. *Mol Cell*.

Lee, C.Y., Conrad, M.N., and Dresser, M.E. (2012). Meiotic chromosome pairing is promoted by telomere-led chromosome movements independent of bouquet formation. *PLoS Genet* 8, e1002730.

Lee, J.H., Mand, M.R., Deshpande, R.A., Kinoshita, E., Yang, S.H., Wyman, C., and Paull, T.T. (2013). Ataxia telangiectasia-mutated (ATM) kinase activity is regulated by ATP-driven conformational changes in the Mre11/Rad50/Nbs1 (MRN) complex. *J Biol Chem* 288, 12840-12851.

Lee, M.-H., Chang, Y.-C., Hong, E.L., Grubb, J., Chang, C.-S., Bishop, D.K., and Wang, T.-F. (2005). Calcium ion promotes yeast Dmc1 activity via formation of long and fine helical filaments with single-stranded DNA. *J Biol Chem* 280, 40980-40984.

Li, J., Harper, L.C., Golubovskaya, I., Wang, C.R., Weber, D., Meeley, R.B., McElver, J., Bowen, B., Cande, W.Z., and Schnable, P.S. (2007). Functional analysis of maize RAD51 in meiosis and double-strand break repair. *Genetics* 176, 1469-1482.

Li, J.F., Norville, J.E., Aach, J., McCormack, M., Zhang, D., Bush, J., Church, G.M., and Sheen, J. (2013). Multiplex and homologous recombination-mediated genome editing in *Arabidopsis* and *Nicotiana benthamiana* using guide RNA and Cas9. *Nat Biotechnol* 31, 688-691.

Li, T., Liu, B., Spalding, M.H., Weeks, D.P., and Yang, B. (2012). High-efficiency TALEN-based gene editing produces disease-resistant rice. *Nat Biotechnol* 30, 390-392.

Li, W., Chen, C., Markmann-Mulisch, U., Timofejeva, L., Schmelzer, E., Ma, H., and Reiss, B. (2004). The *Arabidopsis* AtRAD51 gene is dispensable for vegetative development but required for meiosis. *Proc Natl Acad Sci U S A* 101, 10596-10601.

- Li, W., and Ma, H. (2006). Double-stranded DNA breaks and gene functions in recombination and meiosis. *Cell Res* *16*, 402-412.
- Li, W., Yang, X., Lin, Z., Timofejeva, L., Xiao, R., Makaroff, C.A., and Ma, H. (2005). The AtRAD51C gene is required for normal meiotic chromosome synapsis and double-stranded break repair in Arabidopsis. *Plant Physiol* *138*, 965-976.
- Li, Z., Golub, E.I., Gupta, R., and Radding, C.M. (1997). Recombination activities of HsDmc1 protein, the meiotic human homolog of RecA protein. *Proc Natl Acad Sci U S A* *94*, 11221-11226.
- Libby, B.J., Reinholdt, L.G., and Schimenti, J.C. (2003). Positional cloning and characterization of Mei1, a vertebrate-specific gene required for normal meiotic chromosome synapsis in mice. *Proc Natl Acad Sci U S A* *100*, 15706-15711.
- Libuda, D.E., Uzawa, S., Meyer, B.J., and Villeneuve, A.M. (2013). Meiotic chromosome structures constrain and respond to designation of crossover sites. *Nature* *502*, 703-706.
- Lieber, M.R. (2010). The mechanism of double-strand DNA break repair by the nonhomologous DNA end-joining pathway. *Annu Rev Biochem* *79*, 181-211.
- Lim, D.S., and Hasty, P. (1996). A mutation in mouse rad51 results in an early embryonic lethal that is suppressed by a mutation in p53. *Mol Cell Biol* *16*, 7133-7143.
- Liu, H., Jang, J.K., Kato, N., and McKim, K.S. (2002). mei-P22 encodes a chromosome-associated protein required for the initiation of meiotic recombination in *Drosophila melanogaster*. *Genetics* *162*, 245-258.
- Liu, J., Renault, L., Veaute, X., Fabre, F., Stahlberg, H., and Heyer, W.D. (2011). Rad51 paralogues Rad55-Rad57 balance the antirecombinase Srs2 in Rad51 filament formation. *Nature* *479*, 245-248.

- Liu, N., Schild, D., Thelen, M.P., and Thompson, L.H. (2002b). Involvement of Rad51C in two distinct protein complexes of Rad51 paralogs in human cells. *Nucleic Acids Res* 30, 1009-1015.
- Liu, Y., Deng, Y., Li, G., and Zhao, J. (2013). Replication factor C1 (RFC1) is required for double-strand break repair during meiotic homologous recombination in Arabidopsis. *Plant J* 73, 154-165.
- Liu, Y., Tarsounas, M., O'Regan, P., and West, S.C. (2007). Role of RAD51C and XRCC3 in genetic recombination and DNA repair. *J Biol Chem* 282, 1973-1979.
- Lobachev, K., Vitriol, E., Stemple, J., Resnick, M.A., and Bloom, K. (2004). Chromosome fragmentation after induction of a double-strand break is an active process prevented by the RMX repair complex. *Curr Biol* 14, 2107-2112.
- Loidl, J. (2016). Conservation and Variability of Meiosis Across the Eukaryotes. *Annu Rev Genet* 50, 293-316.
- Lorenz, A., Osman, F., Sun, W., Nandi, S., Steinacher, R., and Whitby, M.C. (2012). The fission yeast FANCM ortholog directs non-crossover recombination during meiosis. *Science* 336, 1585-1588.
- Lovett, S.T. (1994). Sequence of the RAD55 gene of *Saccharomyces cerevisiae*: similarity of RAD55 to prokaryotic RecA and other RecA-like proteins. *Gene* 142, 103-106.
- Lu, P., Han, X., Qi, J., Yang, J., Wijeratne, A.J., Li, T., and Ma, H. (2012). Analysis of Arabidopsis genome-wide variations before and after meiosis and meiotic recombination by resequencing *Landsberg erecta* and all four products of a single meiosis. *Genome Res* 22, 508-518.
- Ma, H. (2006). A molecular portrait of Arabidopsis meiosis. *Arabidopsis Book* 4, e0095.
- Macaisne, N., Novatchkova, M., Peirera, L., Vezon, D., Jolivet, S., Froger, N., Chelysheva, L., Grelon, M., and Mercier, R. (2008). SHOC1, an XPF endonuclease-

related protein, is essential for the formation of class I meiotic crossovers. *Curr Biol* 18, 1432-1437.

Macaisne, N., Vignard, J., and Mercier, R. (2011). SHOC1 and PTD form an XPF-ERCC1-like complex that is required for formation of class I crossovers. *J Cell Sci* 124, 2687-2691.

Macqueen, A.J., and Roeder, G.S. (2009). Fpr3 and Zip3 ensure that initiation of meiotic recombination precedes chromosome synapsis in budding yeast. *Curr Biol* 19, 1519-1526.

Maleki, S., Neale, M.J., Arora, C., Henderson, K.A., and Keeney, S. (2007). Interactions between Mei4, Rec114, and other proteins required for meiotic DNA double-strand break formation in *Saccharomyces cerevisiae*. *Chromosoma* 116, 471-486.

Mali, P., Yang, L., Esvelt, K.M., Aach, J., Guell, M., DiCarlo, J.E., Norville, J.E., and Church, G.M. (2013). RNA-guided human genome engineering via Cas9. *Science* 339, 823-826.

Malik, S.B., Ramesh, M.A., Hulstrand, A.M., and Logsdon, J.M., Jr. (2007). Protist homologs of the meiotic Spo11 gene and topoisomerase VI reveal an evolutionary history of gene duplication and lineage-specific loss. *Mol Biol Evol* 24, 2827-2841.

Mancera, E., Bourgon, R., Brozzi, A., Huber, W., and Steinmetz, L.M. (2008). High-resolution mapping of meiotic crossovers and non-crossovers in yeast. *Nature* 454, 479-485.

Manfrini, N., Guerini, I., Citterio, A., Lucchini, G., and Longhese, M.P. (2010). Processing of meiotic DNA double strand breaks requires cyclin-dependent kinase and multiple nucleases. *J Biol Chem* 285, 11628-11637.

Marston, A.L. (2015). Shugoshins: tension-sensitive pericentromeric adaptors safeguarding chromosome segregation. *Mol Cell Biol* 35, 634-648.

- Marston, A.L., Tham, W.H., Shah, H., and Amon, A. (2004). A genome-wide screen identifies genes required for centromeric cohesion. *Science* *303*, 1367-1370.
- Martini, E., Diaz, R.L., Hunter, N., and Keeney, S. (2006). Crossover homeostasis in yeast meiosis. *Cell* *126*, 285-295.
- Masson, J.Y., Stasiak, A.Z., Stasiak, A., Benson, F.E., and West, S.C. (2001b). Complex formation by the human RAD51C and XRCC3 recombination repair proteins. *Proc Natl Acad Sci U S A* *98*, 8440-8446.
- Masson, J.Y., Tarsounas, M.C., Stasiak, A.Z., Stasiak, A., Shah, R., McIlwraith, M.J., Benson, F.E., and West, S.C. (2001a). Identification and purification of two distinct complexes containing the five RAD51 paralogs. *Genes Dev* *15*, 3296-3307.
- Masson, J.Y., and West, S.C. (2001). The Rad51 and Dmc1 recombinases: a non-identical twin relationship. *Trends Biochem Sci*.
- Matos, J., Blanco, M.G., Maslen, S., Skehel, J.M., and West, S.C. (2011). Regulatory control of the resolution of DNA recombination intermediates during meiosis and mitosis. *Cell* *147*, 158-172.
- Mazina, O.M., Mazin, A.V., Nakagawa, T., Kolodner, R.D., and Kowalczykowski, S.C. (2004). *Saccharomyces cerevisiae* Mer3 helicase stimulates 3'-5' heteroduplex extension by Rad51; implications for crossover control in meiotic recombination. *Cell* *117*, 47-56.
- McKee, B.D., Yan, R., and Tsai, J.H. (2012). Meiosis in male *Drosophila*. *Spermatogenesis* *2*, 167-184.
- McKim, K.S., Green-Marroquin, B.L., Sekelsky, J.J., Chin, G., Steinberg, C., Khodosh, R., and Hawley, R.S. (1998). Meiotic synapsis in the absence of recombination. *Science* *279*, 876-878.
- McMahill, M.S., Sham, C.W., and Bishop, D.K. (2007). Synthesis-dependent strand annealing in meiosis. *PLoS Biol* *5*, e299.

- Mehta, A., and Haber, J.E. (2014). Sources of DNA double-strand breaks and models of recombinational DNA repair. *Cold Spring Harb Perspect Biol* 6, a016428.
- Mercier, R., Jolivet, S., Vezon, D., Huppe, E., Chelysheva, L., Giovanni, M., Nogue, F., Doutriaux, M.P., Horlow, C., Grelon, M., *et al.* (2005). Two meiotic crossover classes cohabit in Arabidopsis: one is dependent on MER3, whereas the other one is not. *Curr Biol* 15, 692-701.
- Mercier, R., Mezard, C., Jenczewski, E., Macaisne, N., and Grelon, M. (2014). The molecular biology of meiosis in plants. *Annu Rev Plant Biol* 66, 297-327.
- Miao, J., Guo, D., Zhang, J., Huang, Q., Qin, G., Zhang, X., Wan, J., Gu, H., and Qu, L.J. (2013). Targeted mutagenesis in rice using CRISPR-Cas system. *Cell Res* 23, 1233-1236.
- Miller, K.A., Sawicka, D., Barsky, D., and Albala, J.S. (2004). Domain mapping of the Rad51 paralog protein complexes. *Nucleic Acids Res* 32, 169-178.
- Miller, K.A., Yoshikawa, D.M., McConnell, I.R., Clark, R., Schild, D., and Albala, J.S. (2002). RAD51C interacts with RAD51B and is central to a larger protein complex in vivo exclusive of RAD51. *J Biol Chem* 277, 8406-8411.
- Mitchell, M.B. (1955). ABERRANT RECOMBINATION OF PYRIDOXINE MUTANTS OF Neurospora. *Proc Natl Acad Sci U S A* 41, 215-220.
- Mockel, C., Lammens, K., Schele, A., and Hopfner, K.P. (2012). ATP driven structural changes of the bacterial Mre11:Rad50 catalytic head complex. *Nucleic Acids Res* 40, 914-927.
- Moens, P.B., Marcon, E., Shore, J.S., Kochakpour, N., and Spyropoulos, B. (2007). Initiation and resolution of interhomolog connections: crossover and non-crossover sites along mouse synaptonemal complexes. *J Cell Sci* 120, 1017-1027.

- Molnar, S.J., Gupta, P.K., Fedak, G., and Wheatcroft, R. (1989). Ribosomal DNA repeat unit polymorphism in 25 *Hordeum* species. *Theor Appl Genet* 78, 387-392.
- Morozumi, Y., Ino, R., Ikawa, S., Mimida, N., Shimizu, T., Toki, S., Ichikawa, H., Shibata, T., and Kurumizaka, H. (2013). Homologous pairing activities of two rice RAD51 proteins, RAD51A1 and RAD51A2. *PLoS One* 8, e75451.
- Morriscal, S.W. (2015). DNA-pairing and annealing processes in homologous recombination and homology-directed repair. *Cold Spring Harb Perspect Biol* 7, a016444.
- Moses, M.J. (1958). The relation between the axial complex of meiotic prophase chromosomes and chromosome pairing in a salamander (*Plethodon cinereus*). *J Biophys Biochem Cytol* 4, 633-638.
- Mussolino, C., and Cathomen, T. (2013). RNA guides genome engineering. *Nat Biotechnol* 31, 208-209.
- Myler, L.R., and Finkelstein, I.J. (2017). Eukaryotic resectosomes: A single-molecule perspective. *Prog Biophys Mol Biol* 127, 119-129.
- Nakagawa, T., and Kolodner, R.D. (2002). *Saccharomyces cerevisiae* Mer3 is a DNA helicase involved in meiotic crossing over. *Mol Cell Biol* 22, 3281-3291.
- Neale, M.J., and Keeney, S. (2006). Clarifying the mechanics of DNA strand exchange in meiotic recombination. *Nature* 442, 153-158.
- Neale, M.J., Pan, J., and Keeney, S. (2005). Endonucleolytic processing of covalent protein-linked DNA double-strand breaks. *Nature* 436, 1053-1057.
- Nimonkar, A.V., Dombrowski, C.C., Siino, J.S., Stasiak, A.Z., Stasiak, A., and Kowalczykowski, S.C. (2012). *Saccharomyces cerevisiae* Dmc1 and Rad51 proteins preferentially function with Tid1 and Rad54 proteins, respectively, to promote DNA strand invasion during genetic recombination. *J Biol Chem* 287, 28727-28737.

- Nishant, K.T., Plys, A.J., and Alani, E. (2008). A mutation in the putative MLH3 endonuclease domain confers a defect in both mismatch repair and meiosis in *Saccharomyces cerevisiae*. *Genetics* *179*, 747-755.
- Nishino, T., Komori, K., Ishino, Y., and Morikawa, K. (2005). Structural and functional analyses of an archaeal XPF/Rad1/Mus81 nuclease: asymmetric DNA binding and cleavage mechanisms. *Structure* *13*, 1183-1192.
- Nonomura, K.I., Nakano, M., Murata, K., Miyoshi, K., Eiguchi, M., Miyao, A., Hirochika, H., and Kurata, N. (2004). An insertional mutation in the rice PAIR2 gene, the ortholog of Arabidopsis ASY1, results in a defect in homologous chromosome pairing during meiosis. *Mol Genet Genomics* *271*, 121-129.
- Ogawa, T., Yu, X., Shinohara, A., and Egelman, E.H. (1993). Similarity of the yeast RAD51 filament to the bacterial RecA filament. *Science* *259*, 1896-1899.
- Oh, S.D., Lao, J.P., Taylor, A.F., Smith, G.R., and Hunter, N. (2008). RecQ helicase, Sgs1, and XPF family endonuclease, Mus81-Mms4, resolve aberrant joint molecules during meiotic recombination. *Mol Cell* *31*, 324-336.
- Oliver-Bonet, M., Campillo, M., Turek, P.J., Ko, E., and Martin, R.H. (2007). Analysis of replication protein A (RPA) in human spermatogenesis. *Mol Hum Reprod* *13*, 837-844.
- Olivier, M., Da Ines, O., Amiard, S., Serra, H., Goubely, C., White, C.I., and Gallego, M.E. (2016). The Structure-Specific Endonucleases MUS81 and SEND1 Are Essential for Telomere Stability in Arabidopsis. *Plant Cell* *28*, 74-86.
- Osakabe, K., Abe, K., Yamanouchi, H., Takyuu, T., Yoshioka, T., Ito, Y., Kato, T., Tabata, S., Kurei, S., Yoshioka, Y., *et al.* (2005). Arabidopsis Rad51B is important for double-strand DNA breaks repair in somatic cells. *Plant Mol Biol* *57*, 819-833.
- Osakabe, K., Yoshioka, T., Ichikawa, H., and Toki, S. (2002). Molecular cloning and characterization of RAD51-like genes from Arabidopsis thaliana. *Plant Mol Biol* *50*, 71-81.

- Osman, K., Higgins, J.D., Sanchez-Moran, E., Armstrong, S.J., and Franklin, F.C.H. (2011). Pathways to meiotic recombination in *Arabidopsis thaliana*. *New Phytol* *190*, 523-544.
- Osman, K., Sanchez-Moran, E., Mann, S.C., Jones, G.H., and Franklin, F.C. (2009). Replication protein A (AtRPA1a) is required for class I crossover formation but is dispensable for meiotic DNA break repair. *EMBO J* *28*, 394-404.
- Page, S.L., and Hawley, R.S. (2004). The genetics and molecular biology of the synaptonemal complex. *Annu Rev Cell Dev Biol* *20*, 525-558.
- Paques, F., and Haber, J.E. (1999). Multiple pathways of recombination induced by double-strand breaks in *Saccharomyces cerevisiae*. *Microbiol Mol Biol Rev* *63*, 349-404.
- Passy, S.I., Yu, X., Li, Z., Radding, C.M., Masson, J.Y., West, S.C., and Egelman, E.H. (1999). Human Dmc1 protein binds DNA as an octameric ring. *Proc Natl Acad Sci U S A* *96*, 10684-10688.
- Paull, T.T., and Gellert, M. (1998). The 3' to 5' exonuclease activity of Mre 11 facilitates repair of DNA double-strand breaks. *Mol Cell* *1*, 969-979.
- Pezza, R.J., Camerini-Otero, R.D., and Bianco, P.R. (2010). Hop2-Mnd1 condenses DNA to stimulate the synapsis phase of DNA strand exchange. *Biophys J* *99*, 3763-3772.
- Pezza, R.J., Voloshin, O.N., Vanevski, F., and Camerini-Otero, R.D. (2007). Hop2/Mnd1 acts on two critical steps in Dmc1-promoted homologous pairing. *Genes Dev* *21*, 1758-1766.
- Pezza, R.J., Voloshin, O.N., Volodin, A.A., Boateng, K.A., Bellani, M.A., Mazin, A.V., and Camerini-Otero, R.D. (2013). The dual role of HOP2 in mammalian meiotic homologous recombination. *Nucleic Acids Res* *42*, 2346-2357.
- Pittman, D.L., Cobb, J., Schimenti, K.J., Wilson, L.A., Cooper, D.M., Brignull, E., Handel, M.A., and Schimenti, J.C. (1998). Meiotic prophase arrest with failure of

chromosome synapsis in mice deficient for Dmc1, a germline-specific RecA homolog. *Mol Cell* 1, 697-705.

Pittman, D.L., and Schimenti, J.C. (2000). Midgestation lethality in mice deficient for the RecA-related gene, Rad51d/Rad51l3. *Genesis* 26, 167-173.

Puizina, J., Siroky, J., Mokros, P., Schweizer, D., and Riha, K. (2004). Mre11 deficiency in Arabidopsis is associated with chromosomal instability in somatic cells and Spo11-dependent genome fragmentation during meiosis. *Plant Cell* 16, 1968-1978.

Qi, J., Chen, Y., Copenhaver, G.P., and Ma, H. (2014). Detection of genomic variations and DNA polymorphisms and impact on analysis of meiotic recombination and genetic mapping. *Proc Natl Acad Sci U S A* 111, 10007-10012.

Qiao, H., Prasada Rao, H.B., Yang, Y., Fong, J.H., Cloutier, J.M., Deacon, D.C., Nagel, K.E., Swartz, R.K., Strong, E., Holloway, J.K., *et al.* (2014). Antagonistic roles of ubiquitin ligase HEI10 and SUMO ligase RNF212 regulate meiotic recombination. *Nat Genet* 46, 194-199.

Rajanikant, C., Melzer, M., Rao, B.J., and Sainis, J.K. (2008). Homologous recombination properties of OsRad51, a recombinase from rice. *Plant Mol Biol* 68, 479-491.

Ramesh, M.A., Malik, S.-B., and Logsdon, J.M. (2005). A phylogenomic inventory of meiotic genes; evidence for sex in Giardia and an early eukaryotic origin of meiosis. *Curr Biol* 15, 185-191.

Ranjha, L., Anand, R., and Cejka, P. (2014). The *Saccharomyces cerevisiae* Mlh1-Mlh3 heterodimer is an endonuclease that preferentially binds to Holliday junctions. *J Biol Chem* 289, 5674-5686.

Reynolds, A., Qiao, H., Yang, Y., Chen, J.K., Jackson, N., Biswas, K., Holloway, J.K., Baudat, F., de Massy, B., Wang, J., *et al.* (2013). RNF212 is a dosage-sensitive regulator of crossing-over during mammalian meiosis. *Nat Genet* 45, 269-278.

- Robert, T., Nore, A., Brun, C., Maffre, C., Crimi, B., Bourbon, H.M., and de Massy, B. (2016a). The TopoVIB-Like protein family is required for meiotic DNA double-strand break formation. *Science* *351*, 943-949.
- Robert, T., Vrielynck, N., Mezard, C., de Massy, B., and Grelon, M. (2016). A new light on the meiotic DSB catalytic complex. *Semin Cell Dev Biol* *54*, 165-176.
- Roberts, N.Y., Osman, K., and Armstrong, S.J. (2009). Telomere distribution and dynamics in somatic and meiotic nuclei of *Arabidopsis thaliana*. *Cytogenet Genome Res* *124*, 193-201.
- Robertson, R.B., Moses, D.N., Kwon, Y., Chan, P., Zhao, W., Chi, P., Klein, H., Sung, P., and Greene, E.C. (2009). Visualizing the disassembly of *S. cerevisiae* Rad51 nucleoprotein filaments. *J Mol Biol* *388*, 703-720.
- Roeder, G.S. (1997). Meiotic chromosomes: it takes two to tango. *Genes Dev* *11*, 2600-2621.
- Rog, O., and Dernburg, A.F. (2013). Chromosome pairing and synapsis during *Caenorhabditis elegans* meiosis. *Curr Opin Cell Biol* *25*, 349-356.
- Rogacheva, M.V., Manhart, C.M., Chen, C., Guarne, A., Surtees, J., and Alani, E. (2014). Mlh1-Mlh3, a meiotic crossover and DNA mismatch repair factor, is a Msh2-Msh3-stimulated endonuclease. *J Biol Chem* *289*, 5664-5673.
- Romanienko, P.J., and Camerini-Otero, R.D. (1999). Cloning, characterization, and localization of mouse and human SP011. *Genomics* *61*, 156-169.
- Ross, K.J., Fransz, P., and Jones, G.H. (1996). A light microscopic atlas of meiosis in *Arabidopsis thaliana*. *Chromosome Res* *4*, 507-516.
- Ross-Macdonald, P., and Roeder, G.S. (1994). Mutation of a meiosis-specific MutS homolog decreases crossing over but not mismatch correction. *Cell* *79*, 1069-1080.

Sancar, A., Lindsey-Boltz, L.A., Unsal-Kacmaz, K., and Linn, S. (2004). Molecular mechanisms of mammalian DNA repair and the DNA damage checkpoints. *Annu Rev Biochem* 73, 39-85.

Sanchez Moran, E., Armstrong, S.J., Santos, J.L., Franklin, F.C., and Jones, G.H. (2001). Chiasma formation in *Arabidopsis thaliana* accession Wassileskija and in two meiotic mutants. *Chromosome Res* 9, 121-128.

Sanchez-Moran, E., Armstrong, S.J., Santos, J.L., Franklin, F.C., and Jones, G.H. (2002). Variation in chiasma frequency among eight accessions of *Arabidopsis thaliana*. *Genetics* 162, 1415-1422.

Sanchez-Moran, E., Santos, J.L., Jones, G.H., and Franklin, F.C. (2007). ASY1 mediates AtDMC1-dependent interhomolog recombination during meiosis in *Arabidopsis*. *Genes Dev* 21, 2220-2233.

Sartori, A.A., Lukas, C., Coates, J., Mistrik, M., Fu, S., Bartek, J., Baer, R., Lukas, J., and Jackson, S.P. (2007). Human CtIP promotes DNA end resection. *Nature* 450, 509-514.

Schild, D., Lio, Y.C., Collins, D.W., Tsomondo, T., and Chen, D.J. (2000). Evidence for simultaneous protein interactions between human Rad51 paralogs. *J Biol Chem* 275, 16443-16449.

Schimpl, S., Fauser, F., and Puchta, H. (2014). The CRISPR/Cas system can be used as nuclease for in planta gene targeting and as paired nickases for directed mutagenesis in *Arabidopsis* resulting in heritable progeny. *Plant J* 80, 1139-1150.

Schwacha, A., and Kleckner, N. (1995). Identification of double Holliday junctions as intermediates in meiotic recombination. *Cell* 83, 783-791.

Schwacha, A., and Kleckner, N. (1997). Interhomolog bias during meiotic recombination: meiotic functions promote a highly differentiated interhomolog-only pathway. *Cell* 90, 1123-1135.

- Seeliger, K., Dukowic-Schulze, S., Wurz-Wildersinn, R., Pacher, M., and Puchta, H. (2012). BRCA2 is a mediator of RAD51- and DMC1-facilitated homologous recombination in *Arabidopsis thaliana*. *New Phytol* *193*, 364-375.
- Segal, D.J., and Meckler, J.F. (2013). Genome engineering at the dawn of the golden age. *Annu Rev Genomics Hum Genet* *14*, 135-158.
- Sehorn, M.G., Sigurdsson, S., Bussen, W., Unger, V.M., and Sung, P. (2004). Human meiotic recombinase Dmc1 promotes ATP-dependent homologous DNA strand exchange. *Nature* *429*, 433-437.
- Serra, H., Da Ines, O., Degroote, F., Gallego, M.E., and White, C.I. (2013). Roles of XRCC2, RAD51B and RAD51D in RAD51-independent SSA recombination. *PLoS Genet* *9*, e1003971.
- Serrentino, M.E., and Borde, V. (2012). The spatial regulation of meiotic recombination hotspots: are all DSB hotspots crossover hotspots? *Exp Cell Res* *318*, 1347-1352.
- Shan, Q., Wang, Y., Li, J., Zhang, Y., Chen, K., Liang, Z., Zhang, K., Liu, J., Xi, J.J., Qiu, J.L., *et al.* (2013). Targeted genome modification of crop plants using a CRISPR-Cas system. *Nat Biotechnol* *31*, 686-688.
- Shannon, M., Richardson, L., Christian, A., Handel, M.A., and Thelen, M.P. (1999). Differential gene expression of mammalian SPO11/TOP6A homologs during meiosis. *FEBS Lett* *462*, 329-334.
- Shaw, P., and Moore, G. (1998). Meiosis: vive la difference! *Curr Opin Plant Biol* *1*, 458-462.
- Sheridan, S.D., Yu, X., Roth, R., Heuser, J.E., Sehorn, M.G., Sung, P., Egelman, E.H., and Bishop, D.K. (2008). A comparative analysis of Dmc1 and Rad51 nucleoprotein filaments. *Nucleic Acids Res* *36*, 4057-4066.

- Shingu, Y., Mikawa, T., Onuma, M., Hirayama, T., and Shibata, T. (2010). A DNA-binding surface of SPO11-1, an Arabidopsis SPO11 orthologue required for normal meiosis. *FEBS J* 277, 2360-2374.
- Shinohara, A., Ogawa, H., and Ogawa, T. (1992). Rad51 protein involved in repair and recombination in *S. cerevisiae* is a RecA-like protein. *Cell* 69, 457-470.
- Shinohara, A., and Ogawa, T. (1999). Rad51/RecA protein families and the associated proteins in eukaryotes. *Mutat Res* 435, 13-21.
- Shinohara, M., Gasior, S.L., Bishop, D.K., and Shinohara, A. (2000). Tid1/Rdh54 promotes colocalization of rad51 and dmc1 during meiotic recombination. *Proc Natl Acad Sci U S A* 97, 10814-10819.
- Shinohara, M., Oh, S.D., Hunter, N., and Shinohara, A. (2008). Crossover assurance and crossover interference are distinctly regulated by the ZMM proteins during yeast meiosis. *Nat Genet* 40, 299-309.
- Shu, Z., Smith, S., Wang, L., Rice, M.C., and Kmiec, E.B. (1999). Disruption of muREC2/RAD51L1 in mice results in early embryonic lethality which can be partially rescued in a p53(-/-) background. *Mol Cell Biol* 19, 8686-8693.
- Siaud, N., Dray, E., Gy, I., Gerard, E., Takvorian, N., and Doutriaux, M.P. (2004). Brca2 is involved in meiosis in *Arabidopsis thaliana* as suggested by its interaction with Dmc1. *EMBO J* 23, 1392-1401.
- Singh, G., Da Ines, O., Gallego, M.E., and White, C.I. (2017). Analysis of the impact of the absence of RAD51 strand exchange activity in *Arabidopsis* meiosis. *PLoS One* 12, e0183006.
- Smith, K.N., and Nicolas, A. (1998). Recombination at work for meiosis. *Curr Opin Genet Dev* 8, 200-211.
- Snowden, T., Acharya, S., Butz, C., Berardini, M., and Fishel, R. (2004). hMSH4-hMSH5 recognizes Holliday Junctions and forms a meiosis-specific sliding clamp that embraces homologous chromosomes. *Mol Cell* 15, 437-451.

- Sonoda, E., Sasaki, M.S., Buerstedde, J.M., Bezzubova, O., Shinohara, A., Ogawa, H., Takata, M., Yamaguchi-Iwai, Y., and Takeda, S. (1998). Rad51-deficient vertebrate cells accumulate chromosomal breaks prior to cell death. *EMBO J* *17*, 598-608.
- Stacey, N.J., Kuromori, T., Azumi, Y., Roberts, G., Breuer, C., Wada, T., Maxwell, A., Roberts, K., and Sugimoto-Shirasu, K. (2006). Arabidopsis SPO11-2 functions with SPO11-1 in meiotic recombination. *Plant J* *48*, 206-216.
- Stahl, F.W., Foss, H.M., Young, L.S., Borts, R.H., Abdullah, M.F., and Copenhaver, G.P. (2004). Does crossover interference count in *Saccharomyces cerevisiae*? *Genetics* *168*, 35-48.
- Stassen, N.Y., Logsdon, J.M., Jr., Vora, G.J., Offenberg, H.H., Palmer, J.D., and Zolan, M.E. (1997). Isolation and characterization of rad51 orthologs from *Coprinus cinereus* and *Lycopersicon esculentum*, and phylogenetic analysis of eukaryotic recA homologs. *Curr Genet* *31*, 144-157.
- Storlazzi, A., Tessé, S., Gargano, S., James, F., Kleckner, N., and Zickler, D. (2003). Meiotic double-strand breaks at the interface of chromosome movement, chromosome remodeling, and reductional division. *Genes Dev* *17*, 2675-2687.
- Streubel, J., Blucher, C., Landgraf, A., and Boch, J. (2012). TAL effector RVD specificities and efficiencies. *Nat Biotechnol* *30*, 593-595.
- Stronghill, P.E., Azimi, W., and Hasenkampf, C.A. (2014). A novel method to follow meiotic progression in *Arabidopsis* using confocal microscopy and 5-ethynyl-2'-deoxyuridine labeling. *Plant Methods* *10*, 33.
- Sturtevant, A.H. (1915). Castle and Wright on Crossing over in Rats. *Science* *42*, 342.
- Su, H., Cheng, Z., Huang, J., Lin, J., Copenhaver, G.P., Ma, H., and Wang, Y. (2017). Arabidopsis RAD51, RAD51C and XRCC3 proteins form a complex and facilitate RAD51 localization on chromosomes for meiotic recombination. *PLoS Genet* *13*, e1006827.

- Subramanian, V.V., and Hochwagen, A. (2011). Centromere clustering: where synapsis begins. *Curr Biol* 21, R920-922.
- Sugiyama, T., and Kowalczykowski, S.C. (2002). Rad52 protein associates with replication protein A (RPA)-single-stranded DNA to accelerate Rad51-mediated displacement of RPA and presynaptic complex formation. *J Biol Chem* 277, 31663-31672.
- Sun, X., Hu, Z., Chen, R., Jiang, Q., Song, G., Zhang, H., and Xi, Y. (2015). Targeted mutagenesis in soybean using the CRISPR-Cas9 system. *Sci Rep* 5, 10342.
- Sun, Y., Ambrose, J.H., Haughey, B.S., Webster, T.D., Pierrie, S.N., Munoz, D.F., Wellman, E.C., Cherian, S., Lewis, S.M., Berchowitz, L.E., *et al.* (2012). Deep genome-wide measurement of meiotic gene conversion using tetrad analysis in *Arabidopsis thaliana*. *PLoS Genet* 8, e1002968.
- Sung, P. (1994). Catalysis of ATP-dependent homologous DNA pairing and strand exchange by yeast RAD51 protein. *Science* 265, 1241-1243.
- Sung, P. (1997). Yeast Rad55 and Rad57 proteins form a heterodimer that functions with replication protein A to promote DNA strand exchange by Rad51 recombinase. *Genes Dev* 11, 1111-1121.
- Sung, P., Krejci, L., Van Komen, S., and Sehorn, M.G. (2003). Rad51 recombinase and recombination mediators. *J Biol Chem* 278, 42729-42732.
- Szekvolgyi, L., Ohta, K., and Nicolas, A. (2015). Initiation of meiotic homologous recombination: flexibility, impact of histone modifications, and chromatin remodeling. *Cold Spring Harb Perspect Biol* 7.
- Takasu, Y., Kobayashi, I., Beumer, K., Uchino, K., Sezutsu, H., Sajwan, S., Carroll, D., Tamura, T., and Zurovec, M. (2010). Targeted mutagenesis in the silkworm *Bombyx mori* using zinc finger nuclease mRNA injection. *Insect Biochem Mol Biol* 40, 759-765.

- Takeo, S., Lake, C.M., Morais-de-Sa, E., Sunkel, C.E., and Hawley, R.S. (2011). Synaptonemal complex-dependent centromeric clustering and the initiation of synapsis in *Drosophila* oocytes. *Curr Biol* 21, 1845-1851.
- Tang, D., Miao, C., Li, Y., Wang, H., Liu, X., Yu, H., and Cheng, Z. (2014). OsRAD51C is essential for double-strand break repair in rice meiosis. *Front Plant Sci* 5, 167.
- Tanneti, N.S., Landy, K., Joyce, E.F., and McKim, K.S. (2011). A pathway for synapsis initiation during zygotene in *Drosophila* oocytes. *Curr Biol* 21, 1852-1857.
- Tauchi, H., Kobayashi, J., Morishima, K., van Gent, D.C., Shiraishi, T., Verkaik, N.S., vanHeems, D., Ito, E., Nakamura, A., Sonoda, E., *et al.* (2002). Nbs1 is essential for DNA repair by homologous recombination in higher vertebrate cells. *Nature* 420, 93-98.
- Taylor, M.R., Spirek, M., Chaurasiya, K.R., Ward, J.D., Carzaniga, R., Yu, X., Egelman, E.H., Collinson, L.M., Rueda, D., Krejci, L., *et al.* (2015). Rad51 Paralogs Remodel Pre-synaptic Rad51 Filaments to Stimulate Homologous Recombination. *Cell* 162, 271-286.
- Tiang, C.L., He, Y., and Pawlowski, W.P. (2012). Chromosome organization and dynamics during interphase, mitosis, and meiosis in plants. *Plant Physiol* 158, 26-34.
- Trujillo, K.M., Roh, D.H., Chen, L., Van Komen, S., Tomkinson, A., and Sung, P. (2003). Yeast xrs2 binds DNA and helps target rad50 and mre11 to DNA ends. *J Biol Chem* 278, 48957-48964.
- Tsai, J.H., and McKee, B.D. (2011). Homologous pairing and the role of pairing centers in meiosis. *J Cell Sci* 124, 1955-1963.
- Tsutsui, Y., Morishita, T., Iwasaki, H., Toh, H., and Shinagawa, H. (2000). A recombination repair gene of *Schizosaccharomyces pombe*, rhp57, is a functional homolog of the *Saccharomyces cerevisiae* RAD57 gene and is phylogenetically related to the human XRCC3 gene. *Genetics* 154, 1451-1461.

Tsuzuki, T., Fujii, Y., Sakumi, K., Tominaga, Y., Nakao, K., Sekiguchi, M., Matsushiro, A., Yoshimura, Y., and Morita T (1996). Targeted disruption of the Rad51 gene leads to lethality in embryonic mice. *Proc Natl Acad Sci U S A* *93*, 6236-6240.

Uanschou, C., Ronceret, A., Von Harder, M., De Muyt, A., Vezon, D., Pereira, L., Chelysheva, L., Kobayashi, W., Kurumizaka, H., Schlogelhofer, P., *et al.* (2013). Sufficient amounts of functional HOP2/MND1 complex promote interhomolog DNA repair but are dispensable for intersister DNA repair during meiosis in Arabidopsis. *Plant Cell* *25*, 4924-4940.

Uanschou, C., Siwiec, T., Pedrosa-Harand, A., Kerzendorfer, C., Sanchez-Moran, E., Novatchkova, M., Akimcheva, S., Woglar, A., Klein, F., and Schlogelhofer, P. (2007). A novel plant gene essential for meiosis is related to the human CtIP and the yeast COM1/SAE2 gene. *EMBO J* *26*, 5061-5070.

Varas, J., Graumann, K., Osman, K., Pradillo, M., Evans, D.E., Santos, J.L., and Armstrong, S.J. (2015). Absence of SUN1 and SUN2 proteins in Arabidopsis thaliana leads to a delay in meiotic progression and defects in synapsis and recombination. *Plant J* *81*, 329-346.

Vignard, J., Siwiec, T., Chelysheva, L., Vrielynck, N., Gonord, F., Armstrong, S.J., Schlogelhofer, P., and Mercier, R. (2007). The interplay of RecA-related proteins and the MND1-HOP2 complex during meiosis in Arabidopsis thaliana. *PLoS Genet* *3*, 1894-1906.

Villeneuve, A.M., and Hillers, K.J. (2001). Whence meiosis? *Cell* *106*, 647-650.

Vrielynck, N., Chambon, A., Vezon, D., Pereira, L., Chelysheva, L., De Muyt, A., Mezard, C., Mayer, C., and Grelon, M. (2016). A DNA topoisomerase VI-like complex initiates meiotic recombination. *Science* *351*, 939-943.

Wang, C., Higgins, J.D., He, Y., Lu, P., Zhang, D., and Liang, W. (2017). Resolvase OsGEN1 Mediates DNA Repair by Homologous Recombination. *Plant Physiol* *173*, 1316-1329.

- Wang, H., Hu, Q., Tang, D., Liu, X., Du, G., Shen, Y., Li, Y., and Cheng, Z. (2016). OsDMC1 Is Not Required for Homologous Pairing in Rice Meiosis. *Plant Physiol* *171*, 230-241.
- Wang, H., Yang, H., Shivalila, C.S., Dawlaty, M.M., Cheng, A.W., Zhang, F., and Jaenisch, R. (2013). One-step generation of mice carrying mutations in multiple genes by CRISPR/Cas-mediated genome engineering. *Cell* *153*, 910-918.
- Wang, K., Wang, M., Tang, D., Shen, Y., Miao, C., Hu, Q., Lu, T., and Cheng, Z. (2012a). The role of rice HEI10 in the formation of meiotic crossovers. *PLoS Genet* *8*, e1002809.
- Wang, Y., Cheng, Z., Huang, J., Shi, Q., Hong, Y., Copenhaver, G.P., Gong, Z., and Ma, H. (2012). The DNA replication factor RFC1 is required for interference-sensitive meiotic crossovers in *Arabidopsis thaliana*. *PLoS Genet* *8*, e1003039.
- Wang, Y., Xiao, R., Wang, H., Cheng, Z., Li, W., Zhu, G., Wang, Y., and Ma, H. (2014). The *Arabidopsis* RAD51 paralogs RAD51B, RAD51D and XRCC2 play partially redundant roles in somatic DNA repair and gene regulation. *New Phytol* *201*, 292-304.
- Wiese, C., Collins, D.W., Albala, J.S., Thompson, L.H., Kronenberg, A., and Schild, D. (2002). Interactions involving the Rad51 paralogs Rad51C and XRCC3 in human cells. *Nucleic Acids Res* *30*, 1001-1008.
- Wijeratne, A.J., Chen, C., Zhang, W., Timofejeva, L., and Ma, H. (2006). The *Arabidopsis thaliana* PARTING DANCERS gene encoding a novel protein is required for normal meiotic homologous recombination. *Mol Biol Cell* *17*, 1331-1343.
- Wijnker, E., Velikkakam James, G., Ding, J., Becker, F., Klasen, J.R., Rawat, V., Rowan, B.A., de Jong, D.F., de Snoo, C.B., Zapata, L., *et al.* (2013). The genomic landscape of meiotic crossovers and gene conversions in *Arabidopsis thaliana*. *Elife* *2*, e01426.

- Wiltzius, J.J., Hohl, M., Fleming, J.C., and Petrini, J.H. (2005). The Rad50 hook domain is a critical determinant of Mre11 complex functions. *Nat Struct Mol Biol* 12, 403-407.
- Wu, H.Y., and Burgess, S.M. (2006). Two distinct surveillance mechanisms monitor meiotic chromosome metabolism in budding yeast. *Curr Biol* 16, 2473-2479.
- Xie, K., and Yang, Y. (2013). RNA-guided genome editing in plants using a CRISPR-Cas system. *Mol Plant* 6, 1975-1983.
- Xu, R.F., Li, H., Qin, R.Y., Li, J., Qiu, C.H., Yang, Y.C., Ma, H., Li, L., Wei, P.C., and Yang, J.B. (2015). Generation of inheritable and "transgene clean" targeted genome-modified rice in later generations using the CRISPR/Cas9 system. *Sci Rep* 5, 11491.
- Yang, S., Yuan, Y., Wang, L., Li, J., Wang, W., Liu, H., Chen, J.Q., Hurst, L.D., and Tian, D. (2012). Great majority of recombination events in Arabidopsis are gene conversion events. *Proc Natl Acad Sci U S A* 109, 20992-20997.
- Yelina, N.E., Ziolkowski, P.A., Miller, N., Zhao, X., Kelly, K.A., Munoz, D.F., Mann, D.J., Copenhaver, G.P., and Henderson, I.R. (2013). High-throughput analysis of meiotic crossover frequency and interference via flow cytometry of fluorescent pollen in Arabidopsis thaliana. *Nat Protoc* 8, 2119-2134.
- Yu, H., Wang, M., Tang, D., Wang, K., Chen, F., Gong, Z., Gu, M., and Cheng, Z. (2010). OsSPO11-1 is essential for both homologous chromosome pairing and crossover formation in rice. *Chromosoma* 119, 625-636.
- Yu, X., Jacobs, S.A., West, S.C., Ogawa, T., and Egelman, E.H. (2001). Domain structure and dynamics in the helical filaments formed by RecA and Rad51 on DNA. *Proc Natl Acad Sci U S A* 98, 8419-8424.
- Zakharyevich, K., Ma, Y., Tang, S., Hwang, P.Y., Boiteux, S., and Hunter, N. (2010). Temporally and biochemically distinct activities of Exo1 during meiosis: double-

strand break resection and resolution of double Holliday junctions. *Mol Cell* *40*, 1001-1015.

Zakharyevich, K., Tang, S., Ma, Y., and Hunter, N. (2012). Delineation of joint molecule resolution pathways in meiosis identifies a crossover-specific resolvase. *Cell* *149*, 334-347.

Zalevsky, J., MacQueen, A.J., Duffy, J.B., Kempthues, K.J., and Villeneuve, A.M. (1999). Crossing over during *Caenorhabditis elegans* meiosis requires a conserved MutS-based pathway that is partially dispensable in budding yeast. *Genetics* *153*, 1271-1283.

Zhang, B., Wang, M., Tang, D., Li, Y., Xu, M., Gu, M., Cheng, Z., and Yu, H. (2015). XRCC3 is essential for proper double-strand break repair and homologous recombination in rice meiosis. *J Exp Bot* *66*, 5713-5725.

Zhang, C., Song, Y., Cheng, Z.H., Wang, Y.X., Zhu, J., Ma, H., Xu, L., and Yang, Z.N. (2012). The *Arabidopsis thaliana* DSB formation (*AtDFO*) gene is required for meiotic double-strand break formation. *Plant J* *72*, 271-281.

Zhang, F., Maeder, M.L., Unger-Wallace, E., Hoshaw, J.P., Reyon, D., Christian, M., Li, X., Pierick, C.J., Dobbs, D., Peterson, T., *et al.* (2010). High frequency targeted mutagenesis in *Arabidopsis thaliana* using zinc finger nucleases. *Proc Natl Acad Sci U S A* *107*, 12028-12033.

Zhang, H., Zhang, J., Wei, P., Zhang, B., Gou, F., Feng, Z., Mao, Y., Yang, L., Zhang, H., Xu, N., *et al.* (2014). The CRISPR/Cas9 system produces specific and homozygous targeted gene editing in rice in one generation. *Plant Biotechnol J* *12*, 797-807.

Zhang, J., and Han, F. (2017). Centromere pairing precedes meiotic chromosome pairing in plants. *Sci China Life Sci*.

Zhang, L., Liang, Z., Hutchinson, J., and Kleckner, N. (2014a). Crossover patterning by the beam-film model: analysis and implications. *PLoS Genet* *10*, e1004042.

Zhang, Y., Zhang, F., Li, X., Baller, J.A., Qi, Y., Starker, C.G., Bogdanove, A.J., and Voytas, D.F. (2013). Transcription activator-like effector nucleases enable efficient plant genome engineering. *Plant Physiol* *161*, 20-27.

Zickler, D. (2006). From early homologue recognition to synaptonemal complex formation. *Chromosoma* *115*, 158-174.

Zickler, D., and Kleckner, N. (1999). Meiotic chromosomes: integrating structure and function. *Annu Rev Genet* *33*, 603-754.

Zickler, D., and Kleckner, N. (2015). Recombination, Pairing, and Synapsis of Homologs during Meiosis. *Cold Spring Harb Perspect Biol* *7*.